Tunable CAR T Cell Responses Achieved by the Disruption of Protein-Protein Interactions via the Administration of a Small Molecule

José António Costa Guerra

Thesis submitted for the Degree of Doctor of Philosophy

Department of Haematology
UCL Cancer Institute
University College London

September 2020

Declaration

I, José António Costa Guerra confirm that the work presented in this thesis is my own. Where information has been derived from other sources, I confirm that this has been indicated in the thesis.

Abstract

Introduction: The adoptive transfer of T-cells engineered to express chimeric antigen receptors (CARs) has significantly widened the applicability of passive immunotherapy in cancer. Up until now, several studies of CAR therapy have emerged as a promising treatment for cancer, although there are serious concerns regarding potential risk of acute and chronic toxicity. Given the ability of CAR T-cells to engraft and proliferate in the patient, toxicity from excessive activity can be progressive and fulminant. This highlights the need for technologies to remotely control and tune the potency of the CAR T-cells after administration. Suicide gene approaches allow a level of control of CAR T-cell therapy. However, as suicide switches result in permanent loss of all engineered T-cells, a new strategy which can temporarily reduce or stop CAR T-cell activity without triggering CAR T-cell apoptosis is desirable. One way to achieve this is to use small molecules that present desired pharmacologic properties, such as tetracycline and analogues doxycycline and minocycline.

Results: Therefore, we developed a Tet-Off signalling switch that enables tetracycline-dependent, titratable, and reversible control over CAR T-cells. The CAR was split into two: an antigen recognition component fused with TetR (Tet repressor) and a signalling component fused with TiP (TetR interacting peptide). Both TiP and tetracycline are known to bind to TetR with a high affinity. We predicted that although TiP bound to the same part of TetR as tetracycline, Tetracycline would bind with a much higher affinity than TiP and hence rapidly displace TiP. First with eGFP, we showed that in the absence of tetracycline such a system results in membrane localization of a TiP fusion protein, with the eGFP being displaced to the cytoplasm in the presence of tetracycline. Next as a CAR, we showed that in the absence of tetracycline, the two CAR components associate and the CAR signals in the presence of cognate antigens. On the addition of tetracycline, TiP was displaced and the receptor stopped signalling. Depending on the concentration of tetracycline present, tetCAR T-cells showed titratable activity, from as strong as that of conventional CAR T-cells to undetectable. Similar results were obtained when using the analogues doxycycline and minocycline. We tested the effectiveness of this tetCAR in murine and human T-cells. These results included IL-2 and IFN-γ production, the tetCAR T-cell ability to control target cell killing and also the killing of multiple types of target cells by the tetCAR T-cells. Regarding reversibility, we showed that the inhibition process is reversible. Once we wash off the tetracycline from the cultures, tetCAR T-cells regain activity.

Conclusion: We successfully generated and controlled the activity of tetCAR T-cells by tetracycline administration.

Impact Statement

Using novel technology, T-cells can be genetically modified to express an artificial receptor protein, called a Chimeric Antigen Receptor (CAR), which allows them to recognize cancer cells. This new CAR T-cell therapy has demonstrated considerable success in treating patients with haematological malignancies. The active and persistent nature of CAR T-cells in the patient is believed to be a main factor explaining their effective elimination of malignant cells. Although such powerful CAR T-cell activity is the desired response, this ability also represents a key challenge in CAR T-cell therapy, as overly active CAR T-cell activity can lead to dangerous inflammatory syndromes and even be fatal. With the aim to find a solution to the complications encountered with constitutive CARs, we have developed a next generation CAR, called tetCAR, which enable us to tune down the CAR T-cell activity by administration of commonly used antibiotics. This strategy is highly innovative and will allow safer CAR T-cell therapy.

Overall, this PhD project provides the pre-clinical development that needs to be performed, in order to achieve the regulatory approval for testing of tetCAR technology in a clinical study. We hope to reproduce the clinical successes seen with standard CAR T-cell therapy against haematological malignancies, but with control of immune toxicity.

The main competing technology is the suicide gene approach. Such suicide switches leading to a complete elimination of the infused T-cells will result in the irreversible and premature end of this expensive treatment. Furthermore, as CAR T-cell persistence is a key factor for lasting remissions, suicide strategies will result in increased relapses. Consequently, implementing our tetCAR technology represents an important safety improvement in CAR T-cell therapy, as it does not eradicate the CAR T-cells but rather restricts their activities, allowing them to persist and continue to act.

In clinical trials, T-cells engineered to express CARs have proven effective against B-cell cancers and as a result, two CAR T-cell therapies, Yescarta (axicabtagene ciloleucel) from Kite Pharma and Kymriah (tisagenlecleucel) from Novartis, have already obtained market authorization. While CAR T-cell therapies are effective, excessive CAR T-cell activity can lead to highly toxic immune activation syndromes. Finding a way to control this would revolutionize the field. With our tetCAR technology, if we achieve the high clinical response rates seen against B-cell cancers but also control the CAR T-cell activity following grafting, we will have the best-in-class therapeutic product in this exciting emerging field. CAR T-cell therapy will not only be safer, but more widely applicable.

Table of Contents

List of Figures

List of Tables

List of Abbreviations

ACT	Adoptive Cell Therapy
ADCC	Antibody Dependent Cellular Cytotoxicity
aGVHD	Acute Graft-Versus-Host Disease
Allo-HSCT	Allogeneic Haematopoietic SCT
BBB	Blood-Brain Barrier
BD	Becton Dickinson
BiTE	Bi-specific T-cell Engager
CAIX	Carbonic Anhydrase 9
CAR	Chimeric Antigen Receptor
CBD	Cell-Binding Domain
CD28TM	CD28 Transmembrane Domain
CD4TM	CD4 Transmembrane Domain
CD8STK	CD8-α Stalk Spacer Domain
CD8TM	CD8 Transmembrane Domain
CDC	Complement Dependent Cellular Cytotoxicity
CNS	Central Nervous System
CR	Complete Remission
CRS	Cytokine Release Syndrome
CS-1	Connecting Segment-1
CTL	Cytotoxic T-Lymphocytes
DMSO	Dimethyl Sulfoxide
DNA	Deoxyribonucleic Acid
dNTP	Deoxyribonucleotide Triphosphate
E. coli	*Escherichia coli*
EDTA	Ethylenediaminetetraacetic Acid
eGFP	Enhanced Green Fluorescent Protein
ELISA	Enzyme-Linked Immunosorbent Assay
Env	Envelope
ER	Endoplasmic Reticulum
FACS	Flow Cytometry Activated Cell Sorting
Fc	Fragment Crystallizable

FCS	Foetal Calf Serum
FITC	Fluorescein Isothiocyanate
GCV	Ganciclovir
HEK	Human Embryonic Kidney
HF	High-Fidelity
HSV-TK	Herpes Simplex Virus Thymidine Kinase
iCasp9	Inducible Caspase 9
ICU	Intensive Care Unit
IFN-γ	Interferon-Gamma
IgD	Immunoglobulin D
IgG	Immunoglobulin G
IL-2	Interleukin-2
IL-6	Interleukin-6
IL-6R	Interleukin-6 Receptor
IMDM	Iscove's Modified Dulbecco's Medium
IP	Intraperitoneal
L	Linker
LTR	Long Terminal Repeat
MA	Matrix
mAb	Monoclonal Antibody
MACS	Magnetic Activated Cell Sorting
MAS	Macrophage Activation Syndrome
MFI	Mean Fluorescence Intensity
MHC	Major Histocompatibility Complex
MLV	Murine Leukaemia Virus
MoMLV	Moloney Murine Leukaemia Virus
Mu	Murine
MUC-1	Mucin-1
NEB	New England Biolabs
NK	Natural Killer
NS	No Significant
NSG	NOD.Cg-Prkdc^{scid} Il2rg^{tm1wjl}/SzJ murine strain
NT	Non-Transduced
PB	Peripheral Blood

PBMC	Peripheral Blood Mononuclear Cells
PBS	Phosphate Buffered Saline
PCR	Polymerase Chain Reaction
PE	Phycoerythrin
PFA	Paraformaldehyde
PHA	Phytohaemagglutinin
PMA	Phorbol Myristate Acetate
RCV	Replication-Competent Vector
RD114	Feline Endogenous Virus Envelope Protein
RN	RetroNectin
RPMI	Roswell Park Memorial Institute
RT	Room Temperature
RV	Retrovirus
sCD19	Soluble CD19
scFv	Single Chain Variable Fragment
SCID	Severe Combined Immunodeficiency
SCT	Stem Cell Transplant
SD	Standard Deviation
SFG	Retroviral Packaging Plasmid
T2A	*Thosea Asigna* Sequence
TAA	Tumour-Associated Antigens
TB	Terrific Broth
TCR	T-Cell Receptor
Tet	Tetracycline
tetCAR	Tetracycline Inducible CAR
TetR	Tet Repressor
TiP	TetR Interacting Peptide
TGF-β	Transforming Growth Factor Beta
TIL	Tumour-Infiltrating Lymphocytes
TM	Transmembrane
TNFr	Tumour Necrosis Factor Receptor
Tregs	Regulatory T-cells
V	Variable
VH	Antibody Heavy Chain

VL	Antibody Light Chain
VLA-4	Very Late Antigen-4
VLA-5	Very Late Antigen-5
VSV-G	Vesicular Stomatitis Virus-G
WT	Wild-Type

Acknowledgements

I would like to express my sincere gratitude to my first supervisor, Dr Martin Pule, for allowing me the opportunity to undertake my PhD in his laboratory.

I would also like to thank my second supervisor, Prof Kwee Yong, for her advice. Many thanks also go to my colleagues within the Pule group for making the laboratory such an enjoyable place to work. I am also grateful to all the members of the Cancer Institute haematology department for sharing with me their scientific expertise.

I would like to dedicate this thesis to my parents Teresa and Carlos, to my brother Gonçalo and to my partner Tanya for their love, endless support and patience. It is not an understatement to say that everything I have achieved is because of them.

Lastly, I would like to express my deepest love and gratitude to my dad, who was battling pancreatic cancer and passed away recently. Dad, your endless support and encouragement has enabled me to follow my chosen career. Without you around, everything would have been so much harder. My life will never be the same, but I know that you will always be that brightest star in the sky protecting me.

CHAPTER 1

INTRODUCTION

1.1 Cancer immunology and Immunotherapy

The immune system plays a complex role in cancer, having been implicated in both the surveillance and eradication of malignantly transformed cells as well as directly promoting tumourigenesis in certain conditions.

Several observations strongly indicate that immune effector cells play a vital role in preventing cancer development. Studies on transgenic mice with knockout genes important for encoding vital components of the immune system and effector cells show a greater susceptibility towards developing certain types of tumours. Further histopathological and clinical observations in human models have suggested the involvement of cytotoxic T-lymphocytes (CTL). Tumour-infiltrating lymphocytes (TIL) have been found in some cancer patients, and immunodeficient patients show an increased risk of developing tumours, particularly of viral aetiology [1]. While antitumour processes are clearly in place and highly varied across tumour types, specific mechanisms developed by tumour cells can result in an overall impairment of the host immune response and subsequent failure to modulate cancer progression. Detection of a tumour by immune cells early during their development subjects them to frequent immune challenges that owing to their genetic instability, induces alterations in a process known as ‘immunosculpting’ or ‘immune selection’. These tumour cell variants are able to manipulate their microenvironment, having negative consequences for the host immune response. Several mechanisms are deployed by tumour cells to escape immune detection: downregulation of their tumour-associated antigens (TAA) [1], impaired access to TAA by concealment under larger proteins (steric hindrance) [2], expression of decoys such as soluble circulating tumour antigens [3] and loss of antigen presenting capacity by downregulation of major histocompatibility (MHC) molecules [4]. Tumour cells may also exert deleterious effects on lymphocytes directly: expression of immune suppressive factors such as TGF-β [3], suppression of co-stimulatory molecules for T-cell activation [5] and recruitment of regulatory T-cells (Tregs), which proceed to eliminate CTLs.

Together, these mechanisms conspire to create a tumour microenvironment that may eventually lead to a clonal exhaustion and/or depletion of cytotoxic T-cells [3]. The importance of augmenting the abilities of the immune system against cancer coupled with a greater understanding of tumour immunology has led to the development of

cancer immunotherapy. The goal of immunotherapy is to reverse the immune suppression induced by cancer, using the following therapeutic strategies: monoclonal antibodies (mAbs), adoptive transfer of immunological cells, cytokine therapies and vaccination [3]. These can also be classified as either active or passive immunotherapy; active immunotherapy involves stimulating the host's immune response by using protein or whole cell vaccinations. The focus in this study is of a potential therapy that aims to initiate an immune response not directly dependent on the intrinsic host immune system. This is referred to as passive immunotherapy.

1.2 Adoptive T-Cell Therapy (ACT)

Adoptive T-cell transfer is an innovative strategy within cancer immunotherapy that involves isolating TAA-specific T lymphocytes from the patient (known as TILs), expanding these *ex vivo* and then transferring them back into the patient. The properties of T-cells make them ideal for cell-based anti-cancer therapy: they display antigen-specificity, hence minimizing the likelihood of non-specific immune activation (and thus, potential side-effects) and they have potent effector functions, propagated by cytokine release, cytolytic activity directly against the tumour cell and the recruitment of other immune cells [6]. Encouraging outcomes of this treatment have been seen in clinical trials involving melanoma patients. Complete responses lasting between 18-75 months were reported in 28% of the patients in a recent trial [7]. There are however limitations to this therapy. The most significant is that this treatment is limited only to those immunogenic tumours that generate a pool of TAA-specific T-cells. Even in such applicable malignancies, *ex vivo* expansion of patient T-cells to therapeutically significant numbers is challenging, and tumour cells can downregulate MHC through which TILs engage their target. As a unique alternative to this technology, the adoptive transfer of T-cells engineered to express chimeric antigen receptors (CARs) significantly widens the applicability of passive immunotherapy in cancer (Figure 1) [8-10].

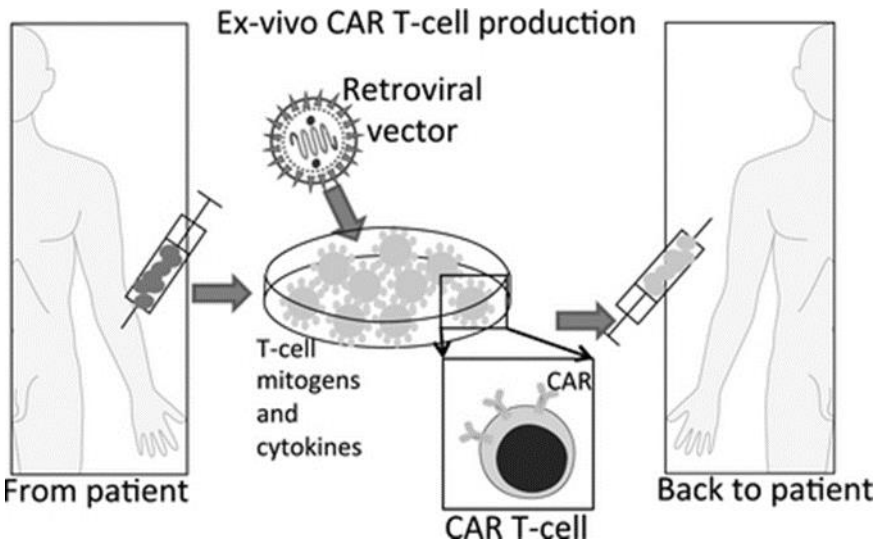

Figure 1. Concept of chimeric antigen receptor (CAR) therapy. T lymphocytes are isolated from the patient and exposed to the viral vector. This results in CAR-expressing T lymphocytes which are expanded *ex vivo* and then transferred back into the patient as treatment [11].

1.3 Chimeric Antigen Receptors (CARs)

CARs are fusion molecules that combine the properties of tumour antigen specificity and binding, followed by the delivery of a T-cell activating signal [12]. The original concept of CAR molecules came from Kuwana et al.'s demonstration of a T-cell receptor (TCR) with its variable domains replaced by an antibody, which assigned it with novel antigenic specificity [10]. A robust technique to generate CAR-grafted T-cells targeted against a chosen native antigen (originally referred to as a 'T-body') was shown by Eshhar et al. [13], whose group also later demonstrated their capability of tissue penetration and target cell destruction [14].

Most CARs contain three main components: (1) an extracellular targeting moiety, (2) an intracellular signalling domain and (3) a 'hinge' or 'spacer' region that separates the other two components from each other. The targeting moiety may be composed of either a single chain variable (antibody) fragment (scFv) or a peptide/ligand motif, allowing for high binding specificity to a wide range of potential antigens.

To optimize the engagement between the targeting moiety and tumour antigen, a hinge region may be included. The characteristics of the target antigen ultimately determine what hinge to use with regards to its size, flexibility and reach. Studies have shown that the presence of the spacer region impacts on CAR functionality. Gilham et al. found that T-cell cytokine release and cytotoxicity was enhanced in the presence of a spacer region [15]. In this case, the CAR binded epitopes that were closer to the cell membrane. Thus, the presence of the spacer region enhanced the 'reach' of the targeting moiety. In another CAR design, an elongated and flexible IgD-derived hinge was shown to decrease steric hindrance of its target protein Mucin-1, thereby enhancing its targetability [16].

The intracellular domain is subject to the most change in the overall CAR design. Its components are variable and can be tailored to deliver a signal that is appropriate for T-cell activation [17]. The combination of choice which gives the most desirable signalling appears to depend on several factors: expression density of the protein antigen on the target cell, structure of the CAR/level of expression and antibody to ligand affinity [18]. The capability of CARs to enable T-cells to activate and perform effector functions stems from the same principle governing TCR activation. Various subunits of the TCR-CD3 complex are responsible for activation and signalling when

the TCR engages with the peptide-MHC complex [19]. However, the TCR subunit ζ was found to be capable of activating the T-cell and propagating effective signalling alone [20, 21]. The CD3ζ subunit has thus become an inclusion in most CAR designs, providing the TCR-like 'signal 1' [13]. CARs containing CD3ζ (or the related Fcϫ) as their subunit are referred to as first generation CARs. But clinical studies involving first generation CARs have shown disappointing results: CAR+ T-cells showed minimal expansion and persistence *in vivo* and a lack of anti-tumour responses [22-24]. To account for these results, one must consider that complete T-cell activation cannot occur with signal 1 alone: in addition, a co-stimulatory signal is also required that is induced through CD28 signalling. However, this signal often cannot come from tumour cells as they downregulate co-stimulatory ligands, leading to the absence of a T-cell 'signal 2' [17]. Second generation CARs were devised to include a co-stimulatory signalling motif in their intracellular domain, as a solution to this problem. The presence of CD28 alongside CD3ζ in the CAR endodomain induced T-cell expansion and cytokine release significantly [25]. The co-stimulatory motif can also be derived from 4-1BB [26] or OX40 [27]. A combination of two or more co-stimulatory domains is incorporated into third generation CARs (Figure 2). Compared to second generation CARs, these appear to display an enhanced effector function *in vivo* when they combine CD28 with 4-1BB [18, 28].

An important rationale of using CARs in the treatment of cancer is their ability to recognise antigen independently of MHC molecules, by binding the protein directly. This is particularly desirable as aberration of MHC molecules is frequently seen in cancer. Moreover, if a protein antigen appears to be critical for growth and survival, its downregulation by the malignant cell as a result of targeting may result in eventual tumour cell death [29]. Another major advantage of using CAR-grafted T-cells is that a polyclonal population of T-cells can all be directed against the same tumour antigen. There is therefore no requirement for isolated tumour-specific lymphocytes from the patient, which as a result of elimination from Tregs are often too low in number.

Several CARs have been developed against tumour-associated antigens, and adoptive transfer approaches using such CAR-expressing T-cells are currently in clinical trial for the treatment of various cancers.

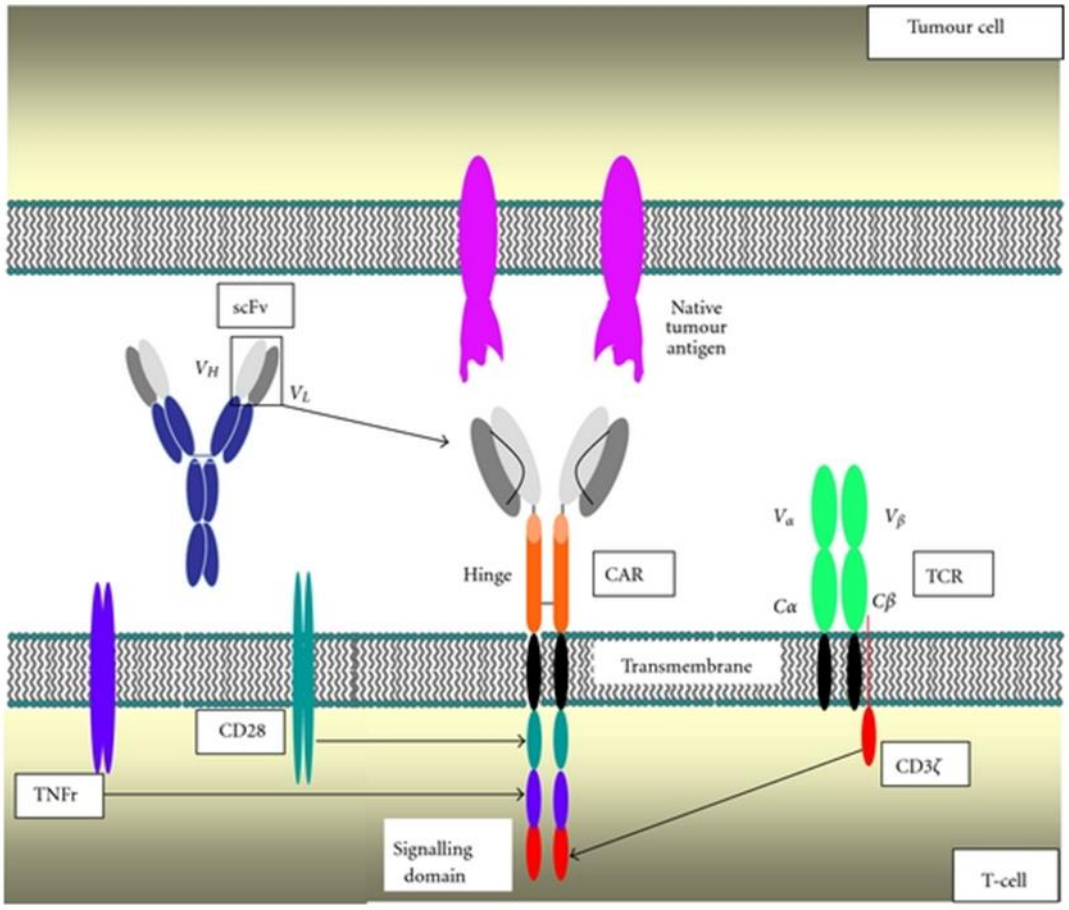

Figure 2. Schematic representation of the chimeric antigen receptor (CAR) structure. These receptors are created by linking a single chain variable fragment (scFv) from a mAb to an intracellular signalling domain via a transmembrane domain (TM). This example shows a "third generation" CAR which endodomain contains CD28, a tumour necrosis factor receptor (TNFr), such as 4-1BB or OX40, and a CD3ζ endodomain [30].

1.4 Chimeric Antigen Receptors toxicity

There have been documented cases of complete remissions in CAR clinical trials [31-40], but toxicity limits broader application. A number of toxicities have been reported from CAR studies, and additional theoretical toxicities exist. Such toxicities include immunological toxicity caused by sustained intense activation of the CAR T-cells resulting in a cytokine release syndrome (CRS) [41] and "On-target off-tumour" toxicity i.e. recognition of the target antigen on normal tissues.

Type	Subtype	Comment
Infusional	Allergic Reaction	As per any blood product
	Reaction to DMSO	As per other cell therapies
	Other Excipients	Albumin, EDTA and salt buffer
Direct effects	Tumour Lysis Syndrome	Due to rapid destruction of tumour
	B cell Aplasia	On-target off-tumour toxicity
	Graft-versus-host Disease	When generated post allo-HSCT
Indirect effects	Cytokine Release Syndrome	Related to immunological activity
	Neurotoxicity	Idiosyncratic syndrome
	Cytopenias	Likely related to marrow macrophage activation after CRS
Gene Vector	Replication-competent vector	Very unlikely due to vector design
	Insertional mutagenesis	Has not been reported in T-cells

Table 1. Possible toxicity from CAR T-cell therapy

Recent clinical data describe a cytokine release syndrome (CRS) which occurs several days after T-cell infusion and is associated with clinical responses. This syndrome resembles that seen in patients with defects in the granule-dependent cytotoxic activity and in patients treated with the CD19 bi-specific T-cell engager (BiTE) therapeutic. CRS is presumed to be caused by persistent antigen-driven activation and proliferation of T-cells which in turn release copious inflammatory cytokines leading to hyper-activation of macrophages and a feed-forward cycle of immune activation. A large spike in serum IL-6 is characteristic, as well as other clinical and laboratory features of CRS. This syndrome can result in a severe systemic illness requiring intensive care unit (ICU) admission. However, it appears to respond quickly and completely to the IL-6 receptor (IL-6R) antagonist tocilizumab in most cases [33, 37, 41-43].

On-target off-tumour toxicity has been reported with other CARs [26, 44-46]. A group of patients treated in Rotterdam with a CAR against the renal cell carcinoma antigen CAIX developed unexpected and treatment limiting biliary toxicity [47]. In another example, one patient died of a respiratory distress syndrome which occurred immediately post-infusion of a large dose of third generation anti-ERBB2 CAR T-cells [48] due to low level of the target antigen in the lungs.

One particularly troublesome toxicity is neurotoxicity of activated T-cells [49-51]. This syndrome can range from mild symptoms such as dysarthria through to confusion, seizures, coma and death [40, 52-60]. The precise pathogenesis is not understood although recent primate studies suggest that it is associated with rapid margination of activated T-cells to the cerebral microenvironment [61]. This toxicity resembles that seen with the bi-specific T-cell engager Blinatumomab, except with this latter agent the toxicity can be ameliorated by stopping the agent. This is not possible with CAR T-cell therapy and unlike CRS an effective way to treat this neurotoxicity is not yet established.

These toxicities are very difficult to predict even with detailed animal studies or primate work. Crucially, unlike small molecules and biologics, CAR T-cells do not have a half-life i.e. one cannot just not give any more and wait for the agent to breakdown/become excreted. CAR T-cells are autonomous – they can engraft and proliferate so toxicity can be progressive and fulminant.

1.5 Small Molecule Control of CAR T-cells

Given that CAR T-cell activity is autonomous and toxicity can be unpredictable and fulminant, strategies have been developed to control CAR T-cell activity "remotely" through the administration of small molecules. These approaches are summarized in the table below.

Method	Description	Advantages and disadvantages
Suicide genes	A small molecule triggers apoptosis of the CAR T-cell hence stopping all toxicity.	Proven and effective. However, results in complete deletion of the CAR T-cells with an increased risk of relapse, when actually only a transient reduction in CAR T-cell activity is required.
Indirect CARs	The CAR does not recognize the target antigen directly, instead it recognizes an adaptor. A targeting / adaptor protein is co-administered. If this latter infusion is stopped the T-cells stop working.	There are two main limitations: A second therapeutic agent needs to be manufactured which is a considerable undertaking. Further, CAR T-cell activity will be limited to bio-availability of the second agent which may in some tissues / tumour cores be limited. Advantage over standard BiTEs is not clear.
Tunable CARs	A small molecule directly controls the CAR T-cell activity either through transcriptional control or through a split CAR approach.	The transcriptional approach requires a complex vector and is likely slow. The split-CAR approach requires experimental small molecule and also requires the patient to stay on a small molecule all the time.

Table 2. Summarized approaches that allow for small molecule control of CAR T-cell activity

1.5.1 Suicide genes

Suicide genes are genetically expressed elements which can conditionally destroy cells which express them. Examples include Herpes simplex virus thymidine kinase (HSV-TK) which renders cells susceptible to Ganciclovir (GCV) [62, 63], inducible Caspase 9 (iCasp9) which renders cells susceptible to a small molecular homodimerizer [64, 65], CD20 and RQR8 which renders cells susceptible to Rituximab (Figure 3) [66-68].

This technology adds a certain amount of safety to CAR T-cell therapy, however there are limitations. Firstly, it is a binary approach wherein all the CAR T-cells are destroyed upon addition of the suicide entity. In addition, medicinal therapeutics often have a therapeutic window. With a suicide gene the potency of the product cannot be tuned such that efficacy with tolerable toxicity can be achieved. In some settings (e.g. paediatric B-ALL), premature depletion of the CAR T-cells increases the risk of relapse.

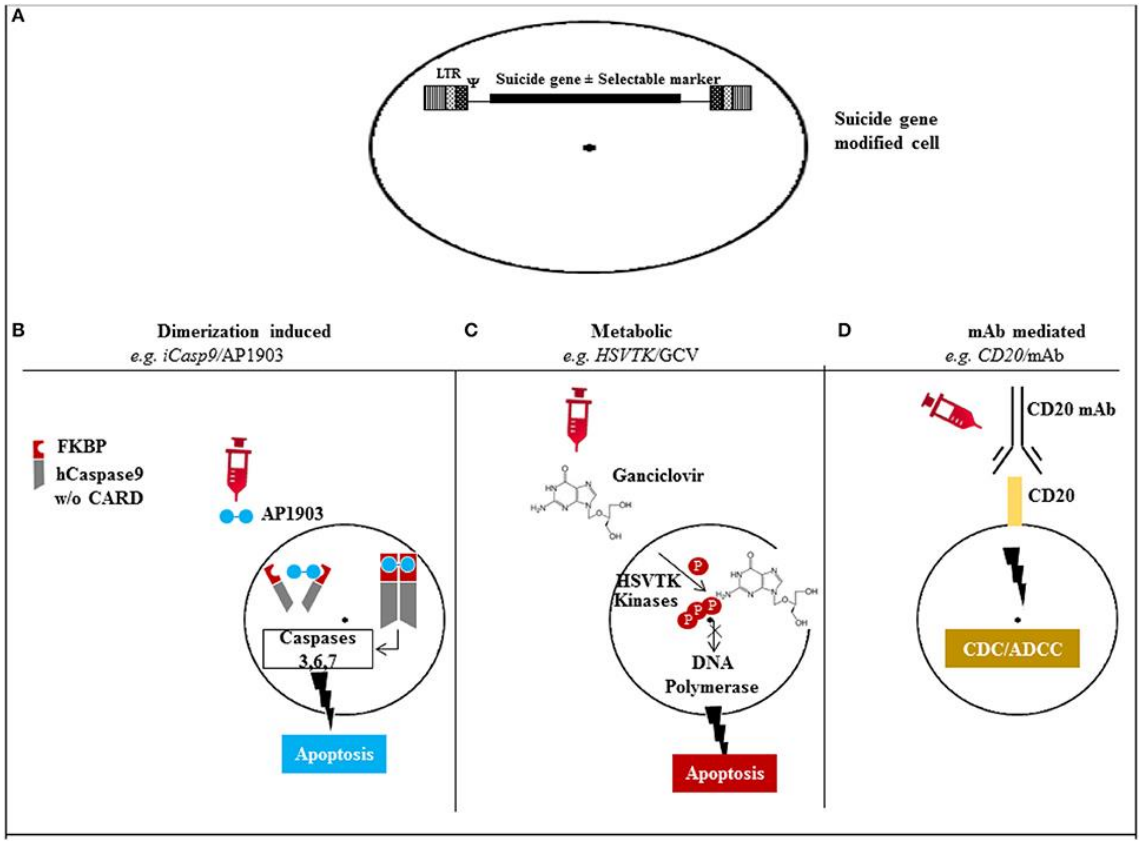

Figure 3. Suicide gene strategies. (a) A suicide gene encodes for a protein which can allow selective elimination of modified cells in case of unacceptable toxicity. (b) The iCasp9 system utilises a synthetic fusion gene construct derived from the human

Caspase9 activation domain fused to a synthetic FKBP12 binding domain. Induction of suicide gene machinery is mediated through therapeutic administration of AP1903. (c) The HSV-TK system involves selective phosphorylation of the non-toxic prodrug ganciclovir by the HSV-TK enzyme generating GCV-triphosphate. Incorporation of this metabolite into DNA results in chain termination and single strand breaks in dividing cells. (d) Surface antigen overexpression on modified cells (e.g., CD20) allows destruction after exposure to the monoclonal antibody (mAb) through complement/antibody dependent cellular cytotoxicity (CDC/ADCC) [69].

1.5.2 Indirect CARs

Here, a "universal" CAR is generated which rather than recognizing the target antigen recognizes an adaptor target. After CAR T-cell infusion, a recombinant "adaptor" protein is also administered which is a fusion between the adaptor target and a targeting domain which recognizes the target antigen. In this setting, the CAR T-cells can only activate if the adaptor protein is co-infused. Stopping administration of the adaptor molecule will stop CAR T-cell activity. There are a few iterations of this approach which in its simplest form the CAR recognizes Fc and the adaptor protein is a therapeutic mAb. Other approaches include the CAR recognizing FITC or a peptide and the adaptor protein being a FITC-conjugated scFv or an scFv linked to the cognate peptide [70-78].

The main limitation for this approach is the need for a second therapeutic agent (i.e. the adaptor) which is burdensome. Another limitation is that CAR T-cell activity is limited by bio-distribution of the adaptor agent. Access to certain sites (e.g. tumour core, past the blood-brain barrier) may be limited. Finally, the advantage of this approach over a BiTE approach is not clear.

1.5.3 Tunable CARs

Here, a small molecule directly controls CAR activity. Importantly, the CAR T-cell is not killed by the small molecule [79-90]. Two such systems have been suggested: in one expression of the CAR is simply controlled by a small molecule. In another system, the CAR is split in two. Recently, Wu et al. showed a design in which the antigen-recognition and signalling components were split into distinct polypeptides appended to heterodimerizing domains that assemble only in the presence of a small molecule (Figure 4) [89]. In this setting, the CAR T-cells can only activate when exposed to both cognate antigen and small molecule. The authors described a system that enables small molecule-dependent, titratable, and reversible control over CAR T-cells.

The latter approach is the most attractive small molecule controllable system but has limitations. Firstly, the choice of small molecule is difficult: the described systems use rapamycin as a proof-of-concept. However, this is an immunosuppressive drug and will inactivate CAR T-cells. Non-immunosuppressive version of rapamycin have been described [91-93], but these agents have never been given to humans and need to be developed as pharmaceutical agents which is burdensome. Other suggests small molecules such as Gibberellin have never been used as drugs. Furthermore, volume of distribution problems are also present. Finally, with this system the patient needs to stay on the small molecule drug or the CAR will not work.

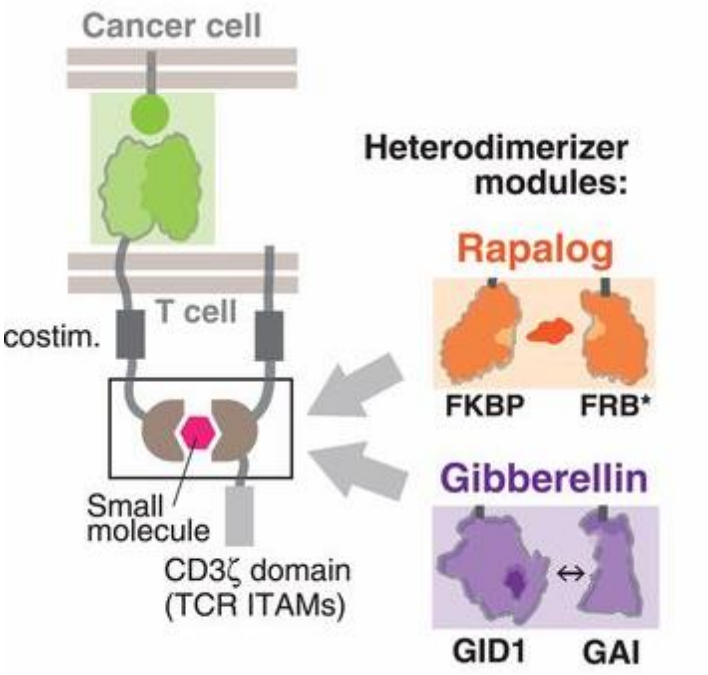

Figure 4. Tunable CAR system. The CAR is split into two: an antigen recognition component and a signalling component. In the presence of a small molecule (e.g., Rapalog or Gibberellin), the two components associate and the CAR signals the presence of cognate antigens. In the absence of the small molecule, the receptor stops signalling [89].

1.6 A Tunable CAR based on small molecule disruption of protein-protein interaction

Here, a CAR is directly inhibited by administration of a small molecule. A split synthetic receptor system is used to separate the antigen-recognition and signalling components into distinct polypeptides appended to heterodimerizing domains to produce an inducible system, where the addition of small molecule inhibits the system. In the absence of small molecule, these two components heterodimerize to assemble a functioning receptor complex. The main aim for this approach is to find a configuration that would strongly impair the CAR activity when in the presence of the small molecule but still allow for strong antigen-induced signalling, comparable to that achieved by the conventional single-component receptor, when the two components are assembled.

1.7 Tetracycline and Tetracycline analogues as small molecules to control CAR therapy

An ideal small molecule for application in such a system would have excellent tissue penetration, low serum protein binding and penetrate the blood-brain barrier well. In addition, the small molecule should have little side-effects and be well tolerated. Tetracycline and analogues doxycycline and minocycline fulfil these criteria well: they are small hydrophobic molecules with excellent tissue penetration. They are used to treat Central Nervous System (CNS) infections so are well known to cross the blood-brain barrier. They are often given over long periods to treat chronic infections and are well tolerated with few pharmacological effects other than their microbiological activity [94-100].

1.8 The TiP system

The Tet operon is a very well understood bacterial operon which has been adapted for use in mammalian cells. Briefly, the Tet repressor (TetR) binds tetracycline as a homodimer, undergoes a conformational change which then modulates DNA binding of the TetR molecules. In 2005, Klotzsche et al. described a phage-display derived peptide which activated the Tet repressor (TetR) [101]. This protein (TetR interacting peptide, or TiP) appeared to have a binding site overlapping but not identical with the tetracycline binding site. Expression of this peptide, even as a fusion with a larger protein, could act as tetracycline to activate TetR. The structure of TiP binding TetR was elucidated crystallographically by others (Figure 5) [102]. We predicted that although TiP bound to the same part of the molecule as tetracycline, Tetracycline would bind with a much higher affinity than TiP and hence rapidly displace TiP. We were not concerned with the DNA binding properties of TetR in this case, only the ability of a protein fused to TiP to heterodimerize to TetR and then to be displaced upon its binding.

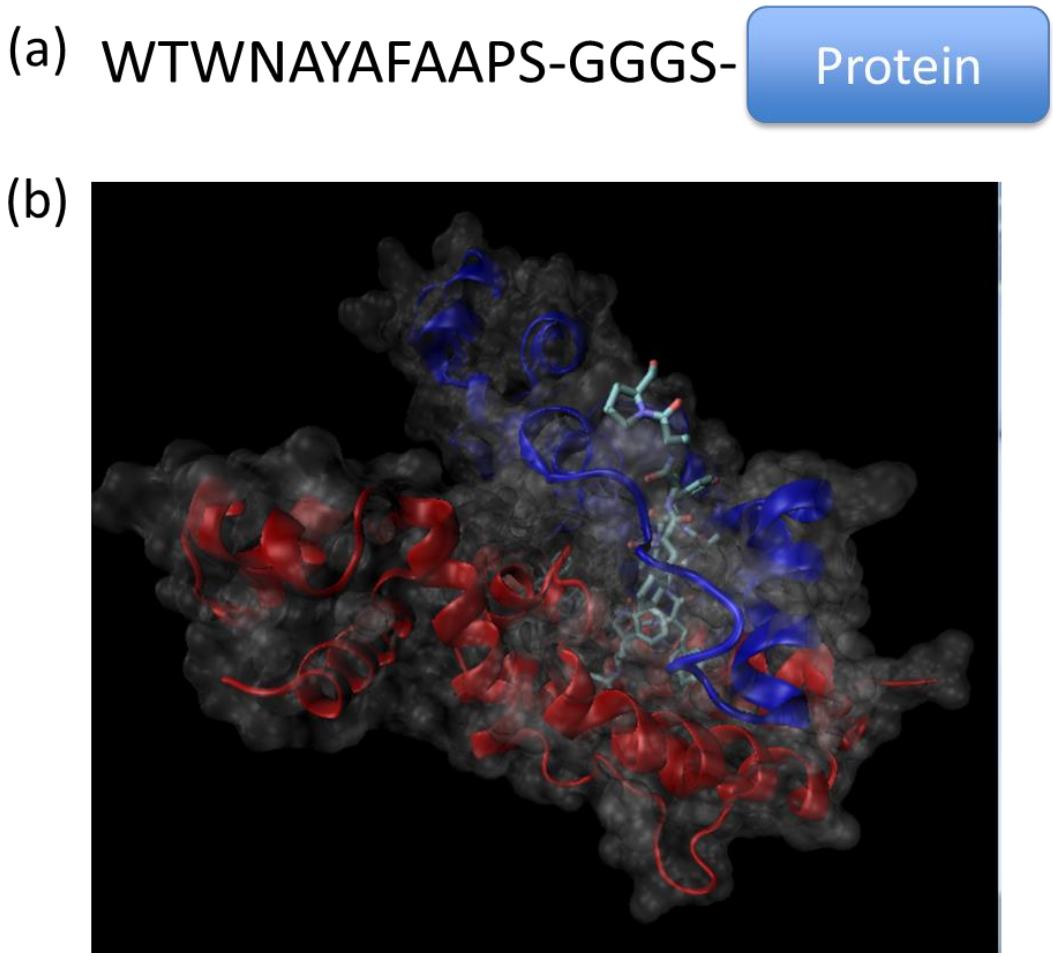

Figure 5. Structures of TetR and TiP. (a) Sequence of TiP attached at the amino-terminus of an arbitrary protein; (b) Crystallography derived structure of TiP interacting with TetR (from PDB 2NS8 and Luckner et al.) [102]. TiP can be seen engaged deep within the TetR homodimer associating with many residues tetracycline associates with.

1.9 Basic concept of tetCAR

The basic concept of the tetCAR is illustrated in Figure 6. Here, the CAR is split into two: an antigen recognition component and a signalling component. The former comprises of an antigen recognizing ectodomain, a transmembrane domain and an intracellular TetR domain. The latter, T-cell signalling domains fused with TiP. In the absence of tetracycline, the two components associate and the CAR signals the presence of cognate antigens (Figure 6a). In the presence of tetracycline, TiP is displaced and the receptor immediately stops signalling (Figure 6b). In summary, the addition of small molecule inhibits the system.

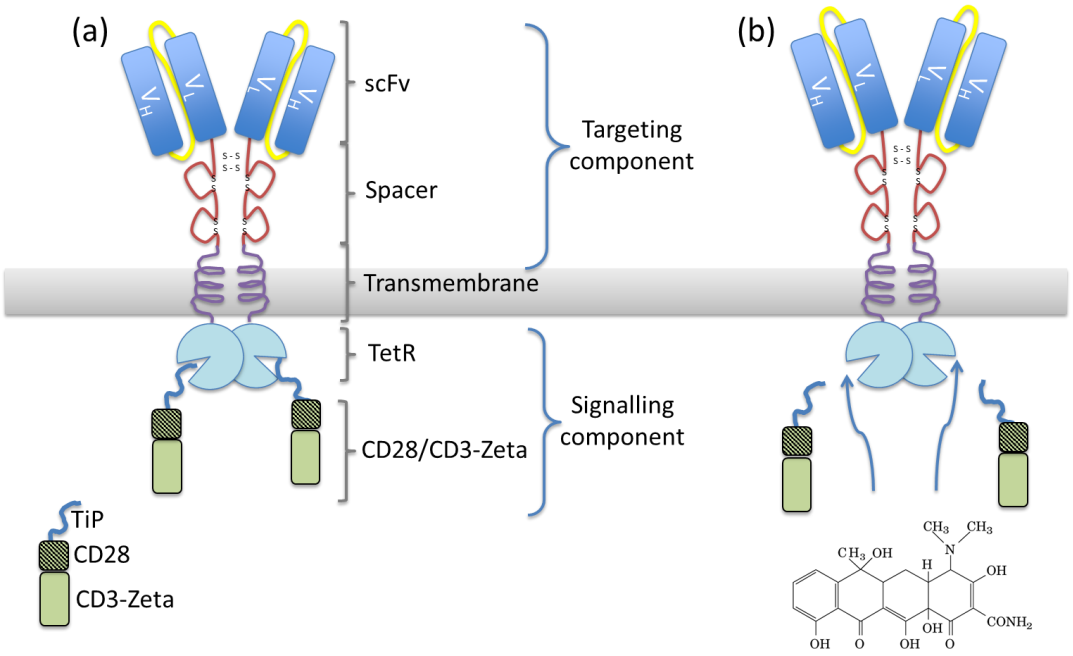

Figure 6. Basic concept of the tetCAR. (a) A membrane spanning receptor component comprises of an extracellular antigen-binding domain, a transmembrane domain and a carefully selected intracellular linker to TetR. A separate molecule: the signalling component comprises of an intracellular protein which is generated by fusion of TiP to one or several T-cell signalling domains. In the absence of tetracycline or tetracycline analogues, the receptor and the signalling components interact and in the presence of cognate antigen the system signals. (b) In the presence of tetracycline or tetracycline analogues, TiP is displaced from TetR and the receptor now can no longer transmit signals even in the presence of cognate antigen.

1.10 Hypothesis

Although TiP bound to the same part of the molecule as tetracycline, we hypothesised that tetracycline would bind with a much higher affinity than TiP and hence rapidly displace TiP. Therefore, we hypothesised that the tetCAR would allow for effective remote control of therapeutic T-cells through disruption of protein-protein interaction. We predicted that the tetCAR would enable complete, titratable and reversible switch off over T-cell activity.

1.11 Aims of this Thesis

This thesis details the work that I have undertaken to investigate the feasibility of using a Tet-Off signalling switch for the remote control of therapeutic CAR T-cells.

The specific aims of this PhD project are:

1. To prove the functionality of the system in terms of membrane assembly.
2. To prove the functionality of the system as a CAR.
3. To prove the effectiveness of the tetCAR in therapeutically relevant T-cells.
4. To develop a promising tetCAR construct and test *in vitro*.
5. To prove the effective tunable control of tetCAR T-cell activity via the administration of tetracycline.
6. To prove the effective reversible control of tetCAR T-cell activity.

CHAPTER 2

MATERIALS AND METHODS

2.1 Molecular Biology

2.1.1 Construction of OFF-switch tetCARs

2.1.1.1 Splicing DNA by overlap extension PCR

The tetCAR constructs were generated via High-Fidelity Phusion PCR (New England Biolabs, USA) of pre-existing DNA fragments in the lab plasmid archive, with constructed forward and reverse primers (Integrated DNA Technologies, Belgium) bridging between different overlapping oligonucleotides. Phusion PCR allows the fusion of several pieces of DNA on certain junctions that are complementary. This occurs in two PCR reactions as depicted in the below schematic Figure 7, whereby in a primary PCR reaction (Table 3) sequences of DNA are amplified with overlapping base pairs at their extremities. Subsequently, in a secondary Phusion PCR reaction (Table 4) complementary sequences overlap and by amplification result in fusion of the two sequences of DNA.

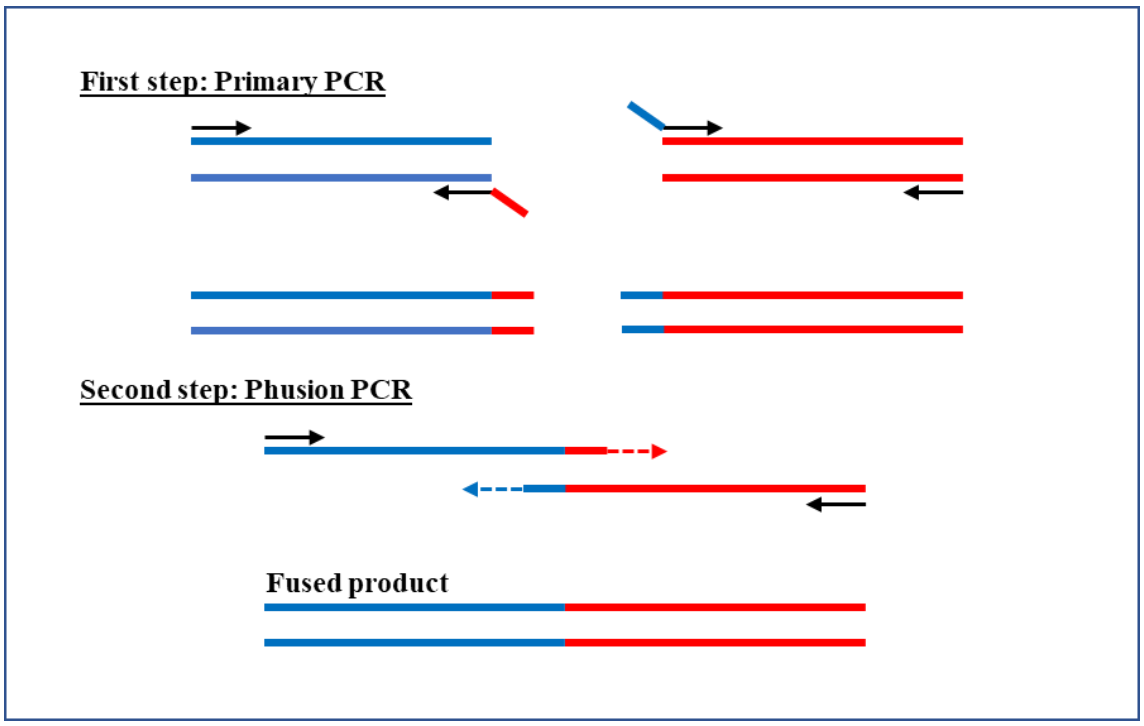

Figure 7. Schematic diagram of Phusion PCR reactions

Reagents	Volume (µL)
5x HF Buffer	10
dNTPs (25µM)	1
Forward primer (25µM)	1
Reverse primer (25µM)	1
Template (200 ng/µL)	1
Phusion Polymerase	0.5
Nuclease-Free Water	35.5

Table 3. Primary PCR reaction

Reagents	Volume (µL)
5x HF Buffer	10
dNTPs (25µM)	1
Forward primer (25µM)	1
Reverse primer (25µM)	1
Template 1	1
Template 2	1
Phusion Polymerase	0.5
Nuclease-Free Water	34.5

Table 4. Secondary phusion PCR reaction

2.1.1.2 Restriction endonuclease digestion

The production of the various tetCAR constructs relied heavily on DNA digestion with restriction enzymes. Restriction digests were performed according to manufacturer's instructions (NEB) to establish cloning fragments of DNA with 'sticky' ends to facilitate DNA ligation. For inserts derived by PCR, the entire sample was digested.

2.1.1.3 Separation and extraction of DNA fragments using agarose gel electrophoresis

The DNA fragments resulting from the restriction digest were separated using agarose gel electrophoresis. 1% agarose gels were prepared and electrophoresed at 110V in 1x TBE buffer until appropriate separation was achieved. Following separation of DNA fragments, bands were visualised using a dark reader blue light box to prevent UV-mediated mutagenesis and excised from the gel with a clean scalpel. The required constructs were isolated and purified from the gel using the QIAquick Gel Extraction Kit (QIAGEN, Germany). Purification was performed according to manufacturer's instructions.

2.1.1.4 Fragment insertion using DNA ligation

New fragments of DNA were inserted into a linearised vector backbone using a ligation reaction. The fragments were inserted into an SFG retroviral vector between the *AgeI* and *MluI* restriction sites. Plasmid maps of the various tetCARs are seen in Figure 8. Ligation was performed using Quick Ligase (New England Biolabs, USA) according to the manufacturer's instructions. Following 5 minutes at room temperature, 2μL of the resulting ligation mixture was used for bacterial transformation of high efficiency C2987 (New England Biolabs, USA) chemically competent *E. coli* bacteria.

2.1.2 Bacterial transformation

Plasmids were amplified by selective growth of transformed chemically competent *E. coli* bacteria. The transformation was carried out as follows: 2μL of ligation mixture was added to the bacteria and incubated at 4°C for 30 minutes. Bacteria were transiently heat-shocked by incubation at 42°C for 35 seconds, followed by incubation at 4°C for 5 minutes. Bacteria were transferred to SOC medium (New England Biolabs, USA) and allowed to recover for 30 minutes on a shaking incubator at 37°C, 220rpm. Subsequently, transformed bacteria were spread on an agar plate infused with appropriate antibiotic and incubated at 37°C overnight.

2.1.3 Isolation of plasmid DNA from *E. coli*

DNA was retrieved from the competent *E. coli* through the rapid alkaline lysis procedure (QIAprep Spin Miniprep Kit, QIAGEN, Germany) reported by Birnboim and Doly [103]. DNA isolation was performed according to manufacturer's instructions. Presence of the tetCAR sequence was verified by means of restriction digestion analysis and sequencing (Beckman Coulter, USA). Bacterial clones that proved to have the correct plasmid sequence were further grown in Terrific Broth (TB) media to generate larger amounts of the plasmid. DNA was retrieved using NucleoBond Xtra Midi kit (MACHEREY-NAGEL, Germany). DNA isolation was performed according to manufacturer's instructions. Midiprep DNA was verified by multiple separate restriction digests cutting in the vector backbone and transgene insert.

2.1.4 Measurement of DNA concentration

The concentration of DNA was determined by measuring absorbance at wavelength 260nm. This was achieved using a NanoDrop Spectrophotometer (Thermo SCIENTIFIC, USA).

(a) **First-generation CD33-targeting tetCAR:**

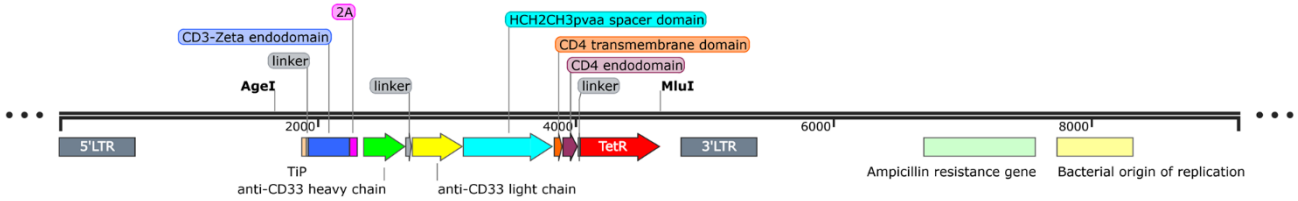

(b) **First-generation CD33-targeting Defective tetCAR:**

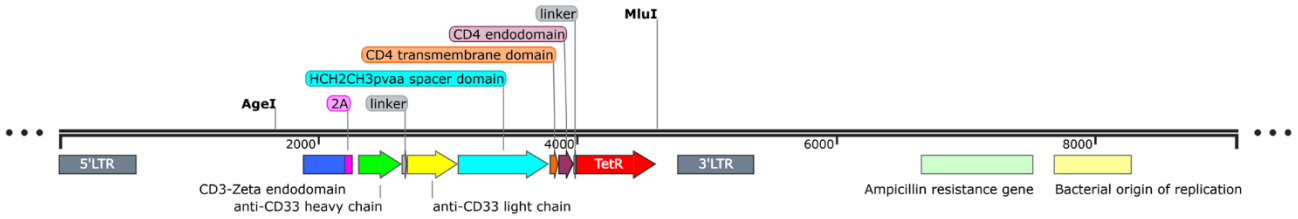

(c) **First-generation CD19-targeting tetCAR:**

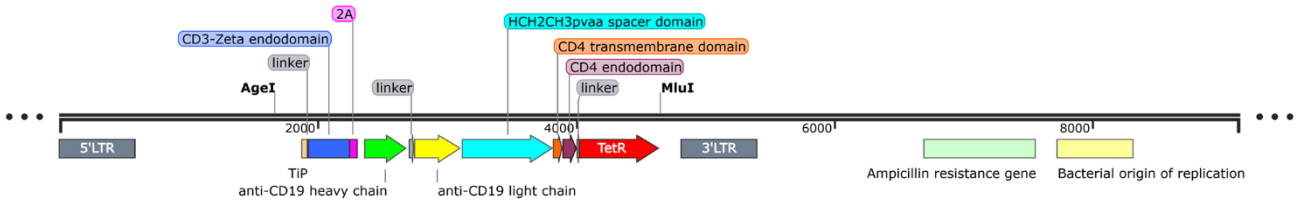

(d) **First-generation CD19-targeting Defective tetCAR:**

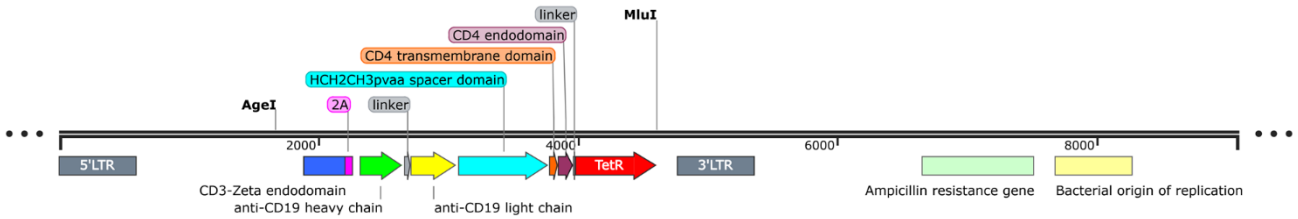

(e) **Second-generation CD19-targeting tetCAR (with 'split' endodomain):**

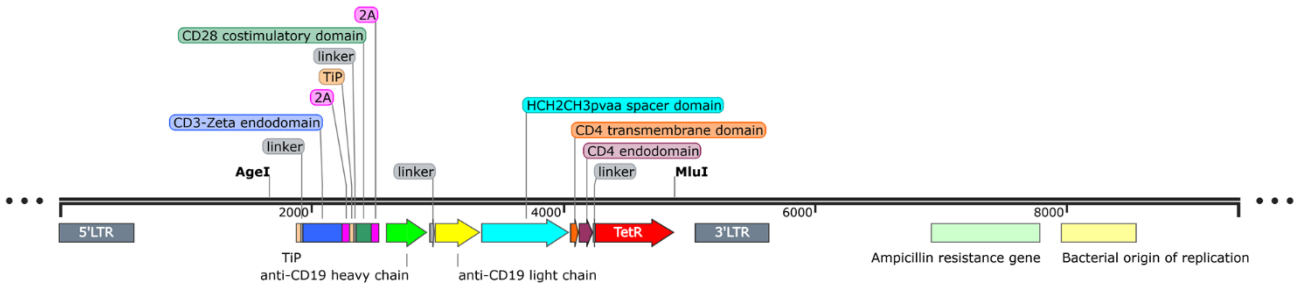

(f) **Second-generation CD19-targeting Defective tetCAR (with 'split' endodomain):**

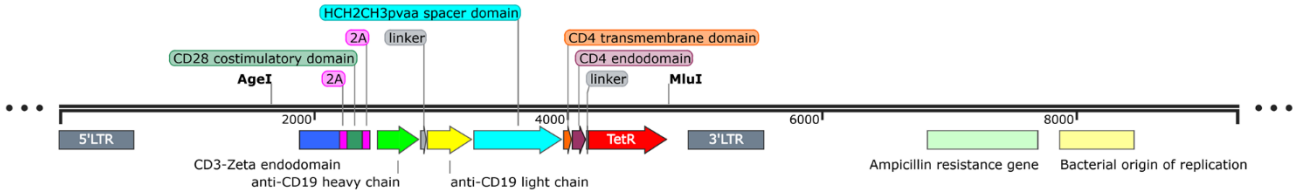

(g) **Third-generation CD19-targeting tetCAR (with 'split' endodomain):**

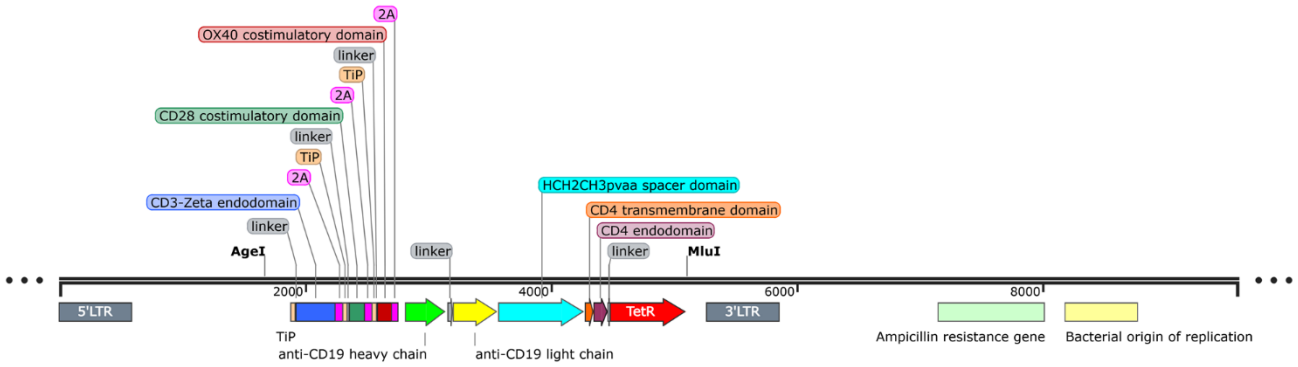

(h) **Third-generation CD19-targeting Defective tetCAR (with 'split' endodomain):**

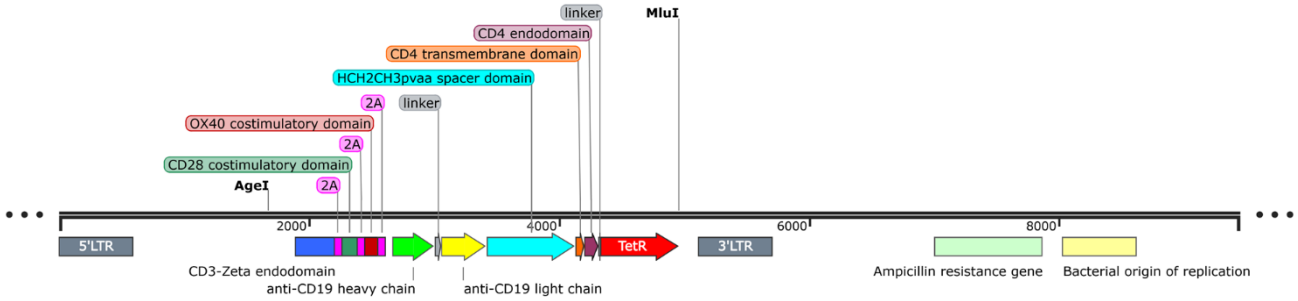

(i) **Second-generation CD19-targeting tetCAR (with 'non-split' endodomain):**

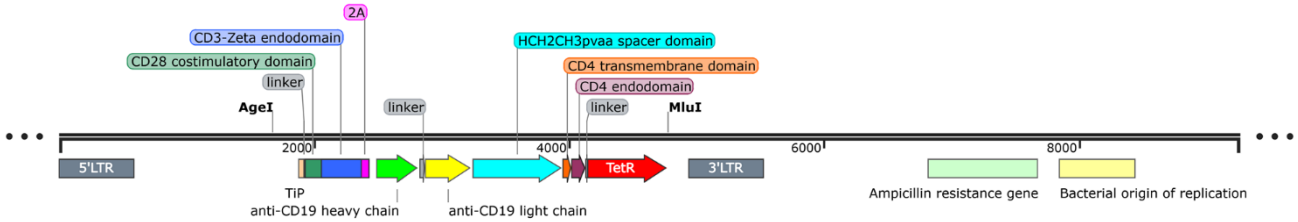

(j) **Second-generation CD19-targeting Defective tetCAR (with 'non-split' endodomain):**

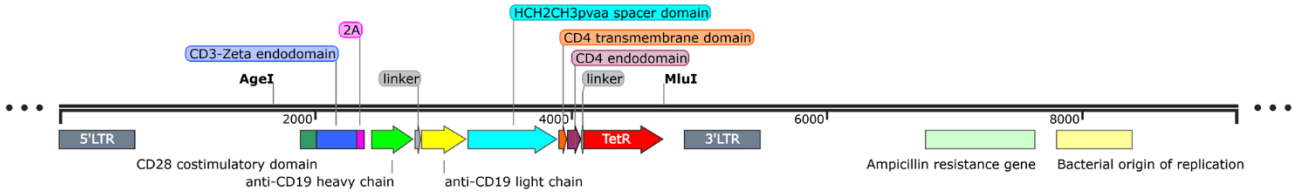

(k) **Second-generation CD19-targeting tetCAR (with CD8TM):**

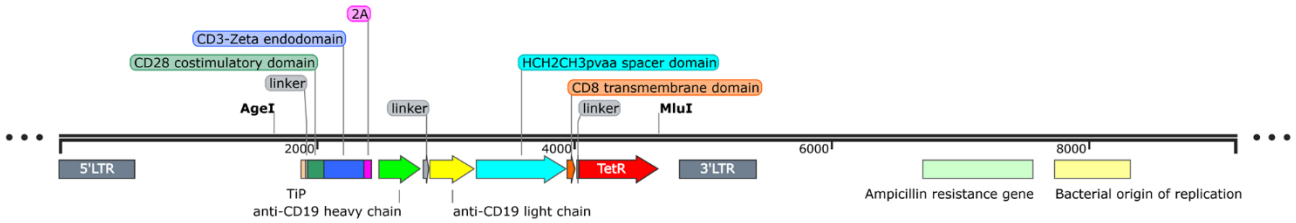

(l) **Second-generation CD19-targeting tetCAR (with CD28TM):**

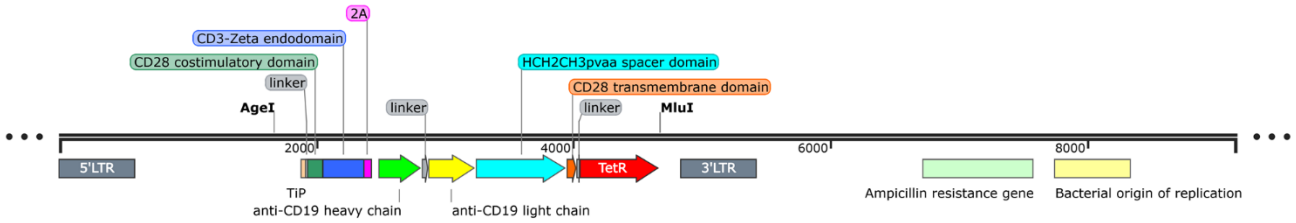

(m) **Second-generation CD19-targeting tetCAR (with CD8STK CD8TM):**

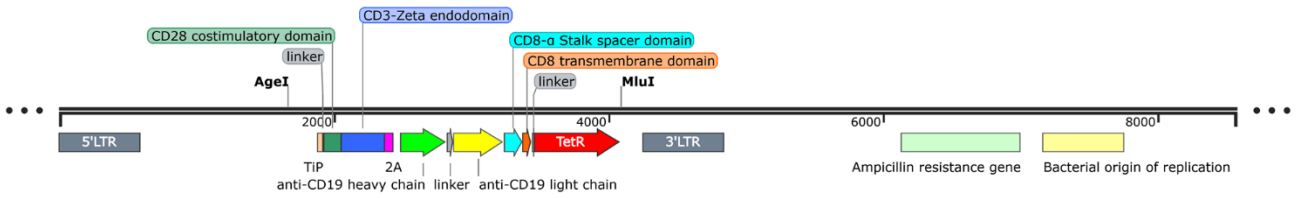

(n) **Second-generation CD19-targeting tetCAR (with CD8STK CD28TM):**

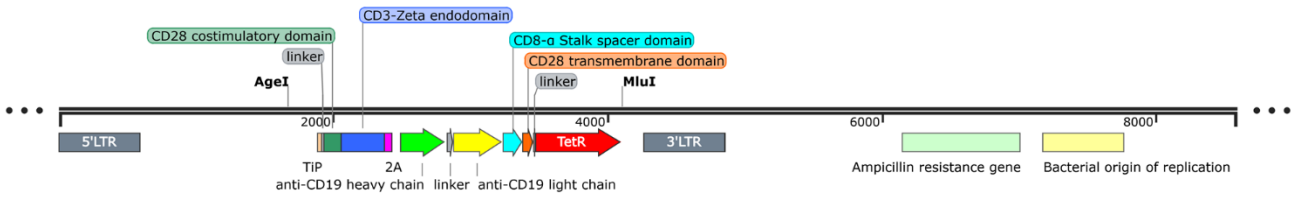

(o) **Third-generation CD19-targeting tetCAR (with CD8TM 4-1BB):**

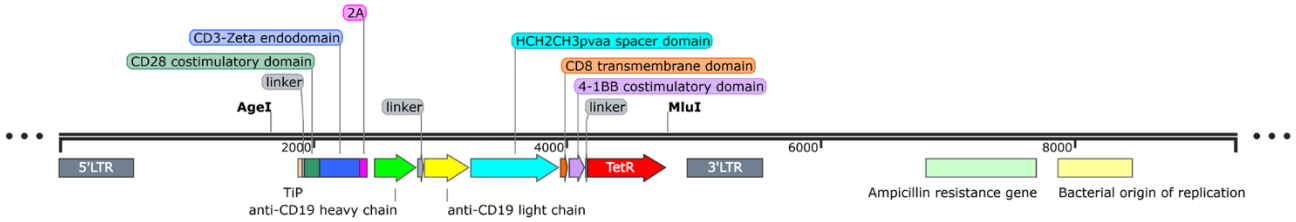

(p) **Third-generation CD19-targeting tetCAR (with CD28TM 4-1BB):**

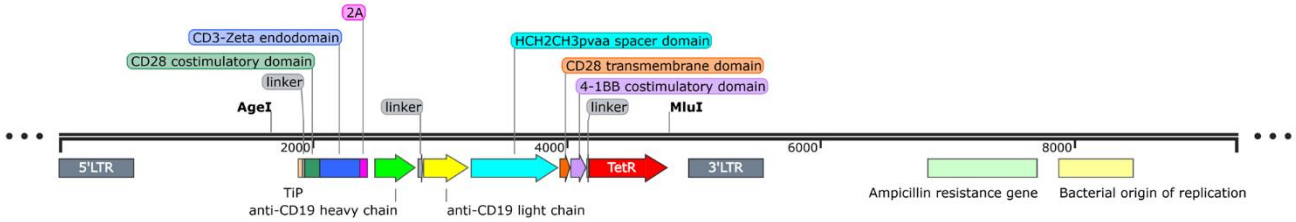

Figure 8. Plasmid maps of the various tetCARs used during this research

2.2 Cell Culture

2.2.1 Primary cells and cell lines

Human and murine T-cells (BW5147 murine cell line) were cultured in RPMI-1640 (Lonza, BE12-167F/12) with 1% Glutamax (Gibco, 35050-061), and 10% Foetal Calf Serum (FCS) (Biosera, FB-1001/500). Primary human T-cells were supplemented with 100 U/mL IL-2. Fresh media and cytokine was supplied two/three times a week.

The cell line of choice for transfection experiments was 293T, which can be efficiently transfected. 293T is an embryonic kidney cell line derived from humans. Cells were cultured in IMDM (Lonza, 12-726F) with 1% Glutamax (Gibco, 35050-061), and 10% FCS (Biosera, FB-1001/500).

The SupT1, Daudi, Nalm6 and Raji target cell lines are all suspension, and were cultured in RPMI-1640 (Lonza, BE12-167F/12), supplemented with 1% Glutamax (Gibco, 35050-061), and 10% FCS (Biosera, FB-1001/500).

2.2.2 Primary cell culture

2.2.2.1 Isolation of Human Peripheral Blood Mononuclear Cells (PBMCs)

Blood samples from healthy donors were obtained on a weekly basis to isolate Human Peripheral Blood Mononuclear Cells (PBMCs). To avoid coagulation, the blood sample was collected into a syringe already containing 500μL of Ethylenediaminetetraacetic acid disodium salt solution (Sigma-Aldrich, USA). PBMCs were isolated based on a ficoll gradient centrifugation method. The blood sample was layered on Ficoll-Paque Premium (GE Healthcare Life Sciences, USA) and centrifuged for 40 minutes at 750g with zero brakes and acceleration to avoid the blood from mixing with the Ficoll-Paque due to its toxic effect over cells. Therefore, it is very crucial to set the acceleration and the brakes to zero. After the initial centrifugation step, the layer formed in the middle, consisting of lymphocytes, was extracted, and transferred to a sterile falcon followed by washing twice using complete RPMI.

2.2.2.2 PBMC stimulation and culture

Finally, isolated PBMCs were counted by trypan blue exclusion at a 1:10 ratio. $1x10^6$ cells/mL of fresh PBMCs, supplemented with 5 μg/mL phytohaemagglutinin (PHA) (Sigma-Aldrich, USA), were seeded into a 24-well tissue culture-treated plate in a total of 2mL per well. After 24 hours, cells were stimulated with 100 U/mL IL-2 (GenScript, USA).

2.2.3 Retroviral work

2.2.3.1 Triple Transfection of 293T cells for Retroviral Production

Generation of retroviral supernatant was achieved by transfecting 293T cells with three plasmids. The essential plasmids for the generation particles are the RD114 plasmid (retroviral pseudotyping with RD114 envelope), Gagpol plasmid (pEQ-Pam3-Epeqpam-env Moloney Murine Leukaemia Virus gagpol expression plasmid), and the SFG retroviral plasmid. The SFG retroviral plasmid, which includes the LTR and the packaging signal, also carries the transgene. The GeneJuice was mixed with the medium and incubated at room temperature for 5 minutes. Then the plasmids were introduced in the mixture followed by 15 minutes incubation before added on 293T cells.

Reagents	**10cm plate**
Plain media	470μL
GeneJuice	30μL
Gagpol	4.7μg
Envelope RD114	3.1μg
SFG plasmid	4.7μg

Table 5. Triple Transfection reaction mixture

2.2.3.2 Retronectin coating preparation of tissue culture plates

To introduce the CAR constructs into T-cells, they were subjected to retroviral-mediated transduction (48 hours after isolation). This ensured integration of the inserted coding DNA into the host T-cell genome, thereby permitting stable CAR expression.
In order to dramatically improve T-cell transduction rates, 24-well non-tissue culture-treated plates were coated with 4μg retronectin (Takara, Japan) the day before. Retronectin is a fragment of the extracellular matrix protein fibronectin that binds the target T-cell through a CS-1 domain and a cell-binding domain (CBD), which interact with the VLA-4 and VLA-5 integrin receptors respectively. Attachment of the virus to the heparin binding domain present in retronectin between the CS-1 and CBD causes co-localisation of the target cell and the virus, thus greatly improving gene transfer efficiency [104, 105].

2.2.3.3 Retroviral-mediated T-cell Transduction

On the day of transduction, the retronectin was aspirated of the wells, replaced with 250μL of viral supernatant and incubated for 30 minutes at room temperature (RT). In the meantime, the cells were harvested and resuspended at $0.5x10^6$ cells/mL. The 250μL of viral supernatant were aspirated. At the end, it was added 0.5mL of cells, 1.5mL of fresh supernatant and 100 U/mL of IL-2 per well. The plate was then centrifuged for 40 minutes at 1000g (RT).

2.3 *In Vitro* Assays

2.3.1 CD56 Depletion

To exclude residual Natural Killer (NK) cells and potential lymphokine activated killer cells prior to functional assays, human PBMCs were subjected to negative selection to eliminate CD56-expressing cells. This was achieved by labelling the cells with CD56 MicroBeads (Miltenyi, Germany). NK cells with surface-bound beads were removed using QuadroMACS Separator (Miltenyi, Germany) and the flow-through containing uncoupled cells was collected. LD Columns were used (Miltenyi, Germany). CD56 Depletion was performed according to manufacturer's instructions.

2.3.2 Co-culture assays

2.3.2.1 Preparation of co-culture

CAR-transduced T-cells were co-cultured with target cells at 1:1 and 4:1 T-cell:target cell ratios in a U-bottom 96 well cell culture plate (Sigma-Aldrich, USA) with varying concentrations of the small molecule, ranging from 0 to 1600nM. Tetracycline hydrochloride (Sigma-Aldrich, USA), Doxycycline hyclate (Sigma-Aldrich, USA) and Minocycline hydrochloride (Sigma-Aldrich, USA) were used as small molecules. The SupT1, Daudi, Nalm6 and Raji target cell lines were used. Human IL-2 (GenScript, USA) was added to a final concentration of 100 U/mL per well. Negative and positive controls were included in the co-culture plate.

2.3.2.2 Detection of cytokine release using Enzyme-Linked Immunosorbent Assay (ELISA)

After overnight incubation, supernatants were collected and analysed with BioLegend Human interferon-gamma (IFN-γ) ELISA MAX Deluxe kit (BioLegend, USA). Measuring the release of specific cytokines by CAR-transduced T-cells during co-

culture with targets provided a quantitative technique for investigating T-cell activation. Cytokine release was detected using a sandwich Enzyme-Linked Immunosorbent Assay (ELISA), tailored to the cytokine of interest. IFN-γ ELISA was performed according to manufacturer's instructions.

2.3.2.3 Flow cytometry-based cell-killing assay

A major purpose of CARs is to redirect primary human T-cell cytotoxicity selectively towards target cells expressing antigens of interest. One method that can be used to demonstrate target cell destruction is to measure target cell viability following co-culture with CAR-transduced T-cells. This can be achieved by using a flow cytometry-based cell-killing assay. After incubation for a designated period of time, cells were stained and analysed by flow cytometry. The staining protocol is detailed below.

2.4 Flow Cytometry

Flow cytometry was an invaluable technique used to probe for protein expression at the cell surface. Determination of protein expression at the cell surface was important for showing the expression of the CAR by the T-cells and for investigating the levels of CD19 expression on target cells. Flow cytometry also enabled the screening of CAR-transduced T-cell cytotoxicity. Flow cytometry was performed using Becton Dickinson (BD) FACSVerse or BD LSRFortessa or Beckman Coulter CytoFLEX instruments.

2.4.1 General staining protocol

Usually $3x10^5$ cells were washed with PBS, stained with antibodies, then washed and resuspended in FACS buffer (1% FCS in PBS) and placed on ice pending analysis. Where multiple staining steps were required, samples were washed with PBS between individual staining steps. Isotype and/or non-transduced controls were included as required to establish an appropriate benchmark for comparison. All staining steps were performed at room temperature in the dark with 20-minute incubation per step unless indicated otherwise.

2.4.2 Staining protocol for verifying CAR expression on T-cells

CAR-transduced T-cells were washed with PBS and resuspended in the remaining volume. During the first staining, cells were incubated with sCD19-Rabbit IgG antibody for 20 minutes at room temperature. After repeating the wash, cells were incubated with anti-Rabbit IgG antibody, conjugated with Phycoerythrin (PE). At the end, the cells were resuspended in 500µL FACS buffer. The gating strategy is shown in Figure 9.

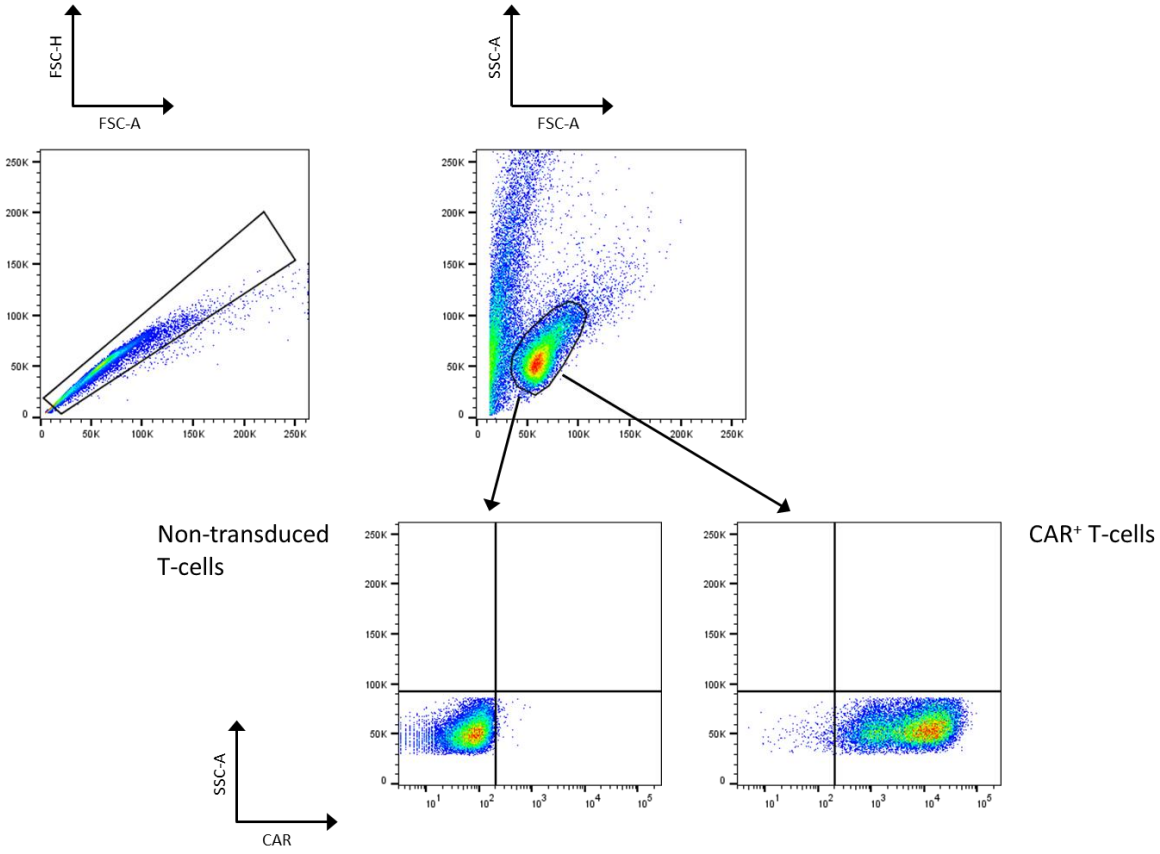

Figure 9. Gating strategy used to verify CAR expression on T-cells. Representative flow cytometry plots illustrating the gating strategy for assessment of CAR transduction efficiency of T-cells. Gating strategy used to identify singlet (top left), viable (top right) T-cell populations. CAR^+ T-cells were gated with reference to non-transduced control T-cells (bottom).

2.4.3 Staining protocol for quantifying CD19 expression on target cells

SupT1, Daudi, Nalm6 and Raji target cell lines were stained on the day before of co-culture, in order to validate their CD19 expression. Target cells were washed with PBS and resuspended in the remaining volume. During the staining, cells were incubated with anti-CD19 antibody conjugated with APC for 20 minutes at room temperature. At the end, the cells were resuspended in 500µL FACS buffer. The gating strategy is shown in Figure 10.

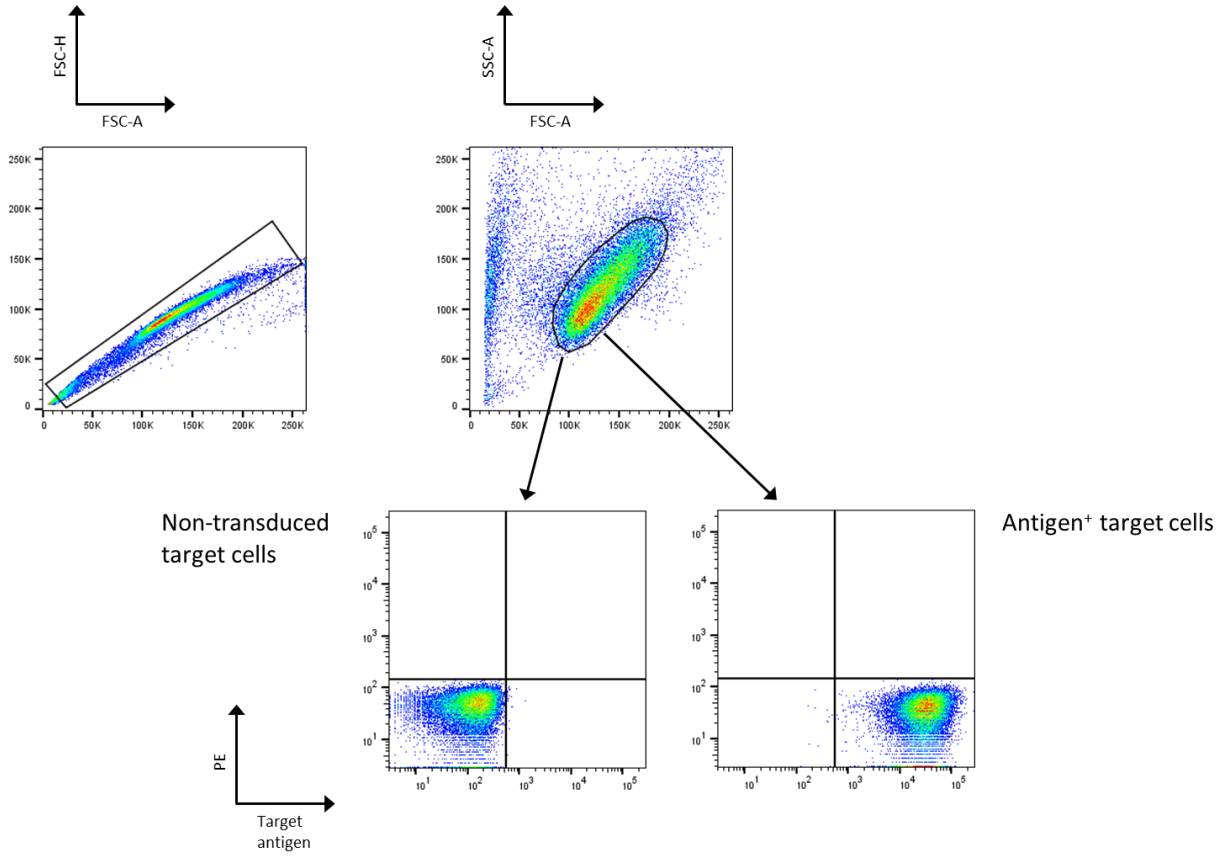

Figure 10. Gating strategy used to quantify antigen expression on target cells. Representative flow cytometry plots illustrating the gating strategy for assessment of the levels of antigen expression on target cell surface. Gating strategy used to identify singlet (top left), viable (top right) target cell populations. Antigen^{+} target cells were gated with reference to non-transduced control target cells (bottom).

2.4.4 Preparation of counting beads

Where it was necessary to enable cellular enumeration within a sample, or to enable effective comparison between samples, samples were supplemented with a pre-determined quantity of fluorescent 'counting beads' as an internal control. Beckman Coulter Flow-Check fluorospheres are supplied at $1x10^6$ beads/mL in an aqueous solution containing preservative surfactant. To prevent toxicity to cellular samples, beads were washed once with PBS prior to addition to samples. Following centrifugation (5 minutes at 400g), beads were resuspended in an equal volume of FACS buffer with 10μL of beads (10000) added to each sample.

2.4.5 Paraformaldehyde (PFA) fixation protocol

Where sample analysis was delayed overnight, following the final wash after antibody staining, samples were fixed by final resuspension into 0.4% PFA-PBS solution and stored at 4°C pending flow cytometry acquisition.

2.4.6 Flow cytometry-based cell-killing assay staining protocol

After incubation for a designated period of time, the plate was centrifuged for 5 minutes at 400g and the supernatants were collected for later quantification by ELISA. Staining of cells for viability and appropriate cell surface markers to allow discrimination between T-cells and target cells was then performed. During the first staining, cells were incubated with anti-CD3 antibody conjugated with PE/Cy7 for 20 minutes at room temperature. After the wash with PBS, cells were incubated with 7-AAD Viability Staining Solution for 10 minutes at room temperature and then analysed by flow cytometry. The gating strategy is shown in Figure 11.

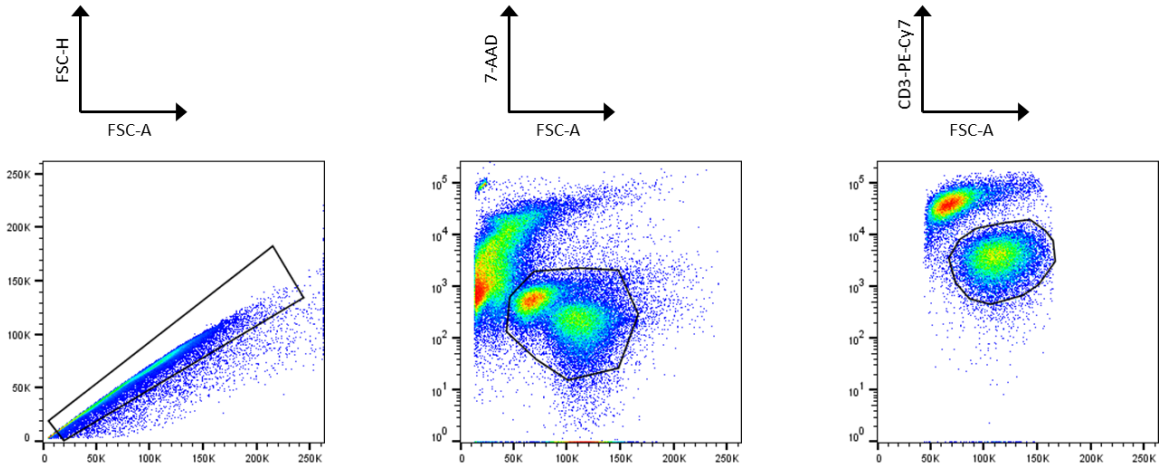

Figure 11. Gating strategy of flow cytometry-based cell-killing assay. Representative flow cytometry plots illustrating the gating strategy for assessment of surviving target cells. Gating strategy used to identify singlet (left), viable (middle) T-cell and target cell populations. Target cells were gated (right).

Antibodies	Supplier	Catalogue No
7-AAD Viability Staining Solution	BioLegend	420404
Flow-Check Fluorospheres	Beckman Coulter	6605359
PE/Cy7 anti-Human CD3 (Clone: SK7)	BioLegend	344816
PE anti-Rabbit IgG	Jackson ImmunoResearch	111-116-144
APC anti-Human CD19 (Clone: HIB19)	BioLegend	302212

Table 6. List of antibodies used. Volume of antibody used as per manufacturer recommendation.

2.5 Imaging assay of GFP tagged tetCAR constructs with Brightfield Microscopy

293T cells were seeded into a 12-well tissue culture-treated plate ($2.5x10^5$ cells per well). After 24 hours, GeneJuice was mixed with the medium and incubated at room temperature for 5 minutes. Then the constructed plasmid was introduced in the mixture followed by 15 minutes incubation before added on 293T cells. After incubating for two days, the cells were harvested and imaged under the brightfield microscope (Zeiss, Germany).

2.6 Statistical Analyses

To investigate for statistical significance, values were subjected to a two-way ANOVA, followed by a Tukey post-hoc test. A P-value < 0.05 was taken as significant. All data was analysed using GraphPad Prism software (version 7).

CHAPTER 3

INITIAL PROOF-OF-CONCEPT EXPERIMENTS

3.1 Test construct with eGFP to demonstrate function of the system

Prior to commencing investigations into the function and efficacy of the tetCAR, it was important to demonstrate that tetCAR works in terms of membrane assembly. Two constructs tagged with green fluorescent protein (GFP) were generated. The first construct consisted of a CAR with TetR as its endodomain and TiP fused to eGFP (Figure 12a). The second, control construct is identical except TiP is absent (Figure 12b). After successful construction, both CARs were transfected in 293T cells and tested in the absence or presence of tetracycline to observe the cell localization of the eGFP.

From the imaging assay, we observed a shift in the pattern of fluorescence with and without tetracycline. In the absence of tetracycline (Figure 12c), the TiP-eGFP CAR-expressing 293T cells presented a clear eGFP fluorescence at the cell membrane while the control CAR-expressing 293T cells showed a cytoplasmic eGFP fluorescence. In the case of TiP-eGFP CAR, this indicates that the two CAR components heterodimerized to assemble a complex. In the presence of tetracycline (Figure 12d), both constructs showed a cytoplasmic eGFP fluorescence. In the case of TiP-eGFP CAR, this suggests that tetracycline displaced TiP.

Taken together, these data show that without tetracycline such a system results in membrane localization of a TiP fusion protein, with the eGFP being displaced to the cytoplasm in the presence of tetracycline.

Figure 12

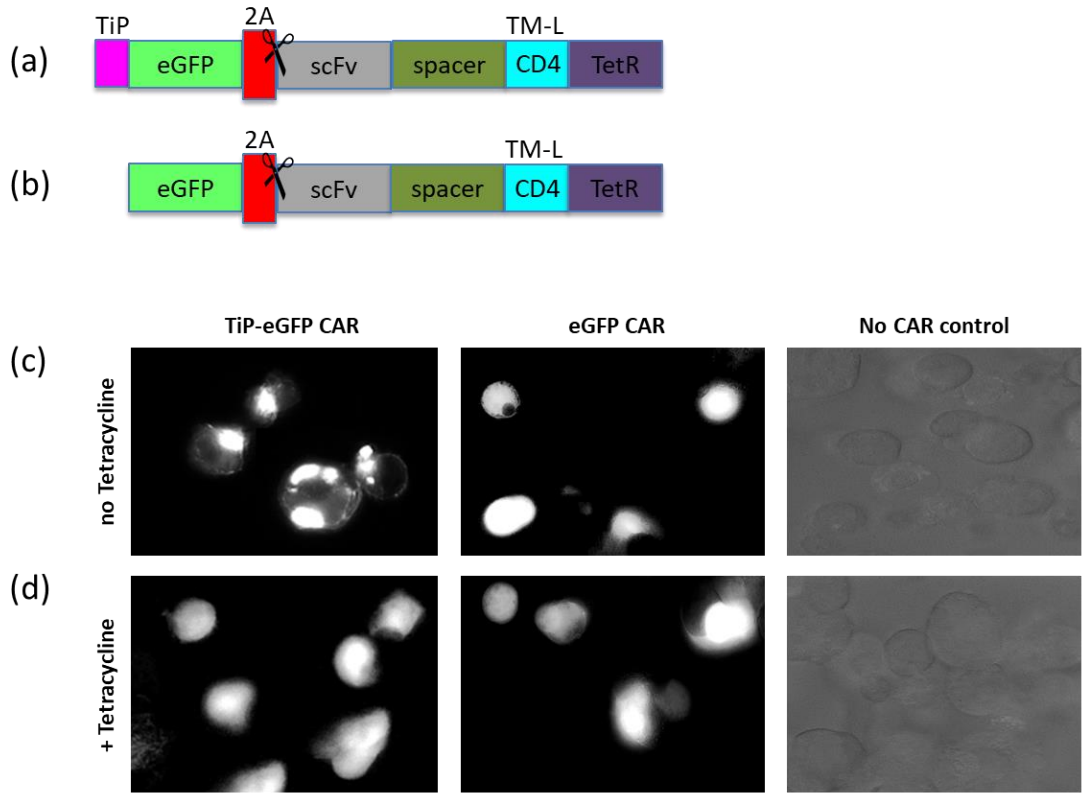

Figure 12. Test construct with eGFP to demonstrate function of the system. (a) A bicistronic construct expressed as a single transcript which self-cleaves at the 2A site (red) to yield: TiP (pink) fused to eGFP (light green); and a CAR with TetR (purple) as its endodomain. (b) A control was also constructed which was identical except TiP was absent. (c) Fluorescent micrograph of 293T cells expressing these constructs in the absence of tetracycline. The TiP-eGFP CAR-expressing 293T cells present a clear eGFP fluorescence at the cell membrane while the control CAR-expressing 293T cells show a cytoplasmic eGFP fluorescence; (d) Fluorescent micrograph of the same cells but now in the presence of tetracycline. Here, the eGFP is cytoplasmic. In the case of TiP-eGFP CAR, this shows that tetracycline has displaced TiP; This work was performed by Khai Kong.

3.2 Function of the initial tetCAR construct

Next, we tested similar constructs in CAR format. Two functional constructs were generated which are identical to the eGFP constructs except they contain CD3-Zeta endodomain instead of eGFP. The CAR is split into two: an antigen recognition component and a signalling component. The former comprises of a CD33 recognizing scFv, a spacer derived from the Fc domain of IgG1, a CD4 derived transmembrane and intracellular domain, and TetR. The latter, CD3-Zeta endodomain fused with TiP (Figure 13a). A control construct was also generated which is identical except TiP is absent from the signalling component (Figure 13b). After successful construction, both CARs were transfected in Human Embryonic Kidney (HEK) 293T cells along with gagpol and vesicular stomatitis virus-G (VSV-G) viral envelope coding plasmids to produce retrovirus. Surface expression of the tetCARs was initially assessed in the HEK 293T cell line following transient transfection. Both tetCARs and the conventional CAR were successfully detected at the cell surface using flow cytometry with an anti-human IgG antibody (Figure 14b).

After collecting the retrovirus supernatant (at 48h and 72h post transfection), BW5 murine T-cells were transduced. Transduction efficiency of the BW5 cells was analysed by flow cytometry (BW5 is a useful cell line for functional work as it released IL-2 upon activation). As shown in Figure 14c, the tetCAR could be detected at the cell surface, thus indicating that this construct was both expressed and trafficked correctly to the plasma membrane. Cell surface expression of the defective tetCAR and conventional CAR was also detected.

Prior to co-culture, a further important goal was to produce and validate a CD33 expressing target cell line. The SupT1 cells provide an elegant model system, as they do not naturally express any antigen. Consequently, the introduction of CD33 into these cells was required. The presence of CD33 at the target cell surface was confirmed using flow cytometry with an anti-human CD33 antibody (Figure 14d). With the ability to achieve expression of the tetCAR at the T-cell surface clearly confirmed, and the CD33 expression of SupT1 cells validated, it was possible to investigate whether this construct was capable of binding the required antigen. As interaction of the CAR with target

antigen was predicted to induce T-cell activation, the release of specific cytokines, such as interleukin-2 (IL-2) was used as a marker of CD33 antigen recognition.
In order to determine the response of tetCAR to antigen stimulation and also to tetracycline, BW5 murine T-cells expressing the tetCAR were co-cultured with wild-type SupT1 cells or SupT1 cells engineered to express CD33 at a 1:4 T-cell:target cell ratio in the absence of tetracycline or in the presence of increasing concentrations of tetracycline (Figure 14e). BW5 cells expressing the defective tetCAR (Figure 14f) and BW5 cells expressing the conventional CAR (Figure 14g) were also tested. After an overnight incubation, supernatant samples were removed and assayed for the presence of IL-2. Subsequent investigations into the release of IL-2 showed that tetracycline decreases murine T-cell IL-2 secretion and hence activation in a dose dependent manner.

The experiment was carried out using concentrations of tetracycline ranging from 0 to 1600 nM. In this experiment tetracycline was serially diluted at 1 in 2 ratio starting from 1600 nM. The conventional CAR, which was used as a positive control, led to consistent secretion of IL-2 by BW5 cells in all tetracycline concentrations. Low levels of IL-2 secretion were observed when the same CAR BW5 cell line was co-cultured with wild-type SupT1 cells (Figure 14g). As expected, no significant IL-2 secretion by defective tetCAR T-cells was detected on either SupT1 CD33 or SupT1 Non-Transduced (NT) cells (Figure 14f). In the tetracycline inducible CAR (also known as tetCAR), the amount of secreted IL-2 was found to decrease with increasing concentrations of tetracycline (Figure 14e). In the absence of tetracycline, IL-2 secretion was analogous to that seen with the positive control. In the presence of 25 nM tetracycline, a minimal concentration of secreted IL-2 was observed. From 50 nM to 1600 nM, no significant IL-2 secretion by tetCAR T-cells was detected on either SupT1 CD33 or SupT1 NT cells. PMA and ionomycin stimulated BW5 cells showed the highest levels of IL-2 secretion.

In summary, our results show a dose dependent reduction in IL-2 secretion with increasing tetracycline concentrations until 50 nM tetracycline, above which the tetCAR is completely switched off.

Figure 13

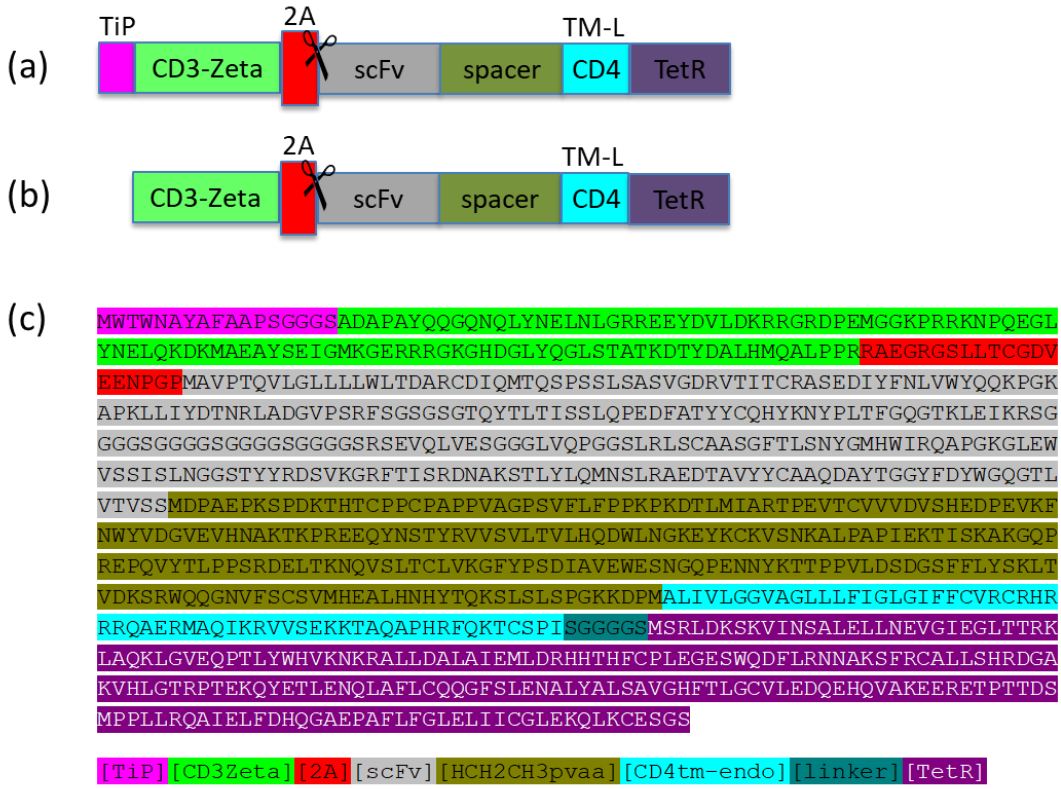

Figure 13. Initial tetCAR construct and control. (a) A bicistronic construct expressed as a single transcript which self-cleaves at the 2A site (red) to yield: a signalling component which comprises of TiP (pink) fused via a flexible linker to the endodomain of CD3-Zeta (light green); and a receptor component which comprises of a CD33 recognizing scFv (grey), a spacer derived from the Fc domain of IgG1 (dark green), a CD4 derived transmembrane and intracellular domain (blue), and TetR (purple). (b) A control was also constructed which was identical except TiP was absent from the signalling component. (c) Annotated amino acid sequence of the basic tetCAR is shown.

Figure 14

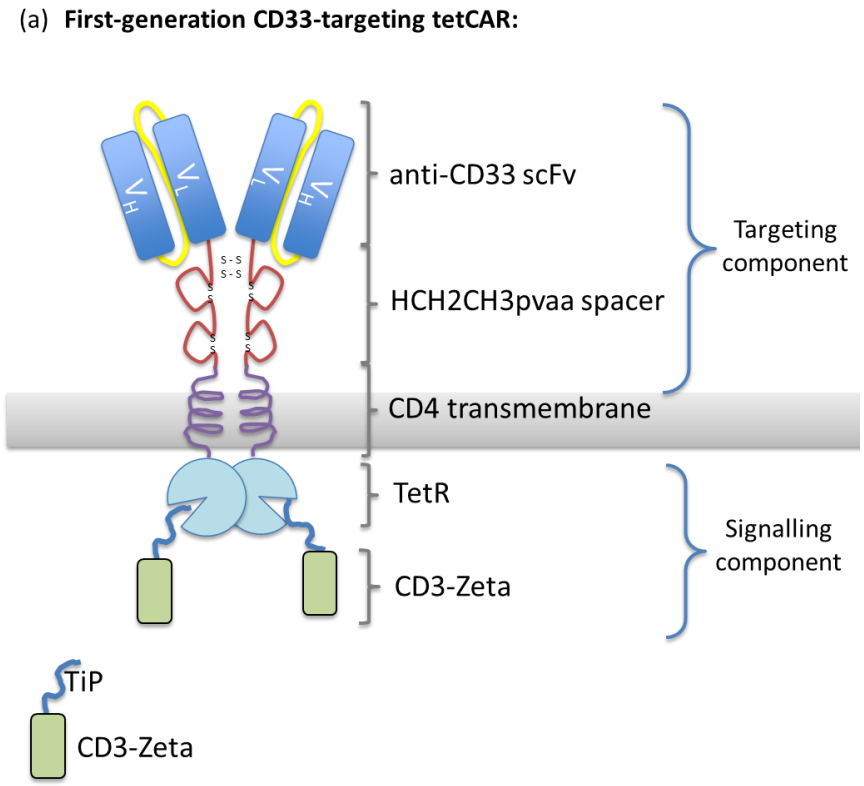

Figure 14. Function of the initial tetCAR construct in comparison with control. (a) Schematic diagram illustrating the initial tetCAR. A bicistronic construct expressed as a single transcript which self-cleaves at the 2A site to yield: a signalling component which comprises of TiP (dark blue) fused via a flexible linker to the endodomain of CD3-Zeta (light green); and a receptor component which comprises of a CD33 recognizing scFv (blue), a spacer derived from the Fc domain of IgG1 (red), a CD4 derived transmembrane and intracellular domain (purple), and TetR (light blue).

(b) **293T cells:**

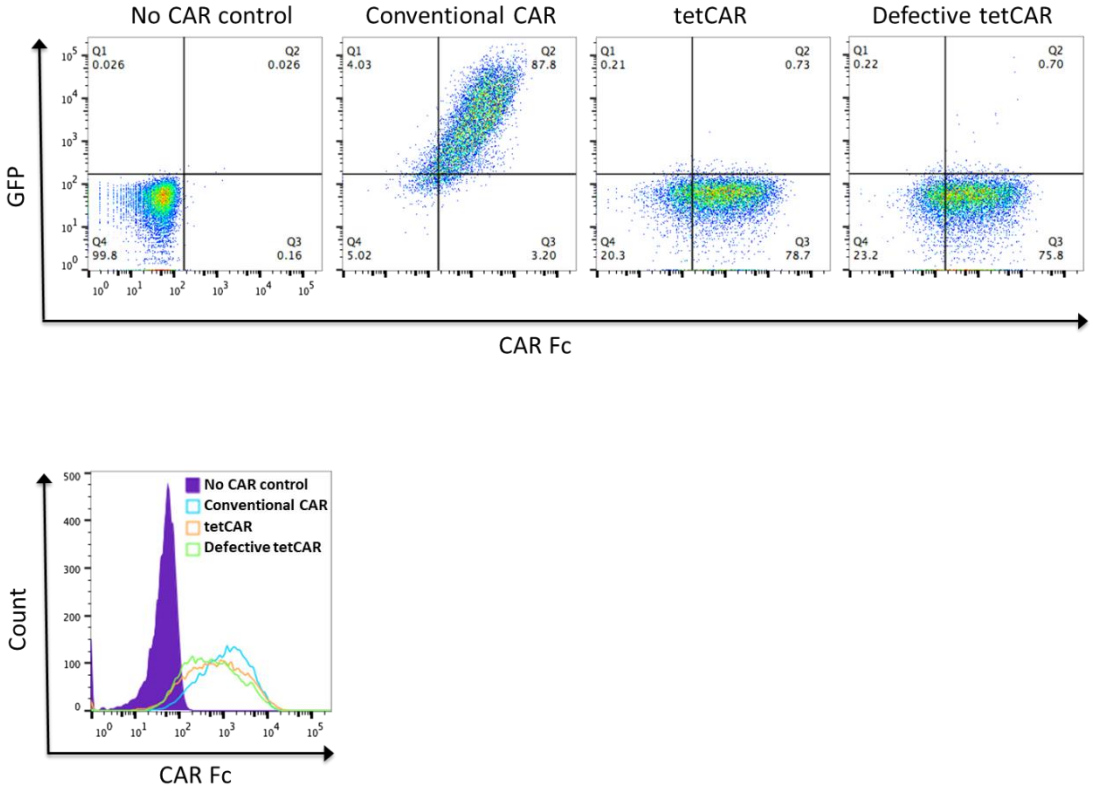

(b) Expression levels of CARs in Human Embryonic Kidney (HEK) 293T cells. Expression of the tetCAR at the surface of HEK 293T cells was compared with the expression of defective tetCAR (with absent TiP domain) and conventional CAR using flow cytometry. The CARs were detected with an anti-human IgG antibody. Staining was compared against Non-Transduced (NT) 293T cells stained using the same antibody.

(c) **BW5 murine T-cells:**

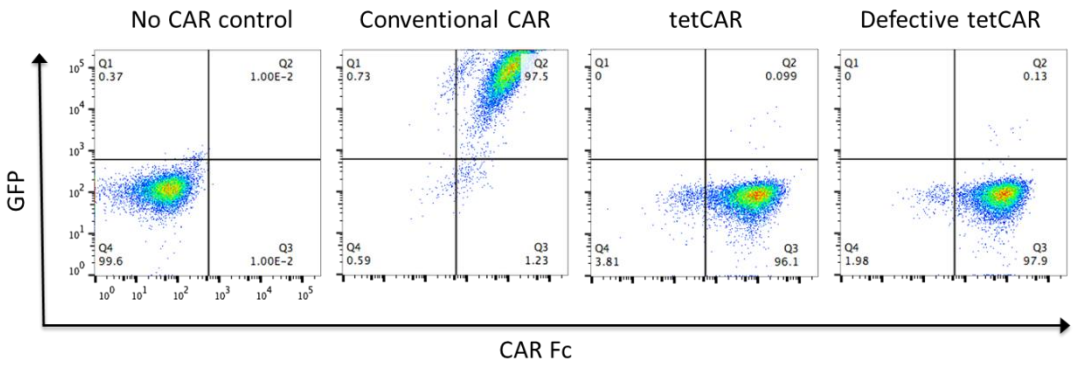

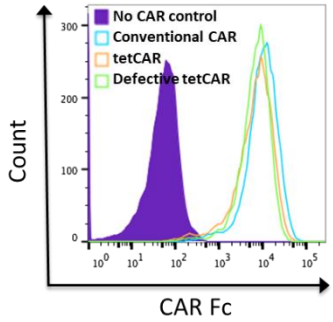

(c) Expression levels of CARs in BW5 murine T-cells. Cells engineered with retroviral constructs encoding CAR molecules were analysed by flow cytometry. Expression of the tetCAR at the surface of BW5 murine T-cells was compared with the expression of defective tetCAR and conventional CAR. The CARs were detected with an anti-human IgG antibody. Staining was compared against NT BW5 cells stained using the same antibody.

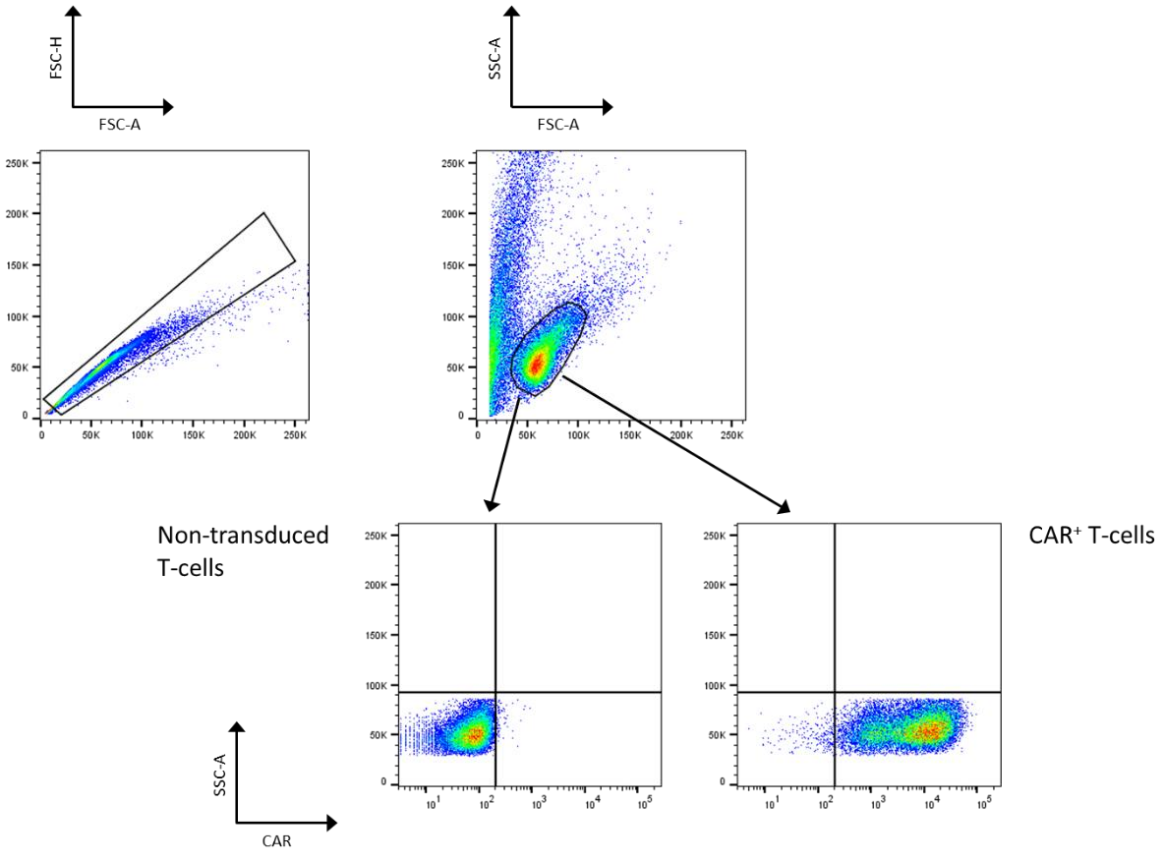

Gating strategy used to verify CAR expression on T-cells. Representative flow cytometry plots illustrating the gating strategy for assessment of CAR transduction efficiency of T-cells. Gating strategy used to identify singlet (top left), viable (top right) T-cell populations. CAR^+ T-cells were gated with reference to non-transduced control T-cells (bottom).

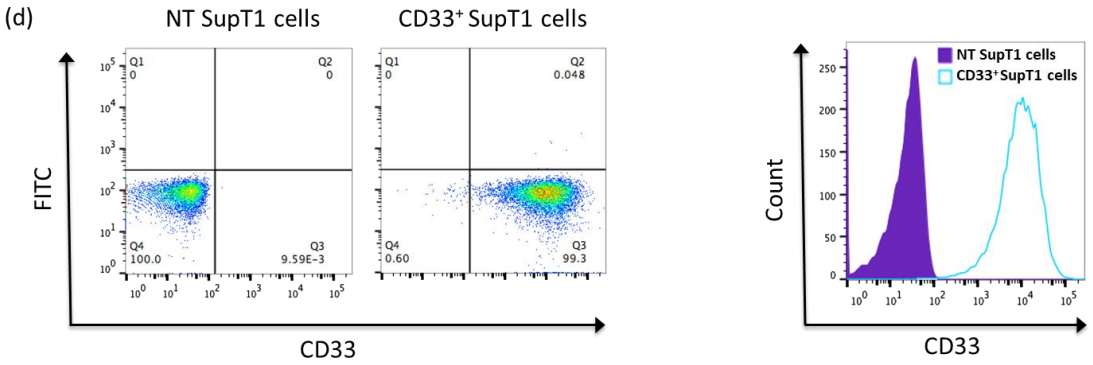

(d) Level of CD33 expression on target cell surface. SupT1 cells were used as target cells in co-culture assays. Non-transduced SupT1 were transduced to stably express CD33. The cells were investigated for the presence of CD33 using flow cytometry. The expression of CD33 was detected using an anti-human CD33 antibody. The level of CD33 expression was compared with that displayed by the NT SupT1 cells stained with the same antibody.

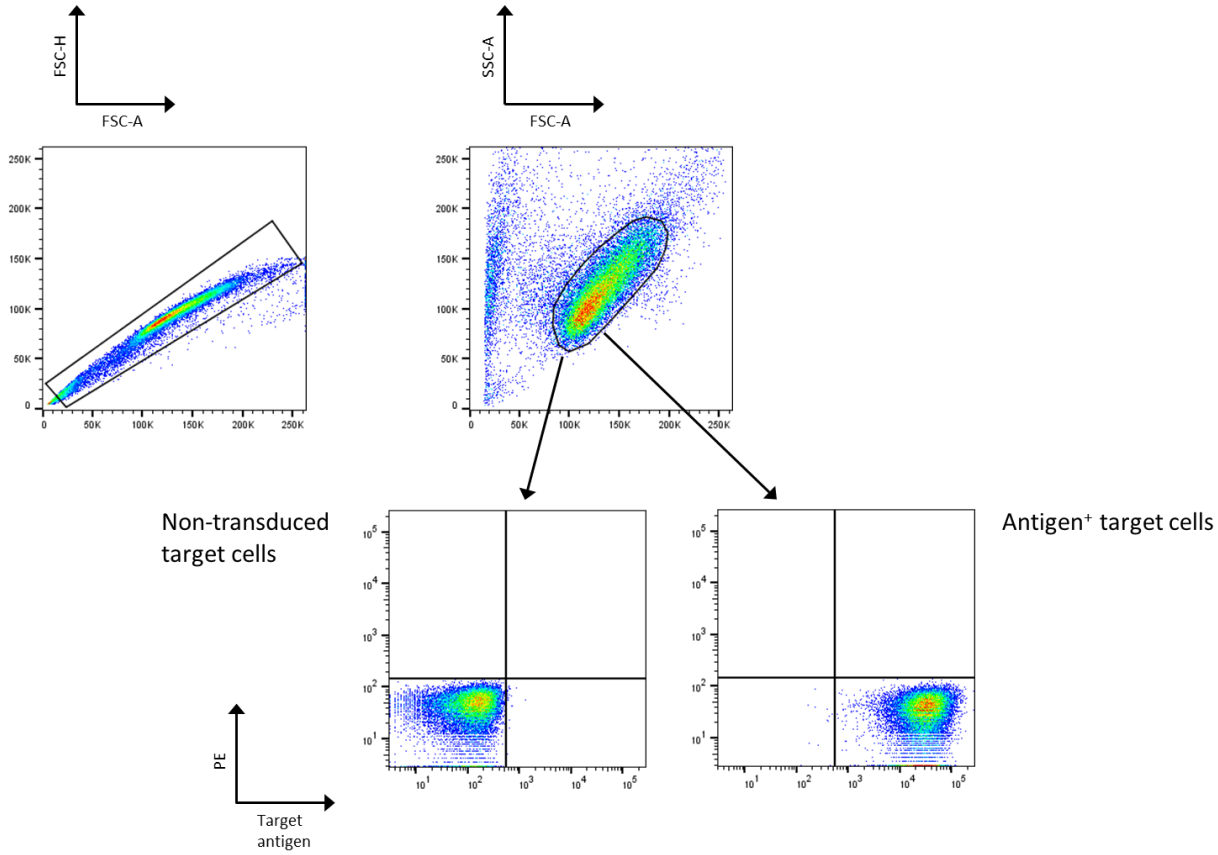

Gating strategy used to quantify antigen expression on target cells. Representative flow cytometry plots illustrating the gating strategy for assessment of the levels of antigen expression on target cell surface. Gating strategy used to identify singlet (top left), viable (top right) target cell populations. Antigen^{+} target cells were gated with reference to non-transduced control target cells (bottom).

(e)

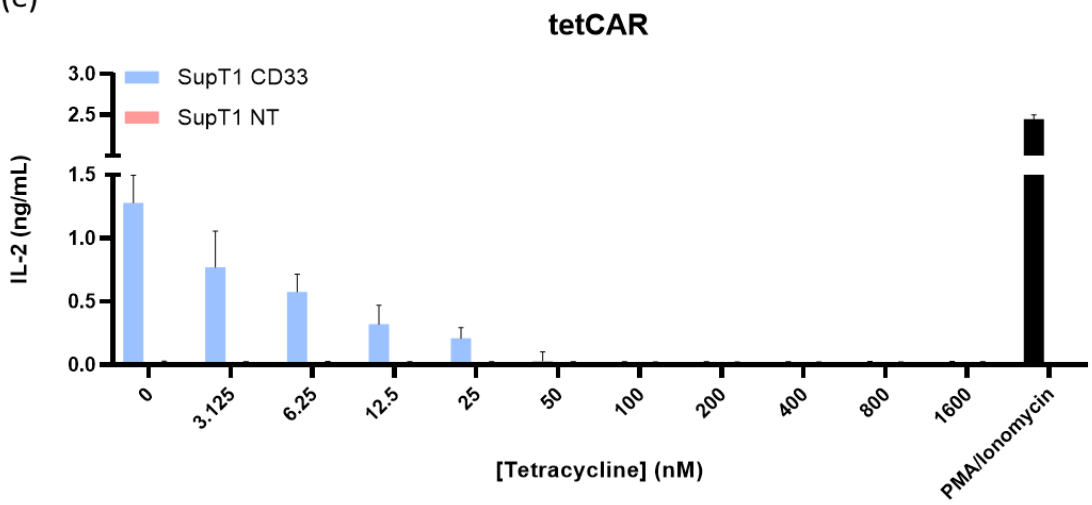

(e) Response of tetCAR to tetracycline and antigen stimulation. BW5 murine T-cells expressing the tetCAR were challenged with wild-type SupT1 cells or SupT1 cells engineered to express CD33 at a 1:4 T-cell:target cell ratio in the absence of tetracycline or in the presence of increasing concentrations of tetracycline. Production of IL-2 after an overnight incubation was quantified by ELISA; n = 3 independent experiments from separate donors, error bars denote SD.

(f)

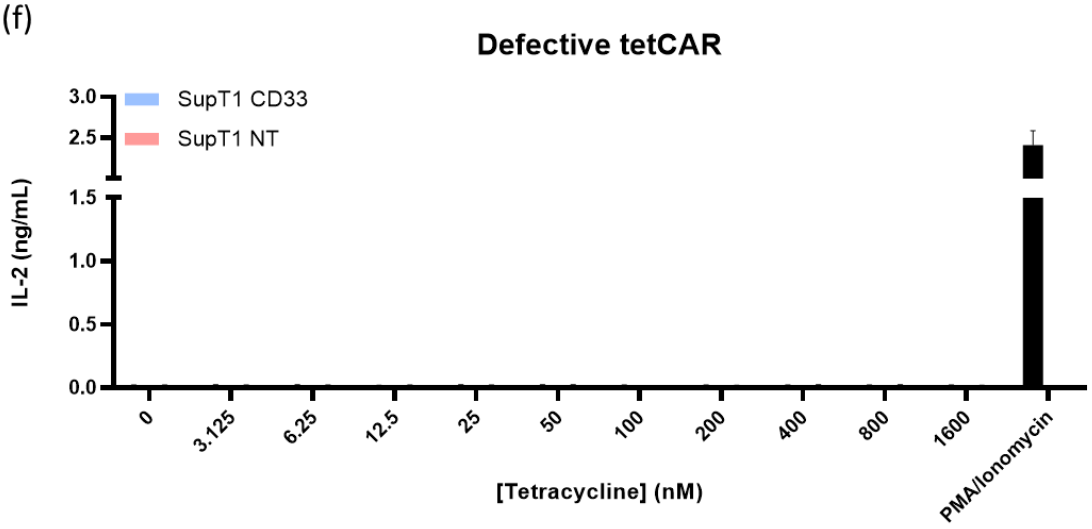

(g)

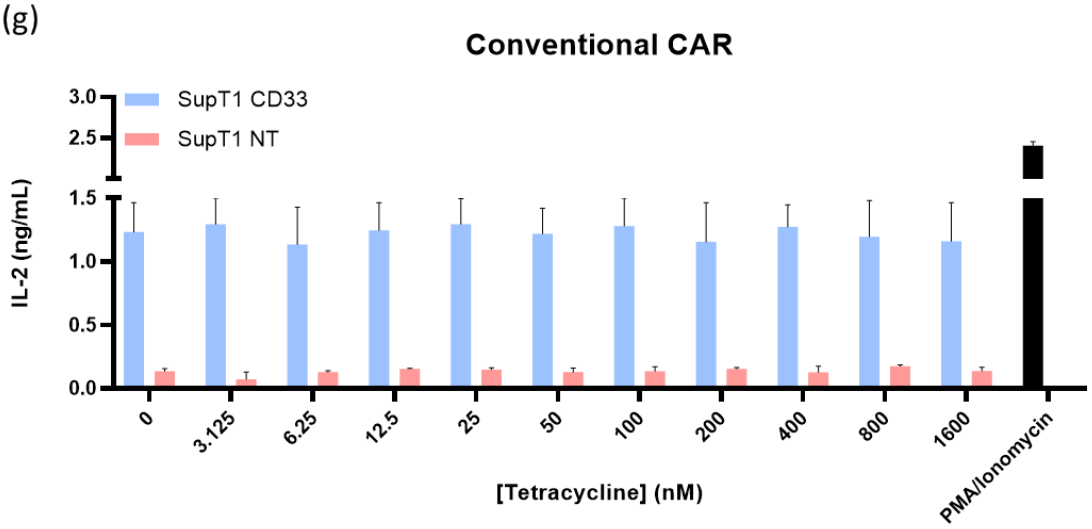

(f) BW5 cells expressing the defective tetCAR and (g) BW5 cells expressing the conventional CAR were also challenged with wild-type SupT1 cells or SupT1 cells engineered to express CD33 at a 1:4 T-cell:target cell ratio in the absence of tetracycline or in the presence of increasing concentrations of tetracycline.

3.3 Response of tetCAR to different small molecules

In order to determine whether the tetCAR would show similar response to different small molecules, we tested doxycycline (Figure 15) and minocycline (Figure 16). The experiments were carried out in parallel and set up as described above for Figure 14. The only modification was the small molecule used in each experiment. As expected, the defective tetCAR T-cells showed similar results in the presence of the three different small molecules. The same was observed with the conventional CAR T-cells. In terms of tetCAR, the amount of secreted IL-2 was undetectable at the lowest concentration of doxycycline (Figure 15a) and also at the lowest concentration of minocycline (Figure 16a). This means that above 3.125 nM doxycycline or minocycline the tetCAR is completely switched off.

These results indicate that the system is more sensitive to doxycycline and minocycline when compared to tetracycline.

Figure 15

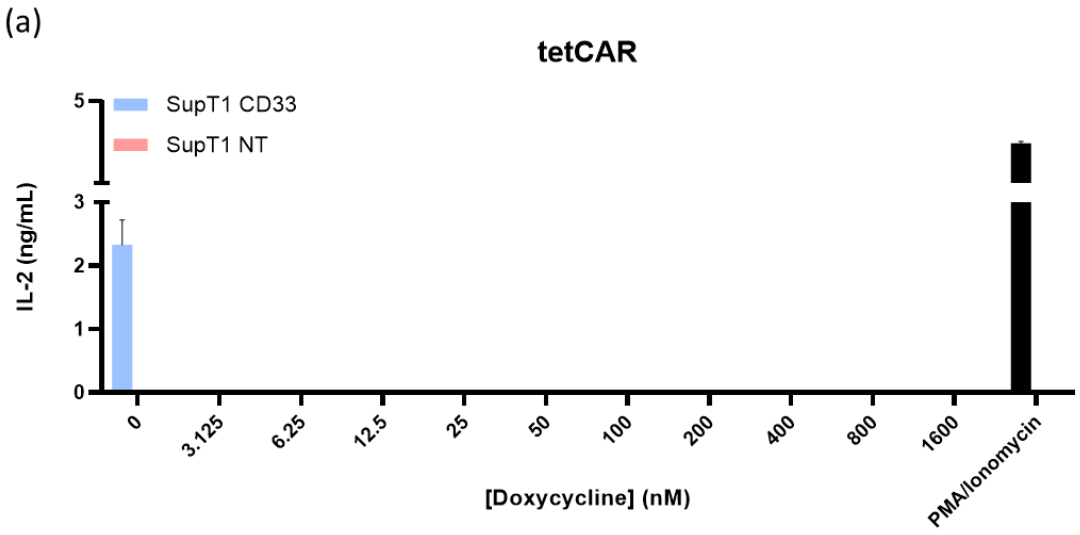

Figure 15. Response of tetCAR to doxycycline, a tetracycline analogue. (a) BW5 murine T-cells expressing the tetCAR were challenged with wild-type SupT1 cells or SupT1 cells engineered to express CD33 at a 1:4 T-cell:target cell ratio in the absence of doxycycline or in the presence of increasing concentrations of doxycycline. Production of IL-2 after an overnight incubation was quantified by ELISA; n = 3 independent experiments from separate donors, error bars denote SD.

(b)

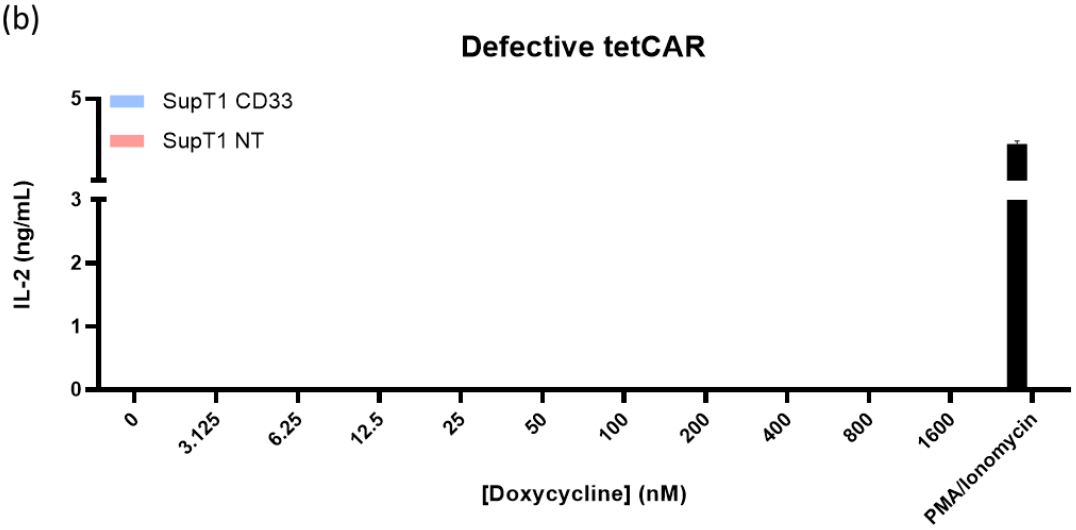

(c)

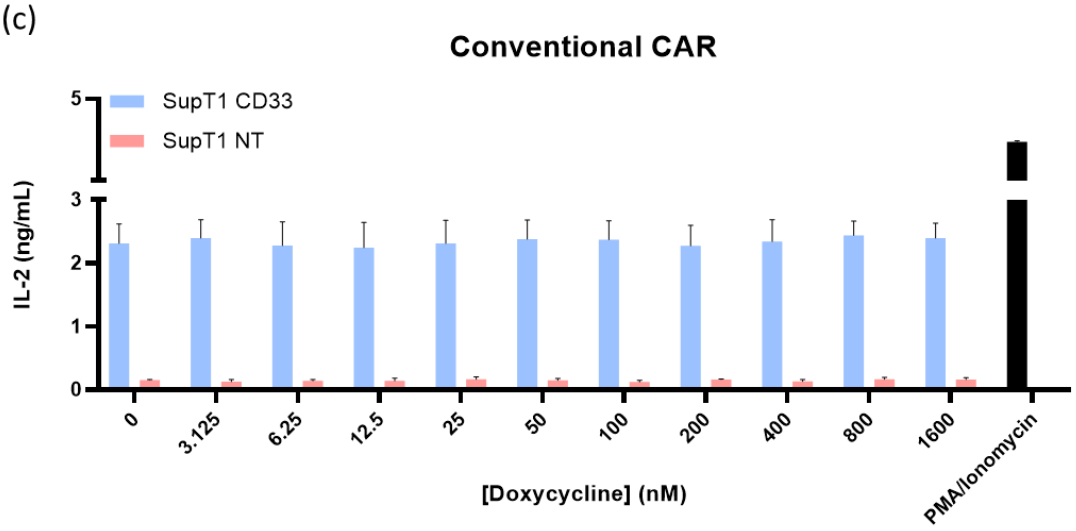

(b) BW5 cells expressing the defective tetCAR and (c) BW5 cells expressing the conventional CAR were also challenged with wild-type SupT1 cells or SupT1 cells engineered to express CD33 at a 1:4 T-cell:target cell ratio in the absence of doxycycline or in the presence of increasing concentrations of doxycycline.

Figure 16

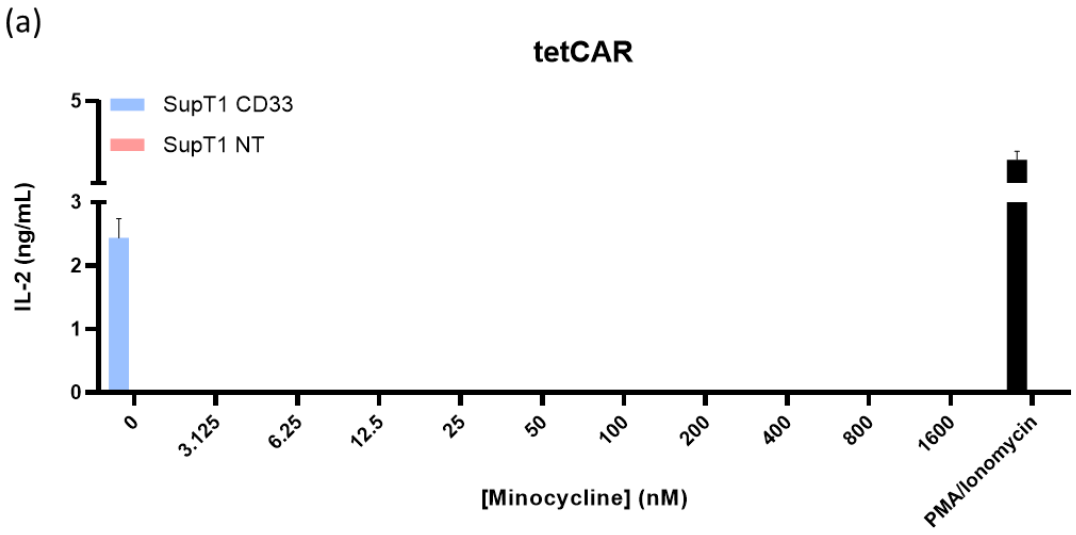

Figure 16. Response of tetCAR to minocycline, another tetracycline analogue. (a) BW5 murine T-cells expressing the tetCAR were challenged with wild-type SupT1 cells or SupT1 cells engineered to express CD33 at a 1:4 T-cell:target cell ratio in the absence of minocycline or in the presence of increasing concentrations of minocycline. Production of IL-2 after an overnight incubation was quantified by ELISA; n = 3 independent experiments from separate donors, error bars denote SD.

(b)

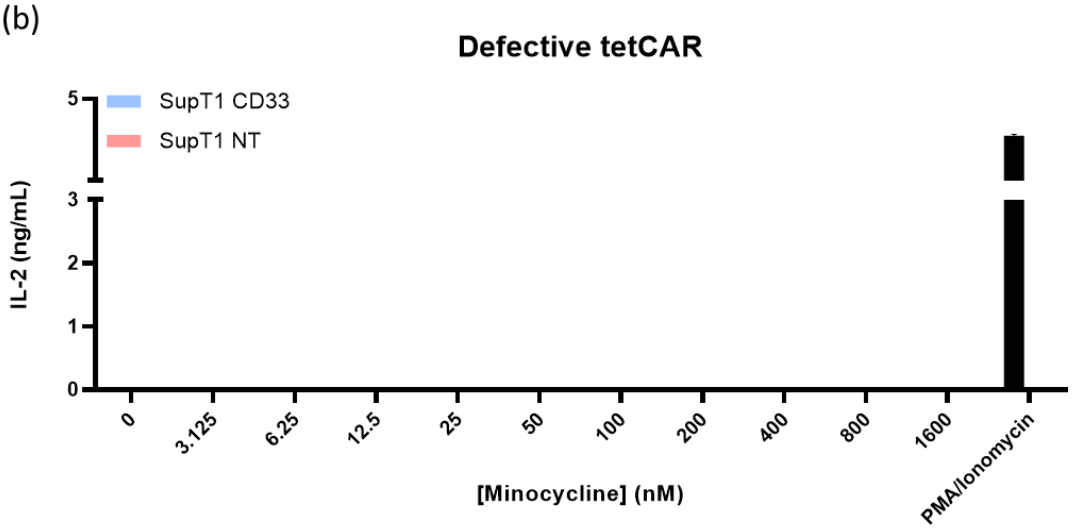

(c)

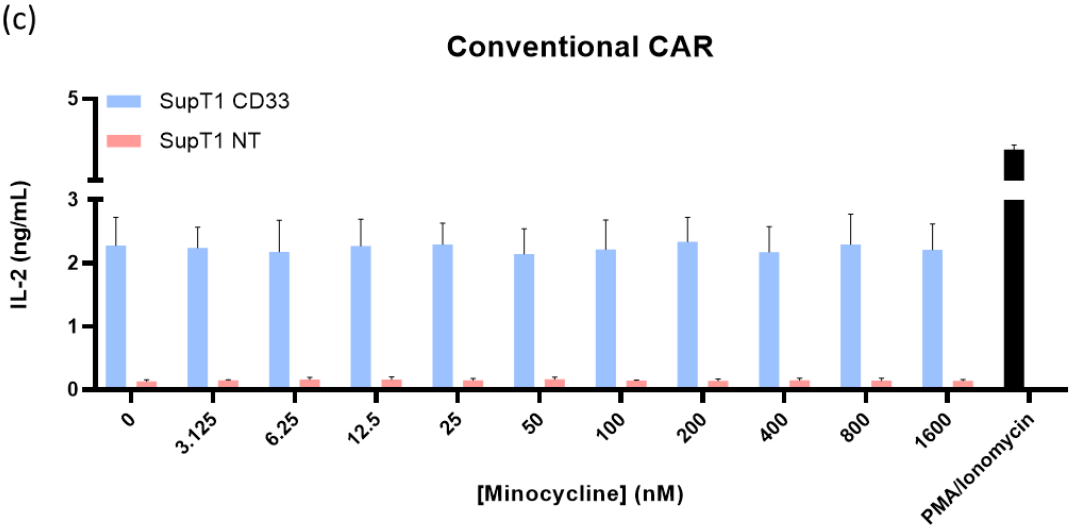

(b) BW5 cells expressing the defective tetCAR and (c) BW5 cells expressing the conventional CAR were also challenged with wild-type SupT1 cells or SupT1 cells engineered to express CD33 at a 1:4 T-cell:target cell ratio in the absence of minocycline or in the presence of increasing concentrations of minocycline.

3.4 Discussion

In this chapter, we have demonstrated function of the tetCAR system. First, we cloned two constructs tagged with eGFP and demonstrated that tetCAR works in terms of membrane assembly. Next, we cloned two functional constructs containing CD3-Zeta endodomain instead of eGFP and demonstrated transduction of BW5 murine T-cells. The T-cells expressing the tetCAR demonstrated specific IL-2 release, and depending on the concentration of tetracycline present, tetCAR T-cells showed titratable activity, from as strong as that of conventional CAR T-cells to undetectable.

After confirming the function of the system in BW5 murine T-cells via the administration of tetracycline, we demonstrated that the tetCAR system is compatible with other alternative small molecules. Using the same range of concentrations, we demonstrated that the tetCAR system is more sensitive to analogues doxycycline and minocycline when compared to tetracycline, as the addition of either tetracycline analogue at the lowest concentration completely inhibited the system.

Ultimately, this highlights the importance of further investigating the function of the tetCAR system in therapeutically relevant T-cells, and also the importance of assessing the titre response of the tetCAR to the different small molecules, which will be explored in the following chapters.

CHAPTER 4

DETERMINATION OF PERFORMANCE OF FIRST-GENERATION CONSTRUCTS

4.1 Function of the initial tetCAR construct in primary human T-cells

After using BW5 murine T-cells for our initial investigations, we tested the effectiveness of this tetCAR in therapeutically relevant T-cells. We expressed the constructs in primary human T-cells and examined the production of the cytokine IFN-γ. Firstly, we analysed the transduction efficiency of the primary human T-cells by flow cytometry. As shown in Figure 17b, the tetCAR could be detected at the cell surface, thus indicating that this construct was both expressed and trafficked correctly to the plasma membrane.

Cell surface expression of the defective tetCAR and conventional CAR was also detected. In order to test the function of the initial tetCAR construct in primary human T-cells, we co-cultured primary human T-cells expressing the tetCAR with wild-type SupT1 cells or SupT1 cells engineered to express CD33 at a 1:1 T-cell:target cell ratio in the absence of tetracycline or in the presence of different concentrations of tetracycline (Figure 17d). Primary human T-cells expressing the defective tetCAR (Figure 17e) and primary human T-cells expressing the conventional CAR (Figure 17f) were also tested. Furthermore, T-cells from the same donor that had not undergone gene transfer (designated non-transduced T-cells) were set up to serve as an additional control (Figure 17g). After an overnight incubation, supernatant samples were removed and assayed for the presence of IFN-γ. The tetCAR led to minimal secretion of IFN-γ by primary human T-cells in the absence of tetracycline. In order to ensure that these results are reproducible, we performed an extra two independent experiments. The results were consistent with the initial findings.

This highlights that the initial CD33-targeting version of the tetCAR construct failed to signal strongly, despite abundant expression in primary human T-cells.

Figure 17

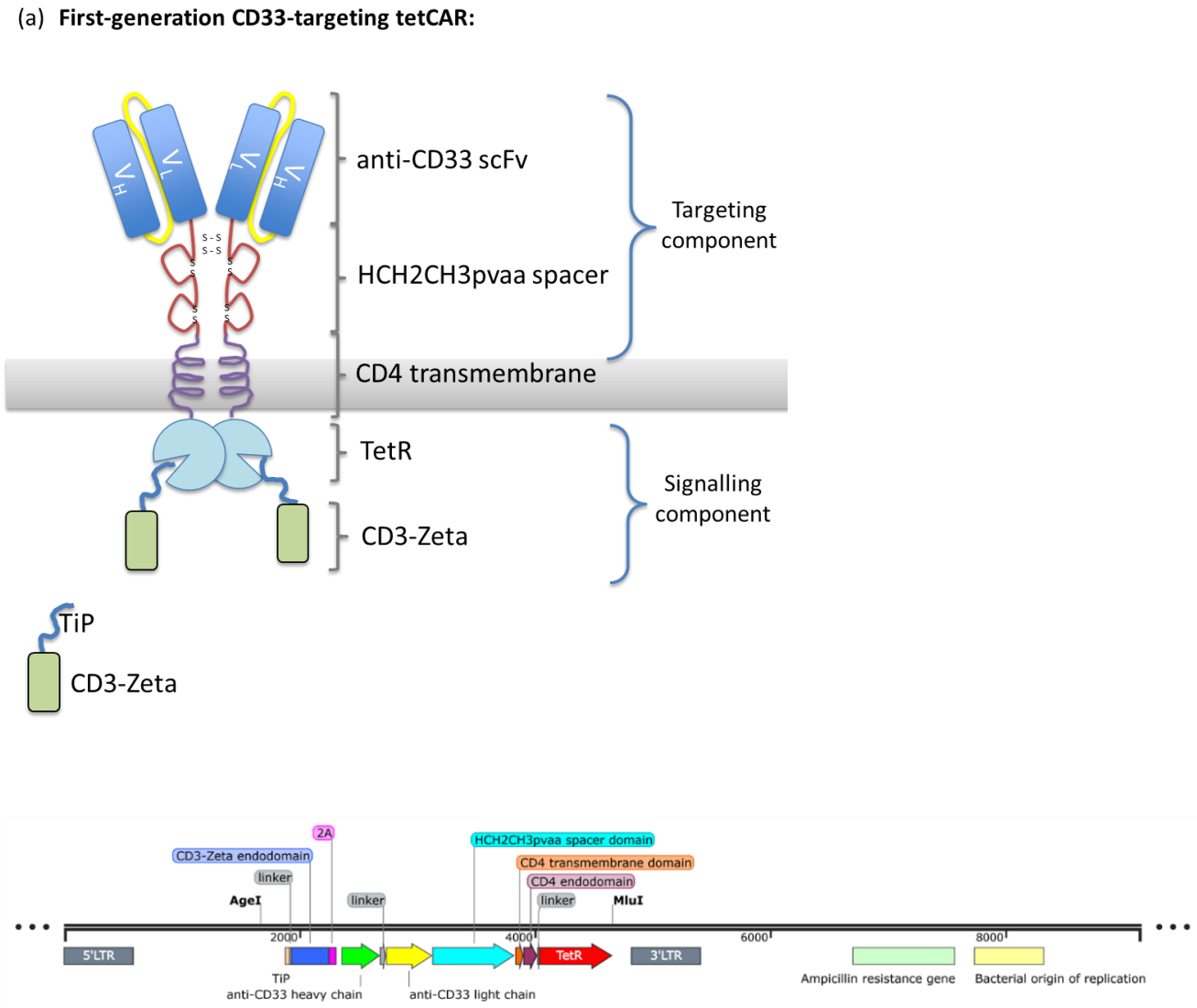

Figure 17. Function of the initial tetCAR construct in primary human T-cells. (a) Schematic diagram illustrating the initial tetCAR (top). A bicistronic construct expressed as a single transcript which self-cleaves at the 2A site to yield: a signalling component which comprises of TiP (dark blue) fused via a flexible linker to the endodomain of CD3-Zeta (light green); and a receptor component which comprises of a CD33 recognizing scFv (blue), a spacer derived from the Fc domain of IgG1 (red), a CD4 derived transmembrane and intracellular domain (purple), and TetR (light blue). Additionally, the plasmid map of the first-generation CD33-targeting tetCAR is also shown (bottom).

(b) **Primary human T-cells:**

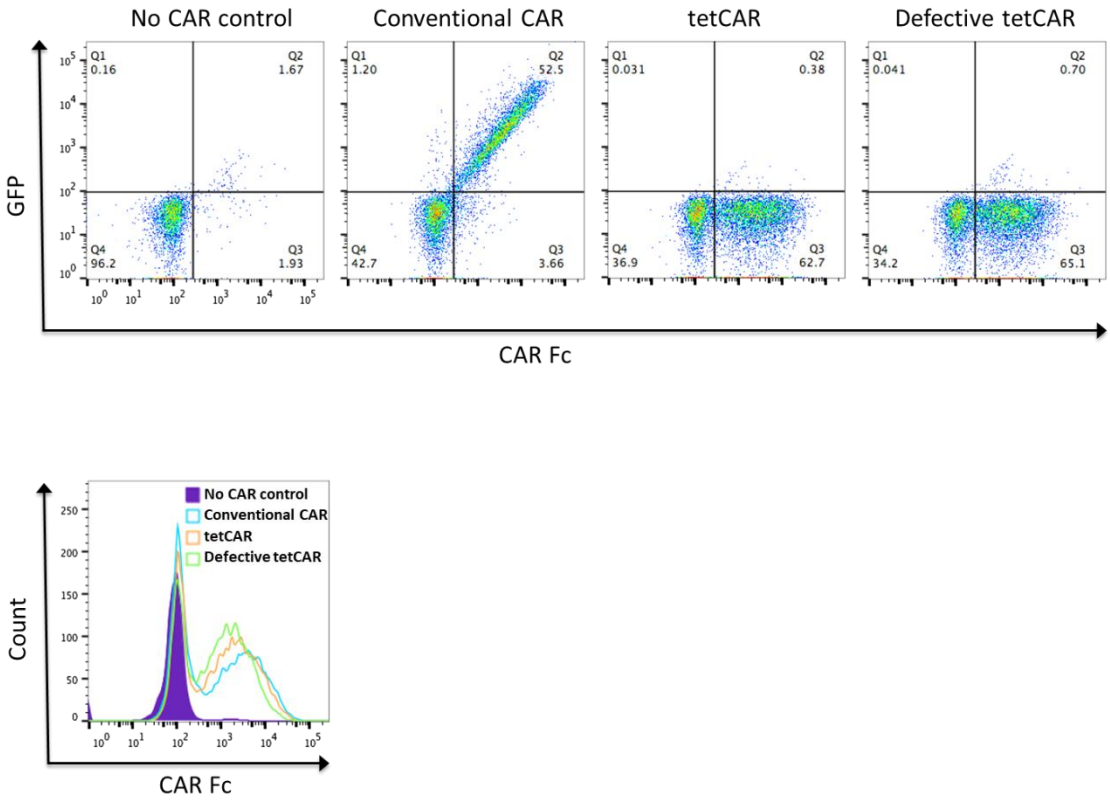

(b) Expression levels of CARs in primary human T-cells. Cells engineered with retroviral constructs encoding CAR molecules were analysed by flow cytometry. Expression of the tetCAR at the surface of primary human T-cells was compared with the expression of defective tetCAR (with absent TiP domain) and conventional CAR. The CARs were detected with an anti-human IgG antibody. Staining was compared against NT T-cells stained using the same antibody.

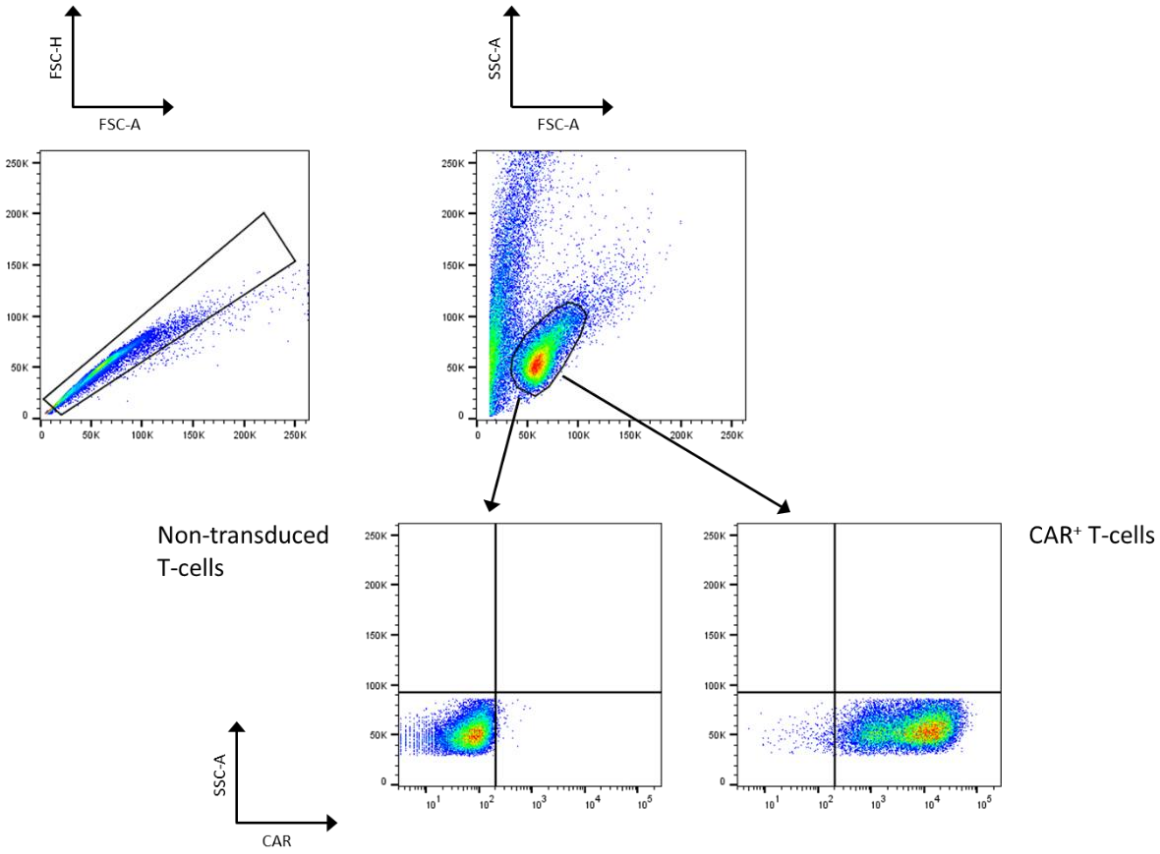

Gating strategy used to verify CAR expression on T-cells. Representative flow cytometry plots illustrating the gating strategy for assessment of CAR transduction efficiency of T-cells. Gating strategy used to identify singlet (top left), viable (top right) T-cell populations. CAR^+ T-cells were gated with reference to non-transduced control T-cells (bottom).

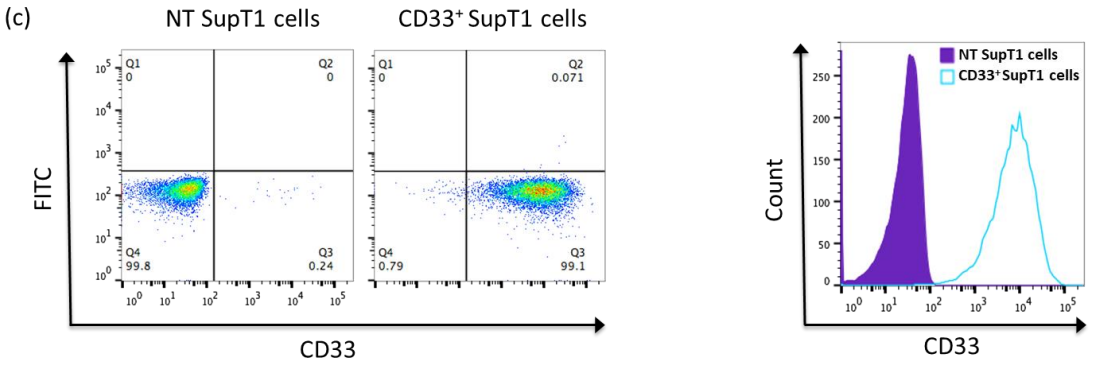

(c) Level of CD33 expression on target cell surface. SupT1 cells were used as target cells in co-culture assays. Non-transduced SupT1 were transduced to stably express CD33. The cells were investigated for the presence of CD33 using flow cytometry. The expression of CD33 was detected using an anti-human CD33 antibody. The level of CD33 expression was compared with that displayed by the NT SupT1 cells stained with the same antibody.

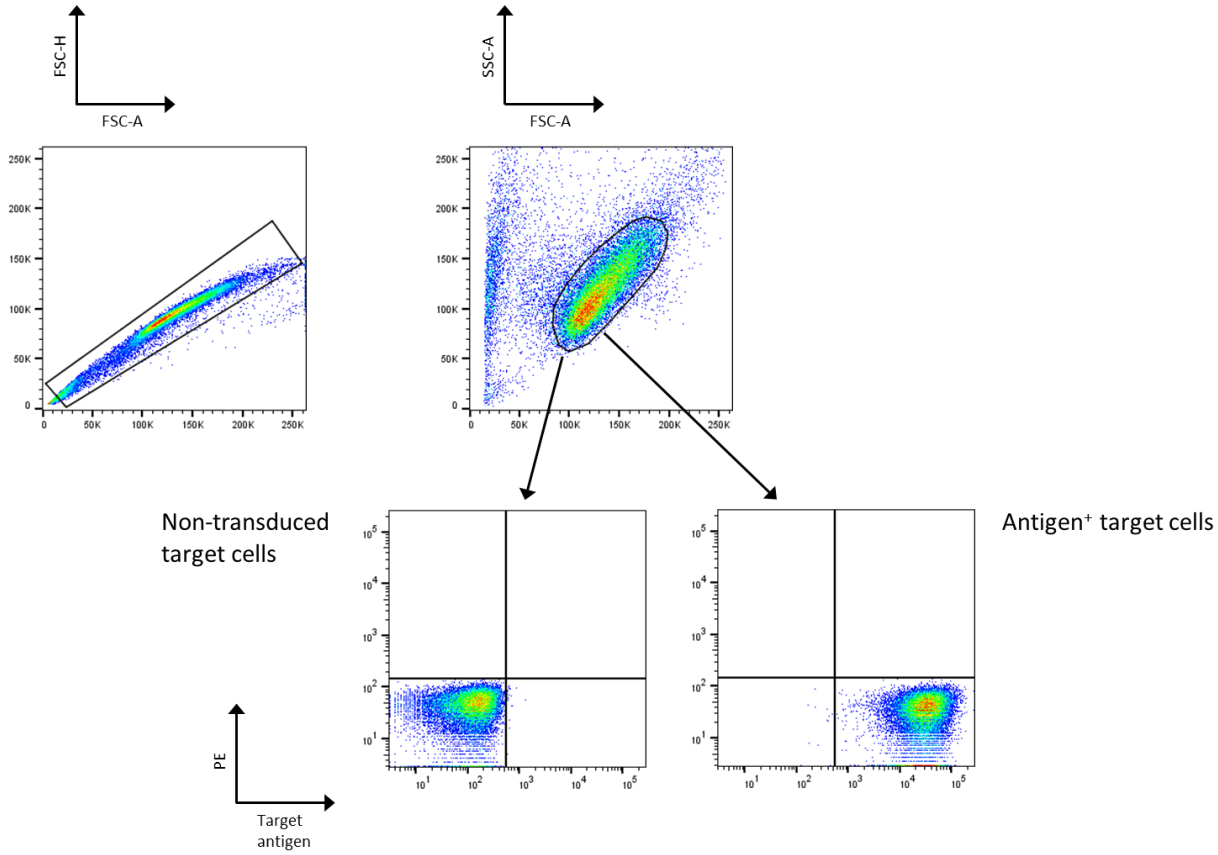

Gating strategy used to quantify antigen expression on target cells. Representative flow cytometry plots illustrating the gating strategy for assessment of the levels of antigen expression on target cell surface. Gating strategy used to identify singlet (top left), viable (top right) target cell populations. Antigen^{+} target cells were gated with reference to non-transduced control target cells (bottom).

(d)

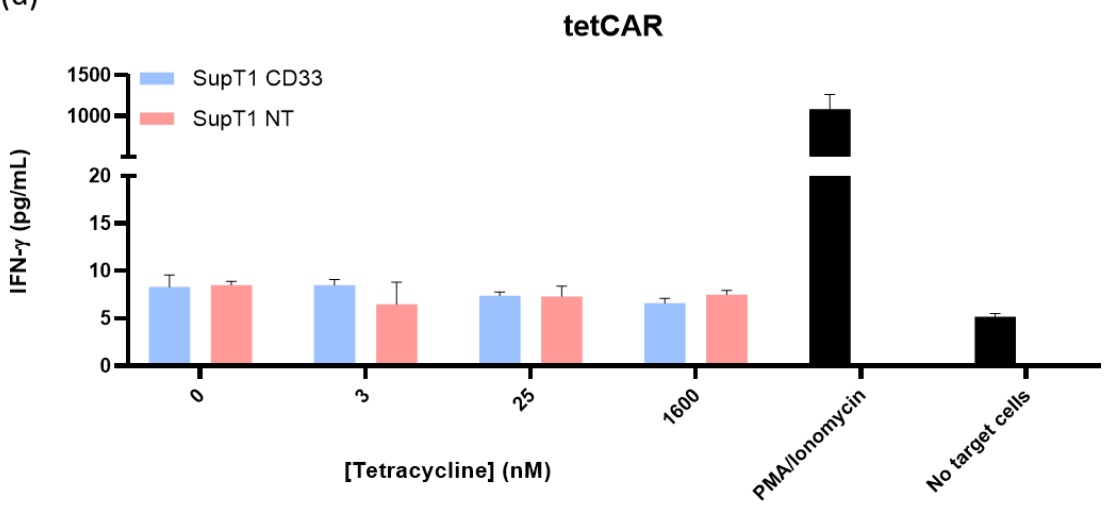

(d) Response of tetCAR to tetracycline and antigen stimulation. Primary human T-cells expressing the tetCAR were challenged with wild-type SupT1 cells or SupT1 cells engineered to express CD33 at a 1:1 T-cell:target cell ratio in the absence of tetracycline or in the presence of different concentrations of tetracycline. Production of IFN-γ after an overnight incubation was quantified by ELISA; n = 3 independent experiments from separate donors, error bars denote SD.

(e)

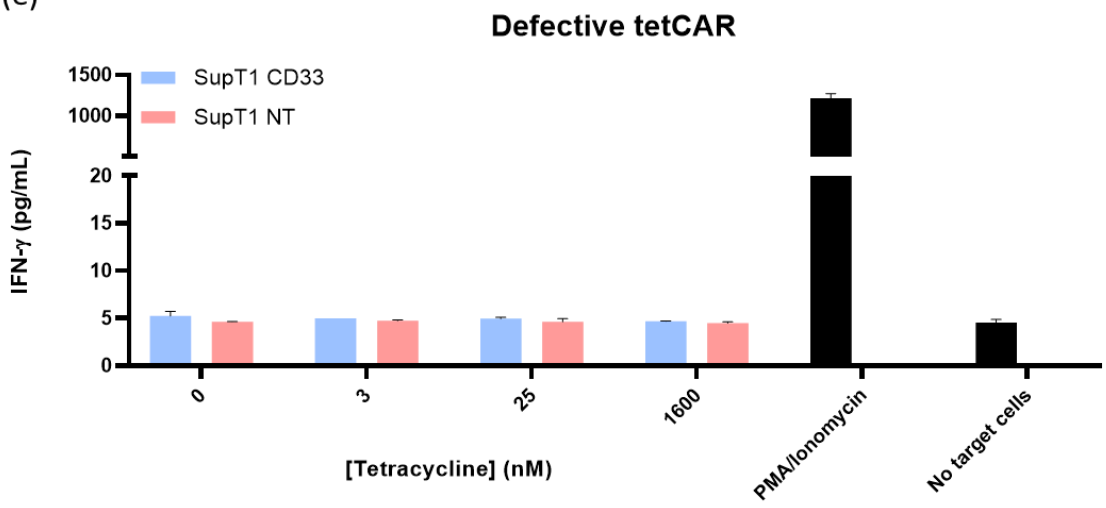
Defective tetCAR
SupT1 CD33
SupT1 NT
IFN-γ (pg/mL)
1500
1000
20
15
10
5
0
0
3
25
1600
PMA/Ionomycin
No target cells
[Tetracycline] (nM)

(f)

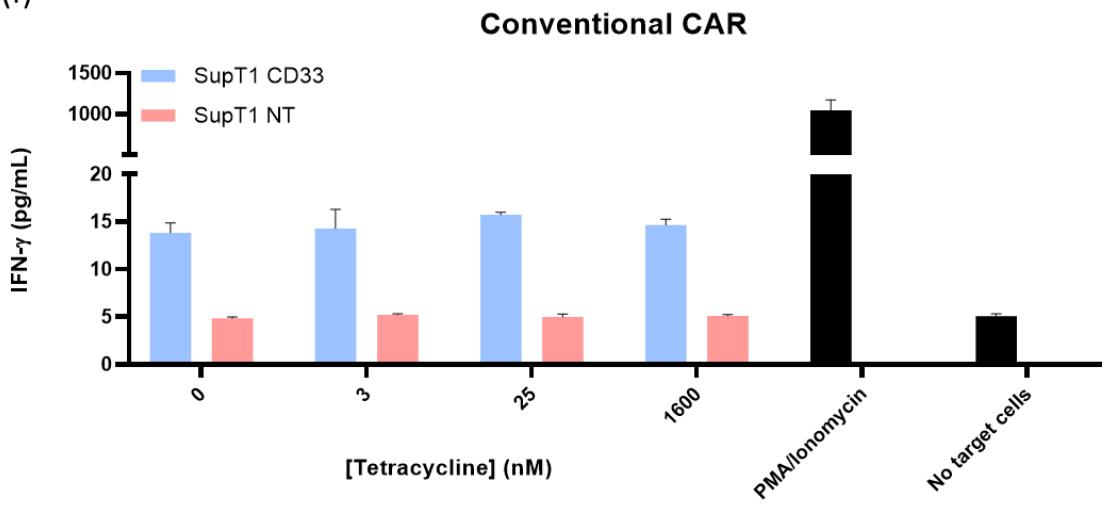
Conventional CAR
SupT1 CD33
SupT1 NT
IFN-γ (pg/mL)
1500
1000
20
15
10
5
0
0
3
25
1600
PMA/Ionomycin
No target cells
[Tetracycline] (nM)

(g)

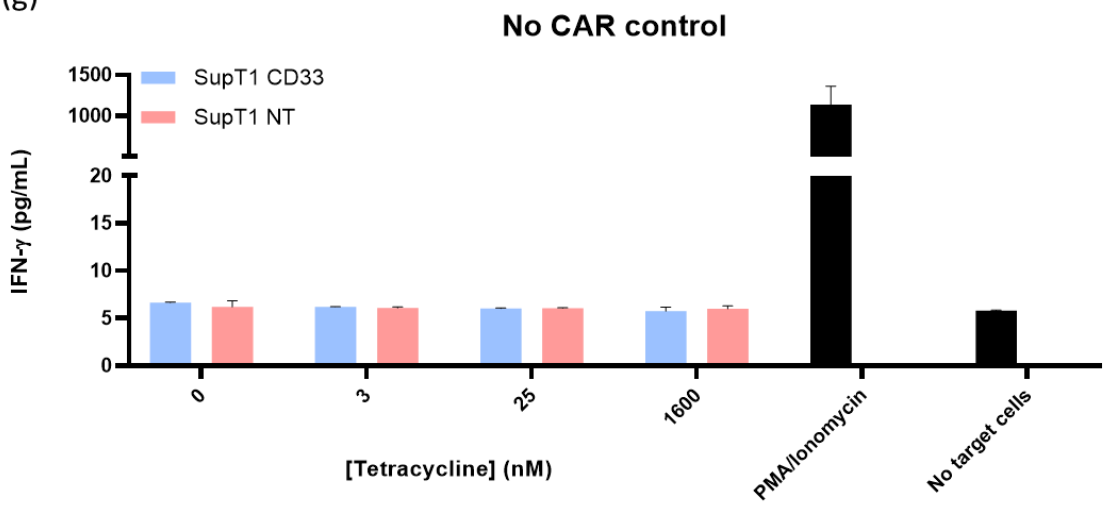

(e) Primary human T-cells expressing the defective tetCAR, (f) primary human T-cells expressing the conventional CAR and (g) non-transduced T-cells were also challenged with wild-type SupT1 cells or SupT1 cells engineered to express CD33 at a 1:1 T-cell:target cell ratio in the absence of tetracycline or in the presence of different concentrations of tetracycline.

4.2 Function of a CD19-targeting version of the tetCAR construct

From previous experiments, we had known that the CD33 scFv used in the CAR was suboptimal. To overcome this problem, we reconstructed the system with a single-chain antibody that recognizes the antigen CD19 instead of the antigen CD33 using a very well characterized anti-CD19 scFv called FMC63. All the other domains of the tetCAR remained the same. As previously carried out for the initial tetCAR, we started by testing the new CD19-targeting version of the tetCAR in BW5 murine T-cells.

The experiments were set up as described above for Figure 14. Surface expression of the tetCARs was initially assessed in the HEK 293T cell line following transient transfection. Both tetCARs and the conventional CAR were successfully detected at the cell surface using flow cytometry with an anti-human IgG antibody (Figure 18b). After collecting the retrovirus supernatant (at 48h and 72h post transfection), BW5 murine T-cells were transduced. Transduction efficiency of the BW5 cells was analysed by flow cytometry. As shown in Figure 18c, the tetCAR could be detected at the cell surface, thus indicating that this construct was both expressed and trafficked correctly to the plasma membrane. Cell surface expression of the defective tetCAR and conventional CAR was also detected. Prior to co-culture, a further important goal was to produce and validate a CD19 expressing target cell line. Consequently, the introduction of CD19 into SupT1 cells was required. The presence of CD19 at the target cell surface was confirmed using flow cytometry with an anti-human CD19 antibody (Figure 18d). With the ability to achieve expression of the tetCAR at the T-cell surface clearly confirmed, and the CD19 expression of SupT1 cells validated, it was possible to investigate whether this construct was capable of binding the required antigen.

As interaction of the CAR with target antigen was predicted to induce T-cell activation, the release of specific cytokines, such as IL-2 was used as a marker of CD19 antigen recognition. In order to determine the response of the new CD19-tetCAR to antigen stimulation and also to tetracycline, BW5 murine T-cells expressing the tetCAR were co-cultured with wild-type SupT1 cells or SupT1 cells engineered to express CD19 at a 1:4 T-cell:target cell ratio in the absence of tetracycline or in the presence of increasing concentrations of tetracycline (Figure 18e). BW5 cells expressing the defective tetCAR

(Figure 18f) and BW5 cells expressing the conventional CAR (Figure 18g) were also tested. After an overnight incubation, supernatant samples were removed and assayed for the presence of IL-2. Subsequent investigations into the release of IL-2 showed that tetracycline decreases murine T-cell IL-2 secretion and hence activation in a dose dependent manner. The experiment was carried out using concentrations of tetracycline ranging from 0 to 1600 nM. In this experiment tetracycline was serially diluted at 1 in 2 ratio starting from 1600 nM.

The conventional CAR, which was used as a positive control, led to consistent secretion of IL-2 by BW5 cells in all tetracycline concentrations. Low levels of IL-2 secretion were observed when the same CAR BW5 cell line was co-cultured with wild-type SupT1 cells (Figure 18g). As expected, no significant IL-2 secretion by defective tetCAR T-cells was detected on either SupT1 CD19 or SupT1 NT cells (Figure 18f). In the tetracycline inducible CAR (also known as tetCAR), the amount of secreted IL-2 was found to decrease with increasing concentrations of tetracycline (Figure 18e). In the absence of tetracycline, IL-2 secretion was analogous to that seen with the positive control. In the presence of 50 nM tetracycline, a minimal concentration of secreted IL-2 was observed. From 100 nM to 1600 nM, no significant IL-2 secretion by tetCAR T-cells was detected on either SupT1 CD19 or SupT1 NT cells. PMA and ionomycin stimulated BW5 cells showed the highest levels of IL-2 secretion.

In summary, our results show that the tetCAR design functions with an alternative antigen-binding domain in BW5 murine T-cells.

Figure 18

(a) **First-generation CD19-targeting tetCAR:**

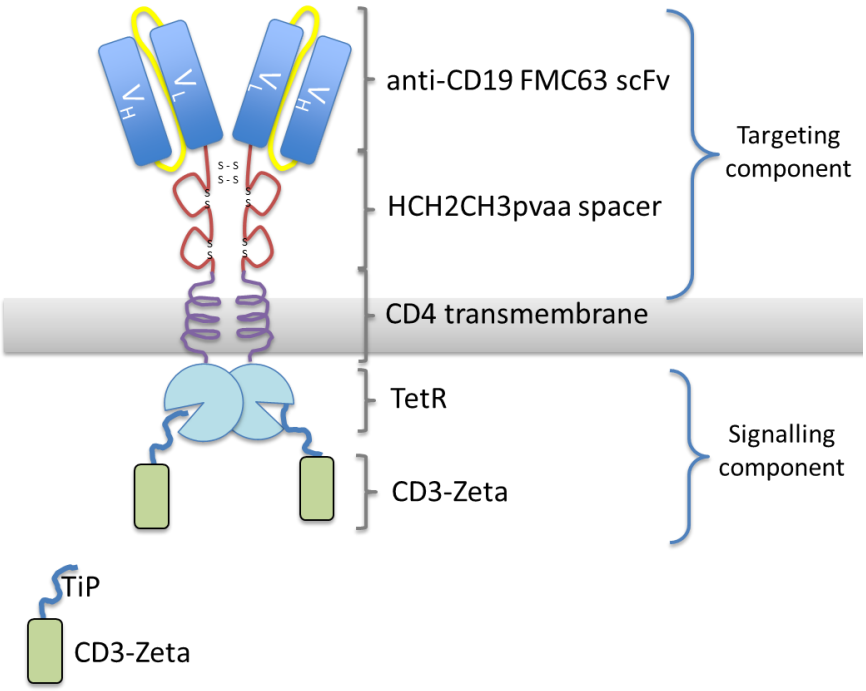

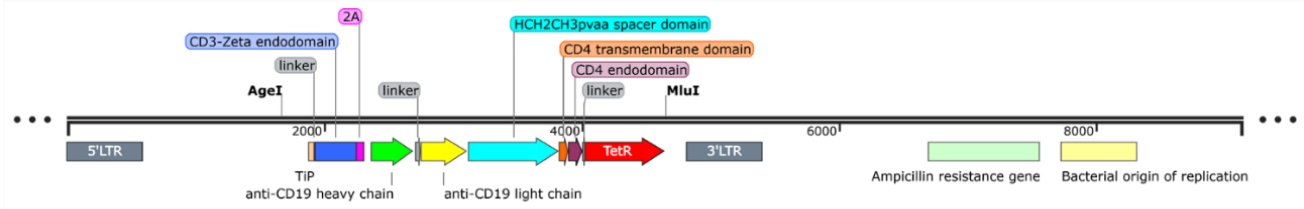

Figure 18. Function of a CD19-targeting version of the tetCAR construct. (a) Schematic diagram illustrating the CD19-targeting tetCAR (top). A bicistronic construct expressed as a single transcript which self-cleaves at the 2A site to yield: a signalling component which comprises of TiP (dark blue) fused via a flexible linker to the endodomain of CD3-Zeta (light green); and a receptor component which comprises of a CD19 recognizing scFv (blue), a spacer derived from the Fc domain of IgG1 (red), a CD4 derived transmembrane and intracellular domain (purple), and TetR (light blue). Additionally, the plasmid map of the first-generation CD19-targeting tetCAR is also shown (bottom).

(b) **293T cells:**

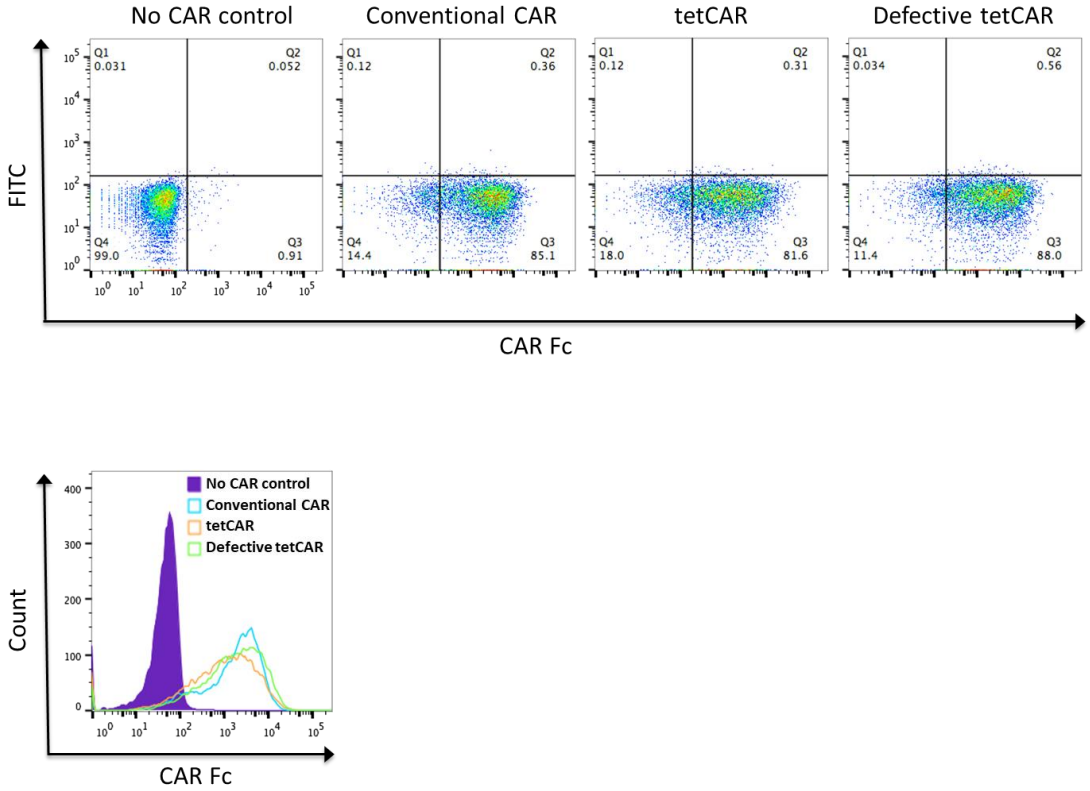

(b) Expression levels of CARs in HEK 293T cells. Expression of the CD19-targeting tetCAR at the surface of HEK 293T cells was compared with the expression of defective tetCAR (with absent TiP domain) and conventional CAR using flow cytometry. The CARs were detected with an anti-human IgG antibody. Staining was compared against NT 293T cells stained using the same antibody.

(c) **BW5 murine T-cells:**

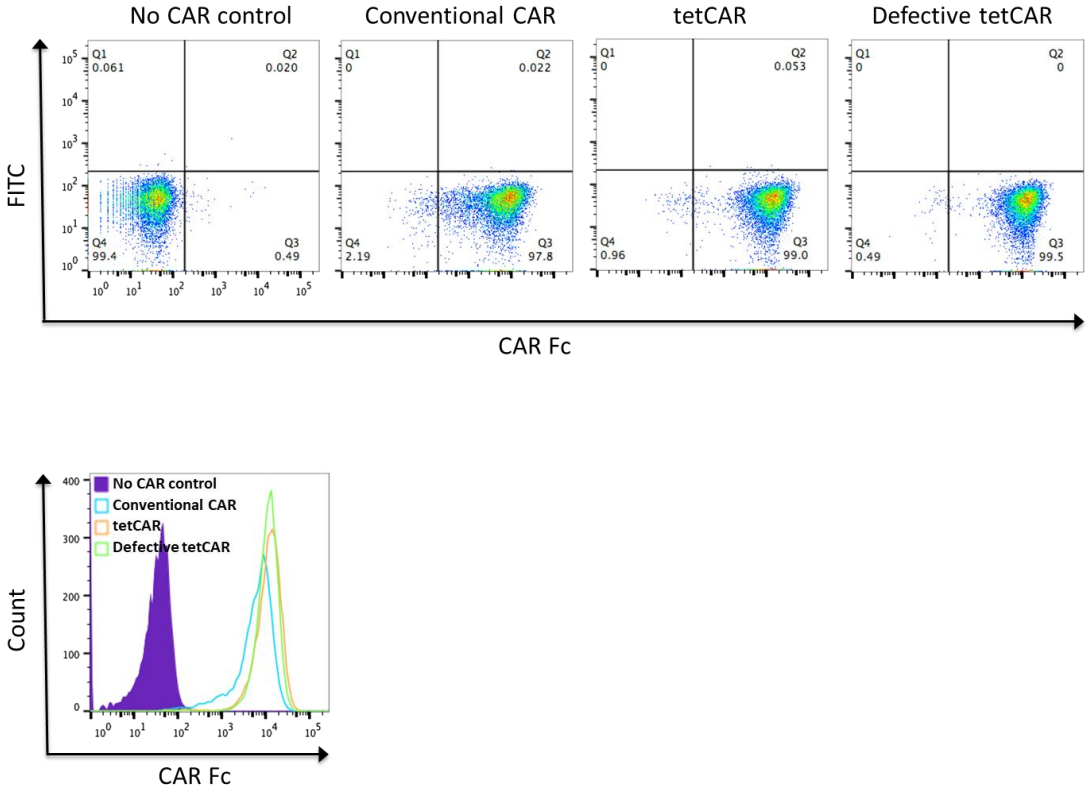

(c) Expression levels of CARs in BW5 murine T-cells. Cells engineered with retroviral constructs encoding CAR molecules were analysed by flow cytometry. Expression of the CD19-targeting tetCAR at the surface of BW5 murine T-cells was compared with the expression of defective tetCAR and conventional CAR. The CARs were detected with an anti-human IgG antibody. Staining was compared against NT BW5 cells stained using the same antibody.

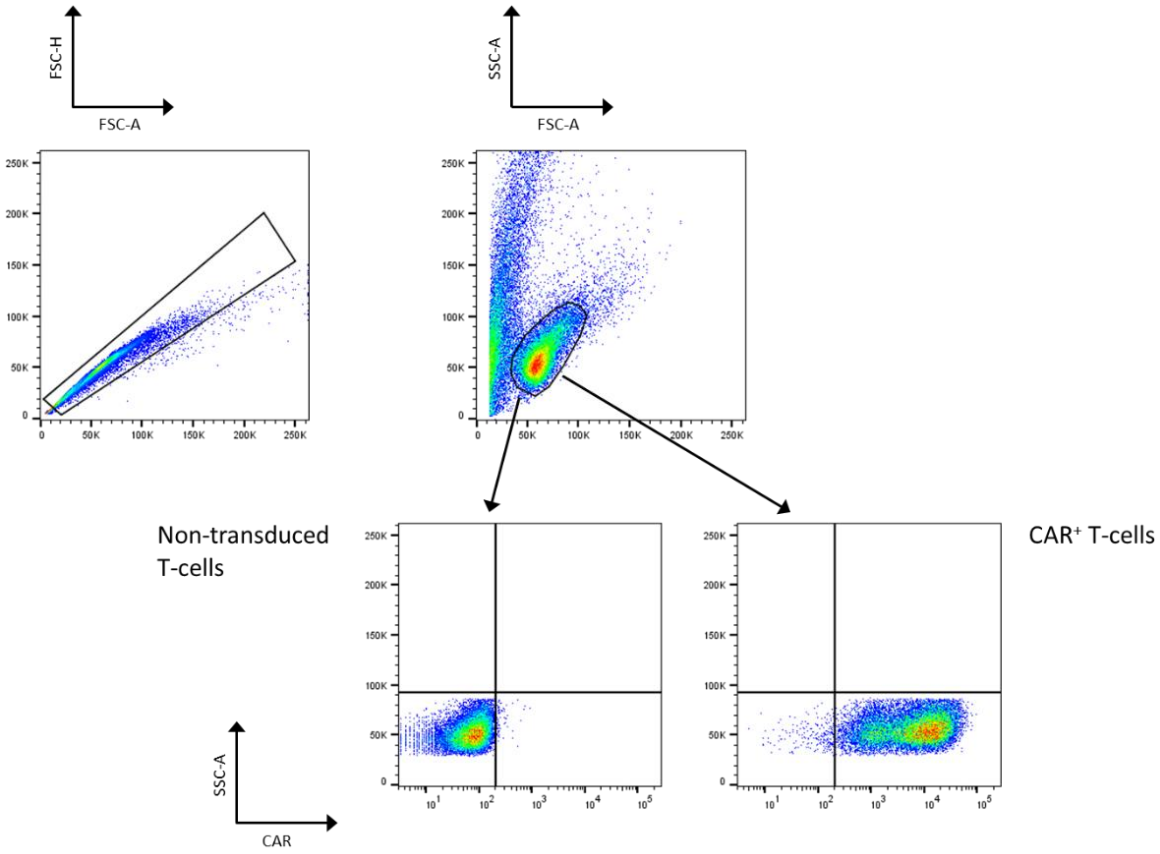

Gating strategy used to verify CAR expression on T-cells. Representative flow cytometry plots illustrating the gating strategy for assessment of CAR transduction efficiency of T-cells. Gating strategy used to identify singlet (top left), viable (top right) T-cell populations. CAR^+ T-cells were gated with reference to non-transduced control T-cells (bottom).

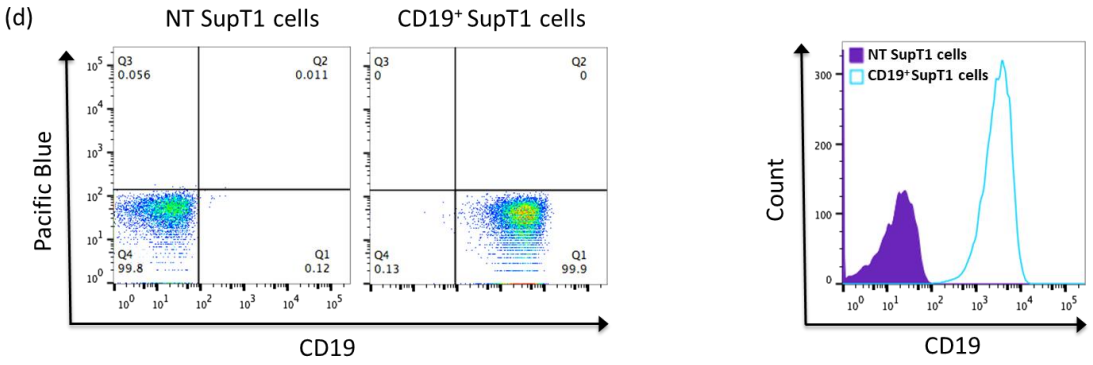

(d) Level of CD19 expression on target cell surface. SupT1 cells were used as target cells in co-culture assays. Non-transduced SupT1 were transduced to stably express CD19. The cells were investigated for the presence of CD19 using flow cytometry. The expression of CD19 was detected using an anti-human CD19 antibody. The level of CD19 expression was compared with that displayed by the NT SupT1 cells stained with the same antibody.

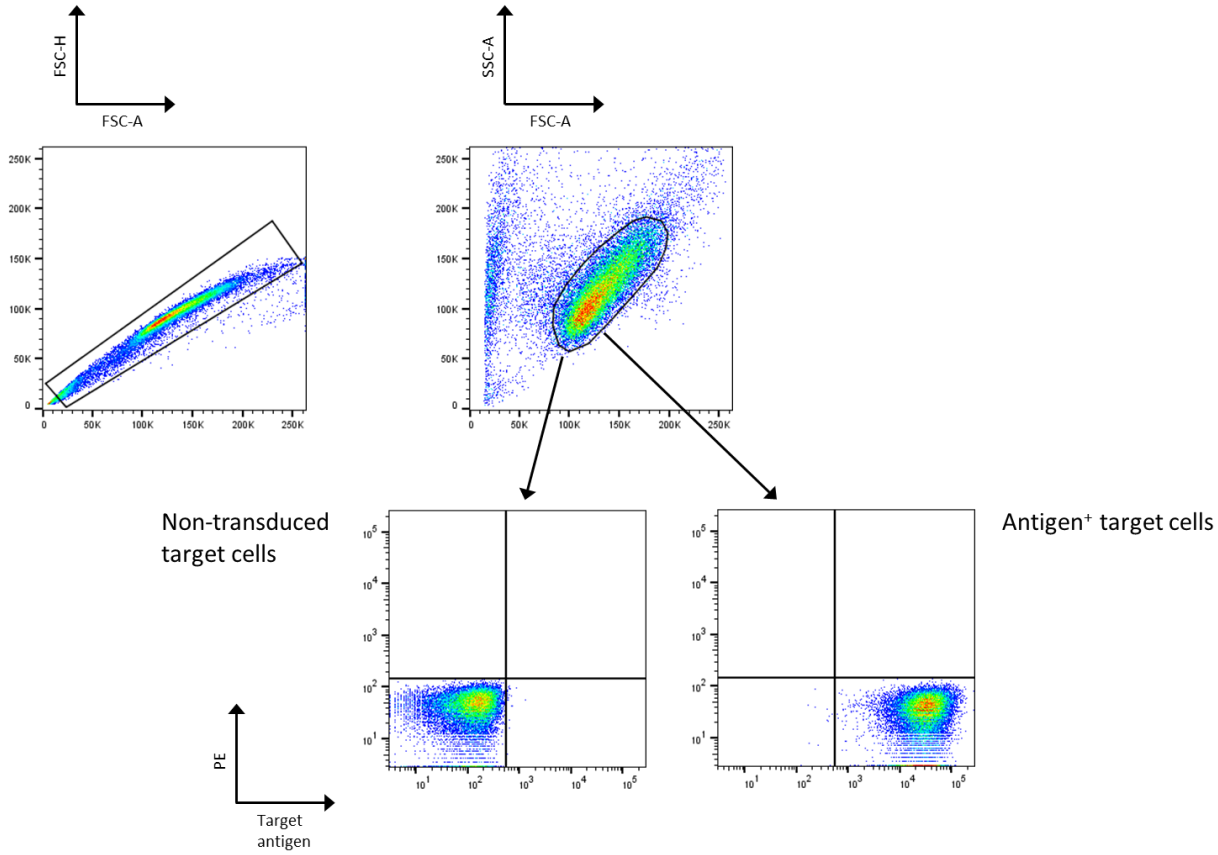

Gating strategy used to quantify antigen expression on target cells. Representative flow cytometry plots illustrating the gating strategy for assessment of the levels of antigen expression on target cell surface. Gating strategy used to identify singlet (top left), viable (top right) target cell populations. Antigen^{+} target cells were gated with reference to non-transduced control target cells (bottom).

(e)

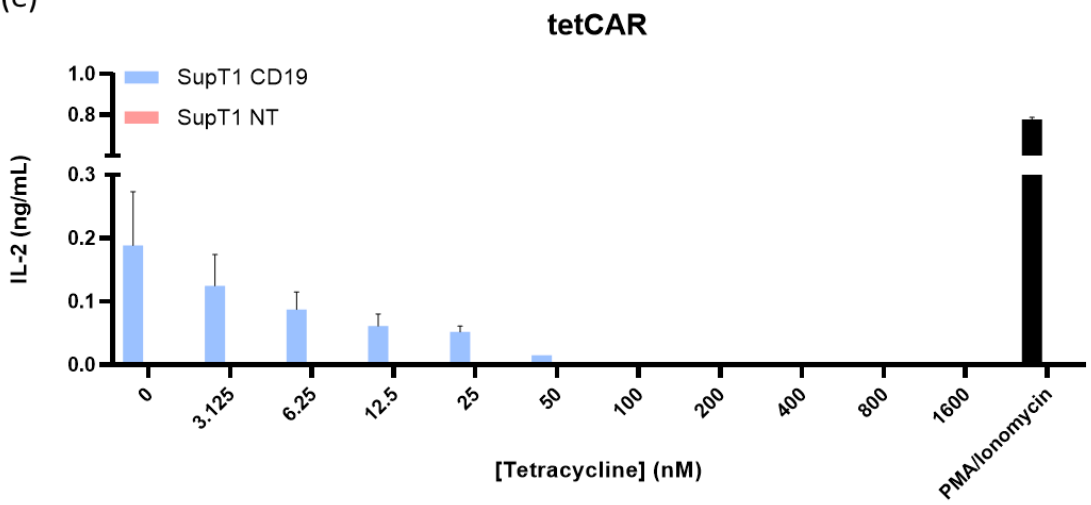

(e) Response of CD19-targeting tetCAR to tetracycline and antigen stimulation. BW5 murine T-cells expressing the CD19-targeting tetCAR were challenged with wild-type SupT1 cells or SupT1 cells engineered to express CD19 at a 1:4 T-cell:target cell ratio in the absence of tetracycline or in the presence of increasing concentrations of tetracycline. Production of IL-2 after an overnight incubation was quantified by ELISA; n = 3 independent experiments from separate donors, error bars denote SD.

(f)

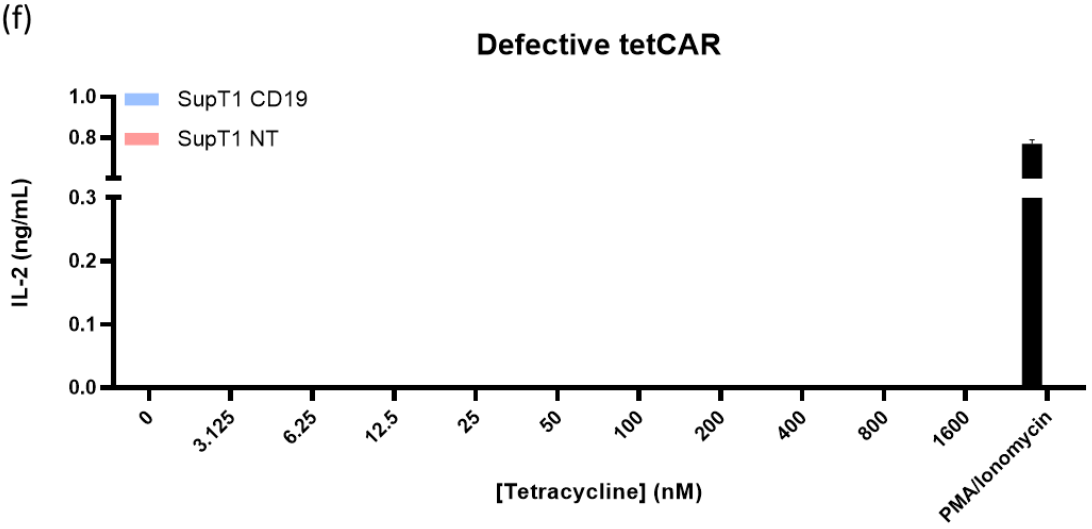

(g)

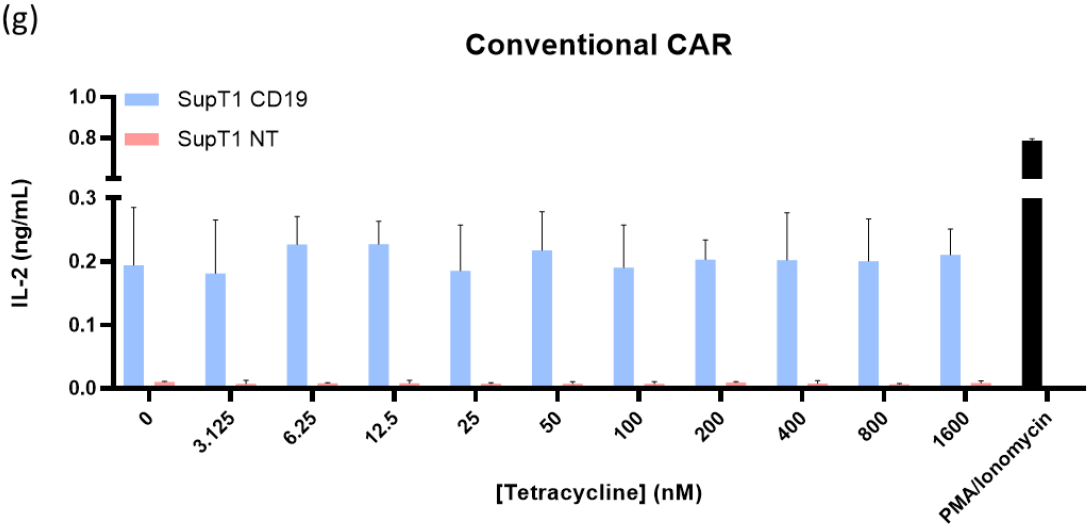

(f) BW5 cells expressing the defective tetCAR and (g) BW5 cells expressing the conventional CAR were also challenged with wild-type SupT1 cells or SupT1 cells engineered to express CD19 at a 1:4 T-cell:target cell ratio in the absence of tetracycline or in the presence of increasing concentrations of tetracycline.

4.3 Function of the CD19-targeting tetCAR construct in primary human T-cells

After showing that the initial CD33-targeting tetCAR construct does not function in primary human T-cells, it became increasingly important to prove that the tetCAR design would function in these therapeutically relevant T-cells when we use an alternative antigen-binding domain. In order to demonstrate this, we expressed the CD19-targeting version of the tetCAR construct in primary human T-cells and examined the production of the cytokine IFN-γ.

Firstly, we analysed the transduction efficiency of the primary human T-cells by flow cytometry. As shown in Figure 19b, the CD19-targeting tetCAR could be detected at the cell surface, thus indicating that this construct was both expressed and trafficked correctly to the plasma membrane. Cell surface expression of the defective tetCAR and conventional CAR was also detected. In order to test the function of the new CD19-targeting tetCAR construct in primary human T-cells, we co-cultured primary human T-cells expressing the tetCAR with wild-type SupT1 cells or SupT1 cells engineered to express CD19 at a 1:1 T-cell:target cell ratio in the absence of tetracycline or in the presence of different concentrations of tetracycline (Figure 19d). Primary human T-cells expressing the defective tetCAR (Figure 19e) and primary human T-cells expressing the conventional CAR (Figure 19f) were also tested. Furthermore, T-cells from the same donor that had not undergone gene transfer (designated non-transduced T-cells) were set up to serve as an additional control (Figure 19g).

After an overnight incubation, supernatant samples were removed and assayed for the presence of IFN-γ. Subsequent investigations into the release of IFN-γ showed that tetracycline decreases human T-cell IFN-γ secretion and hence activation in a dose dependent manner. The experiment was carried out using 3 nM, 25 nM and 1600 nM as tetracycline concentrations. The conventional CAR, which was used as a positive control, led to consistent secretion of IFN-γ by primary human T-cells in all tetracycline concentrations. Low levels of IFN-γ secretion were observed when the same CAR T-cells were co-cultured with wild-type SupT1 cells (Figure 19f). As expected, minimal IFN-γ secretion by defective tetCAR T-cells was detected on either SupT1 CD19 or

SupT1 NT cells (Figure 19e). Similar results were observed with the non-transduced T-cells (Figure 19g). In the tetracycline inducible CAR (also known as tetCAR), the amount of secreted IFN-γ was found to decrease with increasing concentrations of tetracycline (Figure 19d). In the absence of tetracycline, IFN-γ secretion was lower to that seen with the positive control. In the presence of 1600 nM tetracycline, minimal IFN-γ secretion by tetCAR T-cells was detected on either SupT1 CD19 or SupT1 NT cells. PMA and ionomycin stimulated primary human T-cells showed the highest levels of IFN-γ secretion.

Taken together, these data show that the new CD19-targeting tetCAR construct is functional and capable of activating primary human T-cells.

Figure 19

(a) **First-generation CD19-targeting tetCAR:**

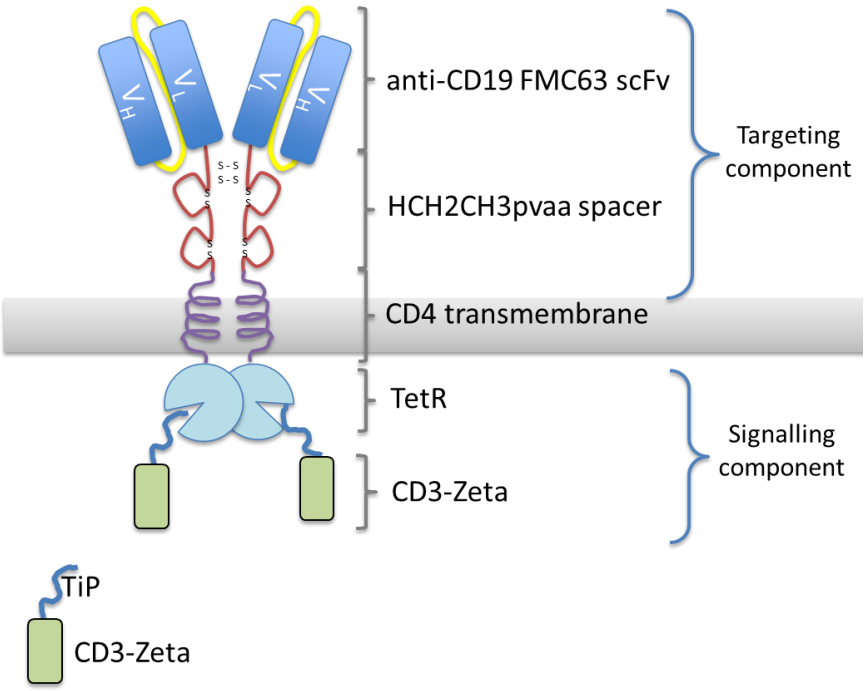

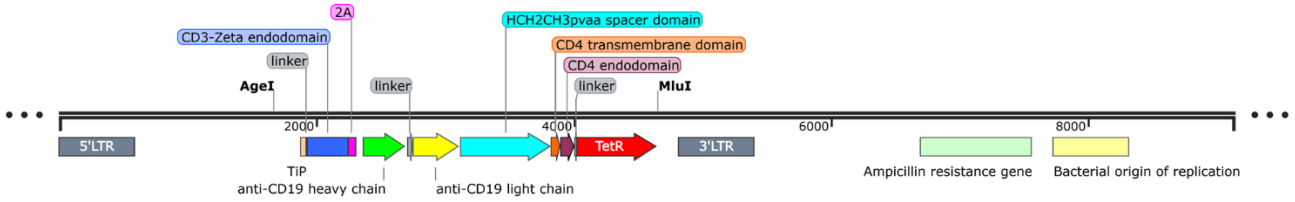

Figure 19. Function of the CD19-targeting tetCAR construct in primary human T-cells. (a) Schematic diagram illustrating the CD19-targeting tetCAR (top). A bicistronic construct expressed as a single transcript which self-cleaves at the 2A site to yield: a signalling component which comprises of TiP (dark blue) fused via a flexible linker to the endodomain of CD3-Zeta (light green); and a receptor component which comprises of a CD19 recognizing scFv (blue), a spacer derived from the Fc domain of IgG1 (red), a CD4 derived transmembrane and intracellular domain (purple), and TetR (light blue). Additionally, the plasmid map of the first-generation CD19-targeting tetCAR is also shown (bottom).

(b) **Primary human T-cells:**

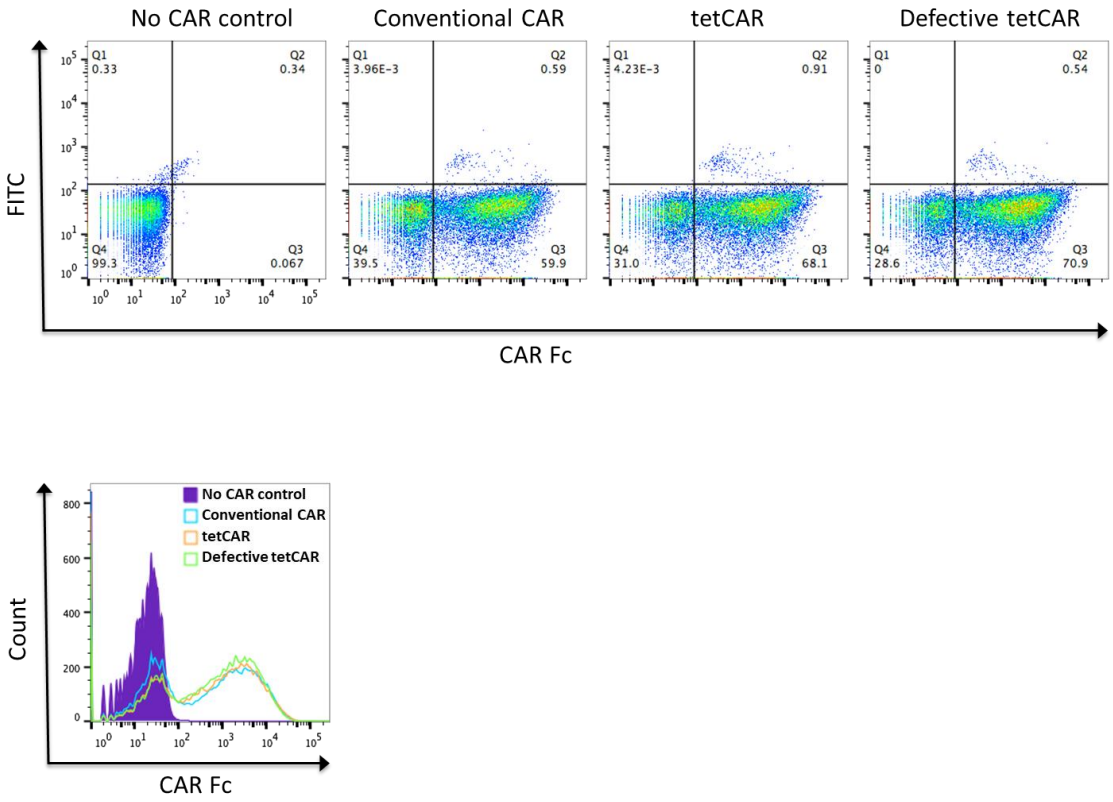

(b) Expression levels of CARs in primary human T-cells. Cells engineered with retroviral constructs encoding CAR molecules were analysed by flow cytometry. Expression of the CD19-targeting tetCAR at the surface of primary human T-cells was compared with the expression of defective tetCAR (with absent TiP domain) and conventional CAR. The CARs were detected with an anti-human IgG antibody. Staining was compared against NT T-cells stained using the same antibody.

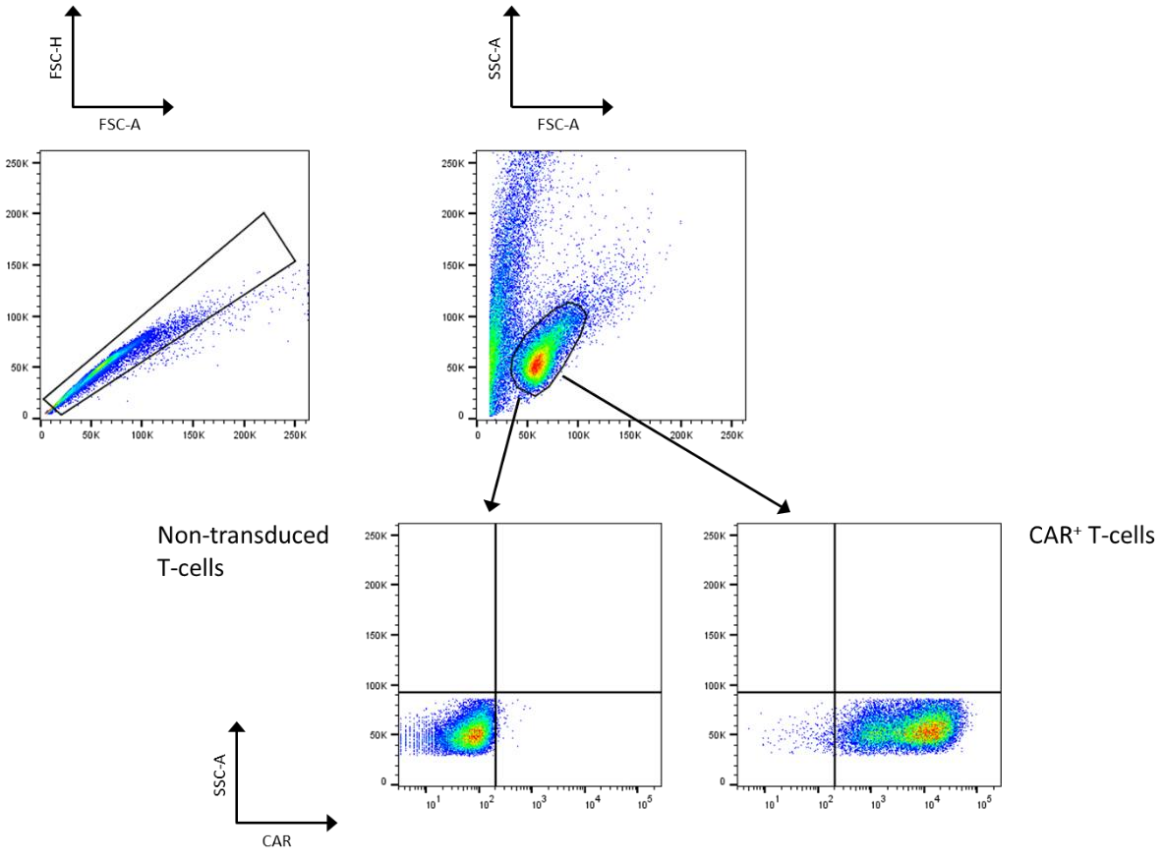

Gating strategy used to verify CAR expression on T-cells. Representative flow cytometry plots illustrating the gating strategy for assessment of CAR transduction efficiency of T-cells. Gating strategy used to identify singlet (top left), viable (top right) T-cell populations. CAR^+ T-cells were gated with reference to non-transduced control T-cells (bottom).

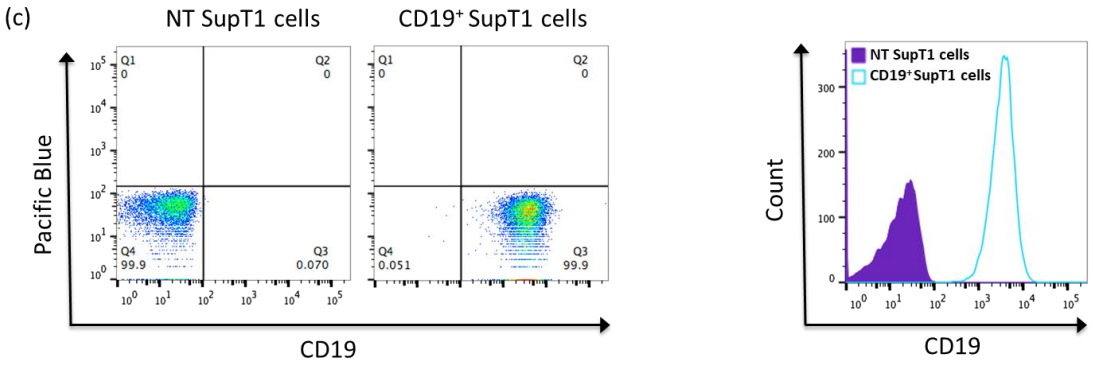

(c) Level of CD19 expression on target cell surface. SupT1 cells were used as target cells in co-culture assays. Non-transduced SupT1 were transduced to stably express CD19. The cells were investigated for the presence of CD19 using flow cytometry. The expression of CD19 was detected using an anti-human CD19 antibody. The level of CD19 expression was compared with that displayed by the NT SupT1 cells stained with the same antibody.

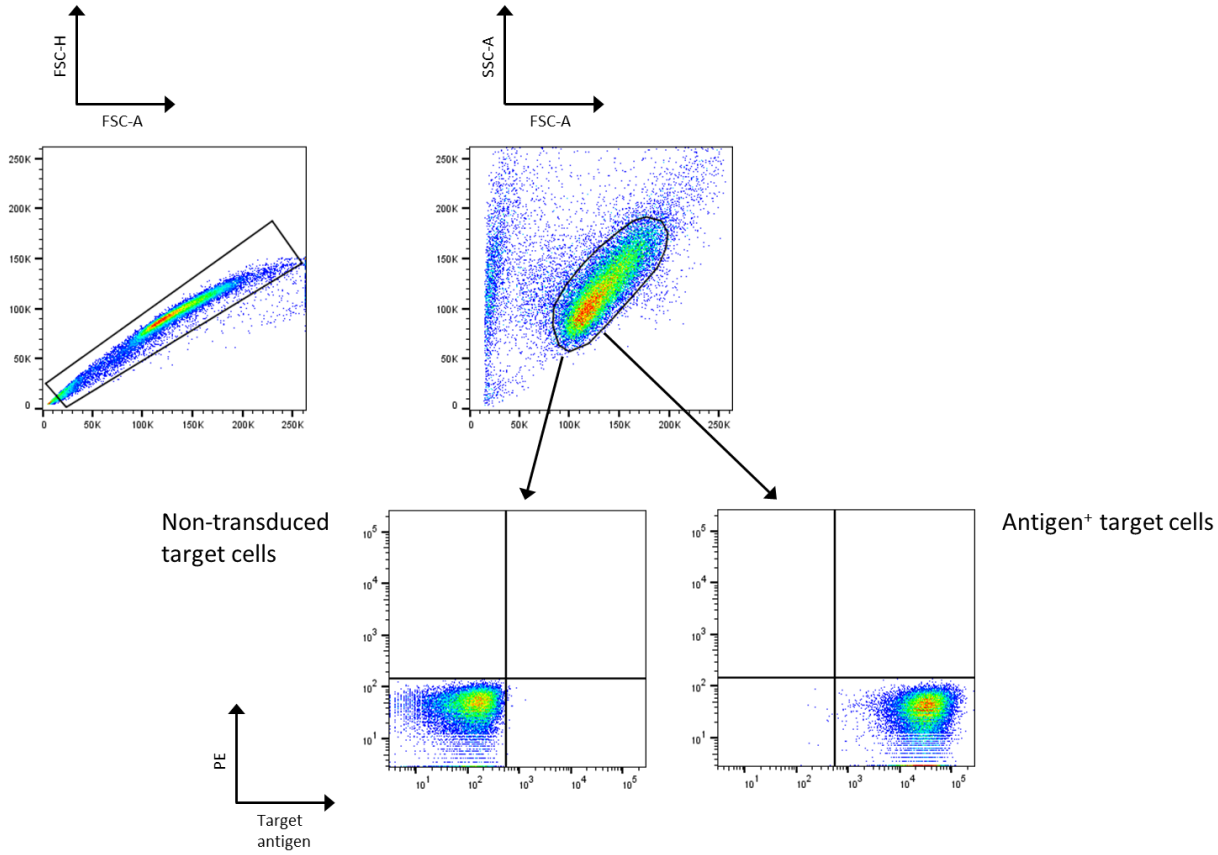

Gating strategy used to quantify antigen expression on target cells. Representative flow cytometry plots illustrating the gating strategy for assessment of the levels of antigen expression on target cell surface. Gating strategy used to identify singlet (top left), viable (top right) target cell populations. Antigen^{+} target cells were gated with reference to non-transduced control target cells (bottom).

(d)

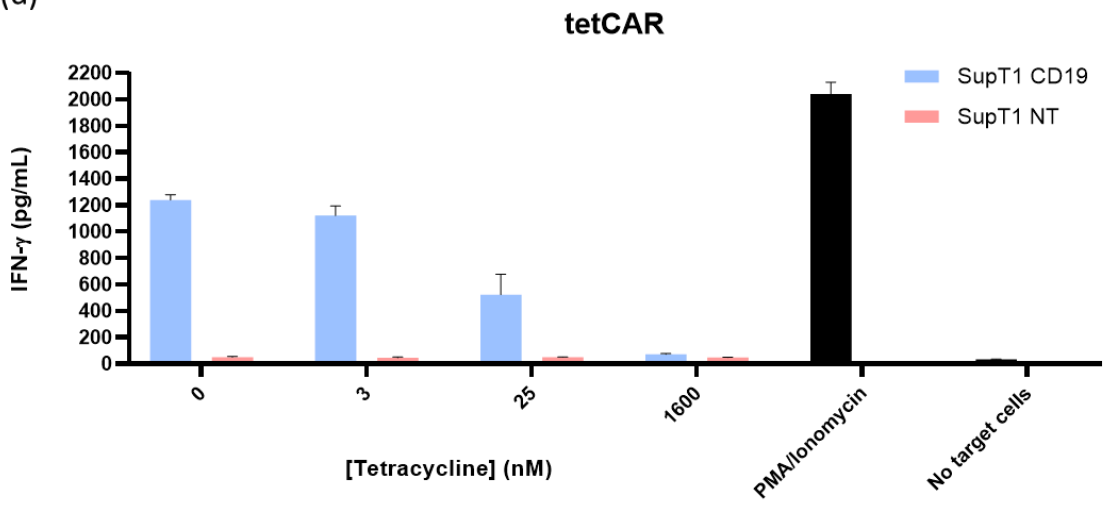

(d) Response of CD19-targeting tetCAR to tetracycline and antigen stimulation. Primary human T-cells expressing the CD19-targeting tetCAR were challenged with wild-type SupT1 cells or SupT1 cells engineered to express CD19 at a 1:1 T-cell:target cell ratio in the absence of tetracycline or in the presence of different concentrations of tetracycline. Production of IFN-γ after an overnight incubation was quantified by ELISA; n = 3 independent experiments from separate donors, error bars denote SD.

(e)

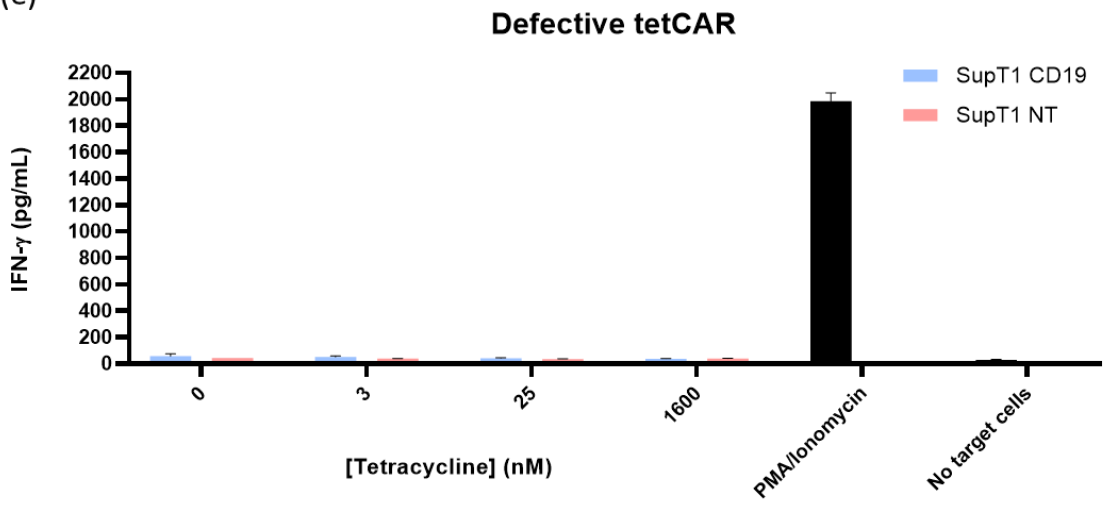
Defective tetCAR
SupT1 CD19
SupT1 NT
IFN-γ (pg/mL)
2200
2000
1800
1600
1400
1200
1000
800
600
400
200
0
0
3
25
1600
PMA/Ionomycin
No target cells
[Tetracycline] (nM)

(f)

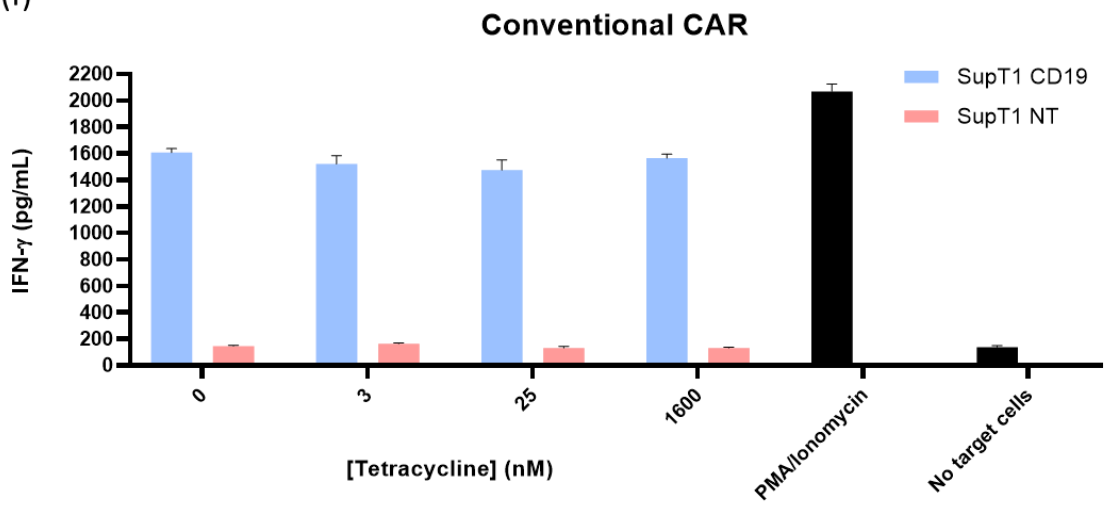
Conventional CAR
SupT1 CD19
SupT1 NT
IFN-γ (pg/mL)
2200
2000
1800
1600
1400
1200
1000
800
600
400
200
0
0
3
25
1600
PMA/Ionomycin
No target cells
[Tetracycline] (nM)

(g)

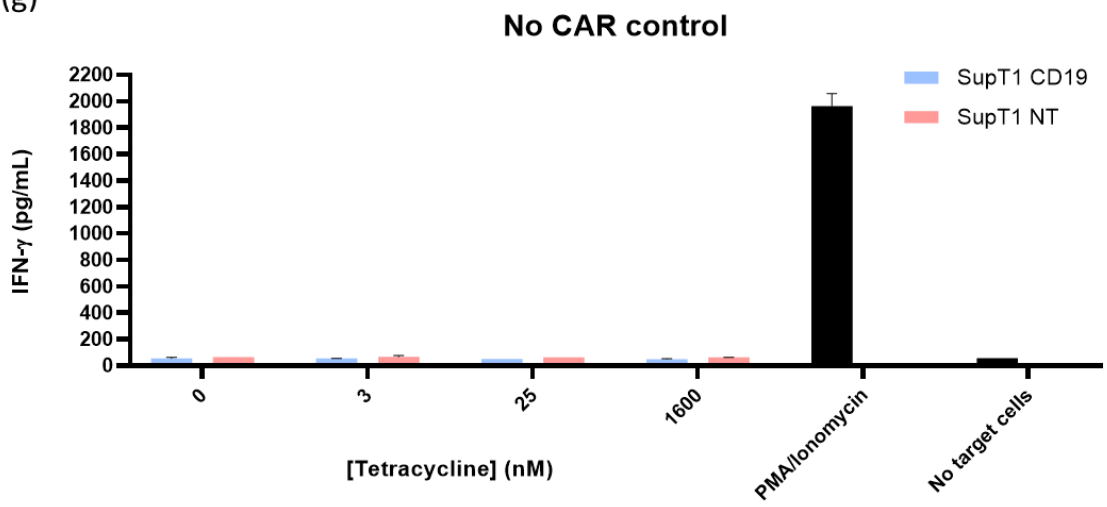

(e) Primary human T-cells expressing the defective tetCAR, (f) primary human T-cells expressing the conventional CAR and (g) non-transduced T-cells were also challenged with wild-type SupT1 cells or SupT1 cells engineered to express CD19 at a 1:1 T-cell:target cell ratio in the absence of tetracycline or in the presence of different concentrations of tetracycline.

4.4 Discussion

In this chapter, we have demonstrated that the tetCAR architecture functions with different binding domains. After confirming the responsiveness to tetracycline and antigen-specific IL-2 release of the initial CD33-targeting version of the tetCAR construct in BW5 murine T-cells, we demonstrated that expression of the same CD33-targeting tetCAR in therapeutically relevant T-cells leads to the loss of functional activity. A possible explanation for this is the potential unstable anti-CD33 scFv, suggesting that stabilization of the binding domains is required to allow full activity. Consequently, we explored replacing the anti-CD33 scFv by an optimised anti-CD19 scFv called FMC63 [106].

After reconstructing the system, we demonstrated that the CD19-targeting version of the tetCAR construct functions in both primary human T-cells and BW5 murine T-cells. Testing of this new tetCAR, in therapeutically relevant T-cells, showed good function and responsiveness to tetracycline but lower cytokine secretion in the absence of tetracycline compared with the conventional CAR, thus suggesting a reduced activation maximum.

As a consequence of these findings, further investigations into the optimal configuration of tetCAR are crucial, and so will be discussed in Chapters 5 and 6.

CHAPTER 5

EFFECT OF SPLITTING CO-STIMULATION

5.1 Function of alternative implementations of the tetCAR construct in primary human T-cells

In addition to testing the effect of alternative antigen-binding domains on the tetCAR function, it was of interest to further investigate the impact of other alternative implementations of the tetCAR, such as splitting co-stimulation. To achieve this, we successfully constructed a second and third-generation alternative implementation of the tetCAR (Figure 20 and Figure 21, respectively). This alternative implementation consisted of a single CAR which is expressed with multiple signalling components all of which comprise of TiP at their amino-terminus but a different individual signalling domain, in contrast to a compound signalling domain. In the case of the second-generation tetCAR, the two different signalling domains comprise of a fusion between TiP and the CD28 endodomain and a fusion between TiP and the CD3-Zeta endodomain (Figure 20a). In the case of the third-generation tetCAR, an additional signalling domain, a fusion between TiP and the OX40 endodomain, is present (Figure 21a). In order to test this, we expressed the two CD19-targeting tetCARs in primary human T-cells and examined the production of the cytokine IFN-γ. These experiments, including the one presented in Figure 19, were carried out in parallel.

Firstly, we analysed the transduction efficiency of the primary human T-cells by flow cytometry. As shown in Figures 20b and 21b, both CD19-targeting tetCARs could be detected at the cell surface, thus indicating that these constructs were both expressed and trafficked correctly to the plasma membrane. Cell surface expression of the defective tetCARs and conventional CARs was also detected. In order to test the function of both CD19-targeting tetCAR constructs in primary human T-cells, we co-cultured primary human T-cells expressing each of the tetCARs with wild-type SupT1 cells or SupT1 cells engineered to express CD19 at a 1:1 T-cell:target cell ratio in the absence of tetracycline or in the presence of different concentrations of tetracycline (Figures 20d and 21c). Primary human T-cells expressing the defective tetCARs (Figures 20e and 21d) and primary human T-cells expressing the conventional CARs (Figures 20f and 21e) were also tested. Furthermore, T-cells from the same donor that had not undergone gene transfer (designated non-transduced T-cells) were set up to serve as an additional control (Figures 20g and 21f).

After an overnight incubation, supernatant samples were removed and assayed for the presence of IFN-γ. Subsequent investigations into the release of IFN-γ showed that tetracycline decreases human T-cell IFN-γ secretion and hence activation in a dose dependent manner. The experiments were carried out using 3 nM, 25 nM and 1600 nM as tetracycline concentrations. Both conventional CARs led to consistent secretion of IFN-γ by primary human T-cells in all tetracycline concentrations (Figures 20f and 21e). As expected, minimal IFN-γ secretion by defective tetCAR T-cells was detected on either SupT1 CD19 or SupT1 NT cells (Figures 20e and 21d). Similar results were observed with the non-transduced T-cells (Figures 20g and 21f). In both tetracycline inducible CARs (also known as tetCARs), the amount of secreted IFN-γ was found to decrease with increasing concentrations of tetracycline (Figures 20d and 21c). In the absence of tetracycline, IFN-γ secretion by the second-generation tetCAR T-cells was slightly higher to that seen with the third-generation tetCAR T-cells. In the presence of 1600 nM tetracycline, minimal IFN-γ secretion by both tetCAR T-cells was detected on either SupT1 CD19 or SupT1 NT cells. PMA and ionomycin stimulated primary human T-cells showed the highest levels of IFN-γ secretion.

These findings confirm that other alternative implementations of the tetCAR are also functional and capable of activating primary human T-cells.

Figure 20

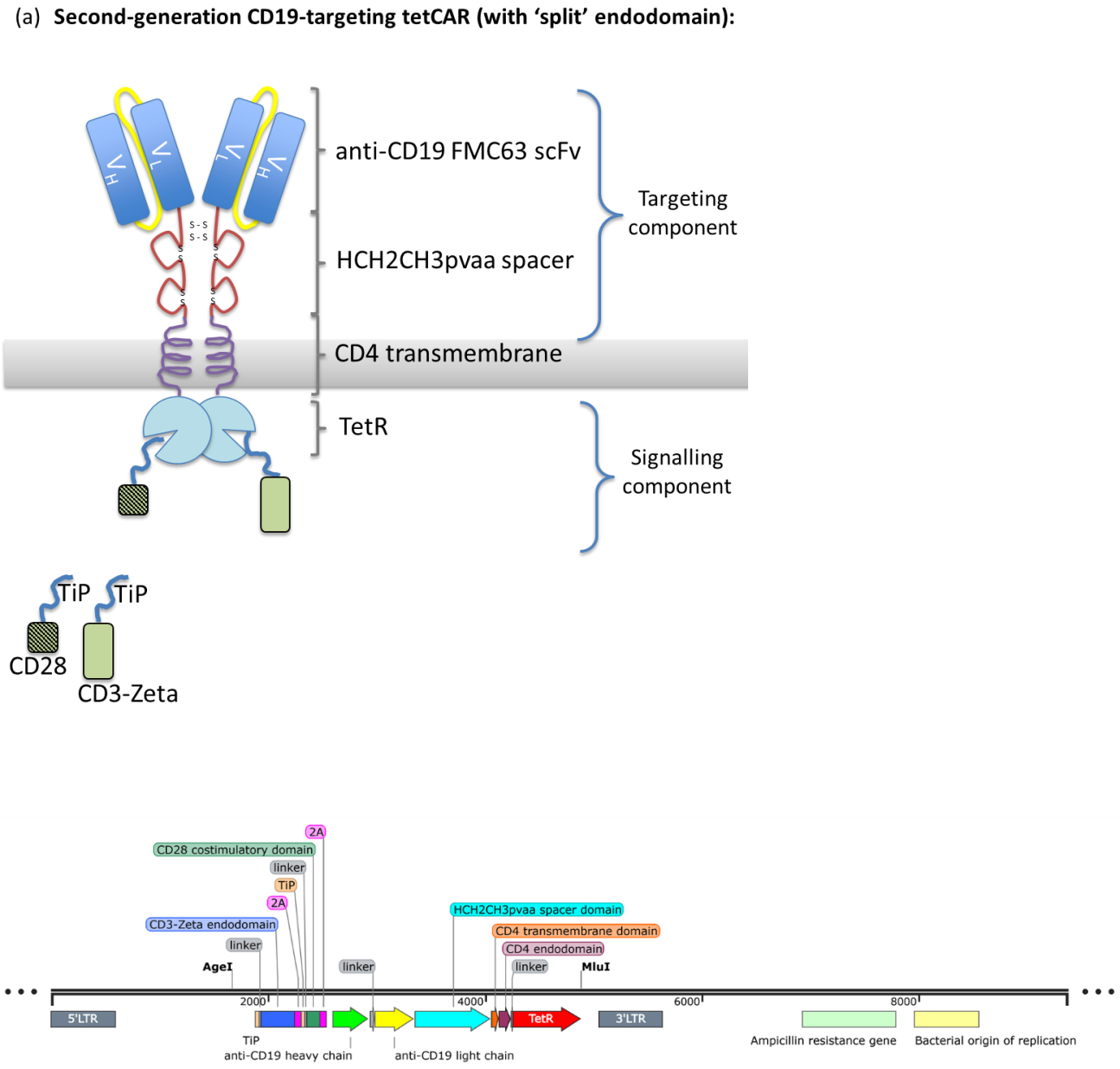

Figure 20. Function of a second-generation alternative implementation of the tetCAR construct in primary human T-cells. (a) Schematic diagram illustrating the second-generation alternative implementation of the tetCAR (top). A single CAR is expressed with multiple signalling components all of which comprise of TiP (dark blue) at their amino-terminus but a different individual signalling domain, in contrast to a compound signalling domain. The two different signalling domains comprise of a fusion between TiP and the CD28 endodomain (diagonal stripes) and a fusion between TiP and the CD3-Zeta endodomain (light green). These randomly interact with the

receptor component, which comprises of a CD19 recognizing scFv (blue), a spacer derived from the Fc domain of IgG1 (red), a CD4 derived transmembrane and intracellular domain (purple), and TetR (light blue). Additionally, the plasmid map of the second-generation CD19-targeting tetCAR (with 'split' endodomain) is also shown (bottom).

(b) **Primary human T-cells:**

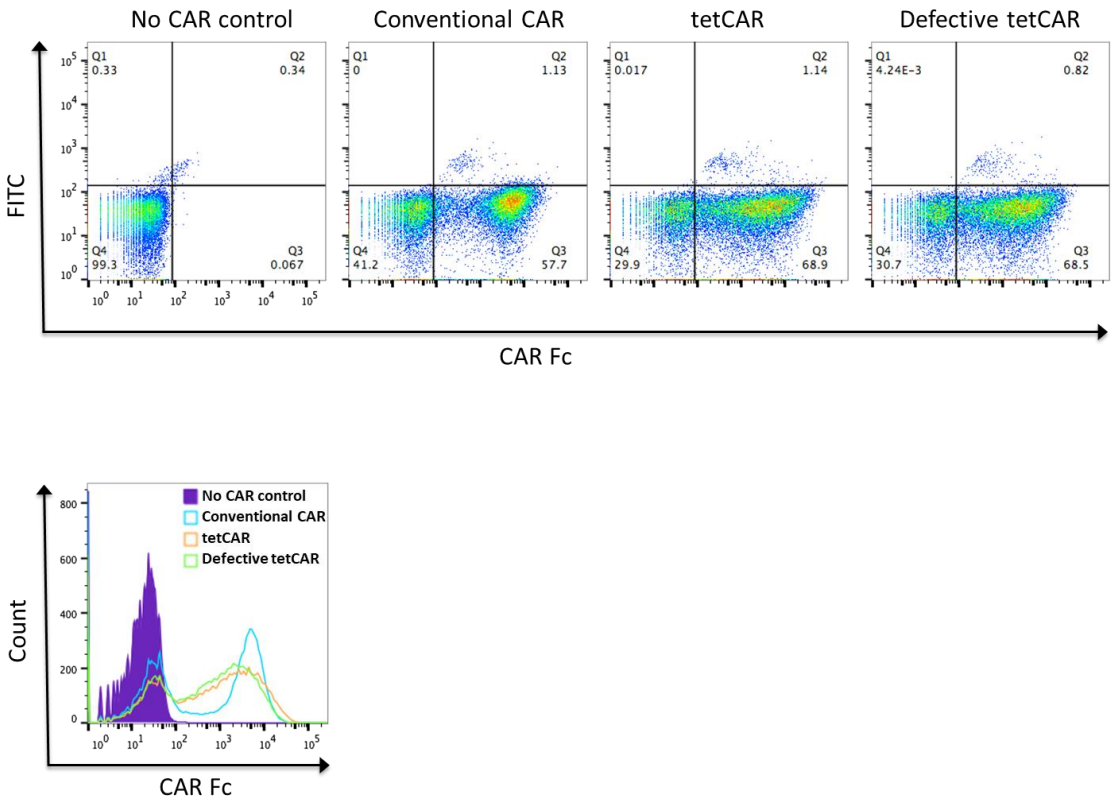

(b) Expression levels of CARs in primary human T-cells. Cells engineered with retroviral constructs encoding CAR molecules were analysed by flow cytometry. Expression of the tetCAR at the surface of primary human T-cells was compared with the expression of defective tetCAR (with absent TiP domain) and conventional CAR. The CARs were detected with an anti-human IgG antibody. Staining was compared against NT T-cells stained using the same antibody.

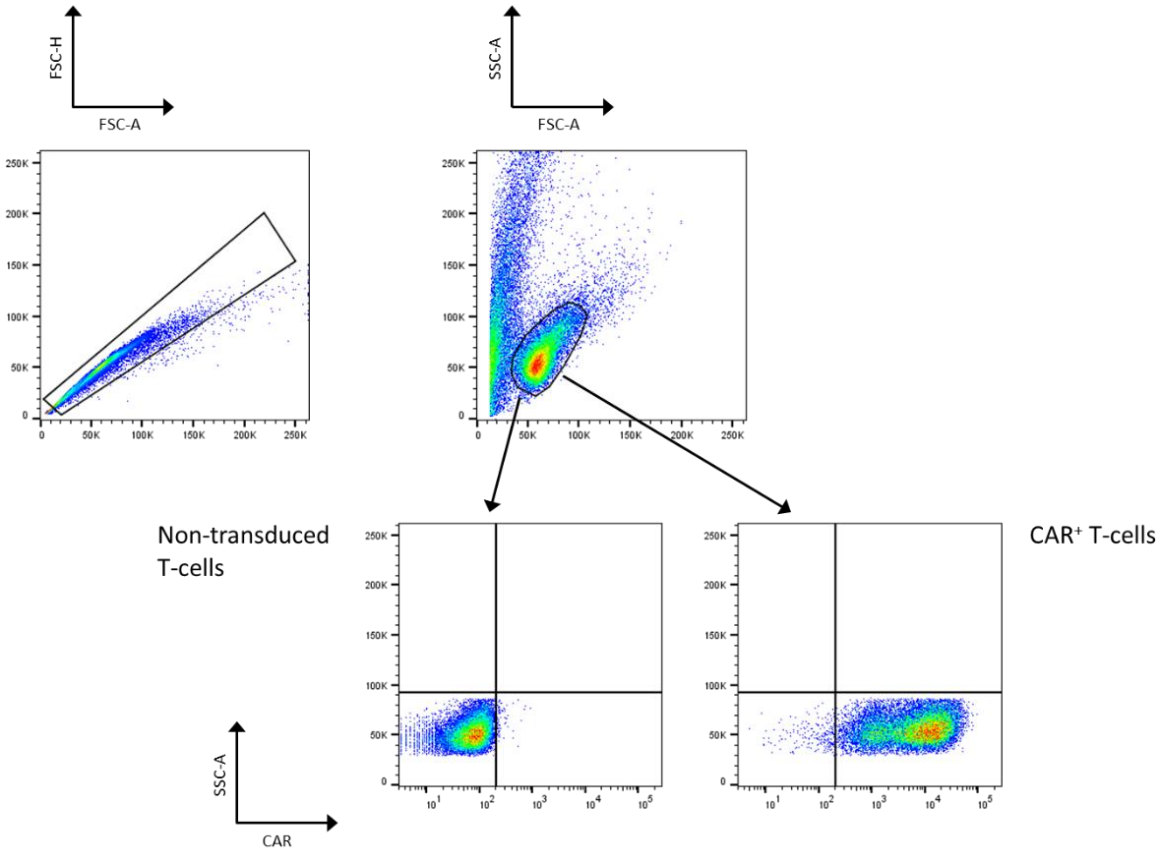

Gating strategy used to verify CAR expression on T-cells. Representative flow cytometry plots illustrating the gating strategy for assessment of CAR transduction efficiency of T-cells. Gating strategy used to identify singlet (top left), viable (top right) T-cell populations. CAR^+ T-cells were gated with reference to non-transduced control T-cells (bottom).

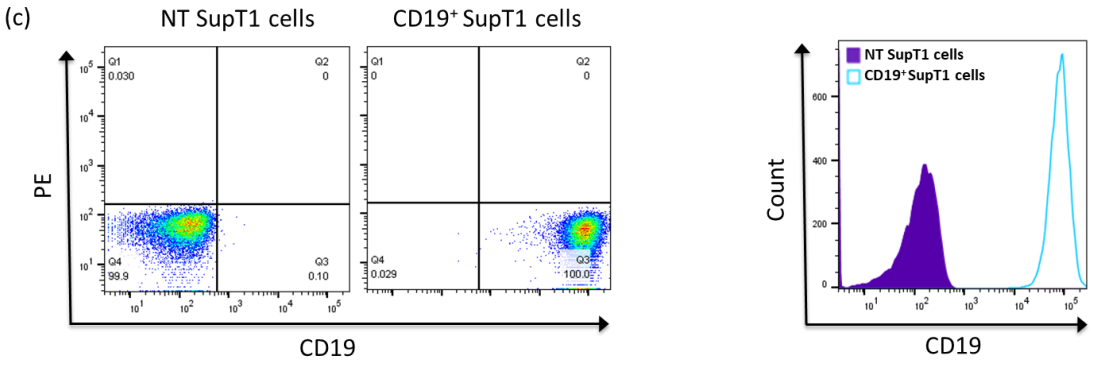

(c) Level of CD19 expression on target cell surface. SupT1 cells were used as target cells in co-culture assays. Non-transduced SupT1 were transduced to stably express CD19. The cells were investigated for the presence of CD19 using flow cytometry. The expression of CD19 was detected using an anti-human CD19 antibody. The level of CD19 expression was compared with that displayed by the NT SupT1 cells stained with the same antibody.

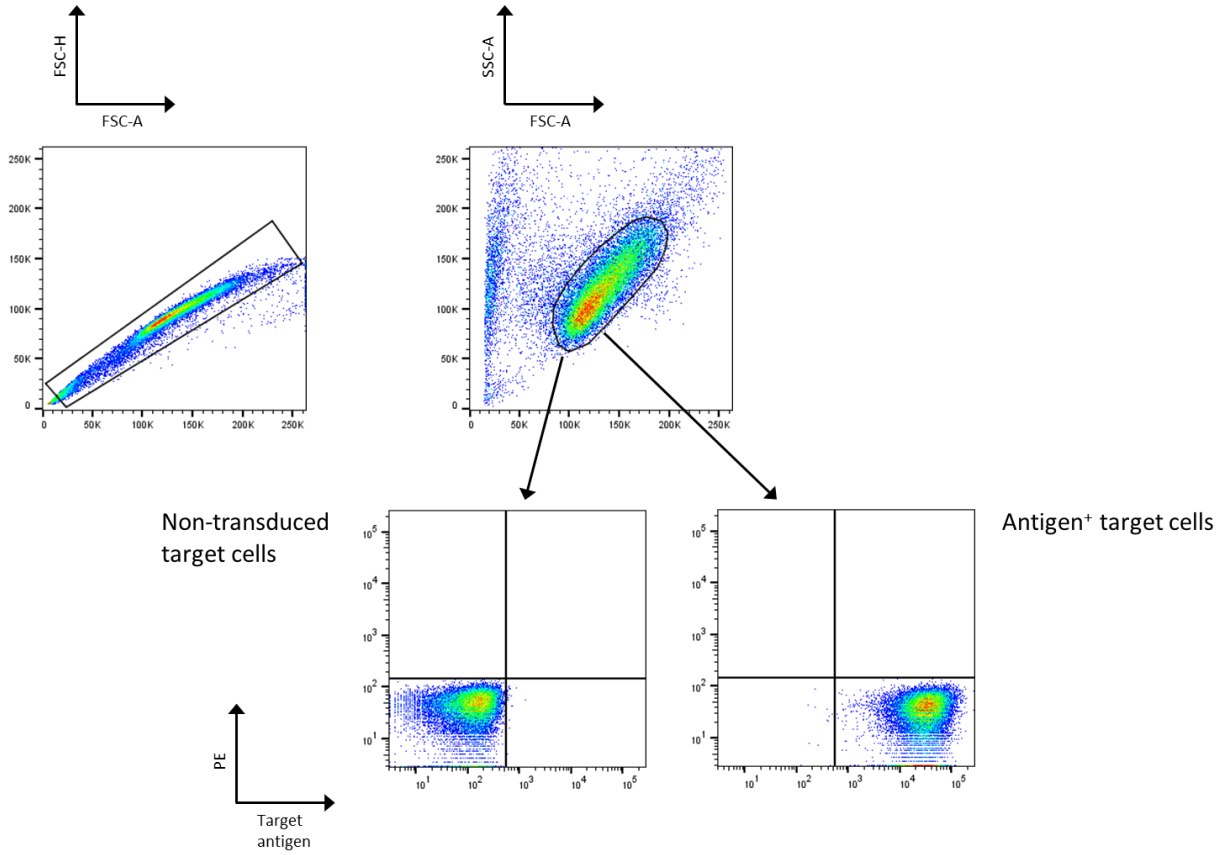

Gating strategy used to quantify antigen expression on target cells. Representative flow cytometry plots illustrating the gating strategy for assessment of the levels of antigen expression on target cell surface. Gating strategy used to identify singlet (top left), viable (top right) target cell populations. Antigen^{+} target cells were gated with reference to non-transduced control target cells (bottom).

(d)

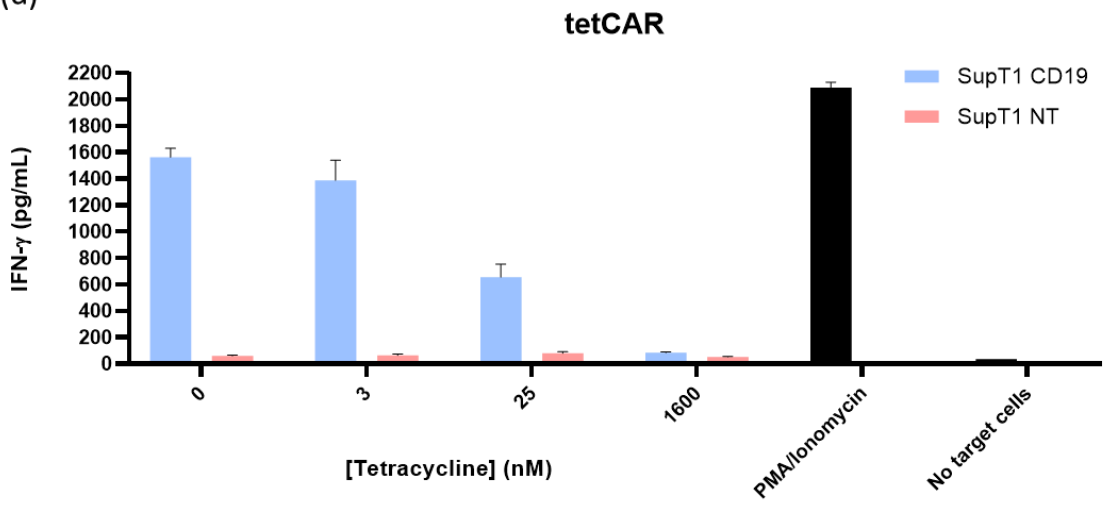

(d) Response of tetCAR to tetracycline and antigen stimulation. Primary human T-cells expressing the tetCAR were challenged with wild-type SupT1 cells or SupT1 cells engineered to express CD19 at a 1:1 T-cell:target cell ratio in the absence of tetracycline or in the presence of different concentrations of tetracycline. Production of IFN-γ after an overnight incubation was quantified by ELISA; n = 3 independent experiments from separate donors, error bars denote SD.

(e)

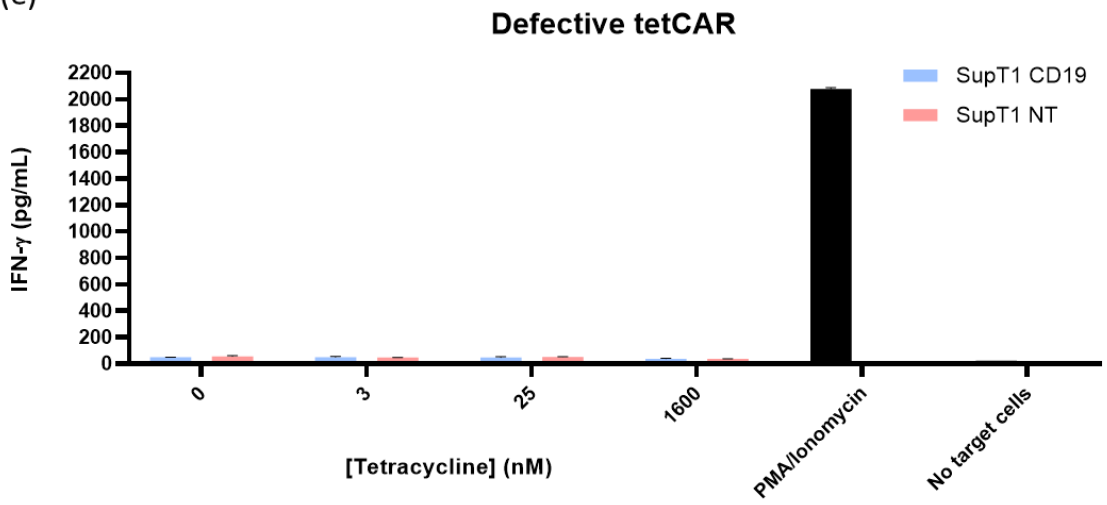
Defective tetCAR
SupT1 CD19
SupT1 NT
IFN-γ (pg/mL)
2200
2000
1800
1600
1400
1200
1000
800
600
400
200
0
0
3
25
1600
PMA/Ionomycin
No target cells
[Tetracycline] (nM)

(f)

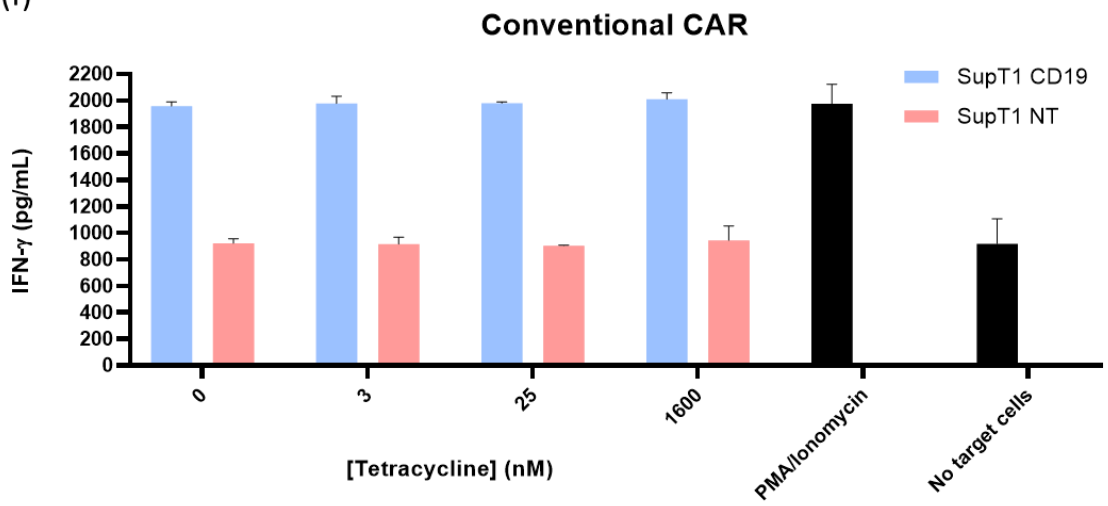
Conventional CAR
SupT1 CD19
SupT1 NT
IFN-γ (pg/mL)
2200
2000
1800
1600
1400
1200
1000
800
600
400
200
0
0
3
25
1600
PMA/Ionomycin
No target cells
[Tetracycline] (nM)

(g)

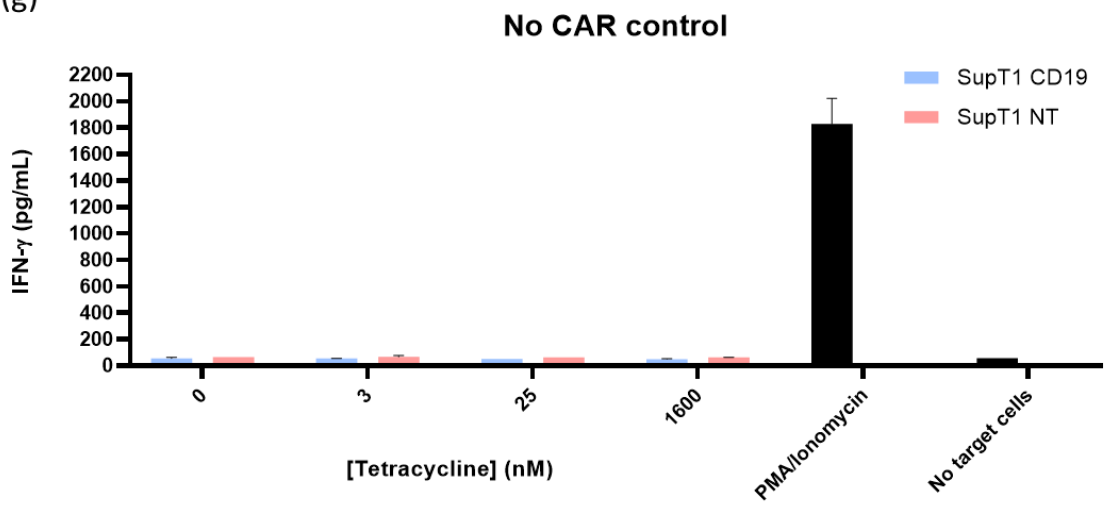

(e) Primary human T-cells expressing the defective tetCAR, (f) primary human T-cells expressing the conventional CAR and (g) non-transduced T-cells were also challenged with wild-type SupT1 cells or SupT1 cells engineered to express CD19 at a 1:1 T-cell:target cell ratio in the absence of tetracycline or in the presence of different concentrations of tetracycline.

Figure 21

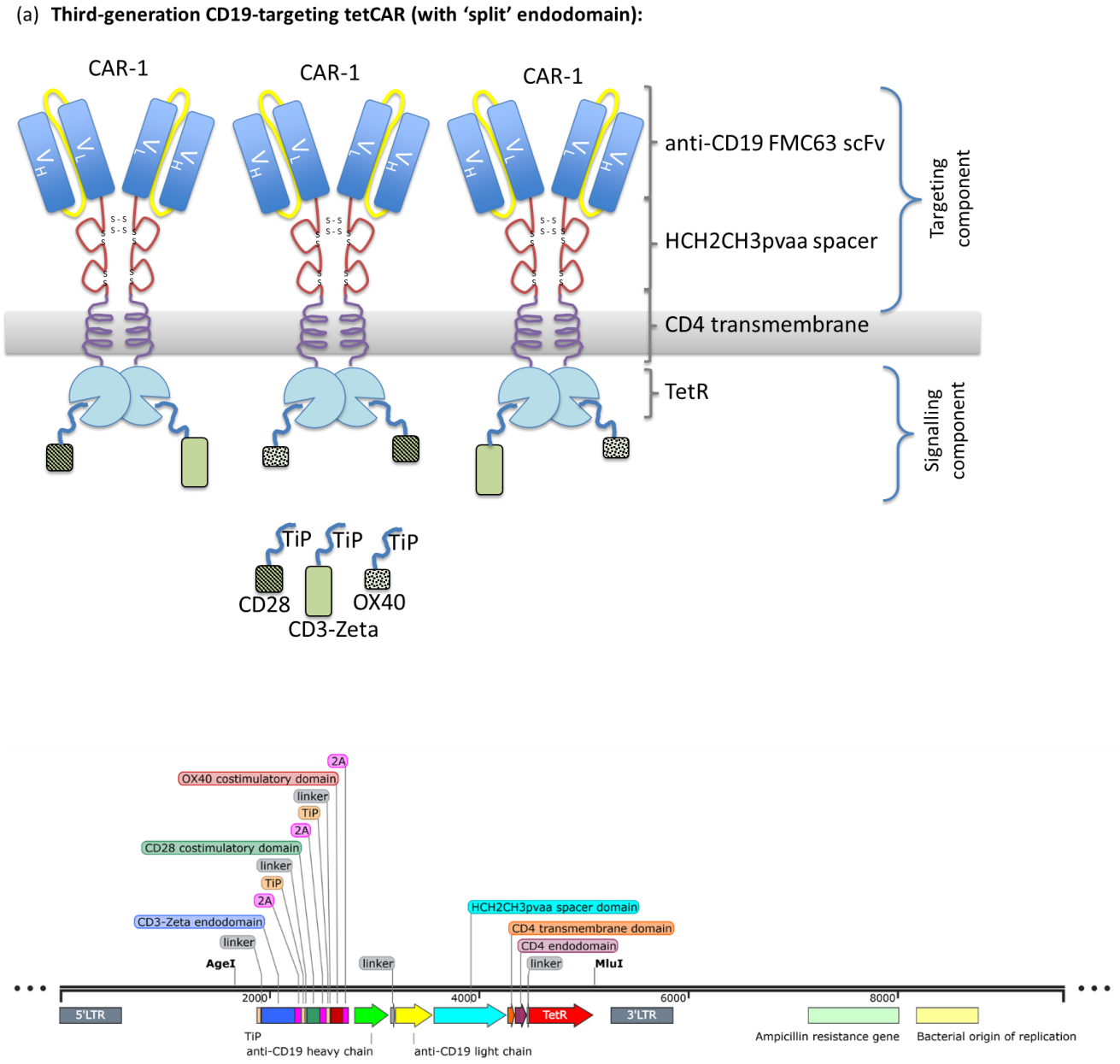

Figure 21. Function of a third-generation alternative implementation of the tetCAR construct in primary human T-cells. (a) Schematic diagram illustrating the third-generation alternative implementation of the tetCAR (top). A single CAR is expressed with multiple signalling components all of which comprise of TiP (dark blue) at their amino-terminus but a different individual signalling domain, in contrast to a compound signalling domain. The three different signalling domains comprise of a fusion between TiP and the CD28 endodomain (diagonal stripes), a fusion between TiP and the OX40 endodomain (large confetti) and a fusion between TiP and the CD3-Zeta

endodomain (light green). These randomly interact with the receptor component, which comprises of a CD19 recognizing scFv (blue), a spacer derived from the Fc domain of IgG1 (red), a CD4 derived transmembrane and intracellular domain (purple), and TetR (light blue). Additionally, the plasmid map of the third-generation CD19-targeting tetCAR (with 'split' endodomain) is also shown (bottom).

(b) **Primary human T-cells:**

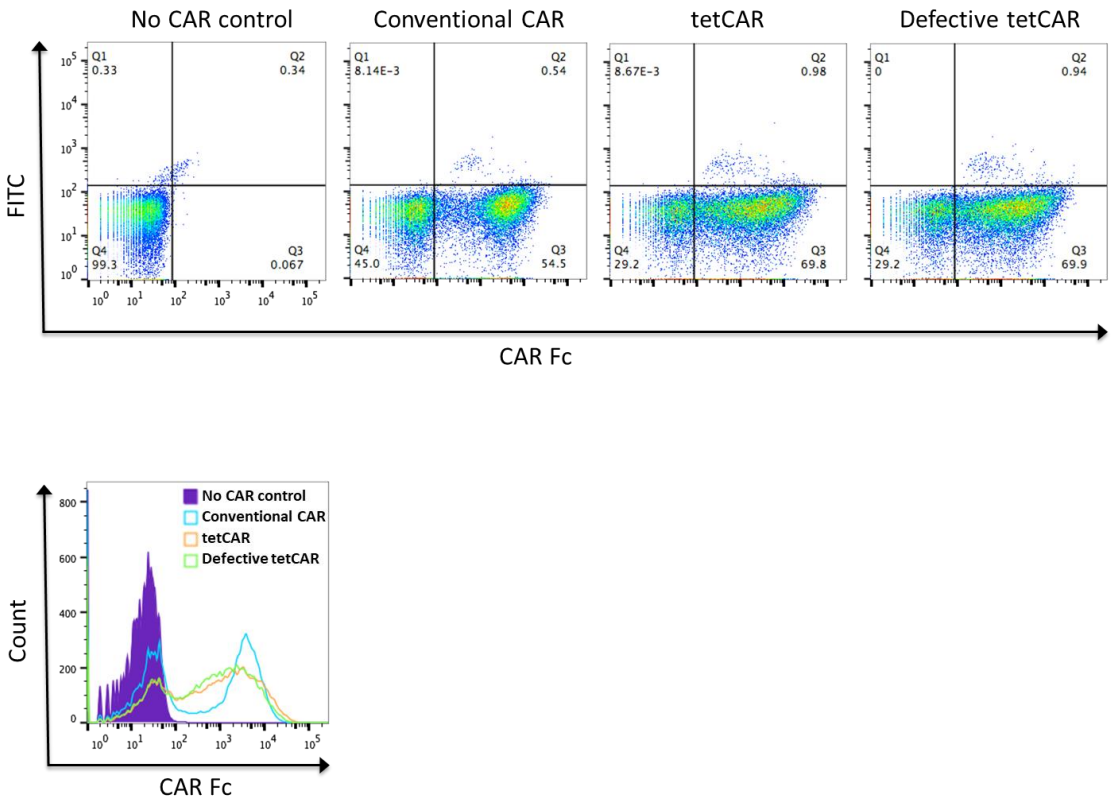

(b) Expression levels of CARs in primary human T-cells. Cells engineered with retroviral constructs encoding CAR molecules were analysed by flow cytometry. Expression of the tetCAR at the surface of primary human T-cells was compared with the expression of defective tetCAR (with absent TiP domain) and conventional CAR. The CARs were detected with an anti-human IgG antibody. Staining was compared against NT T-cells stained using the same antibody.

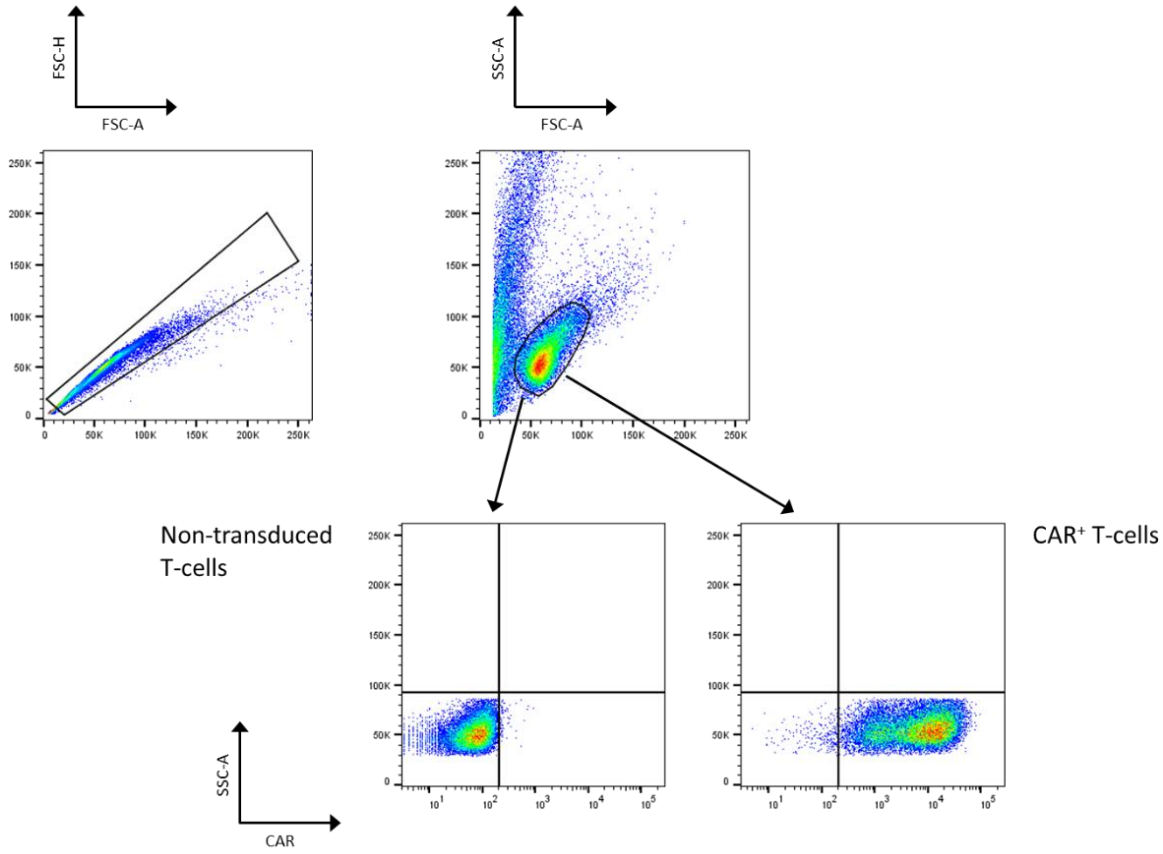

Gating strategy used to verify CAR expression on T-cells. Representative flow cytometry plots illustrating the gating strategy for assessment of CAR transduction efficiency of T-cells. Gating strategy used to identify singlet (top left), viable (top right) T-cell populations. CAR^+ T-cells were gated with reference to non-transduced control T-cells (bottom).

(c)

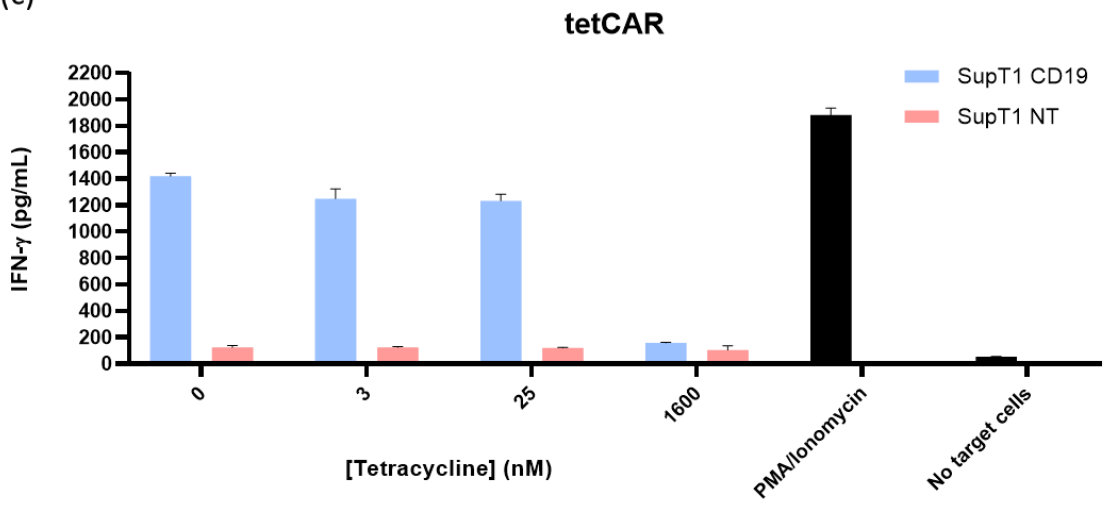

(c) Response of tetCAR to tetracycline and antigen stimulation. Primary human T-cells expressing the tetCAR were challenged with wild-type SupT1 cells or SupT1 cells engineered to express CD19 at a 1:1 T-cell:target cell ratio in the absence of tetracycline or in the presence of different concentrations of tetracycline. Production of IFN-γ after an overnight incubation was quantified by ELISA; n = 3 independent experiments from separate donors, error bars denote SD.

(d)

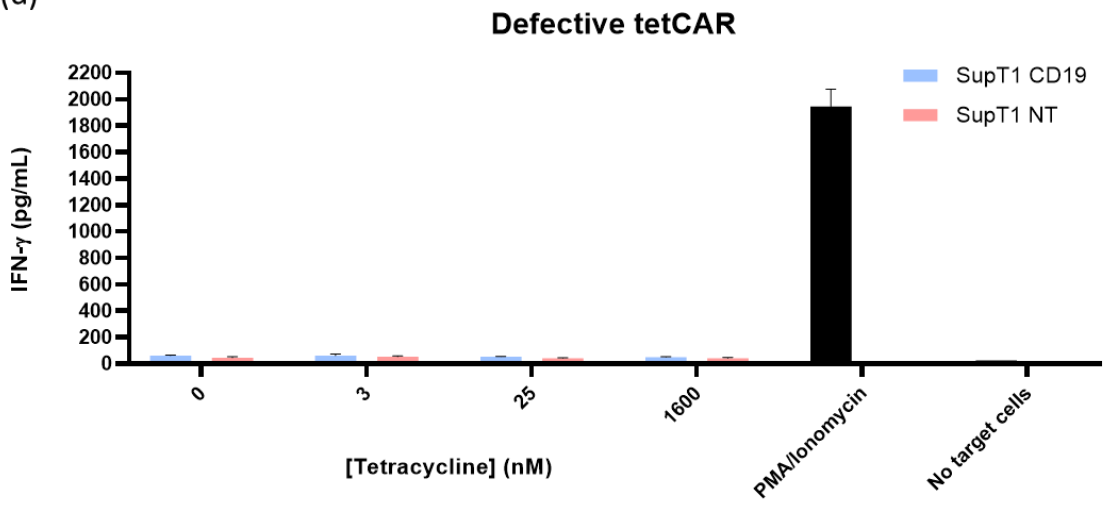
Defective tetCAR
SupT1 CD19
SupT1 NT
IFN-γ (pg/mL)
2200
2000
1800
1600
1400
1200
1000
800
600
400
200
0
0
3
25
1600
PMA/Ionomycin
No target cells
[Tetracycline] (nM)

(e)

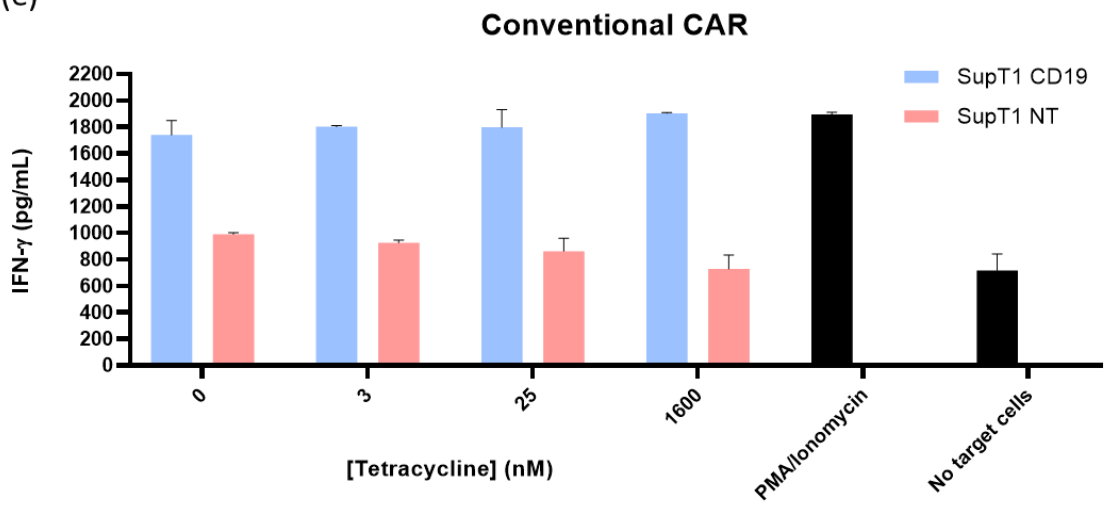
Conventional CAR
SupT1 CD19
SupT1 NT
IFN-γ (pg/mL)
2200
2000
1800
1600
1400
1200
1000
800
600
400
200
0
0
3
25
1600
PMA/Ionomycin
No target cells
[Tetracycline] (nM)

(f)

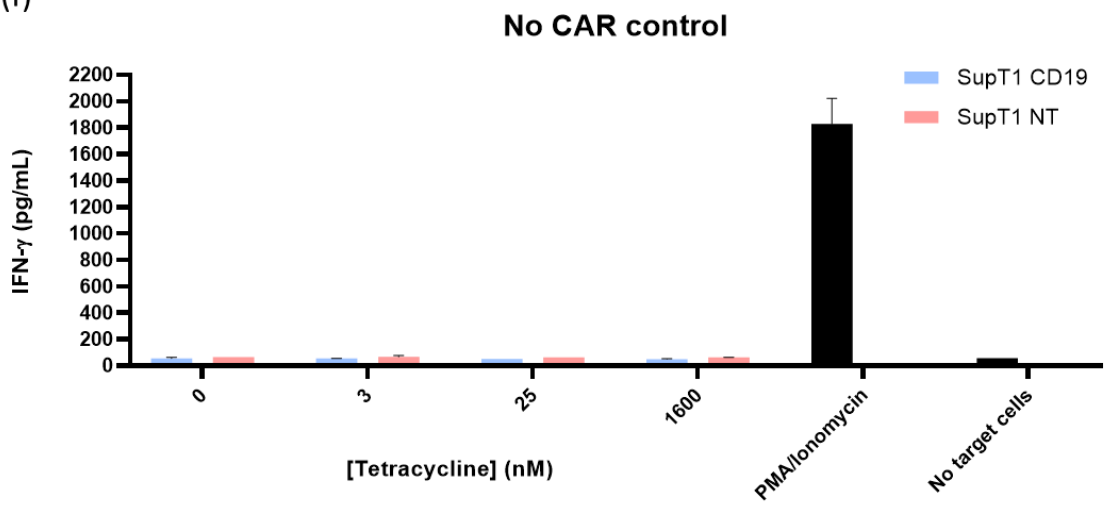

(d) Primary human T-cells expressing the defective tetCAR, (e) primary human T-cells expressing the conventional CAR and (f) non-transduced T-cells were also challenged with wild-type SupT1 cells or SupT1 cells engineered to express CD19 at a 1:1 T-cell:target cell ratio in the absence of tetracycline or in the presence of different concentrations of tetracycline.

5.2 Cytotoxicity activity mediated by tetCAR constructs with different types of endodomain in primary human T-cells

A major purpose of CARs is to redirect primary human T-cell cytotoxicity selectively towards target cells expressing antigens of interest. Therefore, to test whether the above alternative implementation of the tetCAR would function better than the conventional single signalling component tetCAR, we next determined their ability to kill target cells. As the above data showed no significant difference between the second and third-generation tetCARs, it was decided to use the second-generation tetCAR on this experiment. We therefore compared two different second-generation tetCAR constructs. One, a single CAR which is expressed with multiple signalling components all of which comprise of TiP at their amino-terminus but a different individual signalling domain (Figure 22a). The other, a single CAR which is expressed with only one signalling component (Figure 22b). In order to test cell killing, we expressed the two CD19-targeting tetCARs in primary human T-cells and performed a flow cytometry-based cell-killing assay.

Firstly, we analysed the transduction efficiency of the primary human T-cells by flow cytometry. As shown in Figure 22c, both tetCARs (named 'Split' tetCAR and 'Non-split' tetCAR) could be detected at the cell surface, thus indicating that these constructs were both expressed and trafficked correctly to the plasma membrane. Cell surface expression of the defective tetCARs and conventional CAR was also detected. Primary human T-cells expressing the tetCARs were co-cultured with SupT1 cells engineered to express CD19 at a 4:1 T-cell:target cell ratio in the absence of tetracycline or in the presence of 1600 nM tetracycline. Primary human T-cells expressing the conventional CAR were also tested. Furthermore, T-cells from the same donor that had not undergone gene transfer (designated non-transduced T-cells) were set up to serve as an additional control.

After incubation for a designated period of time, surviving target cells were quantified by flow cytometry. A low percentage for survival of $CD19^+$ SupT1 cells indicates a high degree of specific target cell killing by CAR T-cells. In the 72-hour end-point experiment, no cell killing mediated by 'Split' tetCAR T-cells was observed on either

absence or presence of tetracycline (Figure 22d). Similar results were observed with the non-transduced T-cells. On the other hand, slight killing of the $CD19^+$ target cells by 'Non-split' tetCAR T-cells was observed when in the absence of tetracycline. T-cells expressing the conventional CAR induced an efficient target cell killing on either absence or presence of tetracycline. With an extra 24 hours incubation (96-hour end-point experiment), target cell killing mediated by 'Split' tetCAR T-cells was detectable (Figure 22e). However, it was the 'Non-split' tetCAR T-cells that showed the highest degree of target cell killing between the two. In the presence of 1600 nM tetracycline, both tetCARs were completely switched off. A minimal survival of $CD19^+$ target cells was observed with the conventional CAR T-cells on either absence or presence of tetracycline.

Taken together, these data show that the 'Non-split' tetCAR T-cells present an increased ability to kill target cells when compared to the 'Split' tetCAR T-cells. However, even the degree of targeted cell killing by 'Non-split' tetCAR T-cells in the absence of tetracycline did not match the level observed with the conventional CAR T-cells.

Figure 22

(a) **Second-generation CD19-targeting tetCAR (with 'split' endodomain):**

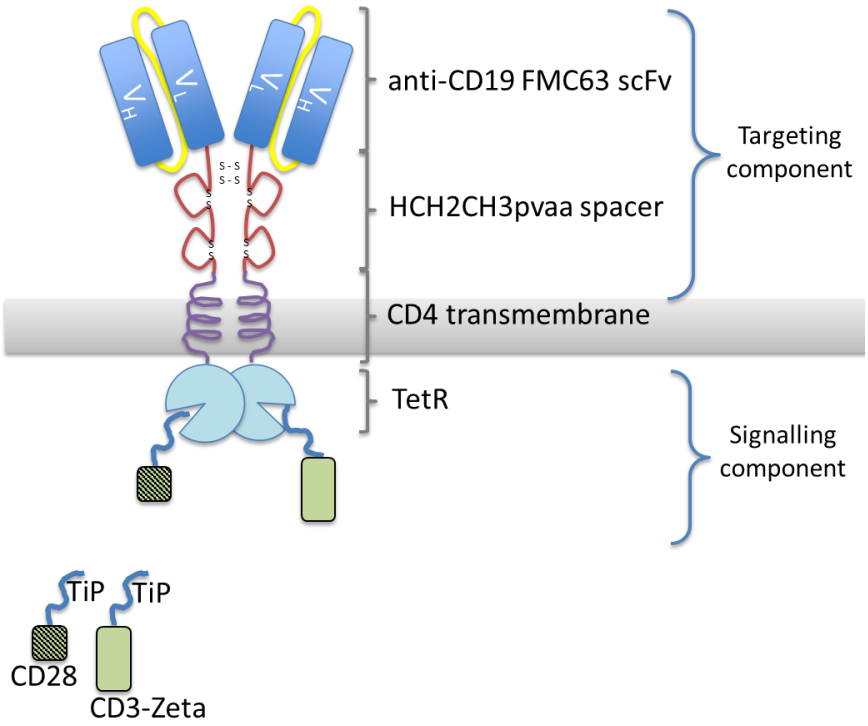

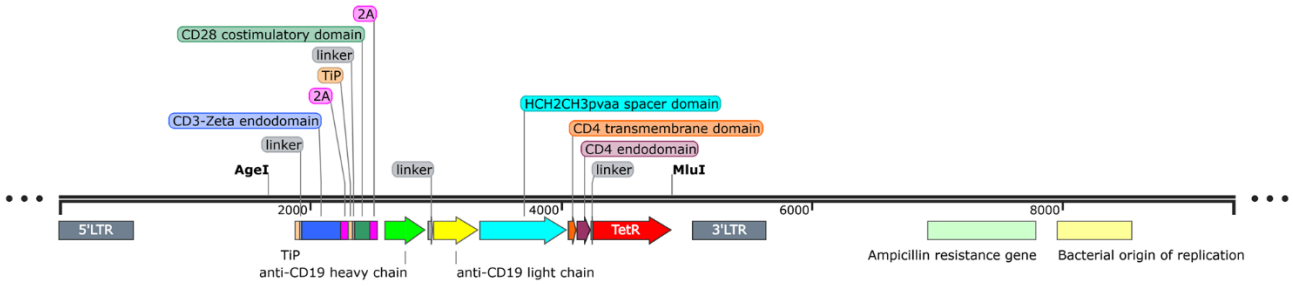

Figure 22. Cytotoxicity activity mediated by tetCAR constructs with different types of endodomain in primary human T-cells. (a) Schematic diagram illustrating the second-generation tetCAR with 'split' endodomain (top). A single CAR is expressed with multiple signalling components all of which comprise of TiP (dark blue) at their amino-terminus but a different individual signalling domain. The two different signalling domains comprise of a fusion between TiP and the CD28 endodomain (diagonal stripes) and a fusion between TiP and the CD3-Zeta endodomain (light green). These randomly interact with the receptor component, which comprises of a CD19 recognizing scFv (blue), a spacer derived from the Fc domain of IgG1 (red), a CD4 derived transmembrane and intracellular domain (purple),

and TetR (light blue). Additionally, the plasmid map of the second-generation CD19-targeting tetCAR (with 'split' endodomain) is also shown (bottom).

(b) **Second-generation CD19-targeting tetCAR (with 'non-split' endodomain):**

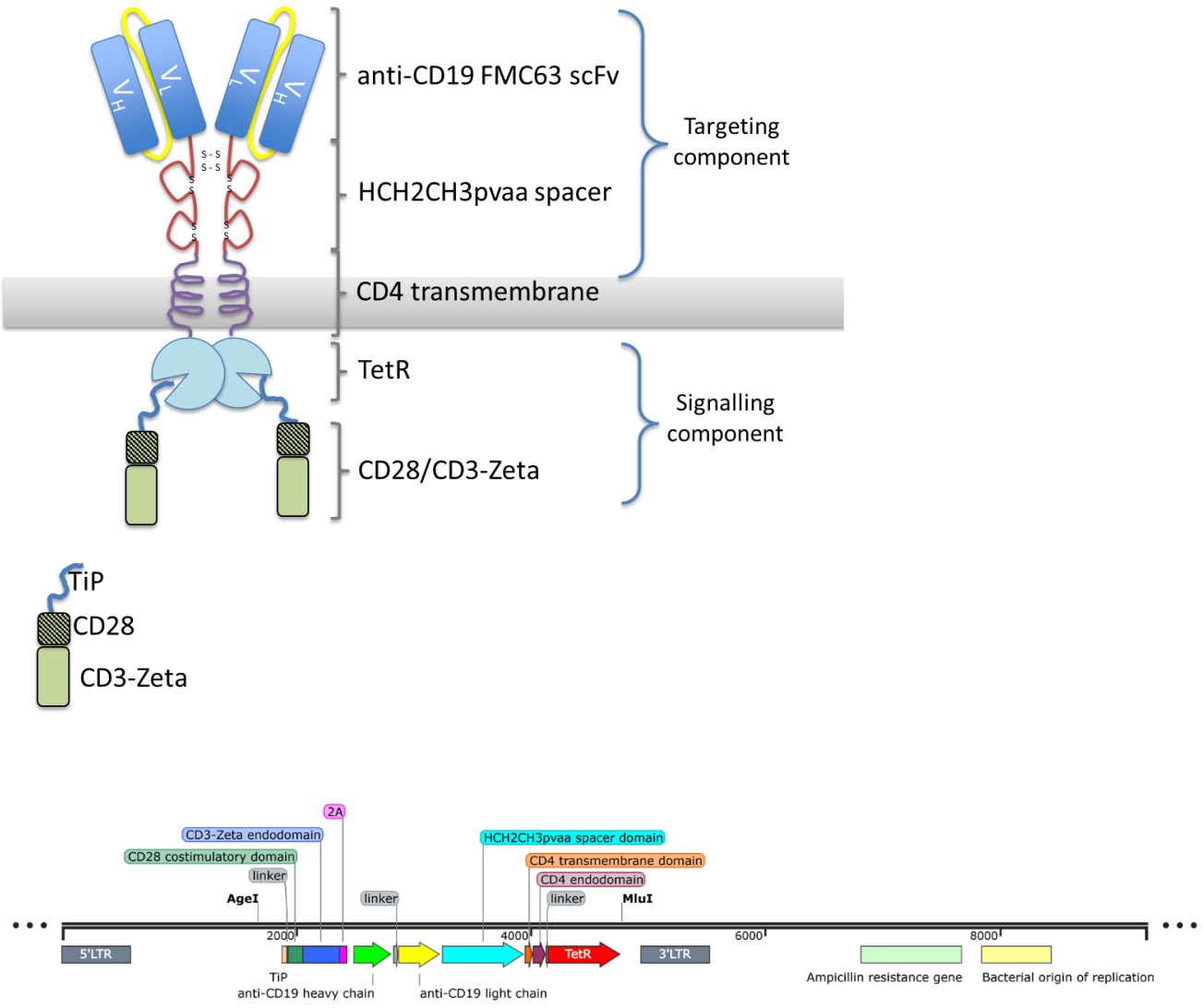

(b) Schematic diagram illustrating the second-generation tetCAR with 'non-split' endodomain (top). A single CAR is expressed with only one signalling component which comprises of TiP (dark blue) fused to the CD28 (diagonal stripes) and CD3-Zeta (light green) endodomain. The receptor component comprises of a CD19 recognizing scFv (blue), a spacer derived from the Fc domain of IgG1 (red), a CD4 derived transmembrane and intracellular domain (purple), and TetR (light blue). Additionally, the plasmid map of the second-generation CD19-targeting tetCAR (with 'non-split' endodomain) is also shown (bottom).

(c) **Primary human T-cells:**

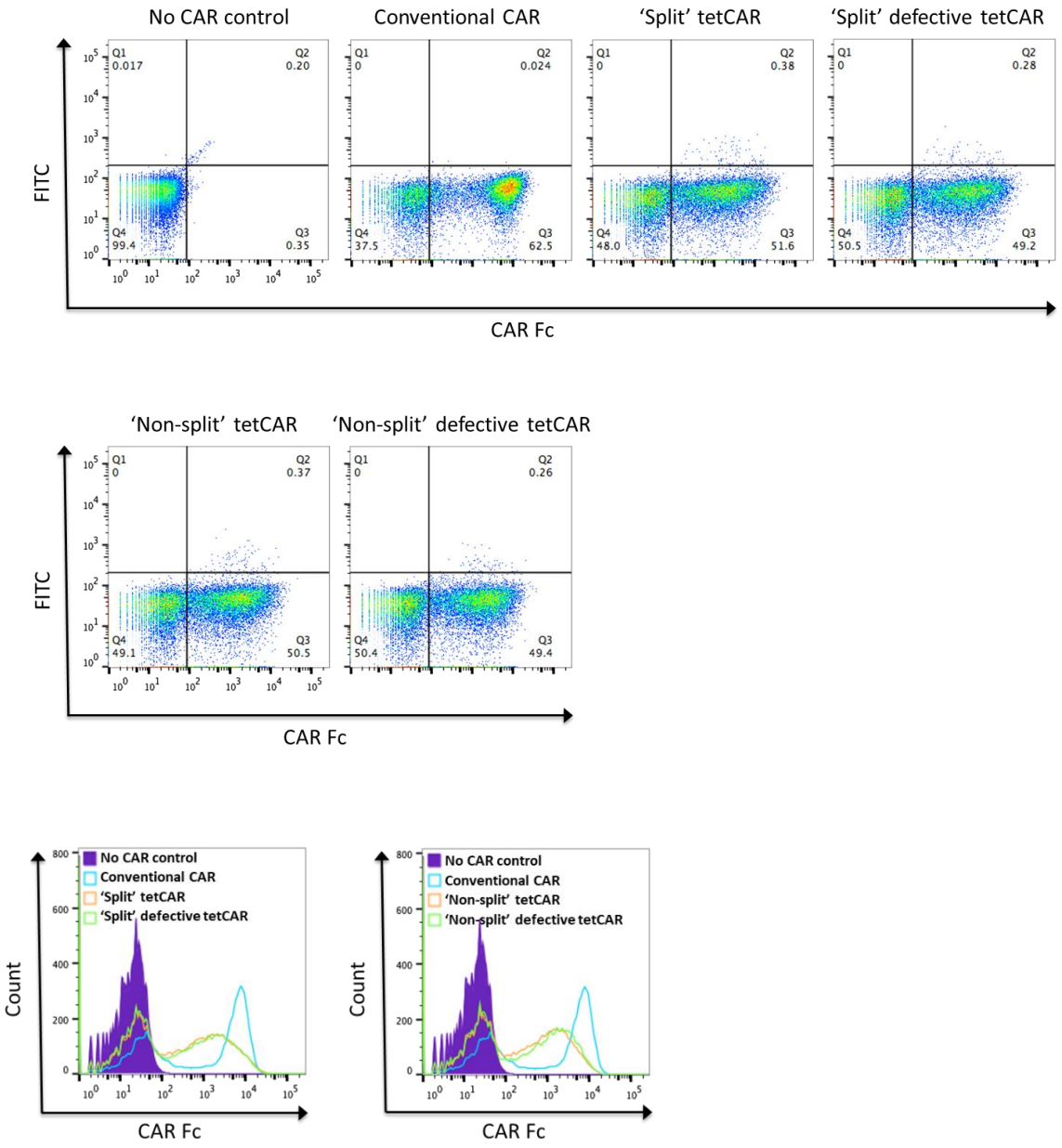

(c) Expression levels of CARs in primary human T-cells. Cells engineered with retroviral constructs encoding CAR molecules were analysed by flow cytometry. Expression of each tetCAR at the surface of primary human T-cells was compared with the expression of their respective defective tetCAR (with absent TiP domain) and conventional CAR. The CARs were detected with an anti-human IgG antibody. Staining was compared against NT T-cells stained using the same antibody.

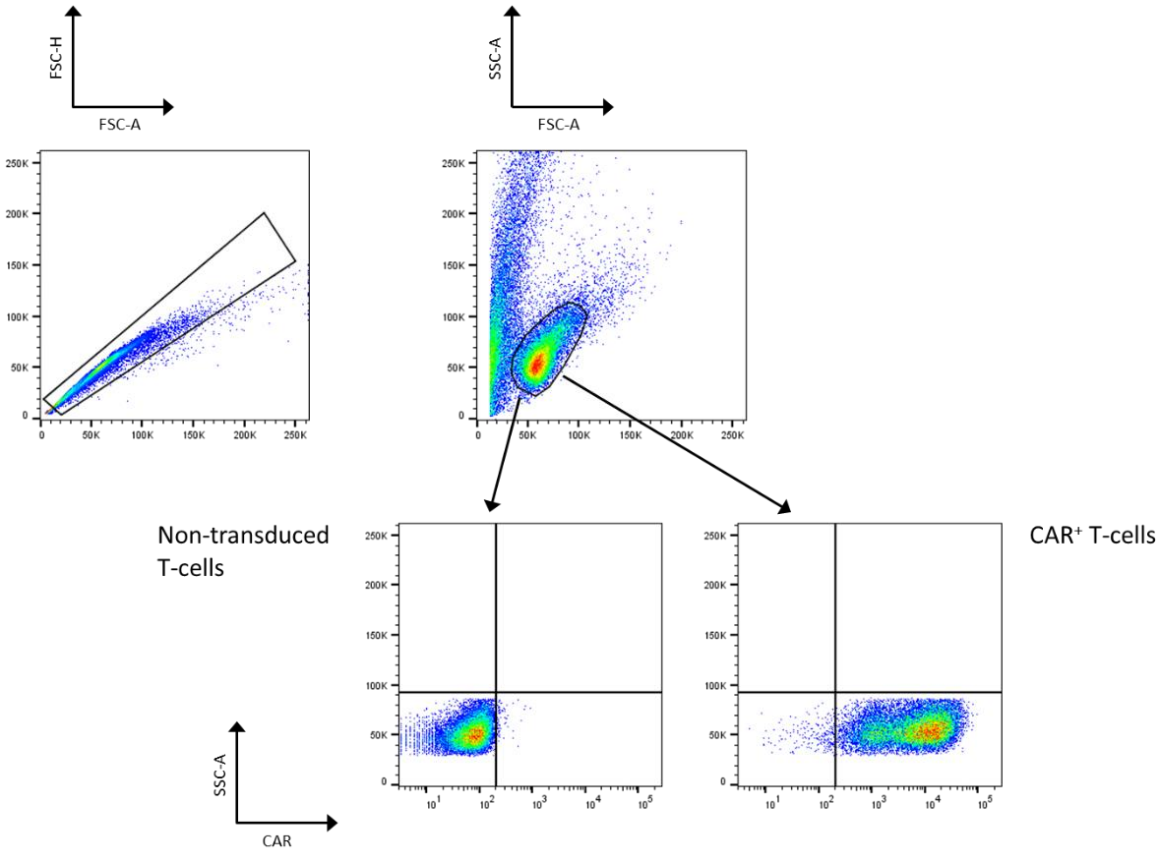

Gating strategy used to verify CAR expression on T-cells. Representative flow cytometry plots illustrating the gating strategy for assessment of CAR transduction efficiency of T-cells. Gating strategy used to identify singlet (top left), viable (top right) T-cell populations. CAR^+ T-cells were gated with reference to non-transduced control T-cells (bottom).

(d)

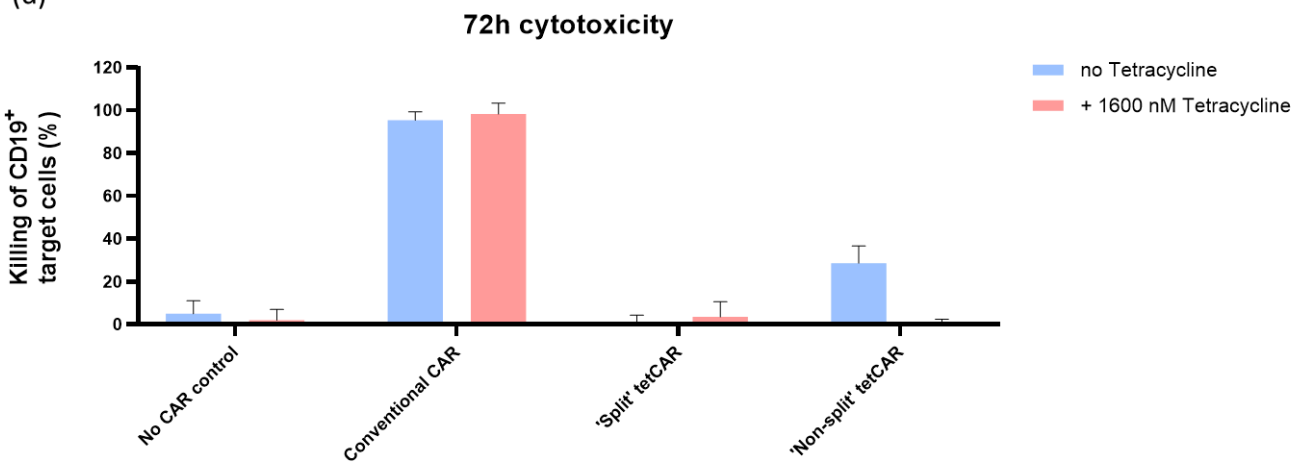

(e)

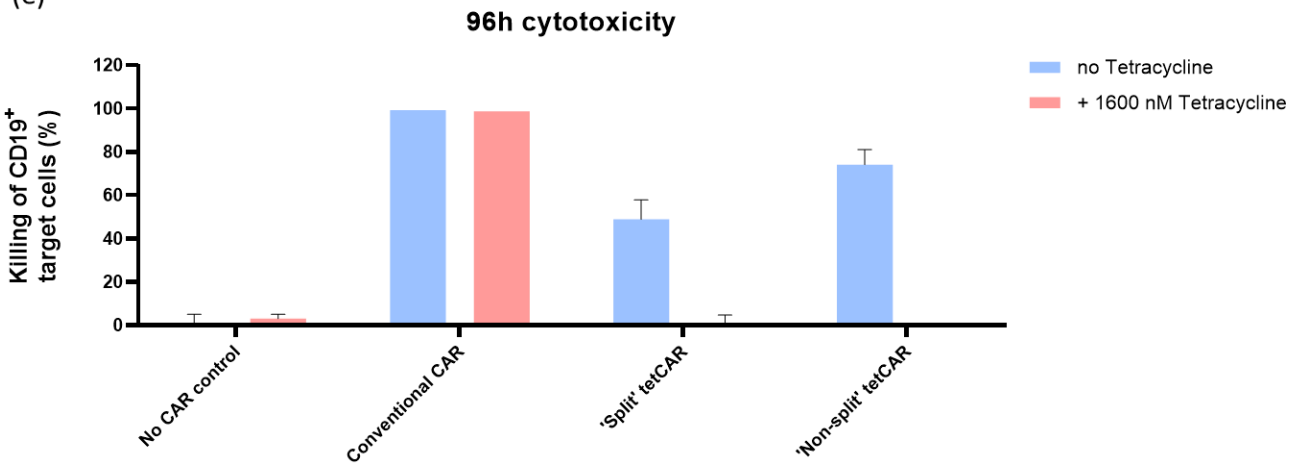

(d) Cytotoxicity activity mediated by tetCARs in a 72-hour and (e) in a 96-hour end-point experiment. Primary human T-cells expressing the tetCARs were challenged with SupT1 cells engineered to express CD19 at a 4:1 T-cell:target cell ratio in the absence of tetracycline or in the presence of 1600 nM tetracycline. Primary human T-cells expressing the conventional CAR and non-transduced T-cells were set-up to serve as control. A low percentage for survival of $CD19^+$ SupT1 cells indicates a high degree of specific target cell killing by CAR T-cells; n = 2 independent experiments from separate donors, error bars denote SD.

5.3 Discussion

In this chapter, we have demonstrated that other alternative implementations of the tetCAR are also functional in therapeutically relevant T-cells. Our goal was to find a configuration of tetCAR that would strongly impair its activity when in the presence of the small molecule but still allow for strong antigen-induced signalling, comparable to that achieved by the conventional single-component receptor, when the two components are assembled. Here, we performed an initial set of experiments to explore the optimal configuration of tetCAR by altering the second component of the bicistronic vector, also known as signalling component. These changes led to the design of a single CAR which is expressed with multiple signalling components all of which comprise of TiP at their amino-terminus but a different individual signalling domain, in contrast to a compound signalling domain. As the TiP domains are identical, each signalling component should be recruited equally to the antigen recognition component and the CAR should transmit an equal CD28, OX40 and CD3-Zeta signal in the absence of tetracycline and upon recognition of the cognate antigen. We hypothesised that lack of steric interaction between the different signalling domains and their second messengers might improve their function.

Unfortunately, whilst the alternative implementations of the tetCAR were functional and capable of activating therapeutically relevant T-cells, there was no evidence of improved functional activity when compared to the compound signalling domain. These results have in fact demonstrated that the ‘Split’ tetCAR T-cells present a reduced cytotoxic capacity compared with the ‘Non-split’ tetCAR T-cells.

In addition, testing of the ‘Non-split’ tetCAR showed good cytotoxic activity and responsiveness to tetracycline but a lower degree of target cell killing in the absence of tetracycline compared with the conventional CAR, thus suggesting a reduced activation maximum. Consequently, we decided to further investigate the optimal configuration of tetCAR, which will be discussed in the following chapter.

CHAPTER 6

IDENTIFICATION OF THE MOST PROMISING SECOND-GENERATION CONSTRUCTS

6.1 Cytotoxicity activity mediated by tetCAR constructs with different components in primary human T-cells

As indicated by the previous results, none of the above tetCARs showed to signal as strongly as the conventional CAR. To be considered a promising construct, the tetCAR needs to show a great balance between the strong antigen-induced signalling (comparable to that of the conventional CAR) and the impaired activity when in the presence of the small molecule. To find a tetCAR design that fulfills the criteria, we constructed and tested a group of tetCAR candidate constructs. As the above data showed that the 'Non-split' tetCAR functions better than the 'Split' tetCAR, it was decided to use the former as template for the design of the new group of constructs. Overall, three major modifications were carried out: replacement of the initial CD4 derived transmembrane and intracellular domain, replacement of the initial spacer derived from the Fc domain of IgG1 and insertion of a 4-1BB costimulatory motif between the transmembrane domain (TM) and TetR. As a result, we successfully constructed a second-generation tetCAR with CD8TM (Figure 23a), a second-generation tetCAR with CD28TM (Figure 23b), a second-generation tetCAR with CD8-α Stalk spacer domain (CD8STK) and CD8TM (Figure 23c), a second-generation tetCAR with CD8STK and CD28TM (Figure 23d), a third-generation tetCAR with CD8TM and 4-1BB (Figure 23e) and a third-generation tetCAR with CD28TM and 4-1BB (Figure 23f). In order to test cell killing, we expressed the CD19-targeting tetCARs in primary human T-cells and performed a flow cytometry-based cell-killing assay.

First, we analysed the transduction efficiency of the primary human T-cells by flow cytometry. As shown in Figure 23g, apart from the 'CD8TM' tetCAR low expression, all the other tetCARs could be detected at the cell surface, thus indicating that these constructs were both expressed and trafficked correctly to the plasma membrane. Cell surface expression of the conventional CAR was also detected. Primary human T-cells expressing the tetCARs were co-cultured with wild-type SupT1 cells or SupT1 cells engineered to express CD19 at a 4:1 T-cell:target cell ratio in the absence of tetracycline or in the presence of 1600 nM tetracycline. Primary human T-cells expressing the conventional CAR were also tested. Furthermore, T-cells from the same donor that had

not undergone gene transfer (designated non-transduced T-cells) were set up to serve as an additional control.

After incubation for 72 hours, surviving target cells were quantified by flow cytometry. A low percentage for survival of $CD19^+$ SupT1 cells indicates a high degree of specific target cell killing by CAR T-cells. In the 72-hour end-point experiment, almost complete killing of the $CD19^+$ target cells was observed with both 'CD8TM 4-1BB' tetCAR T-cells and 'CD28TM 4-1BB' tetCAR T-cells on either absence or presence of tetracycline (Figure 23i). Similar results were observed with the conventional CAR T-cells. In the presence of 1600 nM tetracycline, both 'CD8STK CD8TM' tetCAR T-cells and 'CD8STK CD28TM' tetCAR T-cells showed a minimal target cell killing. In the absence of tetracycline, almost complete killing of the $CD19^+$ target cells was observed with both 'CD8STK CD8TM' tetCAR T-cells and 'CD8STK CD28TM' tetCAR T-cells. A minimal cell killing mediated by non-transduced T-cells was observed on either absence or presence of tetracycline. As expected, minimal killing of the NT target cells was observed (Figure 23j).

In summary, we found two promising tetCAR constructs, the 'CD8STK CD8TM' tetCAR and the 'CD8STK CD28TM' tetCAR.

Figure 23

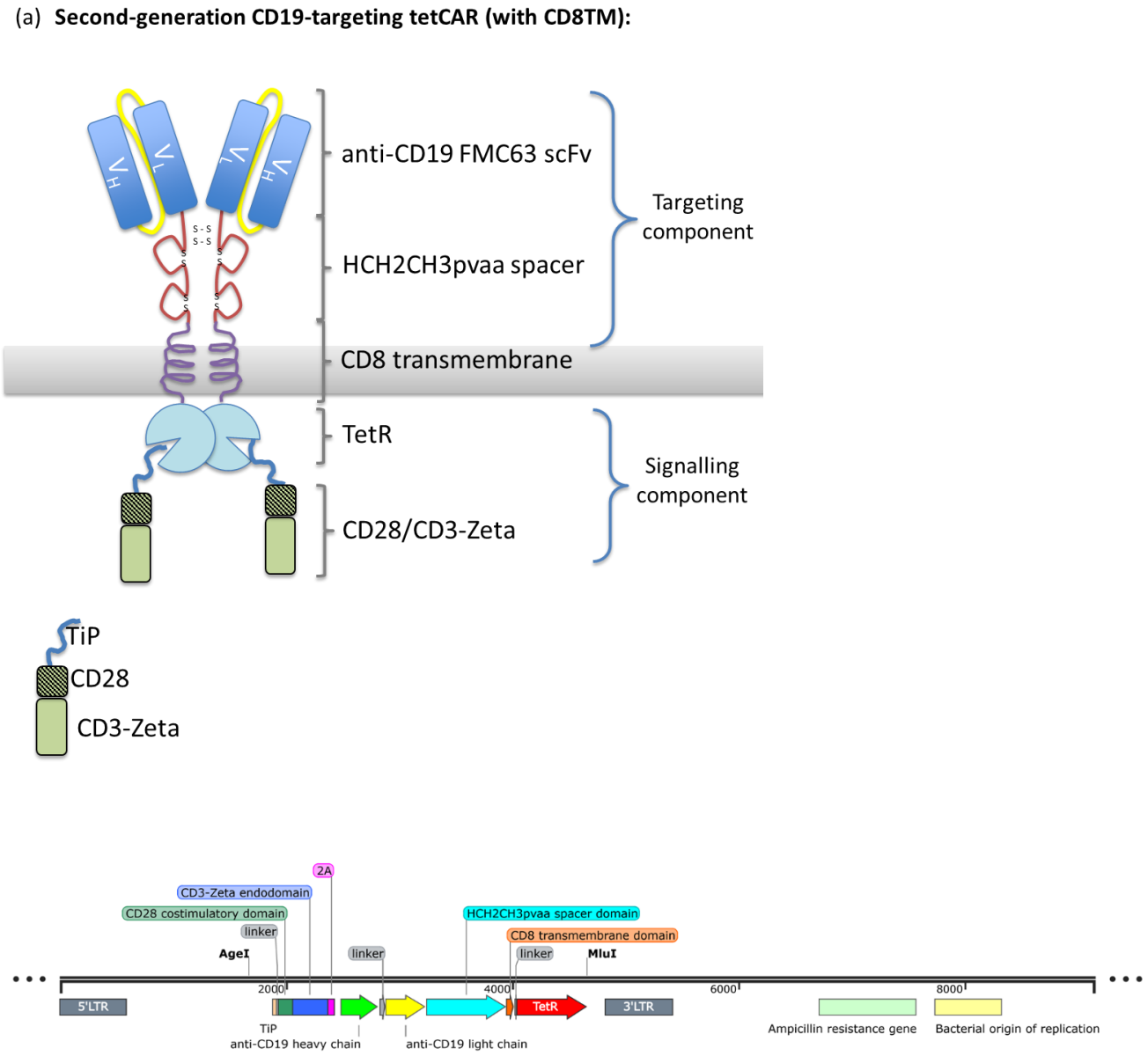

Figure 23. Cytotoxicity activity mediated by tetCAR constructs with different components in primary human T-cells. (a) Schematic diagram illustrating a second-generation tetCAR with CD8TM as transmembrane domain instead of the initial CD4 derived transmembrane and intracellular domain (top). A single CAR is expressed with only one signalling component which comprises of TiP (dark blue) fused to the CD28 (diagonal stripes) and CD3-Zeta (light green) endodomain. The receptor component comprises of a CD19 recognizing scFv (blue), a spacer derived from the Fc domain of IgG1 (red), a CD8 transmembrane domain (purple), and TetR (light blue). Additionally, the plasmid map of the second-generation CD19-targeting tetCAR (with CD8TM) is also shown (bottom).

(b) **Second-generation CD19-targeting tetCAR (with CD28TM):**

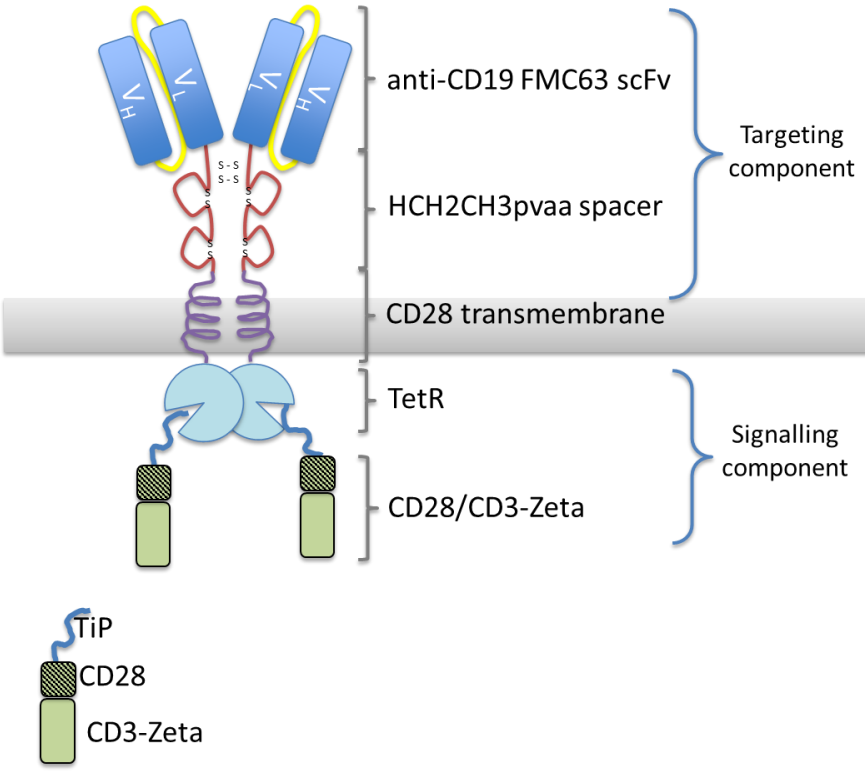

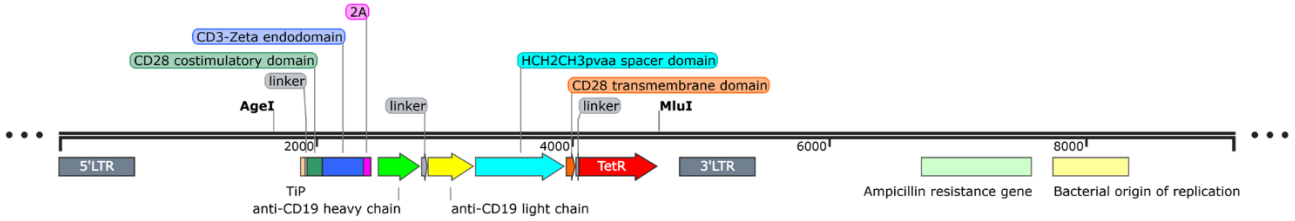

(b) Schematic diagram illustrating a second-generation tetCAR with CD28TM as transmembrane domain instead of the initial CD4 derived transmembrane and intracellular domain (top). A single CAR is expressed with only one signalling component which comprises of TiP (dark blue) fused to the CD28 (diagonal stripes) and CD3-Zeta (light green) endodomain. The receptor component comprises of a CD19 recognizing scFv (blue), a spacer derived from the Fc domain of IgG1 (red), a CD28 transmembrane domain (purple), and TetR (light blue). Additionally, the plasmid map of the second-generation CD19-targeting tetCAR (with CD28TM) is also shown (bottom).

(c) **Second-generation CD19-targeting tetCAR (with CD8STK CD8TM):**

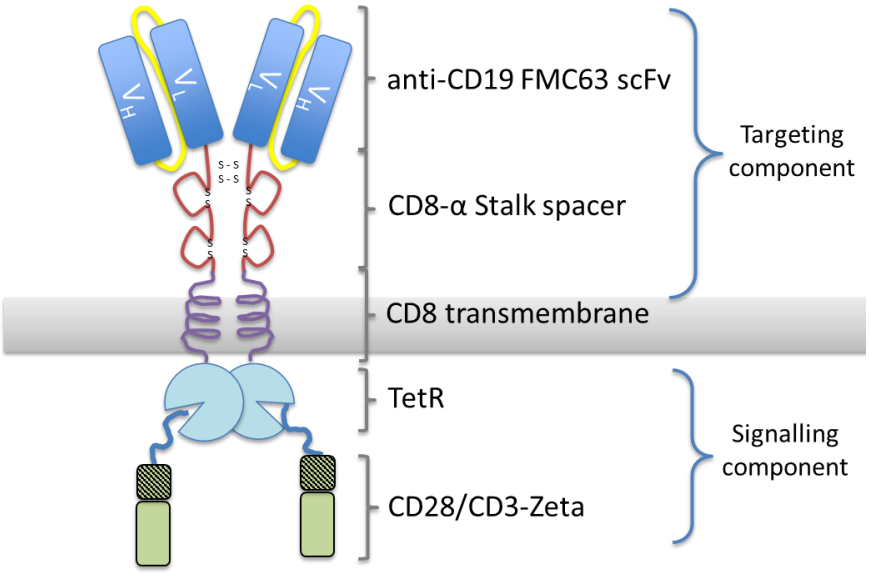

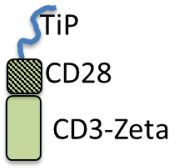

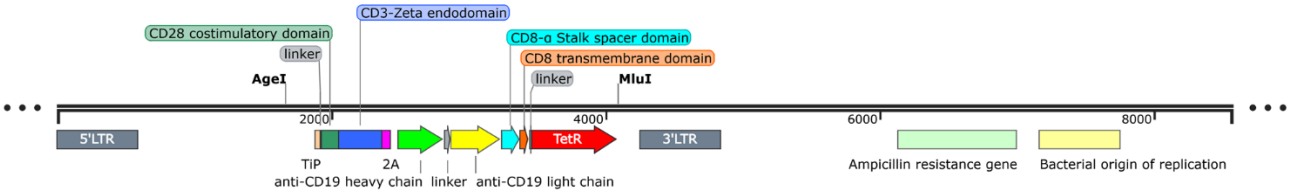

(c) Schematic diagram illustrating a second-generation tetCAR with CD8STK as spacer domain instead of the initial spacer derived from the Fc domain of IgG1 and with CD8TM as transmembrane domain instead of the initial CD4 derived transmembrane and intracellular domain (top). A single CAR is expressed with only one signalling component which comprises of TiP (dark blue) fused to the CD28 (diagonal stripes) and CD3-Zeta (light green) endodomain. The receptor component comprises of a CD19 recognizing scFv (blue), a CD8-α Stalk spacer domain (red), a CD8 transmembrane domain (purple), and TetR (light blue). Additionally, the plasmid map of the second-generation CD19-targeting tetCAR (with CD8STK CD8TM) is also shown (bottom).

(d) **Second-generation CD19-targeting tetCAR (with CD8STK CD28TM):**

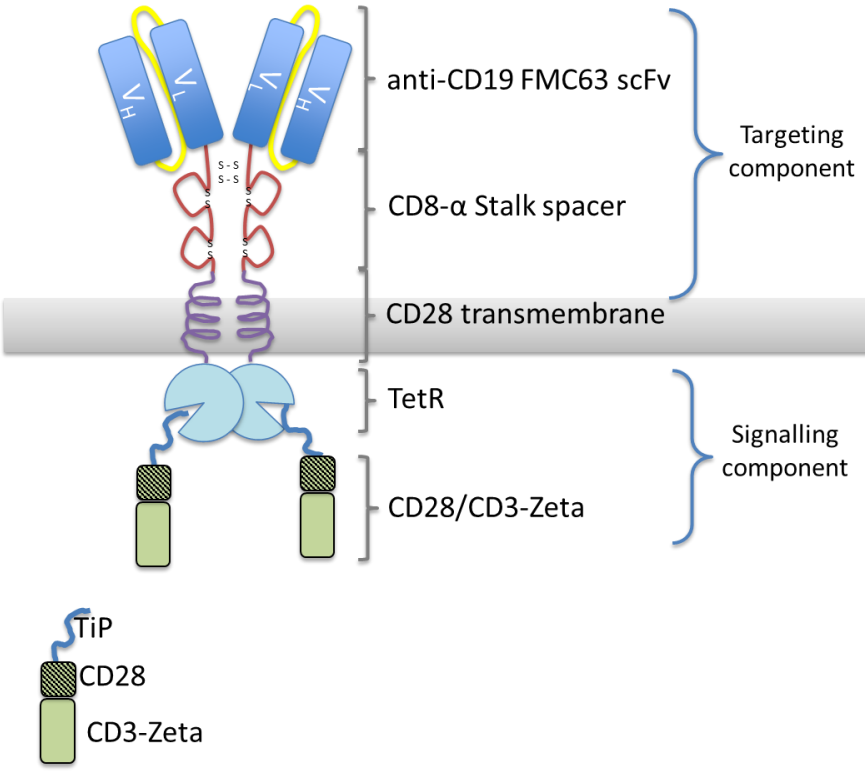

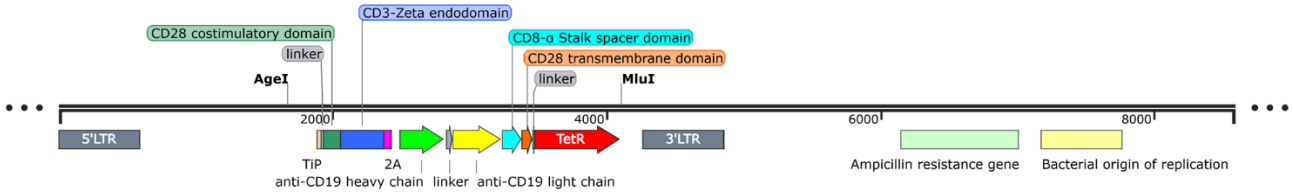

(d) Schematic diagram illustrating a second-generation tetCAR with CD8STK as spacer domain instead of the initial spacer derived from the Fc domain of IgG1 and with CD28TM as transmembrane domain instead of the initial CD4 derived transmembrane and intracellular domain (top). A single CAR is expressed with only one signalling component which comprises of TiP (dark blue) fused to the CD28 (diagonal stripes) and CD3-Zeta (light green) endodomain. The receptor component comprises of a CD19 recognizing scFv (blue), a CD8-α Stalk spacer domain (red), a CD28 transmembrane domain (purple), and TetR (light blue). Additionally, the plasmid map of the second-generation CD19-targeting tetCAR (with CD8STK CD28TM) is also shown (bottom).

(e) **Third-generation CD19-targeting tetCAR (with CD8TM 4-1BB):**

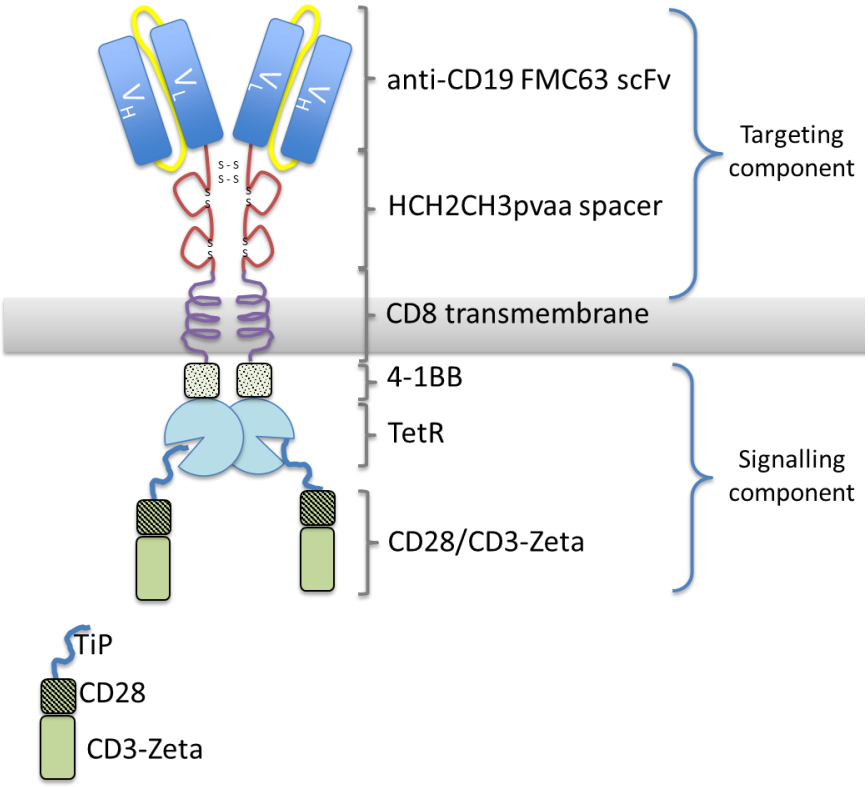

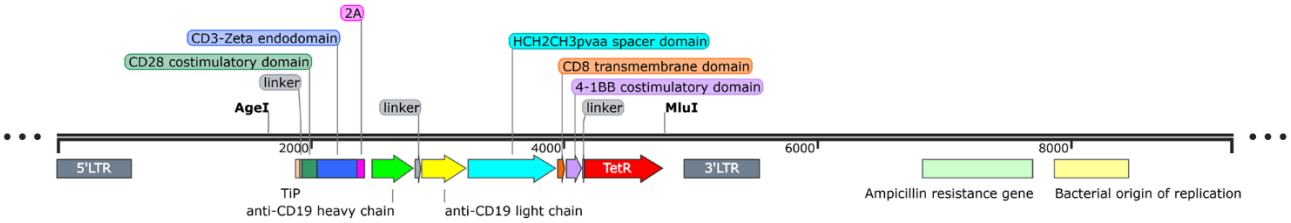

(e) Schematic diagram illustrating a third-generation tetCAR with CD8TM as transmembrane domain instead of the initial CD4 derived transmembrane and intracellular domain (top). A 4-1BB costimulatory motif was inserted between the CD8TM and TetR. A single CAR is expressed with a signalling component which comprises of TiP (dark blue) fused to the CD28 (diagonal stripes) and CD3-Zeta (light green) endodomain. The receptor component comprises of a CD19 recognizing scFv (blue), a spacer derived from the Fc domain of IgG1 (red), a CD8 transmembrane domain (purple), a 4-1BB costimulatory motif (small confetti), and TetR (light blue). Additionally, the plasmid map of the third-generation CD19-targeting tetCAR (with CD8TM 4-1BB) is also shown (bottom).

(f) **Third-generation CD19-targeting tetCAR (with CD28TM 4-1BB):**

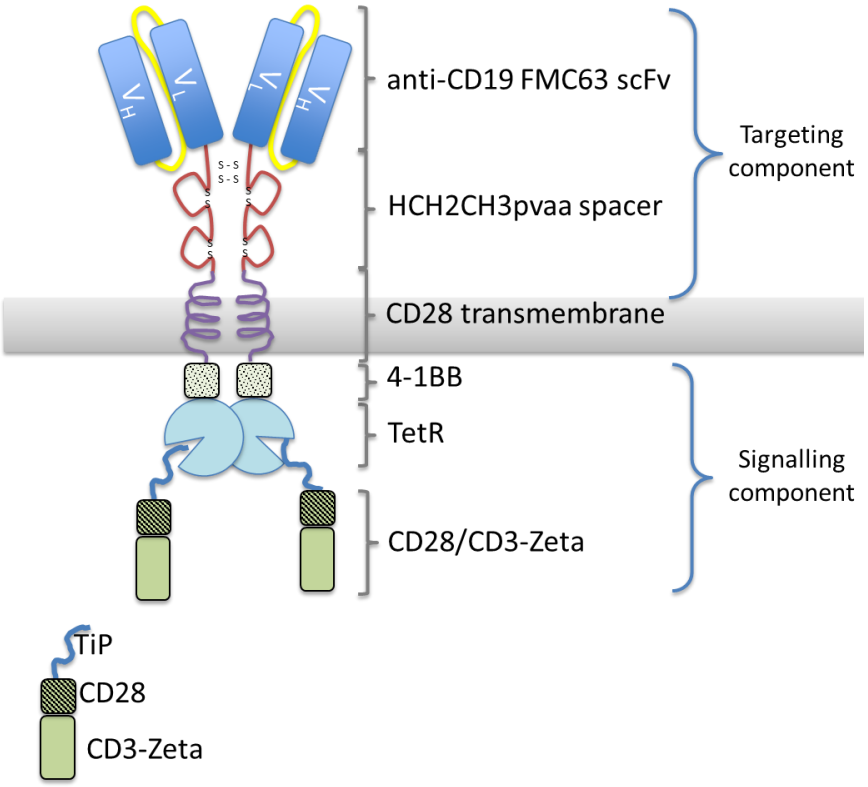

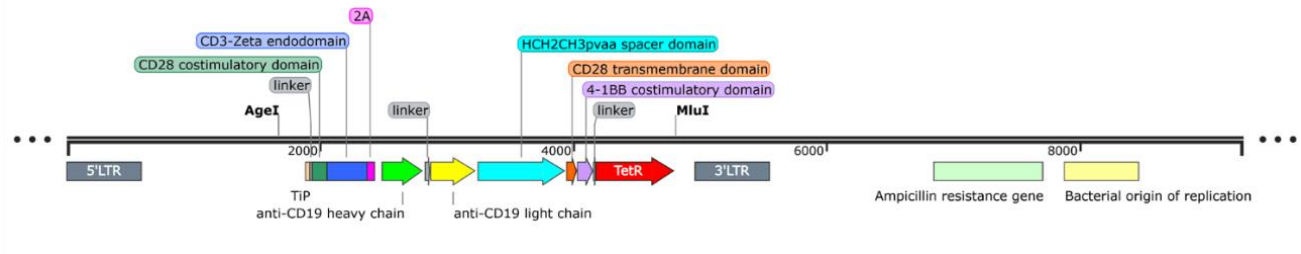

(f) Schematic diagram illustrating a third-generation tetCAR with CD28TM as transmembrane domain instead of the initial CD4 derived transmembrane and intracellular domain (top). A 4-1BB costimulatory motif was inserted between the CD28TM and TetR. A single CAR is expressed with a signalling component which comprises of TiP (dark blue) fused to the CD28 (diagonal stripes) and CD3-Zeta (light green) endodomain. The receptor component comprises of a CD19 recognizing scFv (blue), a spacer derived from the Fc domain of IgG1 (red), a CD28 transmembrane domain (purple), a 4-1BB costimulatory motif (small confetti), and TetR (light blue). Additionally, the plasmid map of the third-generation CD19-targeting tetCAR (with CD28TM 4-1BB) is also shown (bottom).

(g) **Primary human T-cells:**

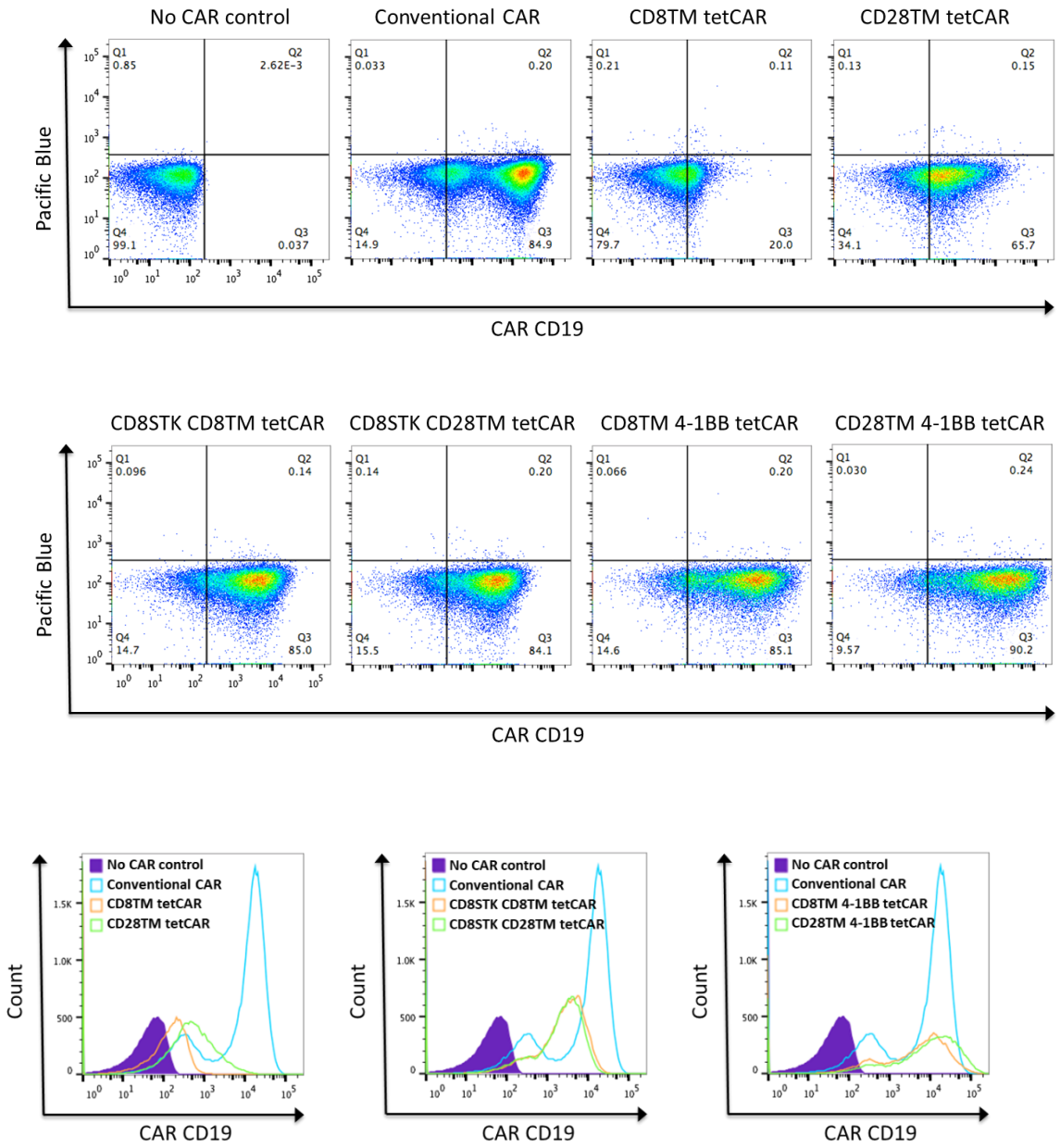

(g) Expression levels of CARs in primary human T-cells. Cells engineered with retroviral constructs encoding CAR molecules were analysed by flow cytometry. Expression of the tetCARs at the surface of primary human T-cells was compared with the expression of conventional CAR. The CARs were detected with soluble CD19 fused to rabbit IgG followed by a directly conjugated anti-Rabbit IgG antibody. Staining was compared against NT T-cells stained using the same antibodies.

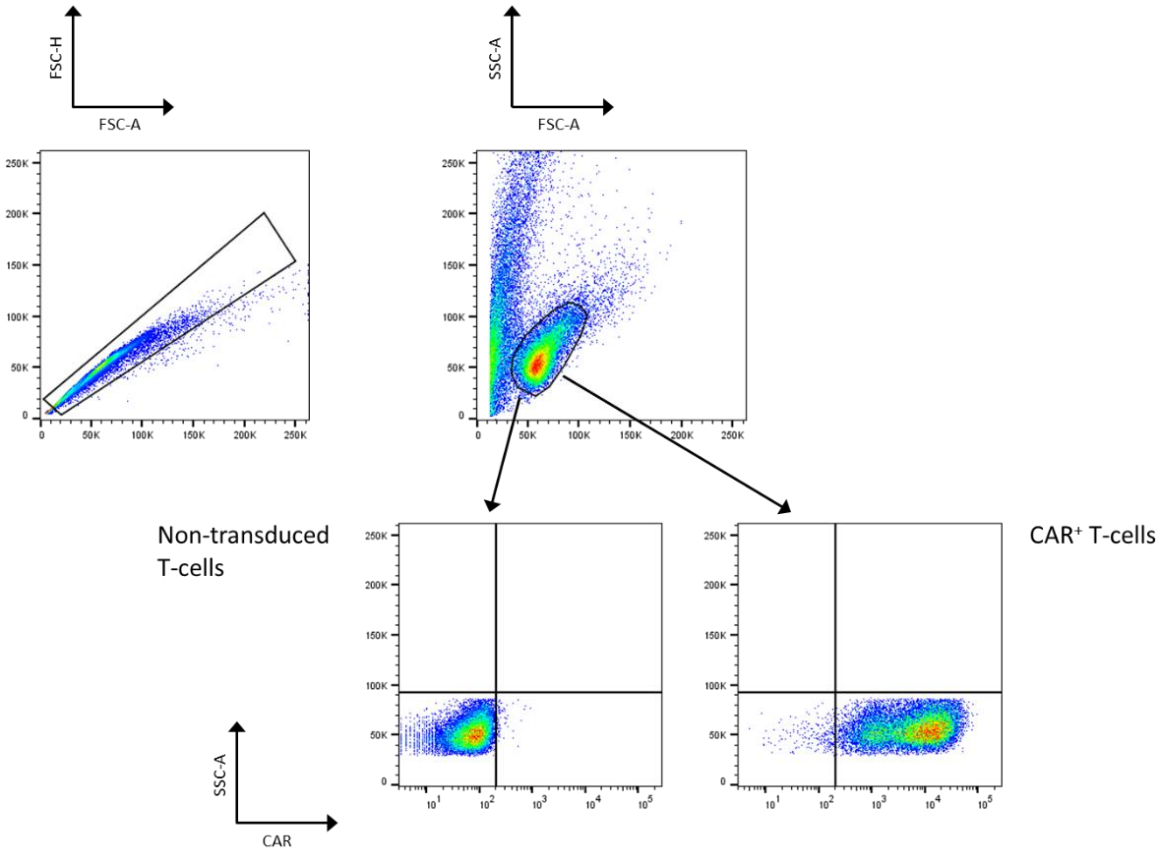

Gating strategy used to verify CAR expression on T-cells. Representative flow cytometry plots illustrating the gating strategy for assessment of CAR transduction efficiency of T-cells. Gating strategy used to identify singlet (top left), viable (top right) T-cell populations. CAR^+ T-cells were gated with reference to non-transduced control T-cells (bottom).

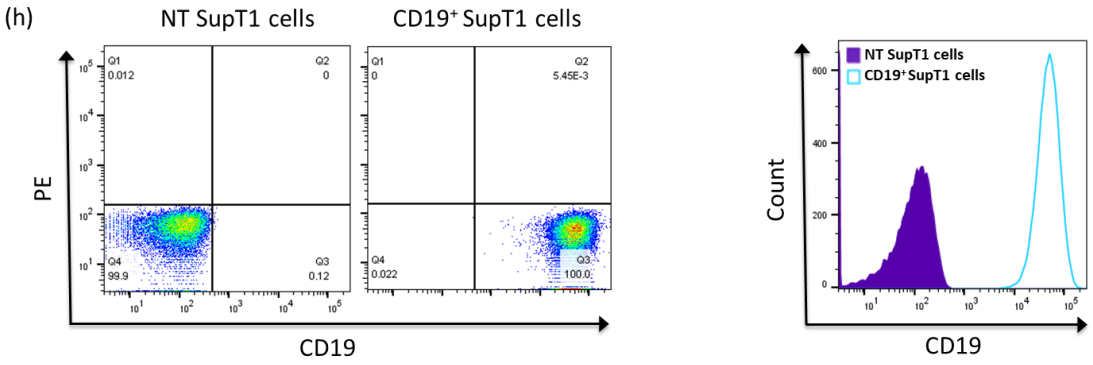

(h) Level of CD19 expression on target cell surface. SupT1 cells were used as target cells in co-culture assays. Non-transduced SupT1 were transduced to stably express CD19. The cells were investigated for the presence of CD19 using flow cytometry. The expression of CD19 was detected using an anti-human CD19 antibody. The level of CD19 expression was compared with that displayed by the NT SupT1 cells stained with the same antibody.

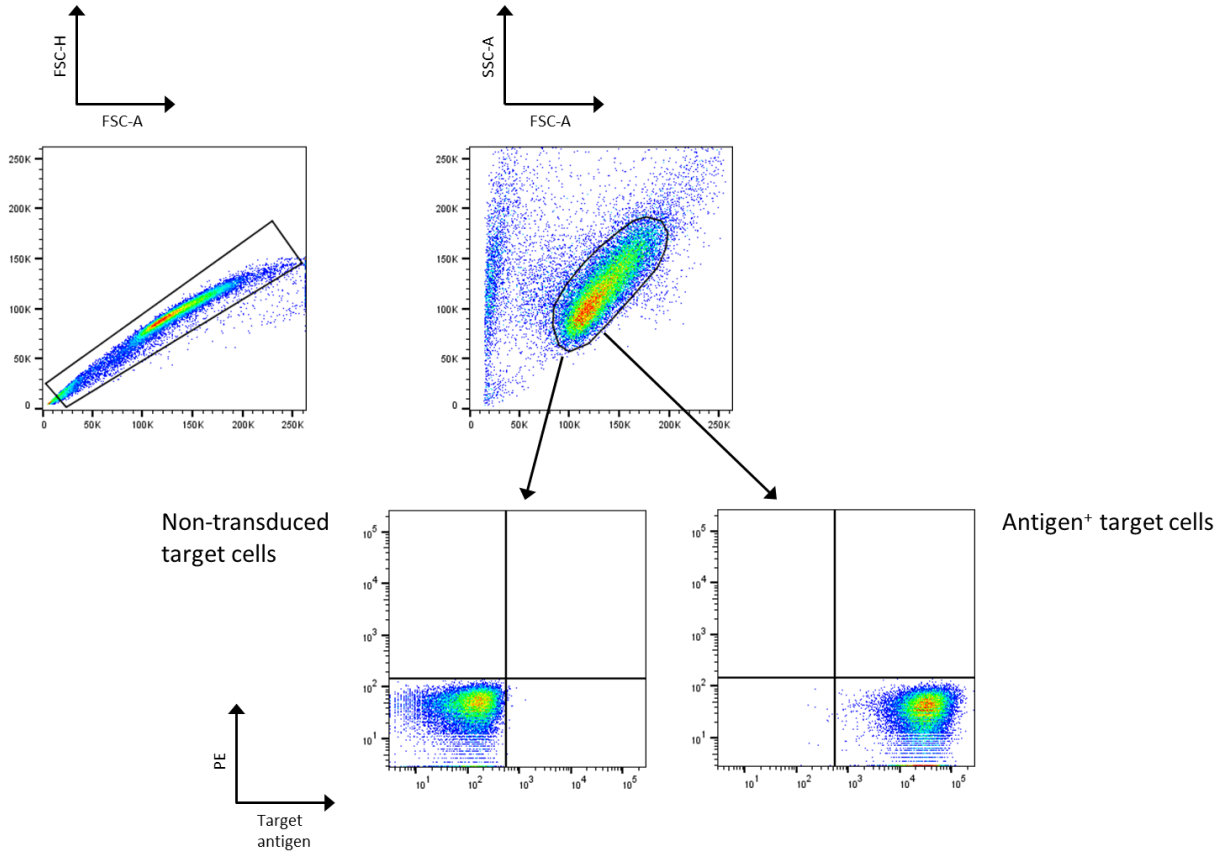

Gating strategy used to quantify antigen expression on target cells. Representative flow cytometry plots illustrating the gating strategy for assessment of the levels of antigen expression on target cell surface. Gating strategy used to identify singlet (top left), viable (top right) target cell populations. Antigen^{+} target cells were gated with reference to non-transduced control target cells (bottom).

(i)

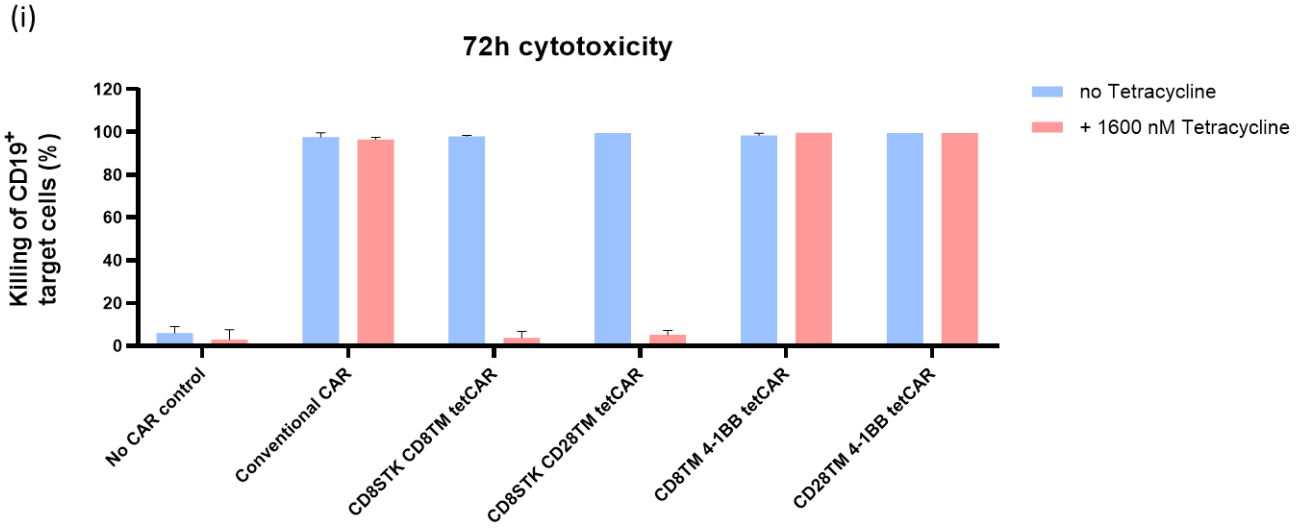

(j)

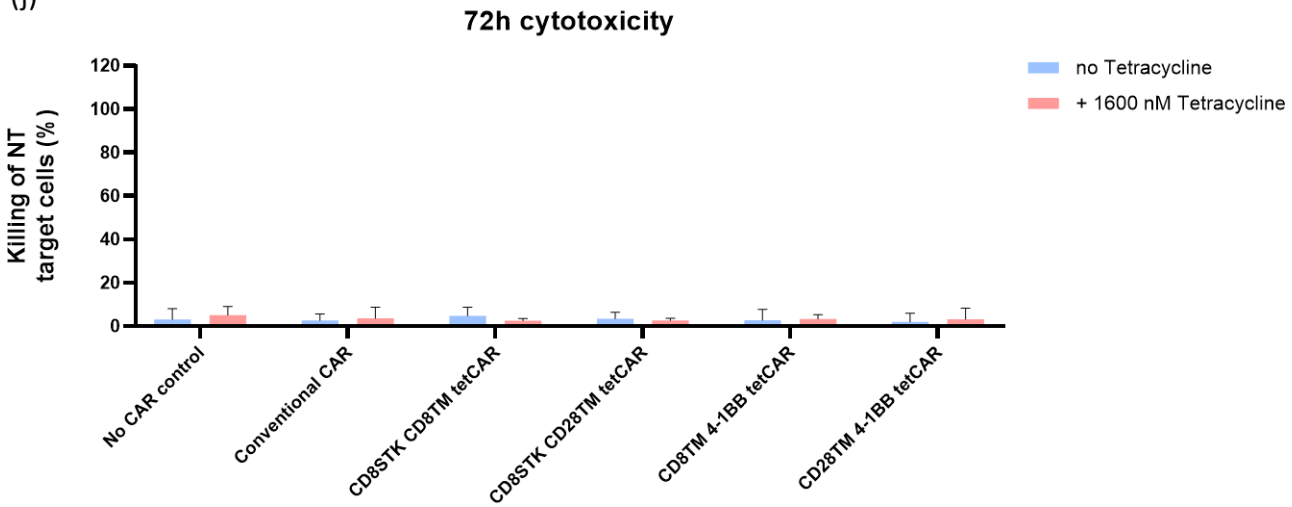

(i) and (j) Cytotoxicity activity mediated by tetCARs in a 72-hour end-point experiment. Primary human T-cells expressing the tetCARs were challenged with (i) SupT1 cells engineered to express CD19 or (j) wild-type SupT1 cells at a 4:1 T-cell:target cell ratio in the absence of tetracycline or in the presence of 1600 nM tetracycline. Primary human T-cells expressing the conventional CAR and non-transduced T-cells were set-up to serve as control. A low percentage for survival of $CD19^+$ SupT1 cells indicates a high degree of specific target cell killing by CAR T-cells; n = 3 independent experiments from separate donors, error bars denote SD.

(k) **72h cytotoxicity (CD19⁺ target cells):**

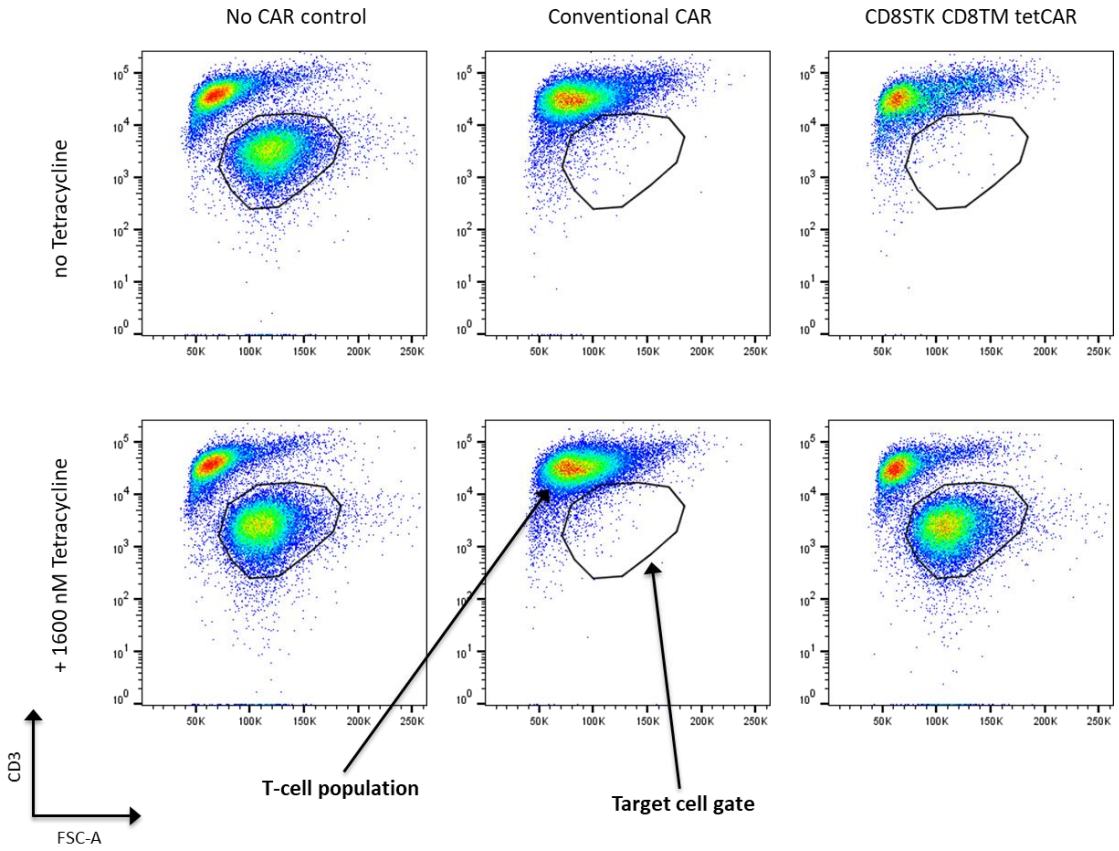

(k) Representative flow cytometry data. Surviving CD19⁺ SupT1 cells at the end of a 72-hour assay were gated. T-cell populations are also indicated on the plots.

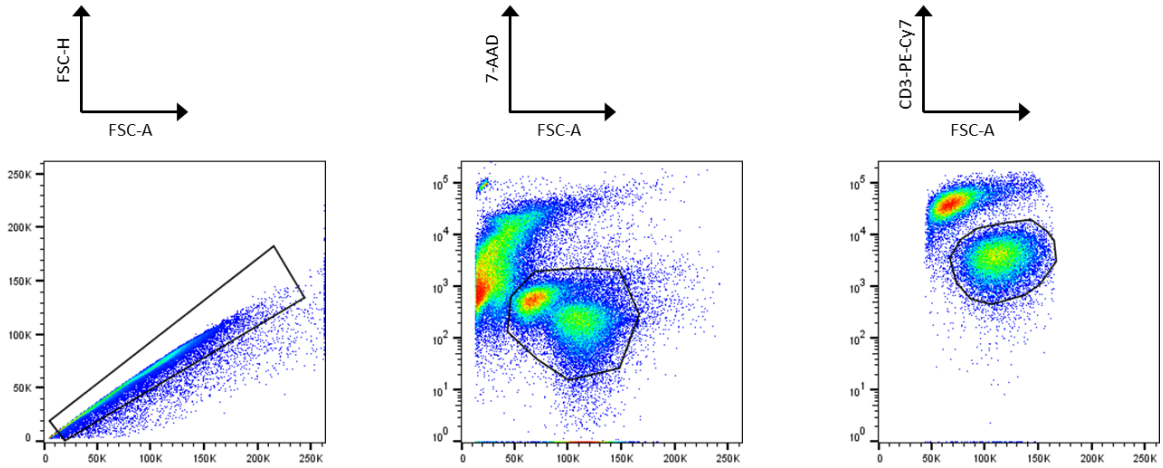

Gating strategy of flow cytometry-based cell-killing assay. Representative flow cytometry plots illustrating the gating strategy for assessment of surviving target cells. Gating strategy used to identify singlet (left), viable (middle) T-cell and target cell populations. Target cells were gated (right).

6.2 Cytokine production by primary tetCAR T-cells

To further assess the function of our group of tetCAR candidate constructs, we also examined the production of the cytokine IFN-γ.

In order to test the function of the CD19-targeting tetCARs in primary human T-cells, we co-cultured primary human T-cells expressing the tetCARs with wild-type SupT1 cells or SupT1 cells engineered to express CD19 at a 4:1 T-cell:target cell ratio in the absence of tetracycline or in the presence of 1600 nM tetracycline. Primary human T-cells expressing the conventional CAR were also tested. Furthermore, T-cells from the same donor that had not undergone gene transfer (designated non-transduced T-cells) were set up to serve as an additional control.

After an overnight incubation, supernatant samples were removed and assayed for the presence of IFN-γ. Subsequent investigations into the release of IFN-γ showed that tetracycline decreases human T-cell IFN-γ secretion and hence activation. When co-cultured with $CD19^+$ target cells, the conventional CAR led to consistent secretion of IFN-γ by primary human T-cells on either absence or presence of tetracycline (Figure 24a). As expected, no IFN-γ secretion by non-transduced T-cells was detected on either absence or presence of tetracycline. When co-cultured with $CD19^+$ target cells, all tetCARs led to consistent secretion of IFN-γ by primary human T-cells in the absence of tetracycline. In the presence of 1600 nM tetracycline, all tetCAR T-cells showed no IFN-γ secretion. As expected, no IFN-γ secretion was observed in the presence of NT target cells (Figure 24b).

These findings confirm that the ‘CD8STK CD8TM’ tetCAR and the ‘CD8STK CD28TM’ tetCAR are promising tetCAR constructs.

Figure 24

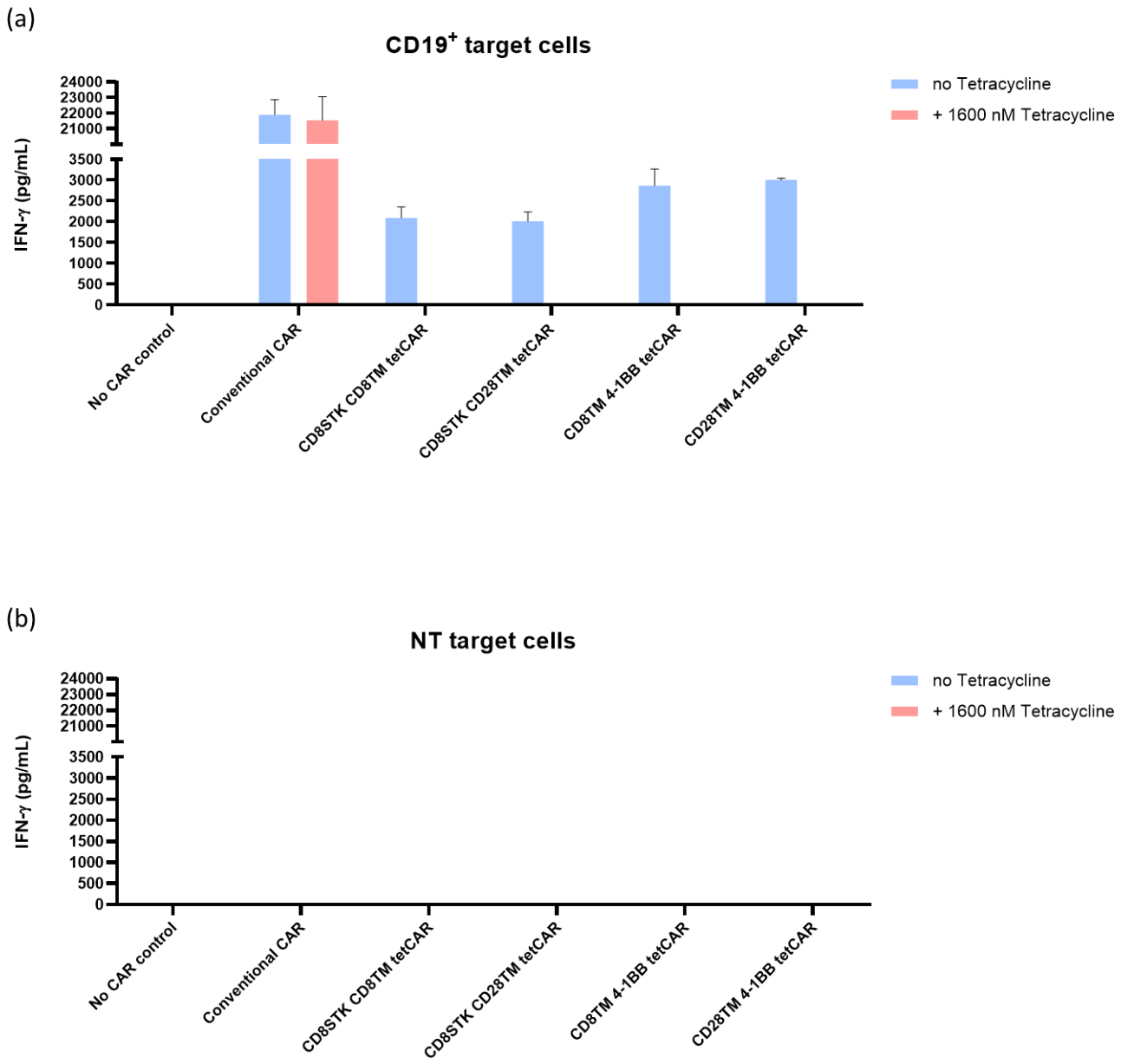

Figure 24. Cytokine production by primary tetCAR T-cells. Primary human T-cells expressing the tetCARs were challenged with (a) SupT1 cells engineered to express CD19 or (b) wild-type SupT1 cells at a 4:1 T-cell:target cell ratio in the absence of tetracycline or in the presence of 1600 nM tetracycline. Primary human T-cells expressing the conventional CAR and non-transduced T-cells were set-up to serve as control. Production of IFN-γ after an overnight incubation was quantified by ELISA; n = 3 independent experiments from separate donors, error bars denote SD.

6.3 Discussion

In this chapter, we have demonstrated successful generation of two promising tetCAR constructs. In the pursuit of finding the optimal configuration of tetCAR, we performed a new set of experiments focussed on altering the first component of the bicistronic vector, also known as antigen recognition component, in contrast to the previous chapter where changes to the signalling component were explored. Overall, three different parts of the tetCAR platform were investigated. Those parts were the transmembrane domain (TM), the spacer domain and the linker between the TM domain and TetR. First, we compared the influence of different transmembrane domains in the antigen recognition component by designing constructs that included the CD8TM or the CD28TM. These are the TM domains most frequently used in CARs [107]. Second, we designed constructs that included the CD8-α Stalk, a spacer commonly employed in CARs, instead of the other commonly used spacer derived from the Fc domain of IgG1 [106]. Overall, a good spacer domain should be able to project the antigen recognition domain away from the membrane and allow it to have the flexibility to bind the target antigen. Third, we investigated the effect of altering the linker fusing the transmembrane domain to TetR by inserting a 4-1BB costimulatory domain between the TM domain and TetR. In addition to increase the length of the linker, this insertion also added a costimulatory signal out of the small molecule control.

After successfully constructing all the different variants of the CD19-targeting tetCAR, we demonstrated transduction of primary human T-cells. Both ‘CD8TM’ tetCAR and ‘CD28TM’ tetCAR showed a lower expression on the cell surface compared with all the other tetCAR variants. An explanation for the reduced expression is the potential decrease of the CAR protein stability.

In the cytotoxicity experiments, testing of the two tetCAR constructs comprising a 4-1BB costimulatory motif between the transmembrane domain and TetR showed a strong cytotoxicity activity either in the absence or presence of tetracycline, suggesting that addition of small molecule did not inhibit the system. On the other hand, both ‘CD8STK CD8TM’ tetCAR and ‘CD8STK CD28TM’ tetCAR showed not only a strong cytotoxicity activity in the absence of tetracycline but also responsiveness to the

small molecule. These results have in fact demonstrated that we found two promising tetCAR constructs, with both ‘CD8STK CD8TM’ tetCAR and ‘CD8STK CD28TM’ tetCAR showing the strongly impaired activity when in the presence of the small molecule and the strong antigen-induced signalling, comparable to that achieved by the conventional single-component receptor, when the two components are assembled.

In addition, we performed cytokine production experiments to further investigate the function of the different variants of the CD19-targeting tetCAR. In contrast to the results achieved with the cytotoxicity experiments, both ‘CD8TM 4-1BB’ tetCAR and ‘CD28TM 4-1BB’ tetCAR showed responsiveness to tetracycline as addition of the small molecule resulted in undetectable levels of cytokine production. A possible explanation for the difference observed between the two sets of experiments is the fast target cell killing when compared to the slower cytokine production, suggesting that the small molecule does not have enough time to act and prevent cell killing [108, 109]. Another interesting observation made in this chapter was that inclusion of the 4-1BB costimulatory domain between the TM domain and TetR seems to be associated with an increase in cytokine production, suggesting that costimulatory domains can be incorporated in the membrane-bound moiety of the tetCAR to enhance responses [110].

Having successfully identified two promising tetCAR constructs, the next phase of the project was to perform a complete *in vitro* test of the tetCAR system, which will be discussed in the following chapter.

CHAPTER 7

IN VITRO TESTING OF THE MOST PROMISING SECOND-GENERATION CONSTRUCTS

7.1 Tunable control of tetCAR T-cell activity by administration of a small molecule

7.1.1 Use of Tetracycline as small molecule

After finding two promising tetCAR constructs, the overall aim was to perform a complete *in vitro* test of the tetCAR system. From previous experiments, we had known that the initial tetCAR constructs allowed for effective tunable control over BW5 murine T-cell activity. In order to further validate the tunability of the system, it was decided to test the two most promising tetCAR constructs in primary human T-cells.

7.1.1.1 Interferon-γ release assay

Firstly, we analysed the transduction efficiency of the primary human T-cells by flow cytometry. As shown in Figure 25c, both tetCARs could be detected at the cell surface, thus indicating that these constructs were both expressed and trafficked correctly to the plasma membrane. Cell surface expression of the conventional CAR was also detected. Primary human T-cells expressing the tetCARs were co-cultured with SupT1 cells engineered to express CD19 at a 4:1 T-cell:target cell ratio in the absence of tetracycline or in the presence of increasing concentrations of tetracycline. Primary human T-cells expressing the conventional CAR were also tested. Furthermore, T-cells from the same donor that had not undergone gene transfer (designated non-transduced T-cells) were set up to serve as an additional control. After an overnight incubation, supernatant samples were removed and assayed for the presence of IFN-γ. Subsequent investigations into the release of IFN-γ showed that tetracycline decreases human T-cell IFN-γ secretion and hence activation in a dose dependent manner. The experiment was carried out using concentrations of tetracycline ranging from 0 to 1600 nM. In this experiment tetracycline was serially diluted at 1 in 2 ratio starting from 1600 nM.

The conventional CAR, which was used as a positive control, led to consistent secretion of IFN-γ by primary human T-cells in all tetracycline concentrations (Figure 25g). As expected, no significant IFN-γ secretion by non-transduced T-cells was detected on either absence or presence of tetracycline (Figure 25h). In both tetracycline inducible

CARs, the amount of secreted IFN-γ was found to decrease with increasing concentrations of tetracycline (Figures 25e and 25f). In the absence of tetracycline, IFN-γ secretion was lower to that seen with the positive control. In the presence of 200 nM tetracycline, the 'CD8STK CD8TM' tetCAR T-cells showed minimal IFN-γ secretion. From 400 nM to 1600 nM, no significant IFN-γ secretion by tetCAR T-cells was detected (Figure 25e). The 'CD8STK CD28TM' tetCAR led to minimal secretion of IFN-γ by primary human T-cells in the presence of 100 nM tetracycline. From 200 nM to 1600 nM, no significant IFN-γ secretion by tetCAR T-cells was observed (Figure 25f).

In summary, the two most promising tetCAR constructs allow for effective tunable control over primary human T-cell activity.

Figure 25

(a) **Second-generation CD19-targeting tetCAR (with CD8STK CD8TM):**

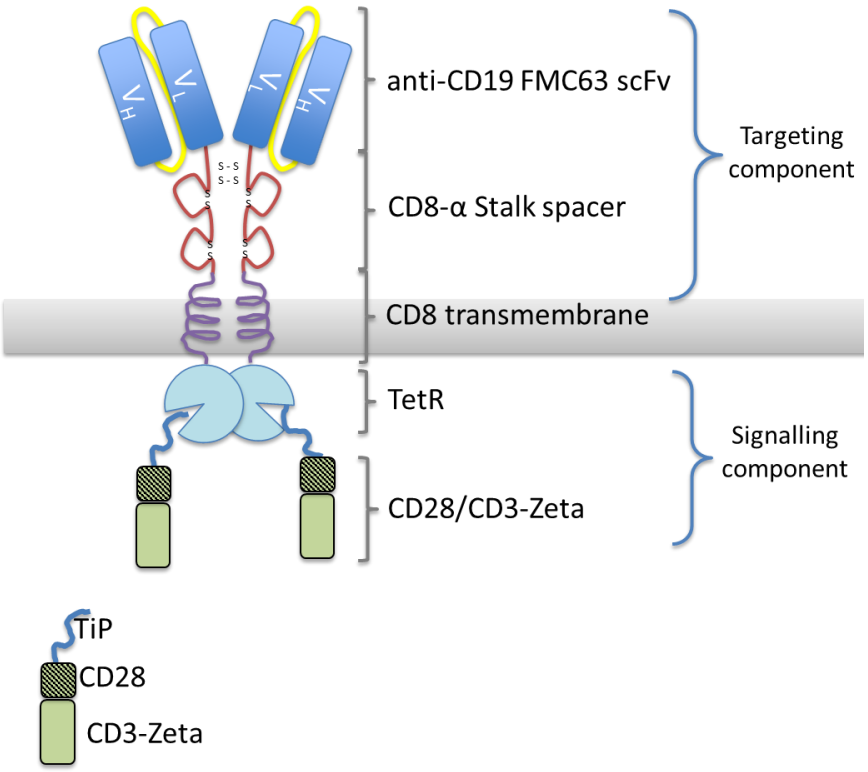

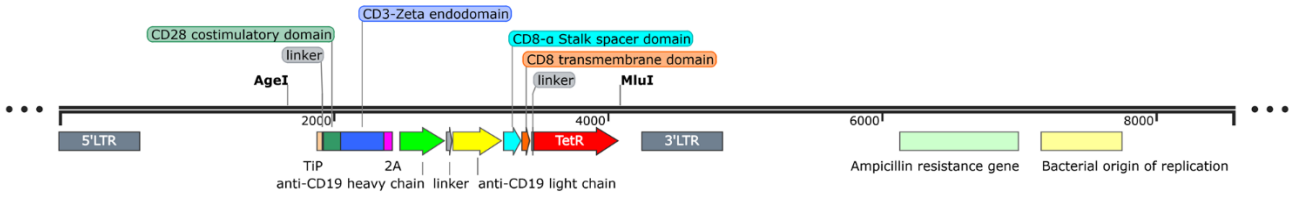

Figure 25. Control of tetCAR T-cell activity by administration of tetracycline. Cytokine production by primary tetCAR T-cells in the presence of $CD19^{+}$ target cells. (a) Schematic diagram illustrating a second-generation tetCAR with CD8STK as spacer domain instead of the initial spacer derived from the Fc domain of IgG1 and with CD8TM as transmembrane domain instead of the initial CD4 derived transmembrane and intracellular domain (top). A single CAR is expressed with only one signalling component which comprises of TiP (dark blue) fused to the CD28 (diagonal stripes) and CD3-Zeta (light green) endodomain. The receptor component comprises of a CD19 recognizing scFv (blue), a CD8-α Stalk spacer domain (red), a CD8 transmembrane domain (purple), and

TetR (light blue). Additionally, the plasmid map of the second-generation CD19-targeting tetCAR (with CD8STK CD8TM) is also shown (bottom).

(b) **Second-generation CD19-targeting tetCAR (with CD8STK CD28TM):**

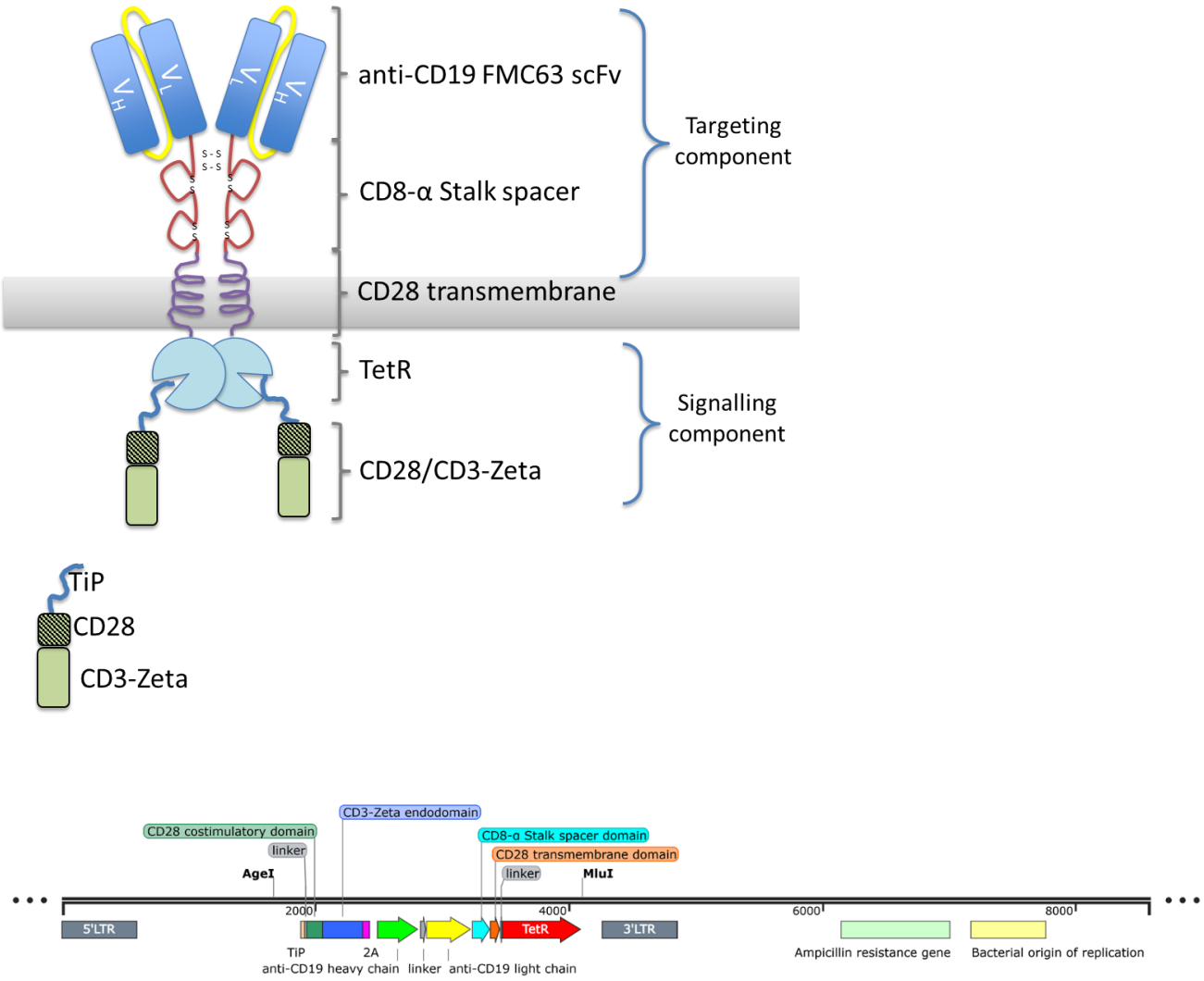

(b) Schematic diagram illustrating a second-generation tetCAR with CD8STK as spacer domain instead of the initial spacer derived from the Fc domain of IgG1 and with CD28TM as transmembrane domain instead of the initial CD4 derived transmembrane and intracellular domain (top). A single CAR is expressed with only one signalling component which comprises of TiP (dark blue) fused to the CD28 (diagonal stripes) and CD3-Zeta (light green) endodomain. The receptor component comprises of a CD19 recognizing scFv (blue), a CD8-α Stalk spacer domain (red), a CD28 transmembrane domain (purple), and TetR (light blue). Additionally, the plasmid map of the second-generation CD19-targeting tetCAR (with CD8STK CD28TM) is also shown (bottom).

(c) **Primary human T-cells:**

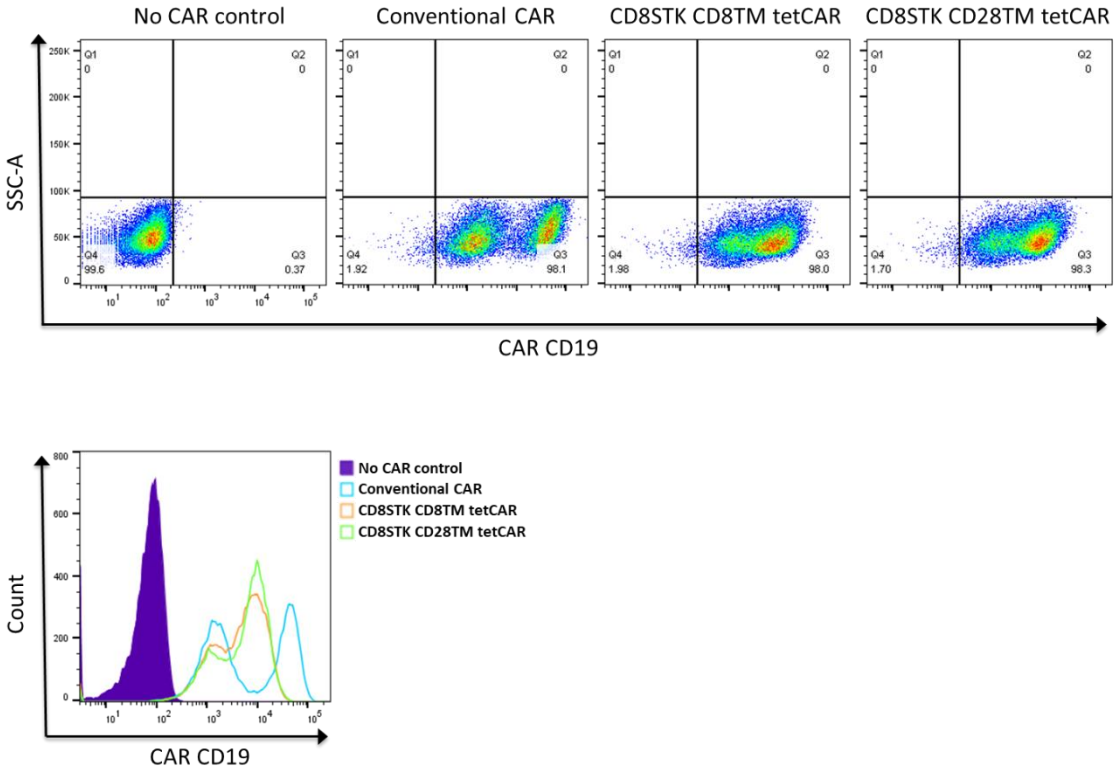

(c) Expression levels of CARs in primary human T-cells. Cells engineered with retroviral constructs encoding CAR molecules were analysed by flow cytometry. Expression of the tetCARs at the surface of primary human T-cells was compared with the expression of conventional CAR. The CARs were detected with soluble CD19 fused to rabbit IgG followed by a directly conjugated anti-Rabbit IgG antibody. Staining was compared against NT T-cells stained using the same antibodies.

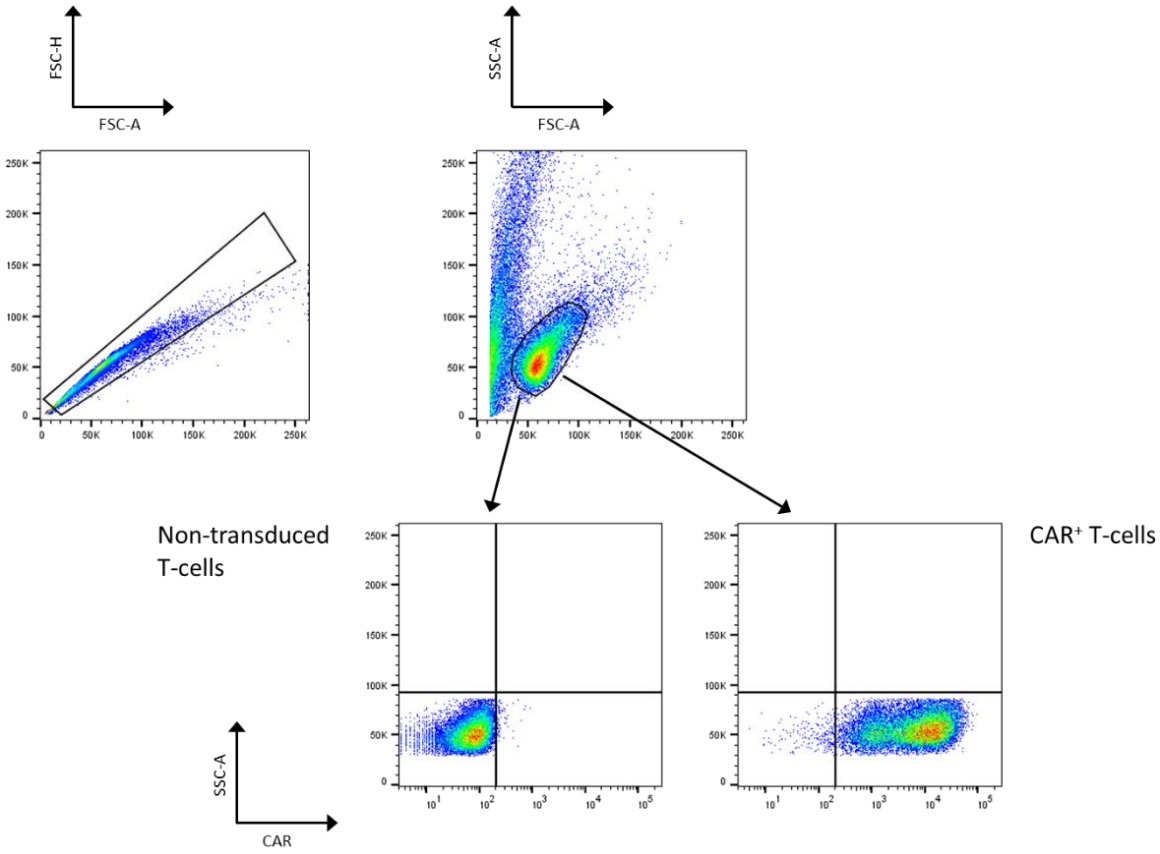

Gating strategy used to verify CAR expression on T-cells. Representative flow cytometry plots illustrating the gating strategy for assessment of CAR transduction efficiency of T-cells. Gating strategy used to identify singlet (top left), viable (top right) T-cell populations. CAR^+ T-cells were gated with reference to non-transduced control T-cells (bottom).

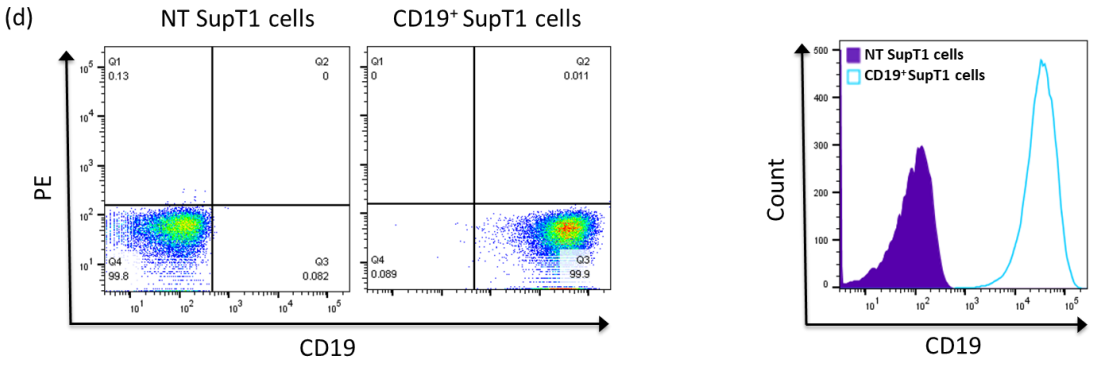

(d) Level of CD19 expression on target cell surface. SupT1 cells were used as target cells in co-culture assays. Non-transduced SupT1 were transduced to stably express CD19. The cells were investigated for the presence of CD19 using flow cytometry. The expression of CD19 was detected using an anti-human CD19 antibody. The level of CD19 expression was compared with that displayed by the NT SupT1 cells stained with the same antibody.

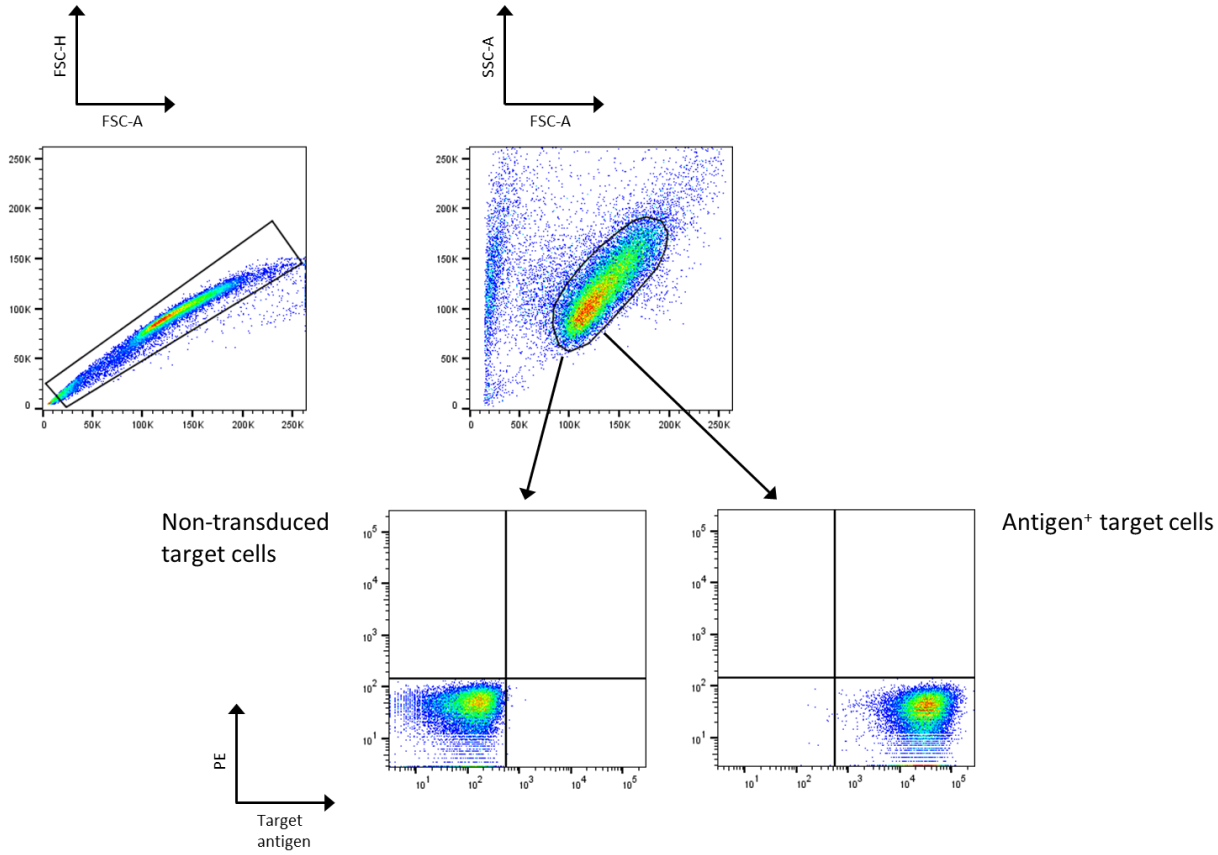

Gating strategy used to quantify antigen expression on target cells. Representative flow cytometry plots illustrating the gating strategy for assessment of the levels of antigen expression on target cell surface. Gating strategy used to identify singlet (top left), viable (top right) target cell populations. Antigen^{+} target cells were gated with reference to non-transduced control target cells (bottom).

(e)

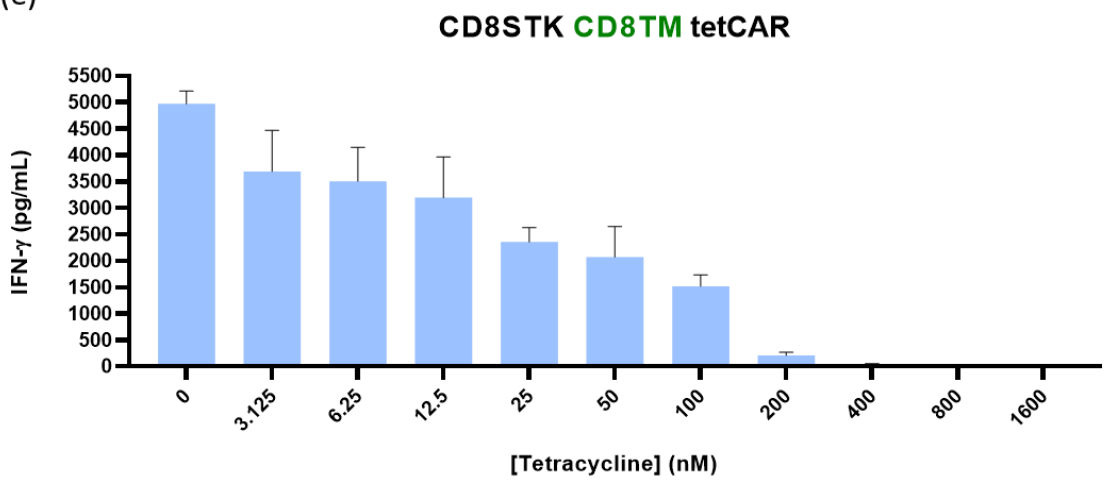

(f)

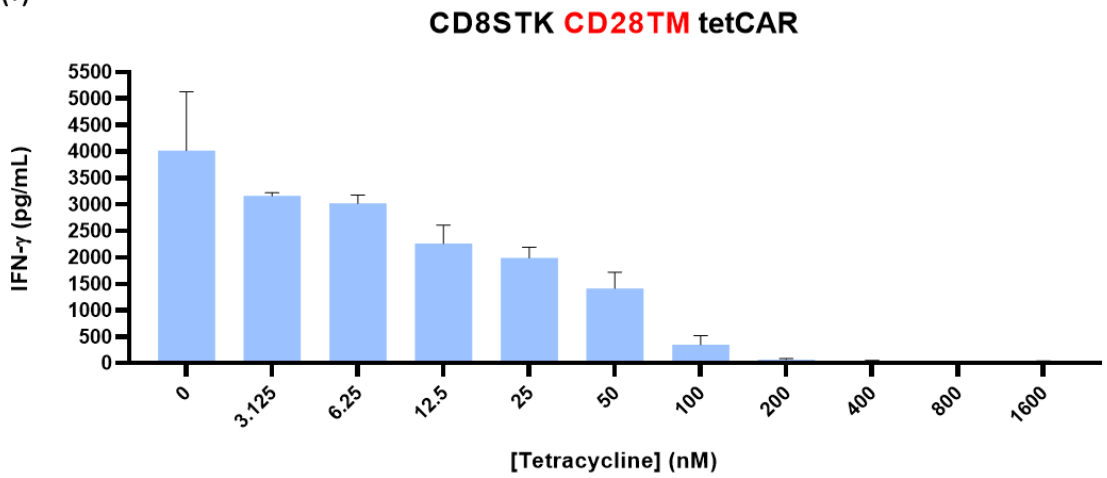

(e) Primary human T-cells expressing the 'CD8STK CD8TM' tetCAR or (f) primary human T-cells expressing the 'CD8STK CD28TM' tetCAR were challenged with SupT1 cells engineered to express CD19 at a 4:1 T-cell:target cell ratio in the absence of tetracycline or in the presence of increasing concentrations of tetracycline.

(g)

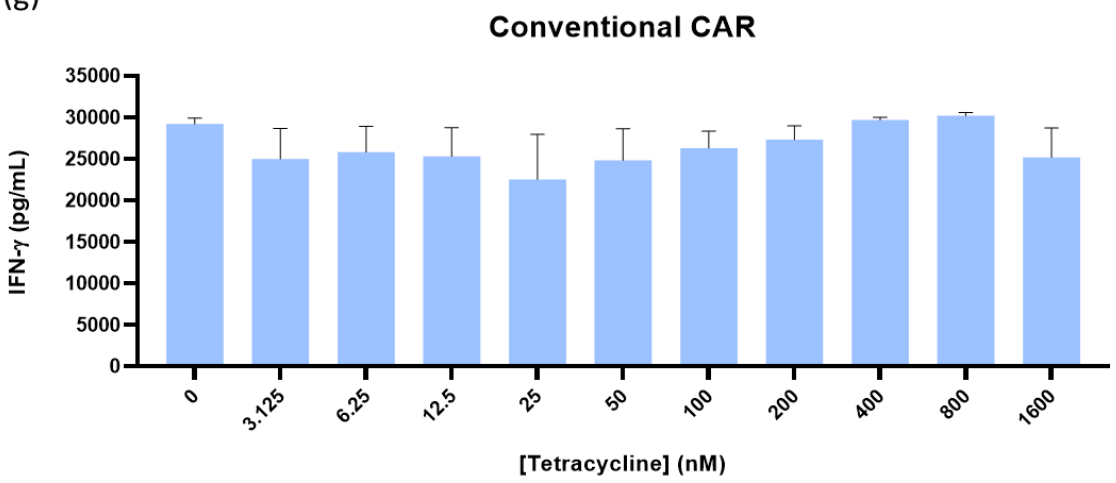

(h)

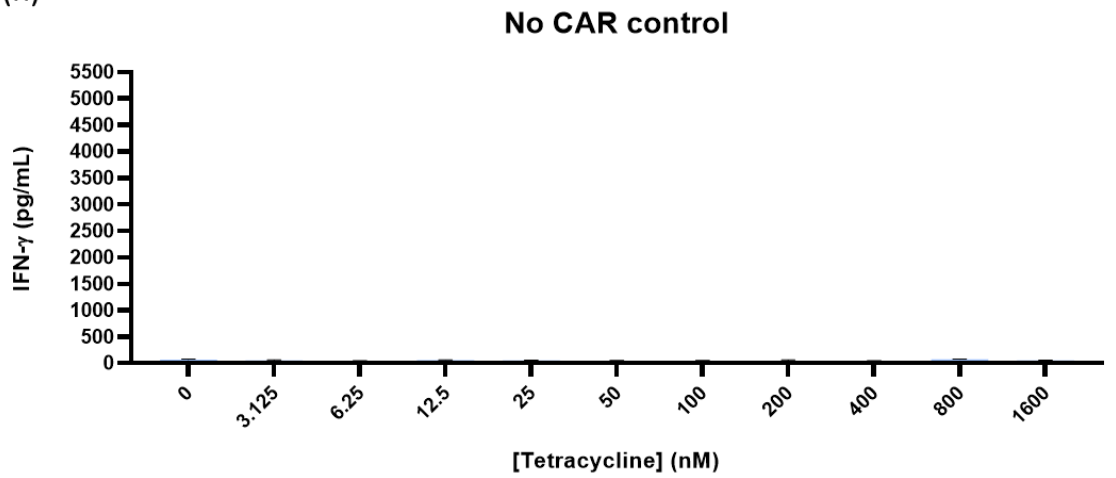

(g) Primary human T-cells expressing the conventional CAR and (h) non-transduced T-cells were set-up to serve as control. Production of IFN-γ after an overnight incubation was quantified by ELISA; n = 3 independent experiments from separate donors, error bars denote SD.

7.1.1.2 Flow cytometry-based cell-killing assay

To further confirm the tunable control of tetCAR T-cell activity by administration of tetracycline, we also performed a flow cytometry-based cell-killing assay.

The experiment was set up as described above for Figure 25. Primary human T-cells expressing the tetCARs were co-cultured with SupT1 cells engineered to express CD19 at a 4:1 T-cell:target cell ratio in the absence of tetracycline or in the presence of increasing concentrations of tetracycline. Primary human T-cells expressing the conventional CAR were also tested. Furthermore, T-cells from the same donor that had not undergone gene transfer (designated non-transduced T-cells) were set up to serve as an additional control. After incubation for 72 hours, surviving target cells were quantified by flow cytometry. A low percentage for survival of $CD19^+$ SupT1 cells indicates a high degree of specific target cell killing by CAR T-cells. The experiment was carried out using concentrations of tetracycline ranging from 0 to 1600 nM. In this experiment tetracycline was serially diluted at 1 in 2 ratio starting from 1600 nM.

In the 72-hour end-point experiment, almost complete killing of the $CD19^+$ target cells was observed with the 'CD8STK CD8TM' tetCAR T-cells between 0 and 100 nM tetracycline (Figure 26a). Similar results were observed with the 'CD8STK CD28TM' tetCAR T-cells between 0 and 50 nM tetracycline (Figure 26b). From 100 nM to 1600 nM with the 'CD8STK CD8TM' tetCAR T-cells and from 50 nM to 1600 nM with the 'CD8STK CD28TM' tetCAR T-cells, the percentage for killing of $CD19^+$ SupT1 cells was found to decrease with increasing concentrations of tetracycline (Figures 26a and 26b). In the presence of 1600 nM tetracycline, both 'CD8STK CD8TM' tetCAR T-cells and 'CD8STK CD28TM' tetCAR T-cells showed no target cell killing. The conventional CAR T-cells showed an almost complete killing of the $CD19^+$ target cells in all tetracycline concentrations (Figure 26c). As expected, no cell killing mediated by non-transduced T-cells was observed on either absence or presence of tetracycline (Figure 26d).

These findings confirm the tunability of the system in therapeutically relevant T-cells via the administration of tetracycline.

Figure 26

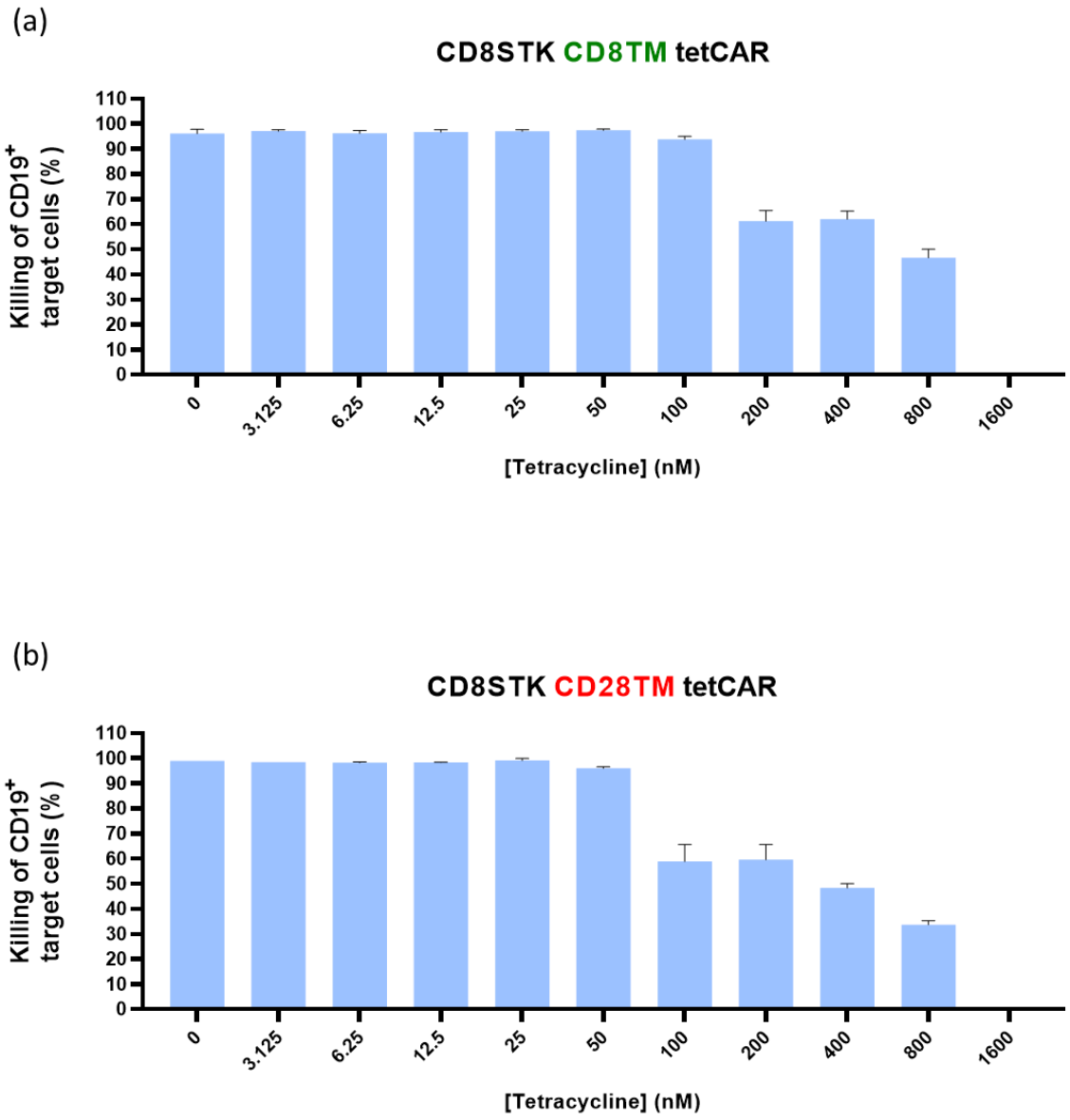

Figure 26. Control of tetCAR T-cell activity by administration of tetracycline. Cytotoxicity activity mediated by tetCARs in a 72-hour end-point experiment. (a) Primary human T-cells expressing the 'CD8STK CD8TM' tetCAR or (b) primary human T-cells expressing the 'CD8STK CD28TM' tetCAR were challenged with SupT1 cells engineered to express CD19 at a 4:1 T-cell:target cell ratio in the absence of tetracycline or in the presence of increasing concentrations of tetracycline.

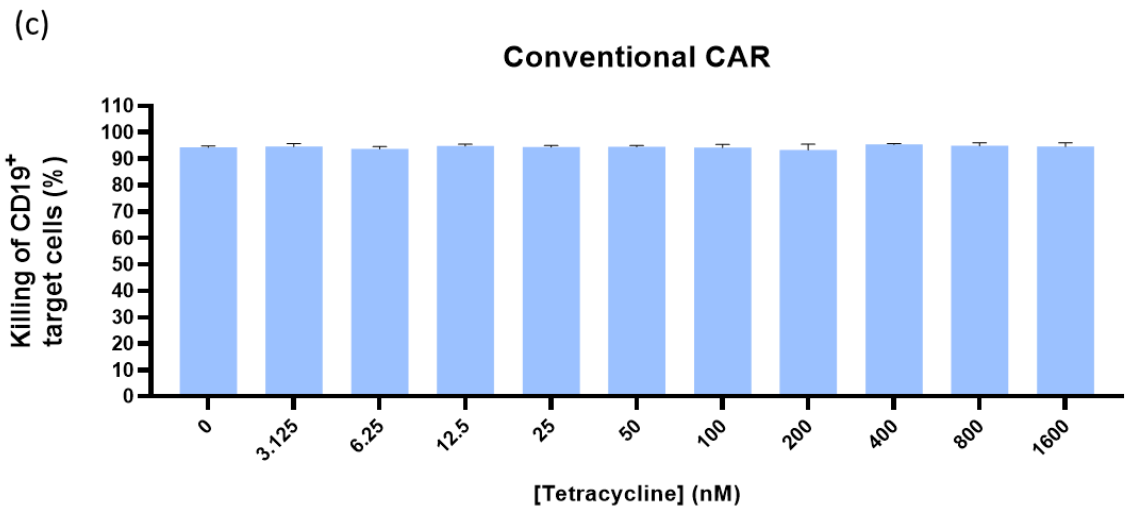

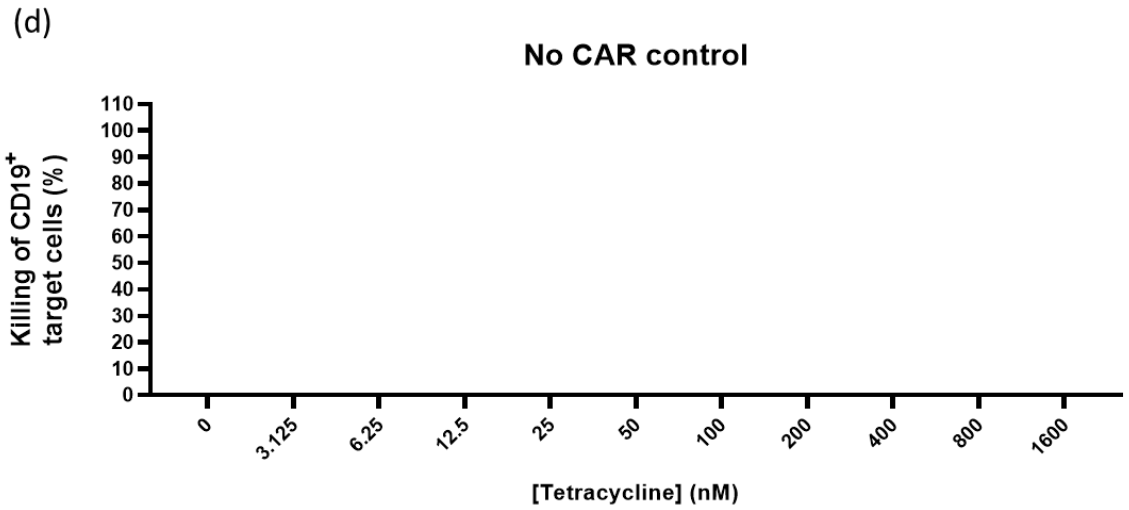

(c) Primary human T-cells expressing the conventional CAR and (d) non-transduced T-cells were set-up to serve as control. A low percentage for survival of $CD19^+$ SupT1 cells indicates a high degree of specific target cell killing by CAR T-cells; n = 3 independent experiments from separate donors, error bars denote SD.

7.1.2 Use of Doxycycline and Minocycline as alternative small molecules

As previously demonstrated in BW5 murine T-cells, the tetCAR system is more sensitive to doxycycline and minocycline when compared to tetracycline. In order to further investigate this, it was decided to test doxycycline and minocycline in primary human T-cells.

7.1.2.1 Testing of drug concentrations ranging from 0 to 1600 nM

The experiments were set up as described above for Figure 25 and Figure 26. The only modification was the small molecule used in each experiment. The experiments were carried out using concentrations of doxycycline or minocycline ranging from 0 to 1600 nM. In these experiments small molecule was serially diluted at 1 in 2 ratio starting from 1600 nM.

After an overnight incubation, supernatant samples were removed and assayed for the presence of IFN-γ. Subsequent investigations into the release of IFN-γ showed that both doxycycline and minocycline decrease human T-cell IFN-γ secretion and hence activation. The conventional CAR, which was used as a positive control, led to consistent secretion of IFN-γ by primary human T-cells in all doxycycline concentrations (Figure 27c) and also in all minocycline concentrations (Figure 29c). As expected, no significant IFN-γ secretion by non-transduced T-cells was detected on either doxycycline (Figure 27d) or minocycline (Figure 29d) experiments. In both tetracycline inducible CARs, the amount of secreted IFN-γ was undetectable at the lowest concentration of doxycycline (Figures 27a and 27b) and also at the lowest concentration of minocycline (Figures 29a and 29b). This means that above 3.125 nM doxycycline or minocycline both tetCARs are completely switched off.
Thus, it can be concluded that a similar pattern is observed in both primary human T-cells and BW5 murine T-cells.

To further assess the response of tetCAR T-cell activity to tetracycline analogues, we also performed a flow cytometry-based cell-killing assay.

After incubation for 72 hours, surviving target cells were quantified by flow cytometry. A low percentage for survival of $CD19^+$ SupT1 cells indicates a high degree of specific target cell killing by CAR T-cells. In the 72-hour end-point experiment, almost complete killing of the $CD19^+$ target cells was observed with the conventional CAR T-cells in the presence of either doxycycline (Figure 28c) or minocycline (Figure 30c). As expected, no cell killing mediated by non-transduced T-cells was observed on either doxycycline (Figure 28d) or minocycline (Figure 30d) experiments. In the presence of all doxycycline (Figures 28a and 28b) and minocycline (Figures 30a and 30b) concentrations, both tetCAR T-cells showed a lower degree of target cell killing when compared to the presence of tetracycline.

These results confirm that the tetCAR system is more sensitive to doxycycline and minocycline when compared to tetracycline.

Figure 27

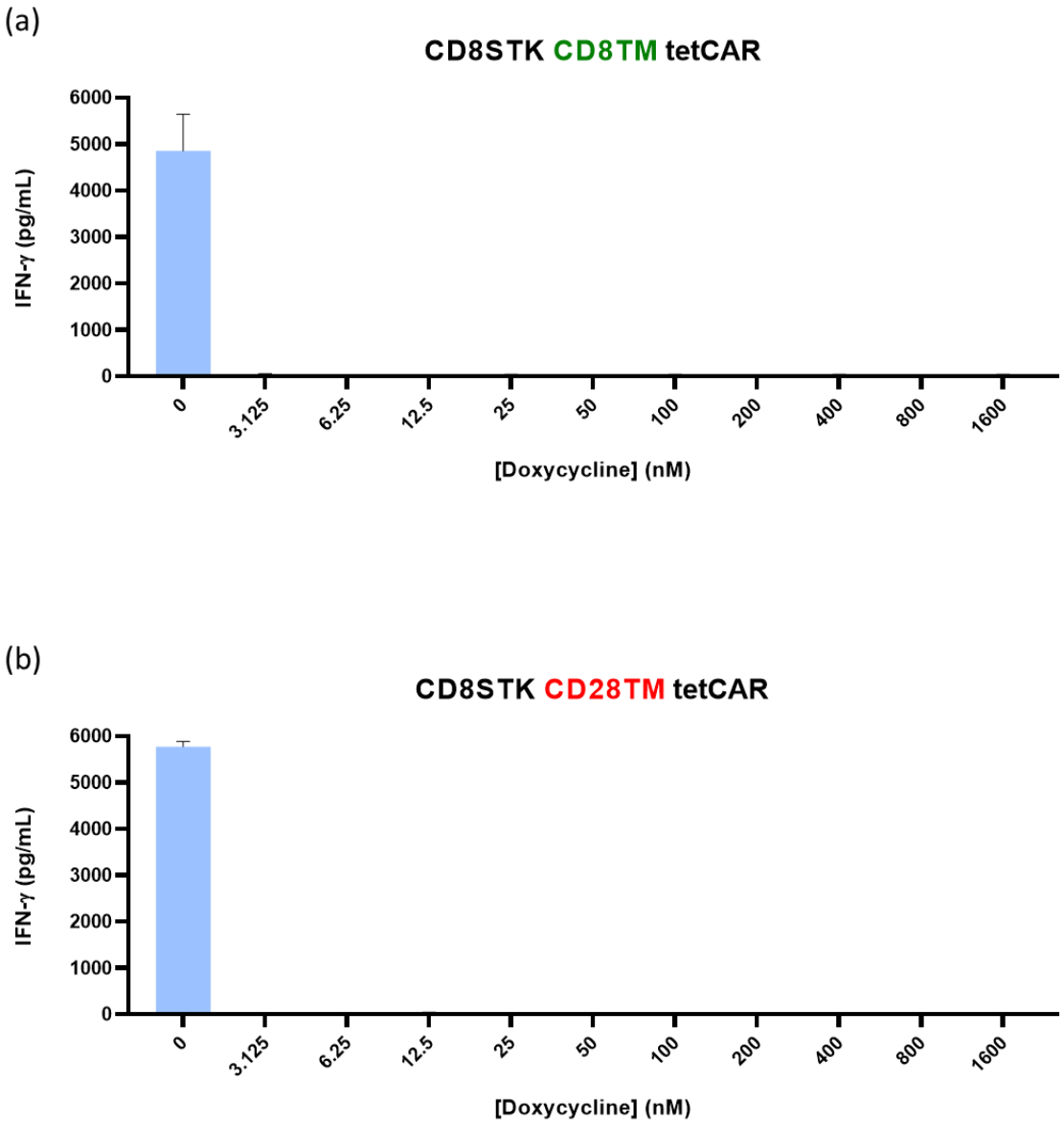

Figure 27. Response of tetCAR T-cell activity to doxycycline, a tetracycline analogue. Cytokine production by primary tetCAR T-cells in the presence of $CD19^{+}$ target cells. (a) Primary human T-cells expressing the 'CD8STK CD8TM' tetCAR or (b) primary human T-cells expressing the 'CD8STK CD28TM' tetCAR were challenged with SupT1 cells engineered to express CD19 at a 4:1 T-cell:target cell ratio in the absence of doxycycline or in the presence of increasing concentrations of doxycycline.

(c)

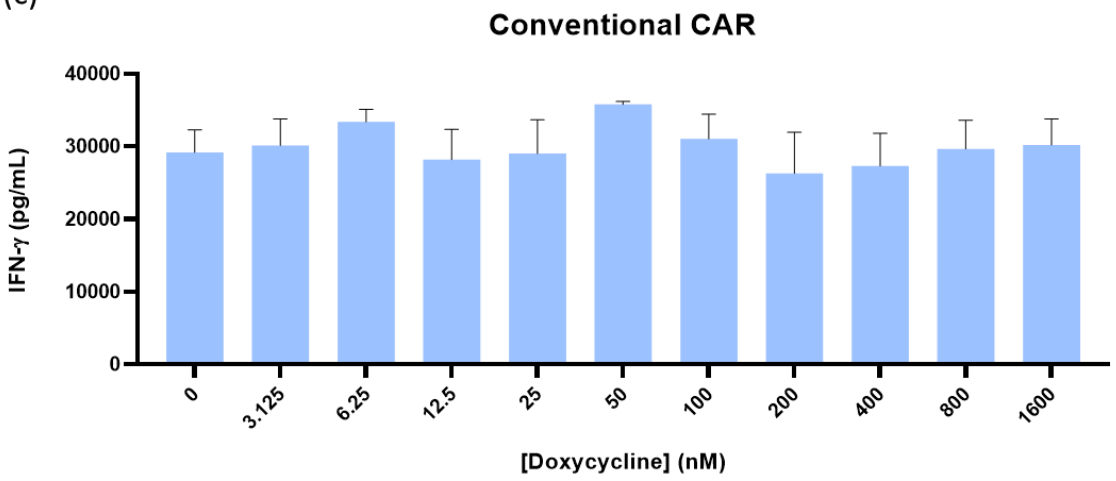

(d)

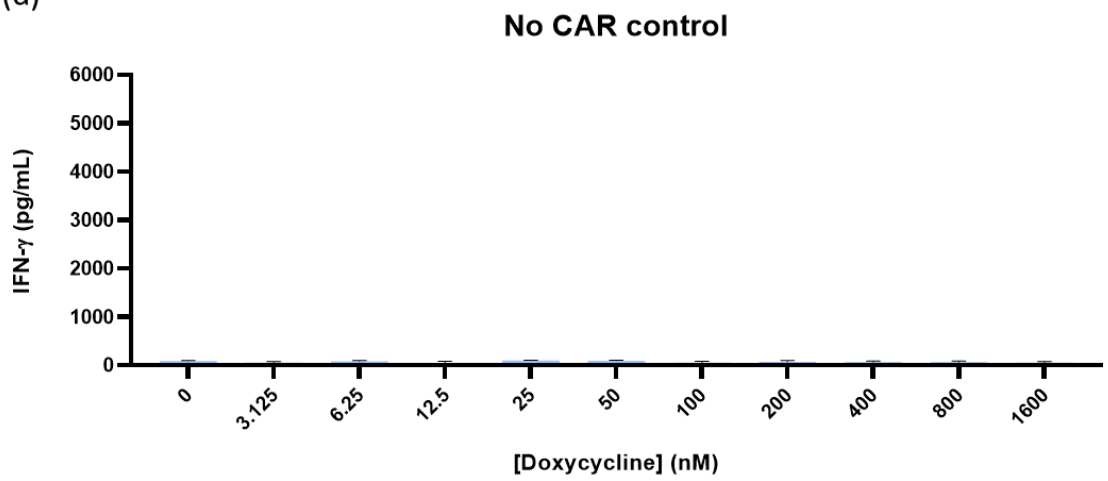

(c) Primary human T-cells expressing the conventional CAR and (d) non-transduced T-cells were set-up to serve as control. Production of IFN-γ after an overnight incubation was quantified by ELISA; n = 2 independent experiments from separate donors, error bars denote SD.

Figure 28

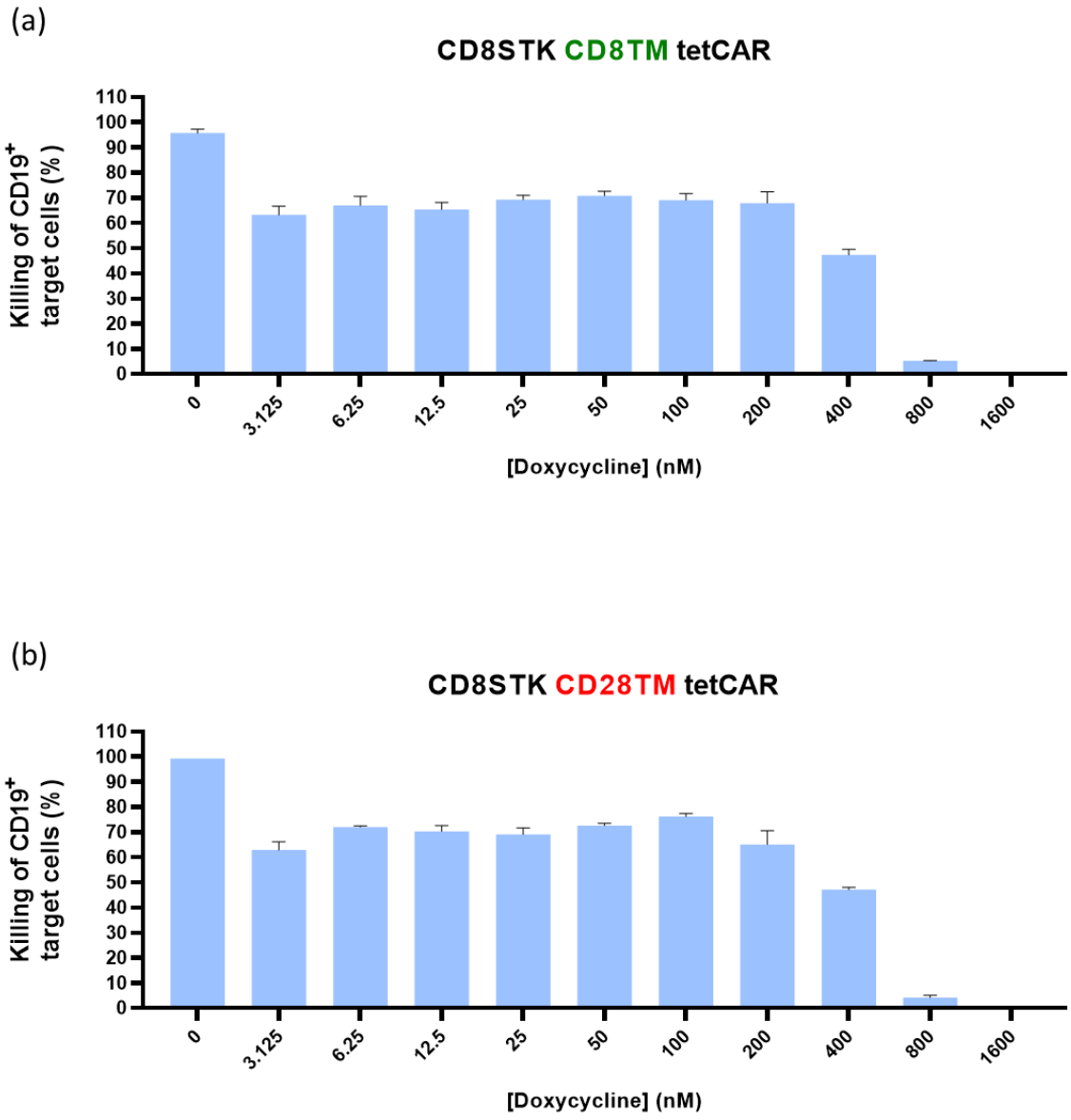

Figure 28. Response of tetCAR T-cell activity to doxycycline, a tetracycline analogue. Cytotoxicity activity mediated by tetCARs in a 72-hour end-point experiment. (a) Primary human T-cells expressing the 'CD8STK CD8TM' tetCAR or (b) primary human T-cells expressing the 'CD8STK CD28TM' tetCAR were challenged with SupT1 cells engineered to express CD19 at a 4:1 T-cell:target cell ratio in the absence of doxycycline or in the presence of increasing concentrations of doxycycline.

(c)

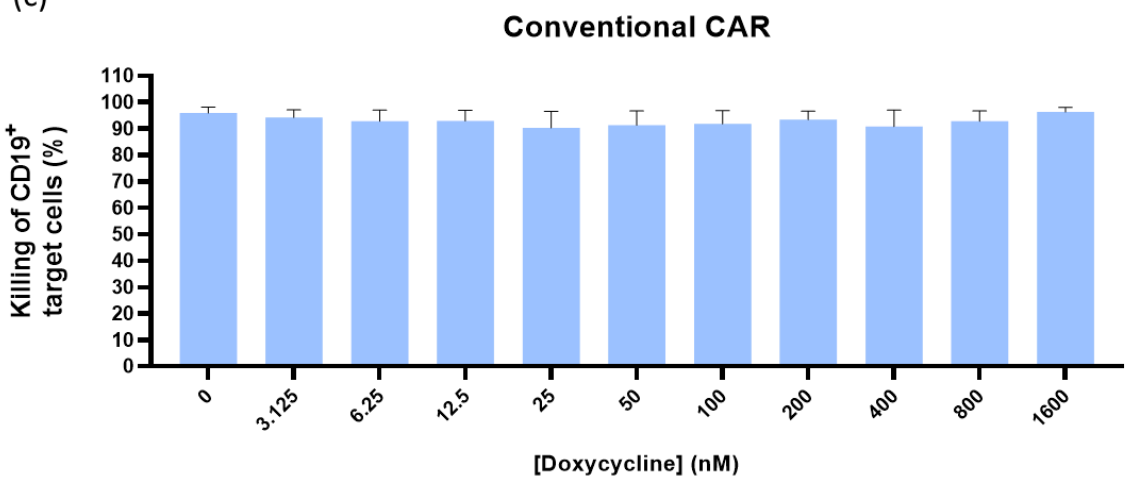

(d)

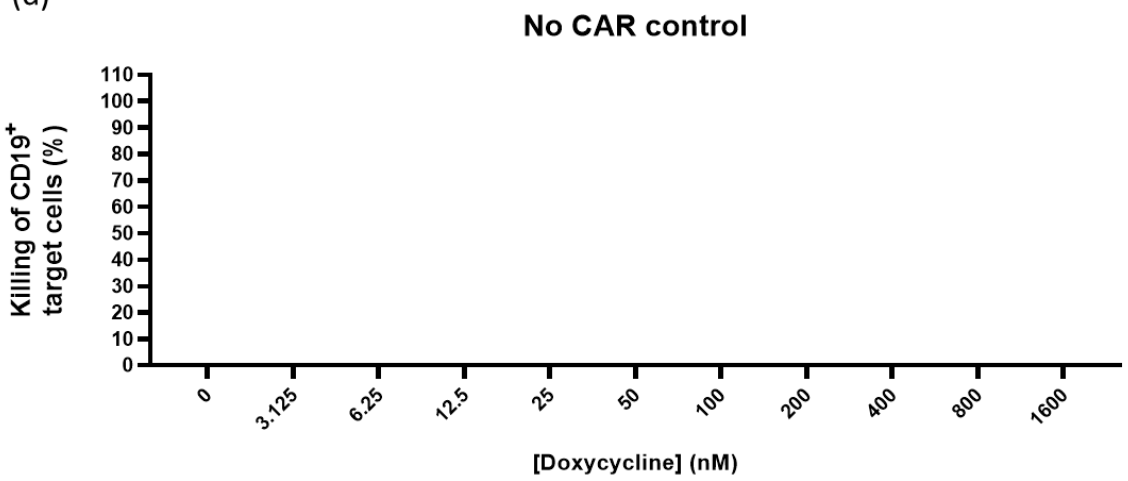

(c) Primary human T-cells expressing the conventional CAR and (d) non-transduced T-cells were set-up to serve as control. A low percentage for survival of $CD19^+$ SupT1 cells indicates a high degree of specific target cell killing by CAR T-cells; n = 2 independent experiments from separate donors, error bars denote SD.

Figure 29

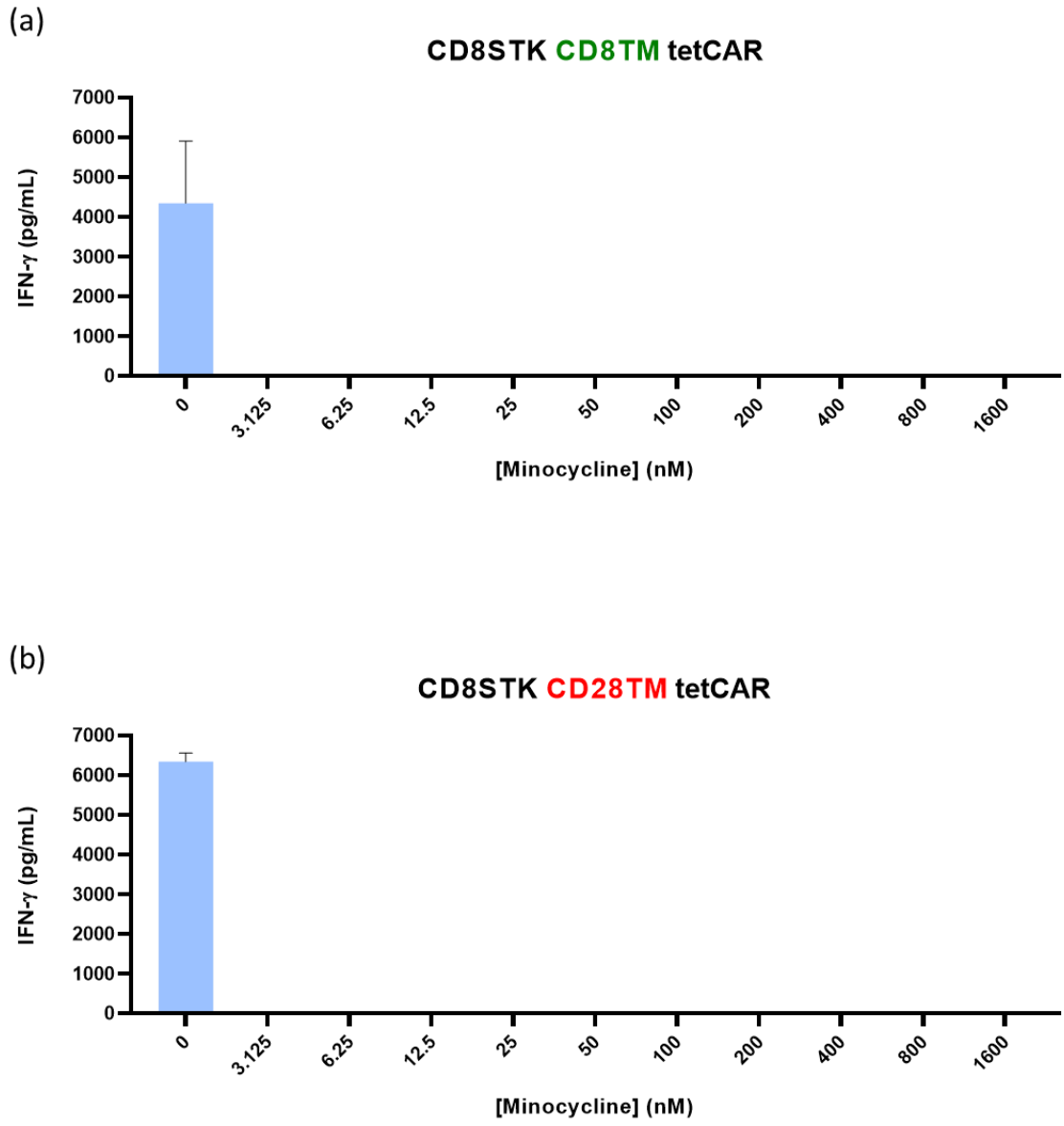

Figure 29. Response of tetCAR T-cell activity to minocycline, another tetracycline analogue. Cytokine production by primary tetCAR T-cells in the presence of $CD19^{+}$ target cells. (a) Primary human T-cells expressing the 'CD8STK CD8TM' tetCAR or (b) primary human T-cells expressing the 'CD8STK CD28TM' tetCAR were challenged with SupT1 cells engineered to express CD19 at a 4:1 T-cell:target cell ratio in the absence of minocycline or in the presence of increasing concentrations of minocycline.

(c)

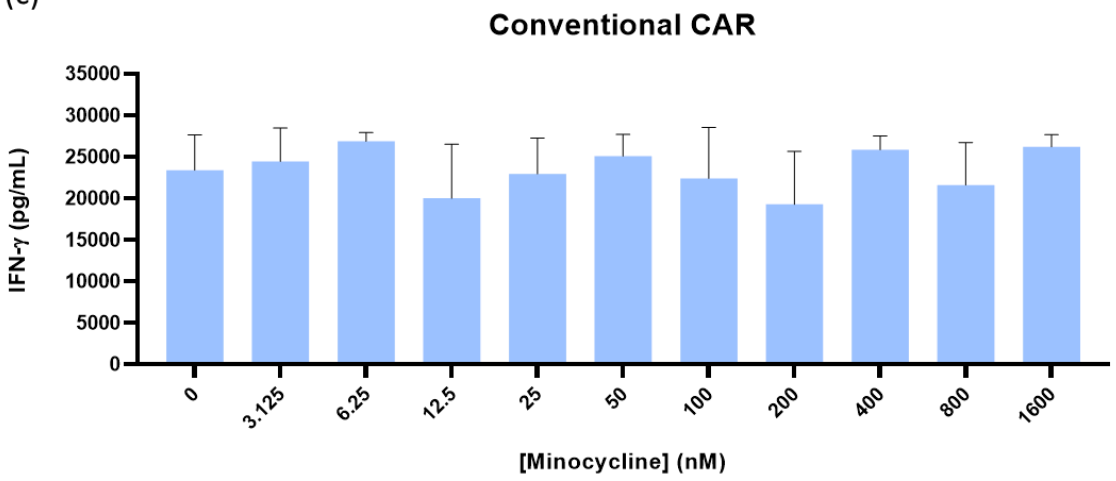

(d)

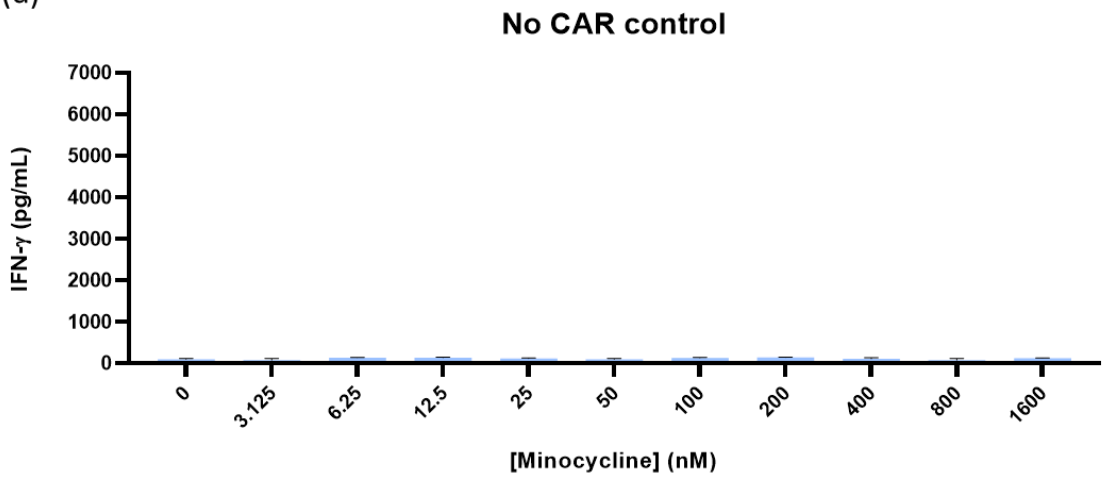

(c) Primary human T-cells expressing the conventional CAR and (d) non-transduced T-cells were set-up to serve as control. Production of IFN-γ after an overnight incubation was quantified by ELISA; n = 2 independent experiments from separate donors, error bars denote SD.

Figure 30

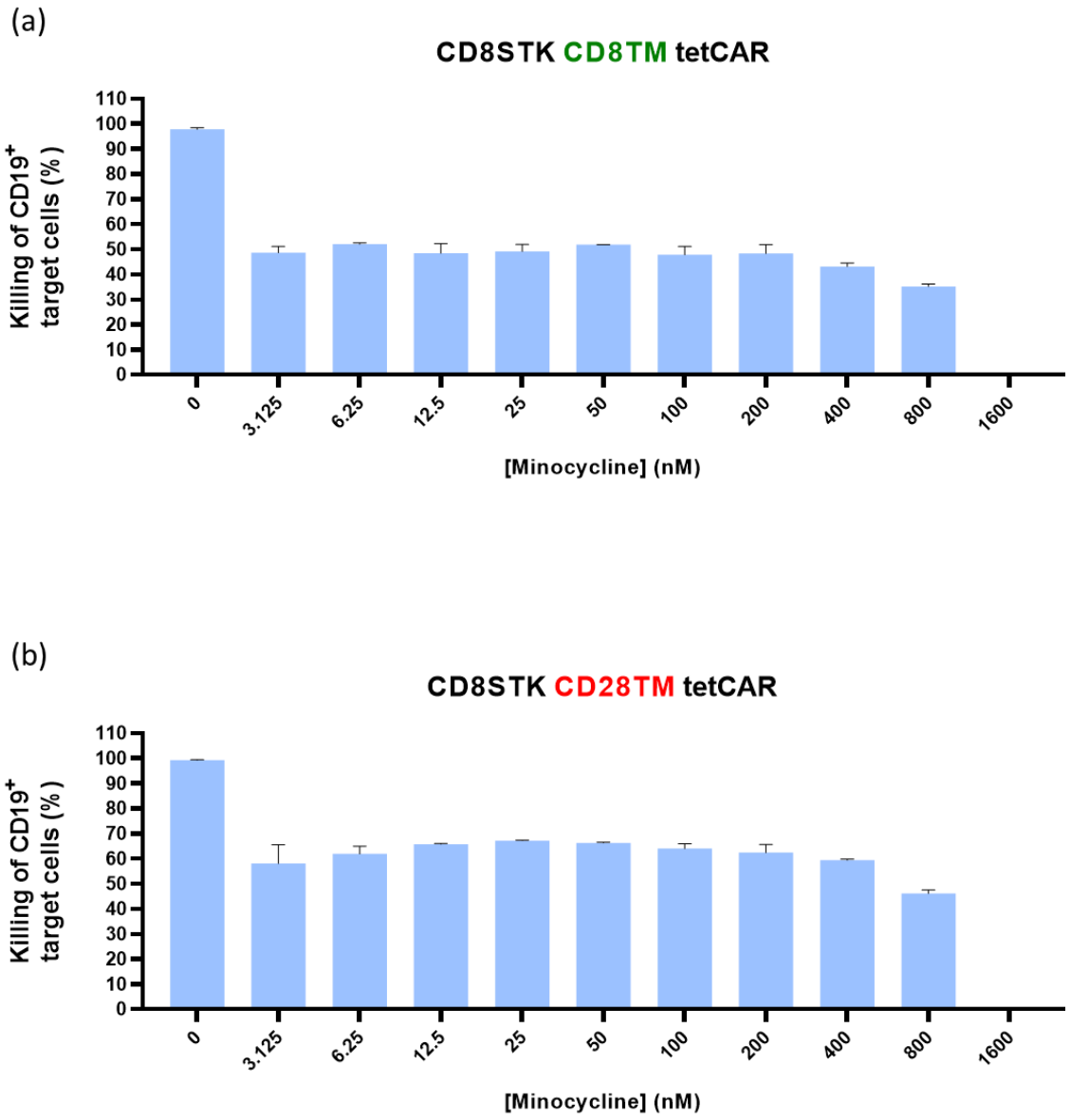

Figure 30. Response of tetCAR T-cell activity to minocycline, another tetracycline analogue. Cytotoxicity activity mediated by tetCARs in a 72-hour end-point experiment. (a) Primary human T-cells expressing the 'CD8STK CD8TM' tetCAR or (b) primary human T-cells expressing the 'CD8STK CD28TM' tetCAR were challenged with SupT1 cells engineered to express CD19 at a 4:1 T-cell:target cell ratio in the absence of minocycline or in the presence of increasing concentrations of minocycline.

(c)

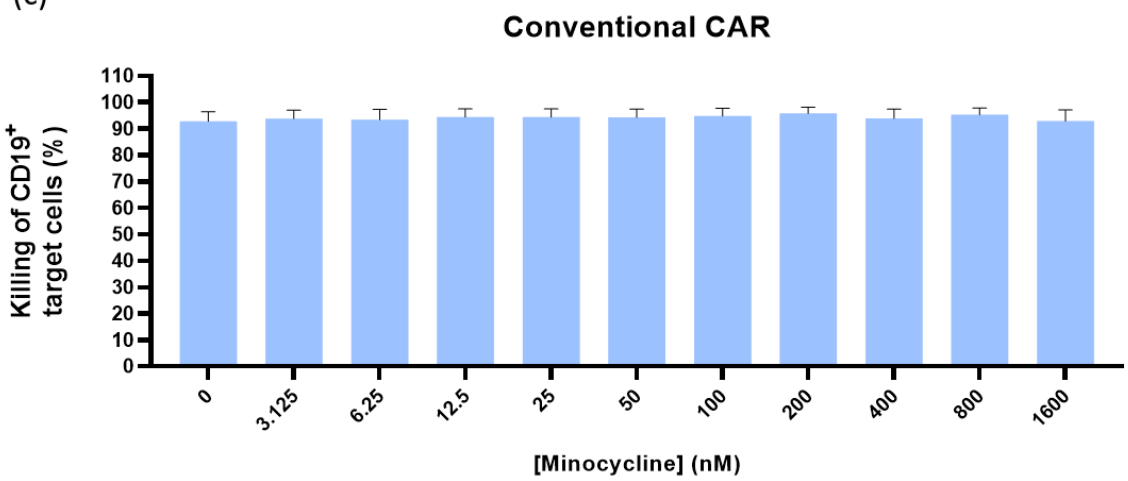

(d)

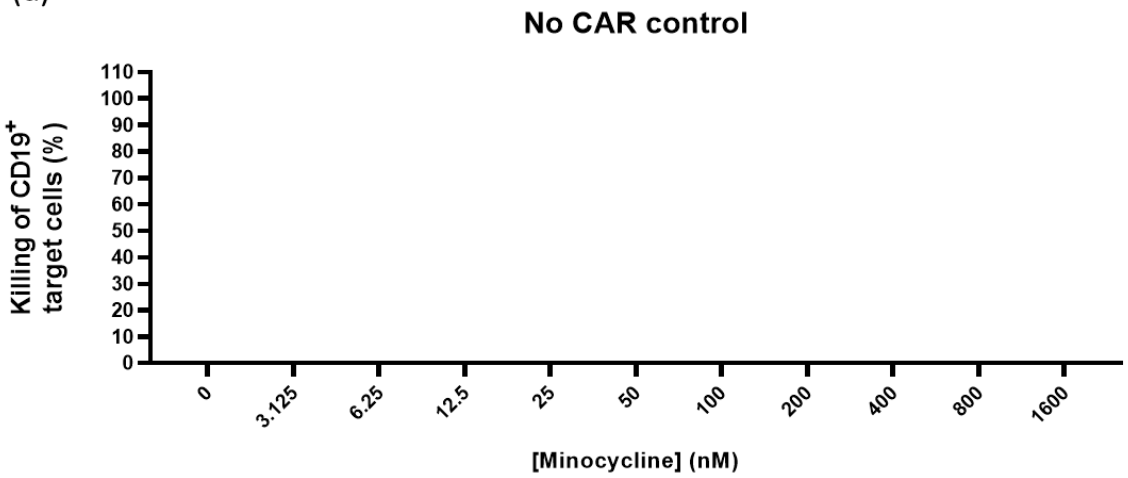

(c) Primary human T-cells expressing the conventional CAR and (d) non-transduced T-cells were set-up to serve as control. A low percentage for survival of $CD19^+$ SupT1 cells indicates a high degree of specific target cell killing by CAR T-cells; n = 2 independent experiments from separate donors, error bars denote SD.

7.1.2.2 Testing of drug concentrations ranging from 0 to 3.125 nM

After demonstrating that the tetCAR system is compatible with other alternative small molecules, it was of interest to assess the titre response of the two most promising tetCARs to doxycycline and minocycline. To achieve this, a new range of small molecule concentrations was tested. From the previous cytokine production experiment, we know that both tetCAR T-cells showed no IFN-γ secretion at the lowest doxycycline or minocycline concentration. Thus, it was decided to test a range of concentrations where the 3.125 nM is our highest dose.

The experiments were set up as described above for Figure 25 and Figure 26. The only modifications were the small molecule used in each experiment and the range of concentrations. The experiments were carried out using concentrations of doxycycline or minocycline ranging from 0 to 3.125 nM. In these experiments small molecule was serially diluted at 1 in 2 ratio starting from 3.125 nM.

After an overnight incubation, supernatant samples were removed and assayed for the presence of IFN-γ. Subsequent investigations into the release of IFN-γ showed that both doxycycline and minocycline decrease human T-cell IFN-γ secretion and hence activation in a dose dependent manner. The conventional CAR, which was used as a positive control, led to consistent secretion of IFN-γ by primary human T-cells in all doxycycline concentrations (Figure 31c) and also in all minocycline concentrations (Figure 33c). As expected, minimal IFN-γ secretion by non-transduced T-cells was detected on either doxycycline (Figure 31d) or minocycline (Figure 33d) experiments. In both tetracycline inducible CARs, the amount of secreted IFN-γ was found to decrease with increasing concentrations of doxycycline (Figures 31a and 31b) and also with increasing concentrations of minocycline (Figures 33a and 33b).
These data show that both tetCAR constructs allow for effective tunable control over T-cell activity via the administration of tetracycline analogues.

To further validate the titratable response of the two most promising tetCARs to doxycycline and minocycline, we also performed a flow cytometry-based cell-killing assay.

After incubation for 72 hours, surviving target cells were quantified by flow cytometry. A low percentage for survival of $CD19^+$ SupT1 cells indicates a high degree of specific target cell killing by CAR T-cells. In the 72-hour end-point experiment, almost complete killing of the $CD19^+$ target cells was observed with the conventional CAR T-cells in the presence of either doxycycline (Figure 32c) or minocycline (Figure 34c). As expected, no cell killing mediated by non-transduced T-cells was observed on either doxycycline (Figure 32d) or minocycline (Figure 34d) experiments. In both tetracycline inducible CARs, the percentage for killing of $CD19^+$ SupT1 cells was found to decrease with increasing concentrations of doxycycline (Figures 32a and 32b) and also with increasing concentrations of minocycline (Figures 34a and 34b).

Taken together, these findings confirm the tunability of the system in therapeutically relevant T-cells via the administration of alternative small molecules.

Figure 31

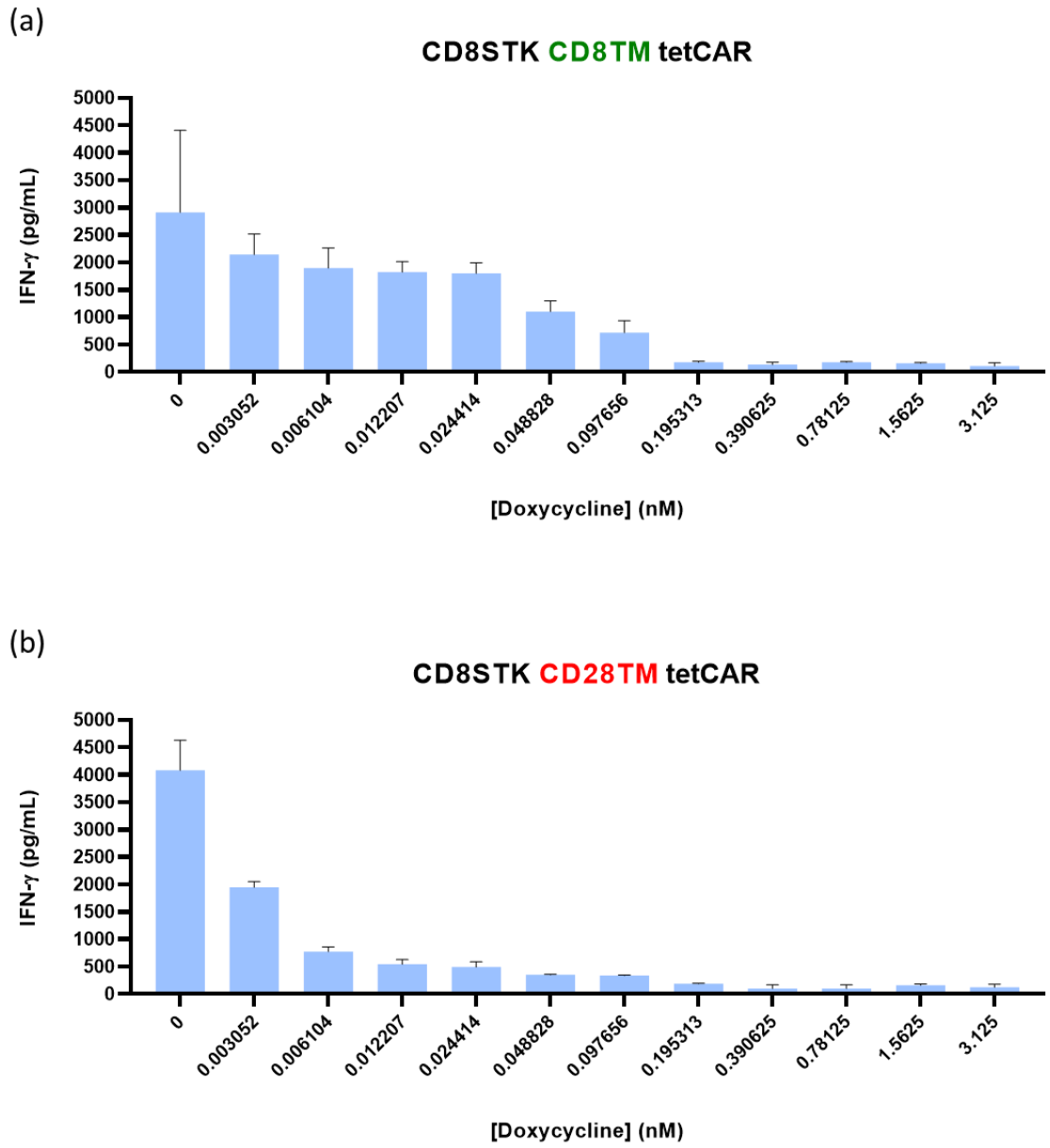

Figure 31. Control of tetCAR T-cell activity by administration of doxycycline, a tetracycline analogue. Cytokine production by primary tetCAR T-cells in the presence of $CD19^{+}$ target cells. (a) Primary human T-cells expressing the 'CD8STK CD8TM' tetCAR or (b) primary human T-cells expressing the 'CD8STK CD28TM' tetCAR were challenged with SupT1 cells engineered to express CD19 at a 4:1 T-cell:target cell ratio in the absence of doxycycline or in the presence of increasing concentrations of doxycycline.

(c)

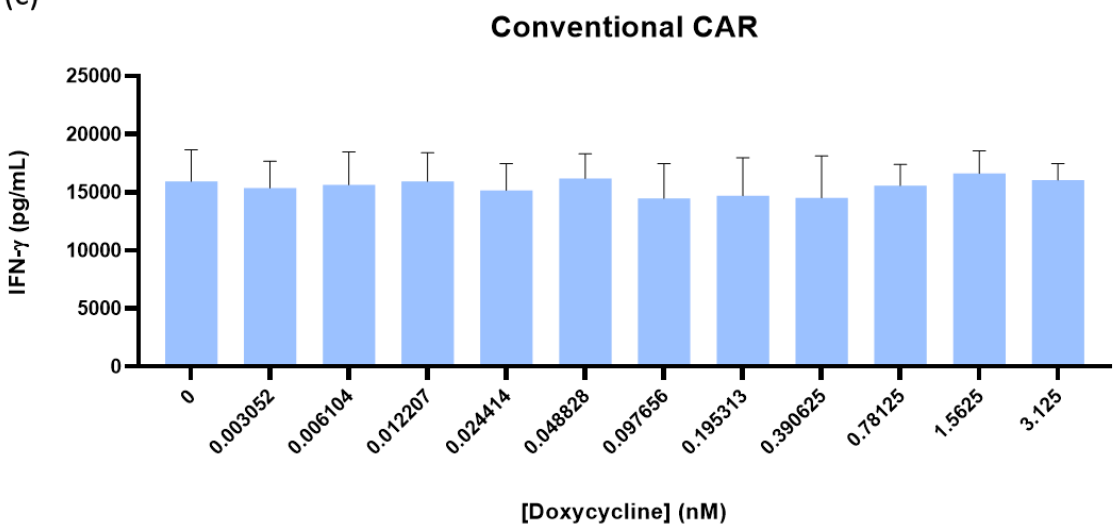

(d)

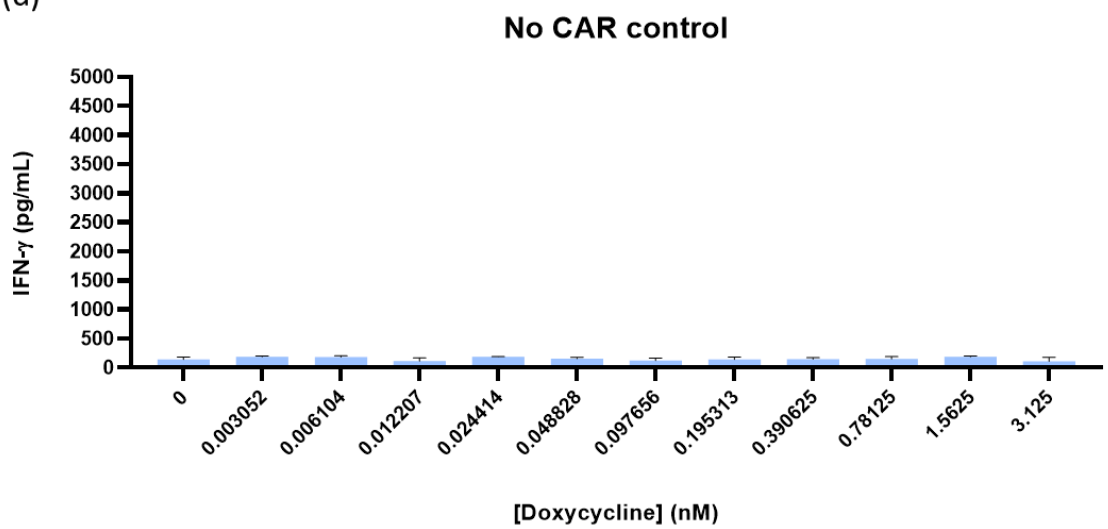

(c) Primary human T-cells expressing the conventional CAR and (d) non-transduced T-cells were set-up to serve as control. Production of IFN-γ after an overnight incubation was quantified by ELISA; n = 2 independent experiments from separate donors, error bars denote SD.

Figure 32

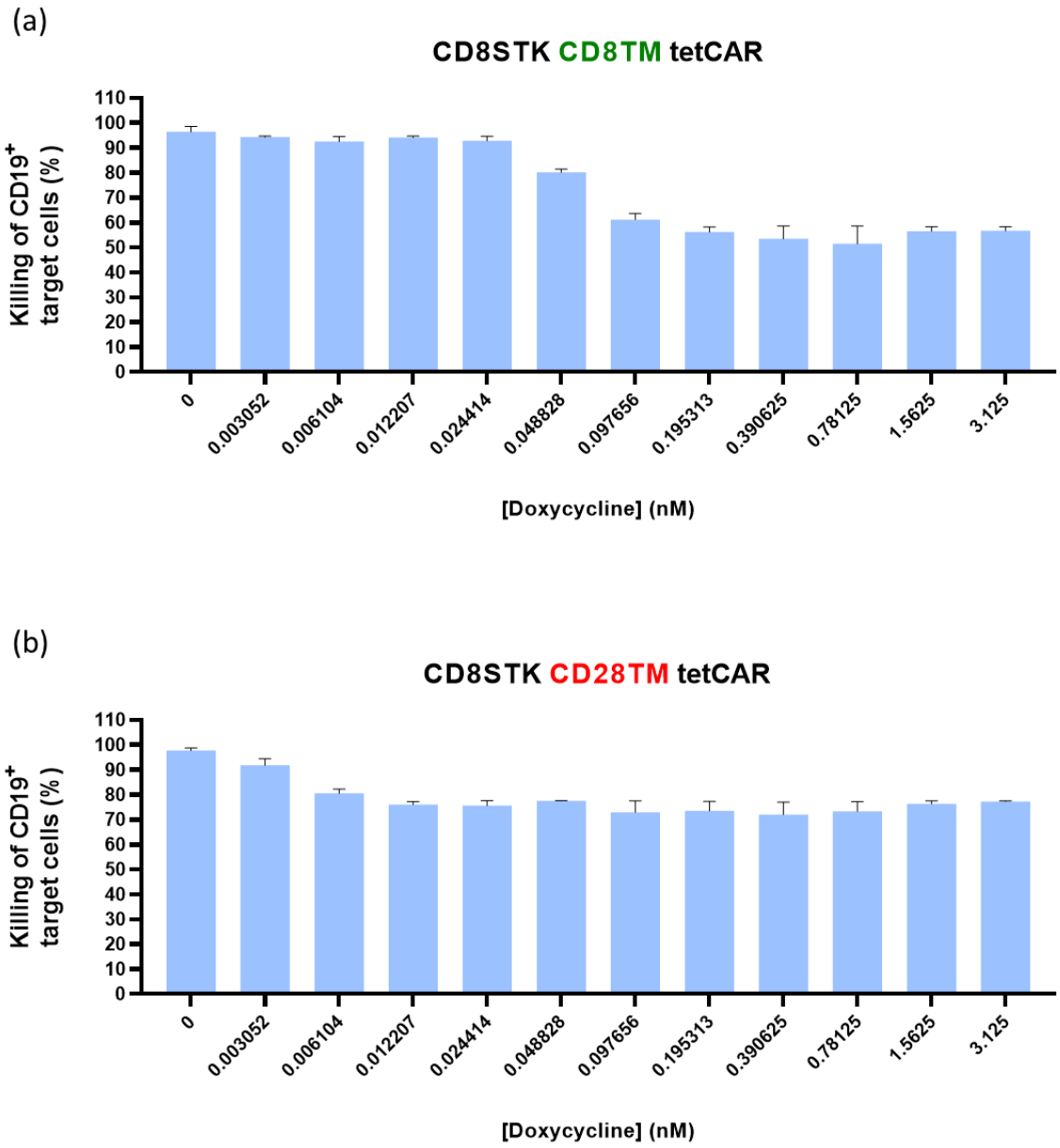

Figure 32. Control of tetCAR T-cell activity by administration of doxycycline, a tetracycline analogue. Cytotoxicity activity mediated by tetCARs in a 72-hour end-point experiment. (a) Primary human T-cells expressing the 'CD8STK CD8TM' tetCAR or (b) primary human T-cells expressing the 'CD8STK CD28TM' tetCAR were challenged with SupT1 cells engineered to express CD19 at a 4:1 T-cell:target cell ratio in the absence of doxycycline or in the presence of increasing concentrations of doxycycline.

(c)

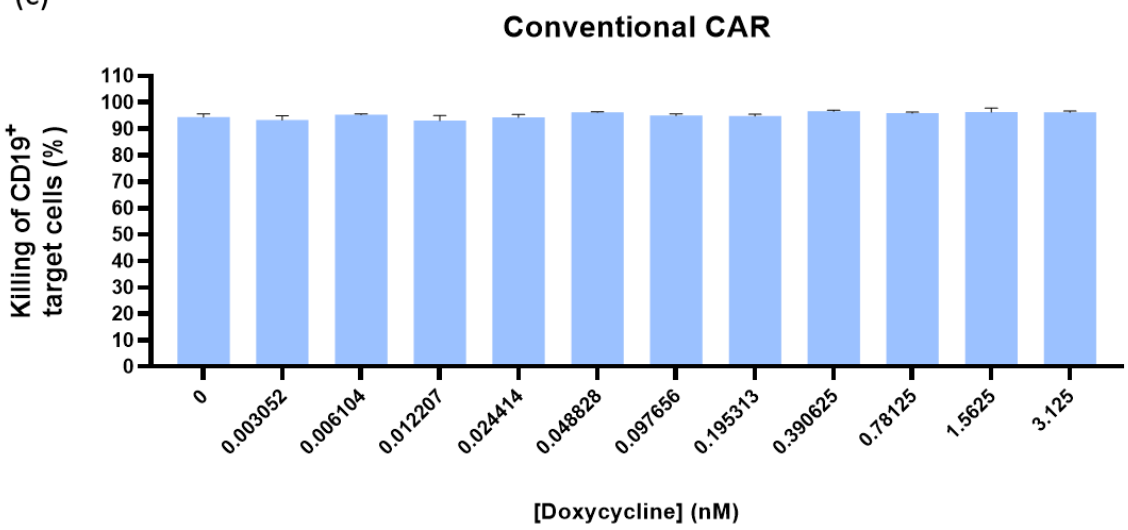

(d)

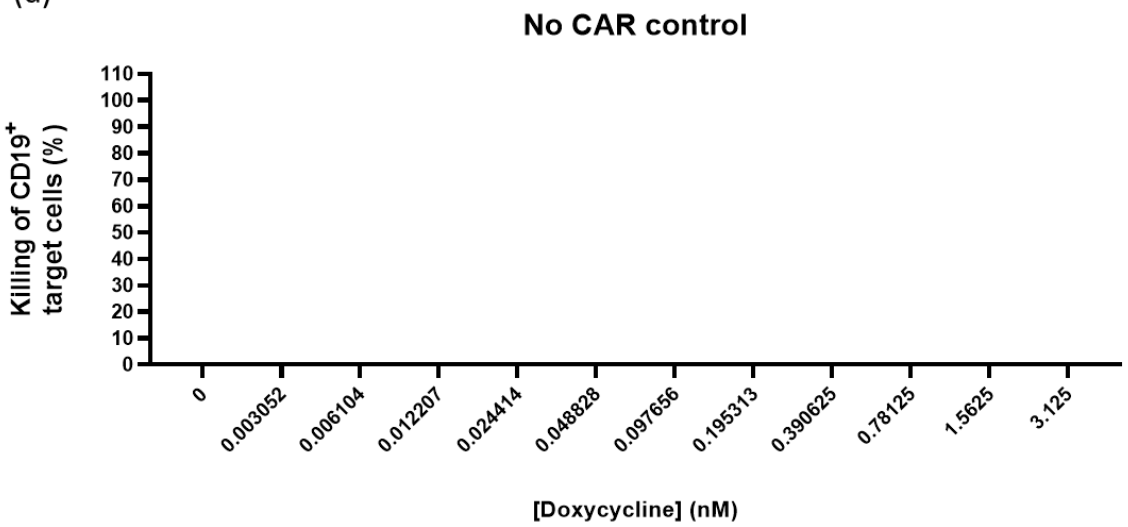

(c) Primary human T-cells expressing the conventional CAR and (d) non-transduced T-cells were set-up to serve as control. A low percentage for survival of $CD19^+$ SupT1 cells indicates a high degree of specific target cell killing by CAR T-cells; n = 2 independent experiments from separate donors, error bars denote SD.

Figure 33

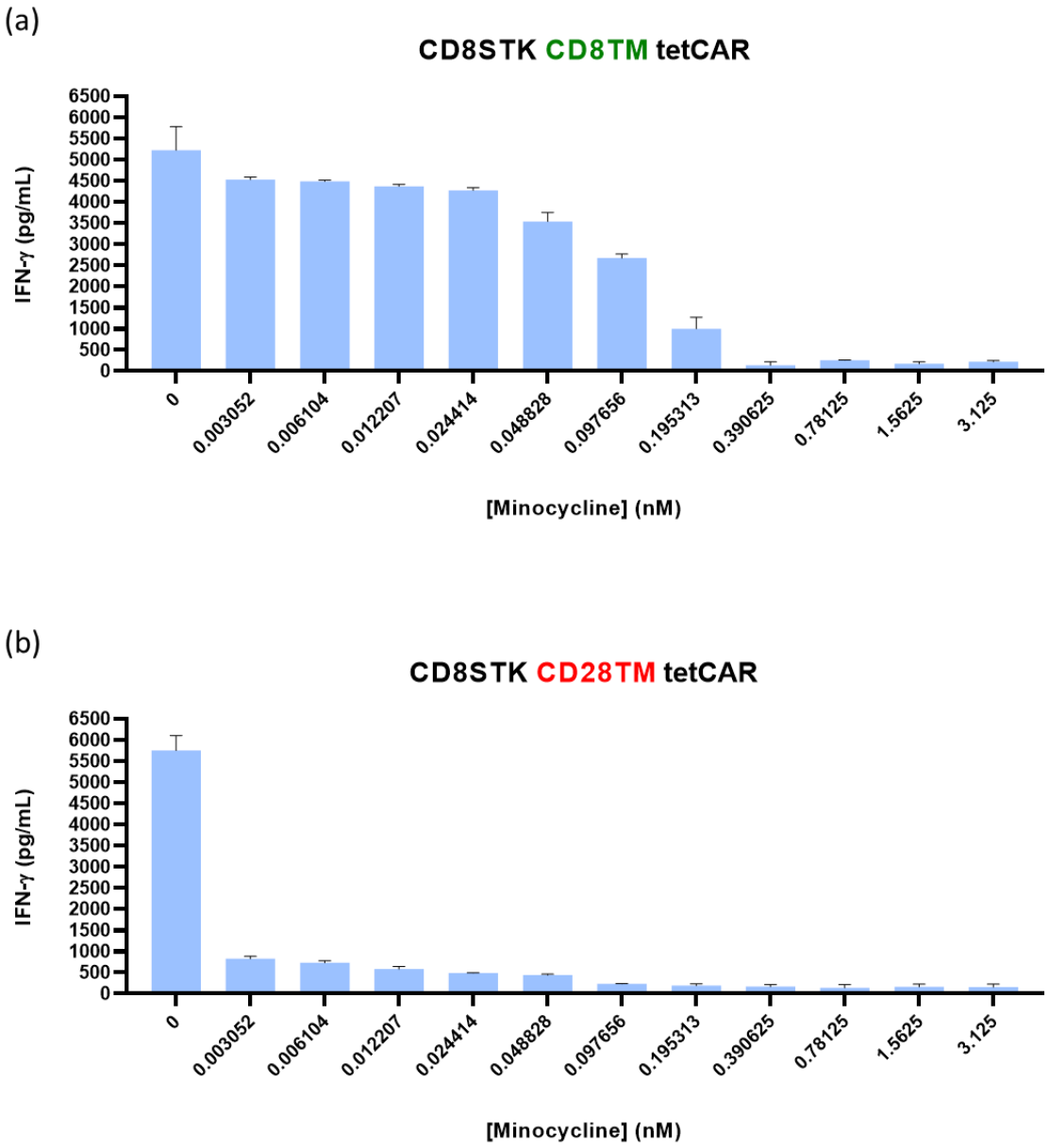

Figure 33. Control of tetCAR T-cell activity by administration of minocycline, another tetracycline analogue. Cytokine production by primary tetCAR T-cells in the presence of $CD19^{+}$ target cells. (a) Primary human T-cells expressing the 'CD8STK CD8TM' tetCAR or (b) primary human T-cells expressing the 'CD8STK CD28TM' tetCAR were challenged with SupT1 cells engineered to express CD19 at a 4:1 T-cell:target cell ratio in the absence of minocycline or in the presence of increasing concentrations of minocycline.

(c)

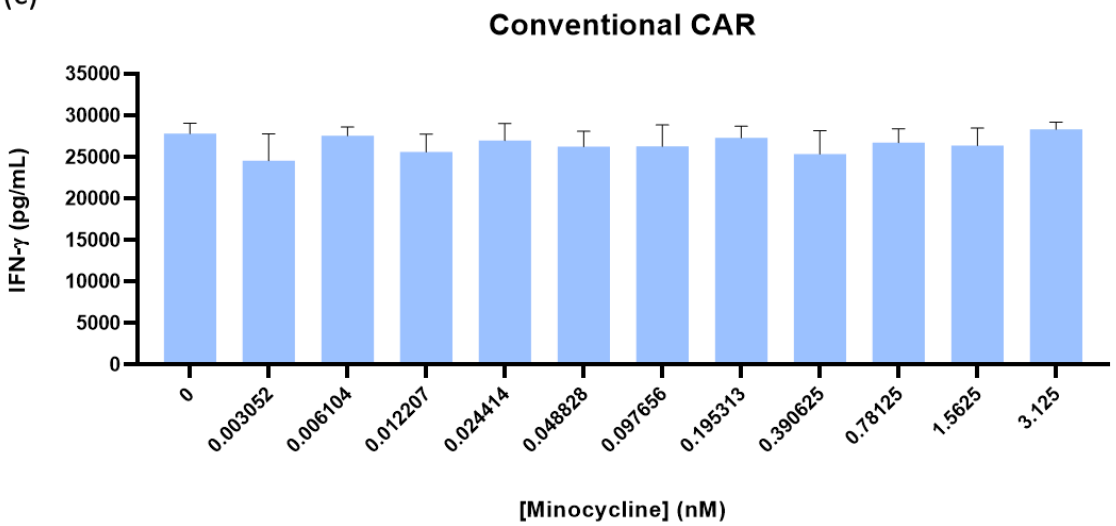

(d)

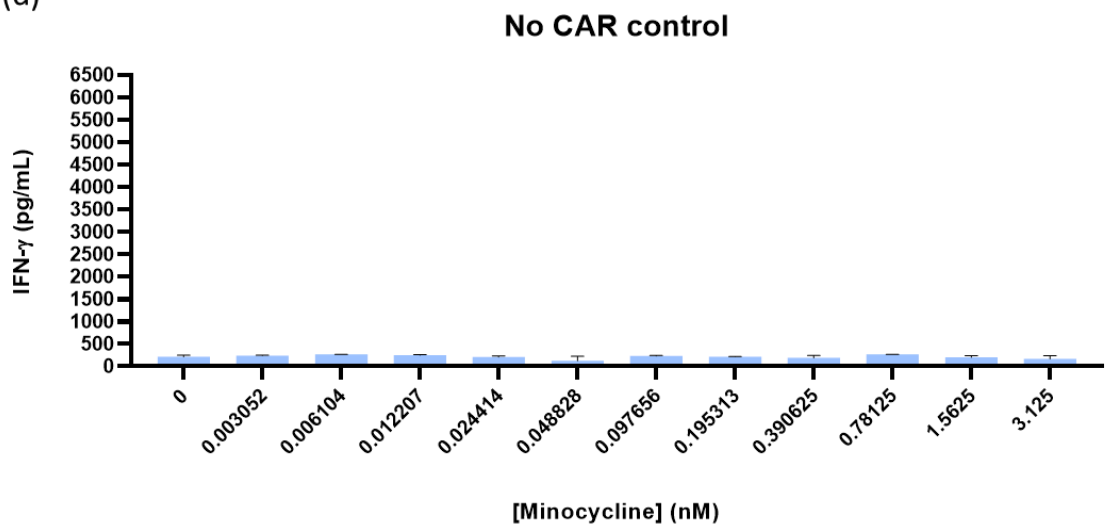

(c) Primary human T-cells expressing the conventional CAR and (d) non-transduced T-cells were set-up to serve as control. Production of IFN-γ after an overnight incubation was quantified by ELISA; n = 2 independent experiments from separate donors, error bars denote SD.

Figure 34

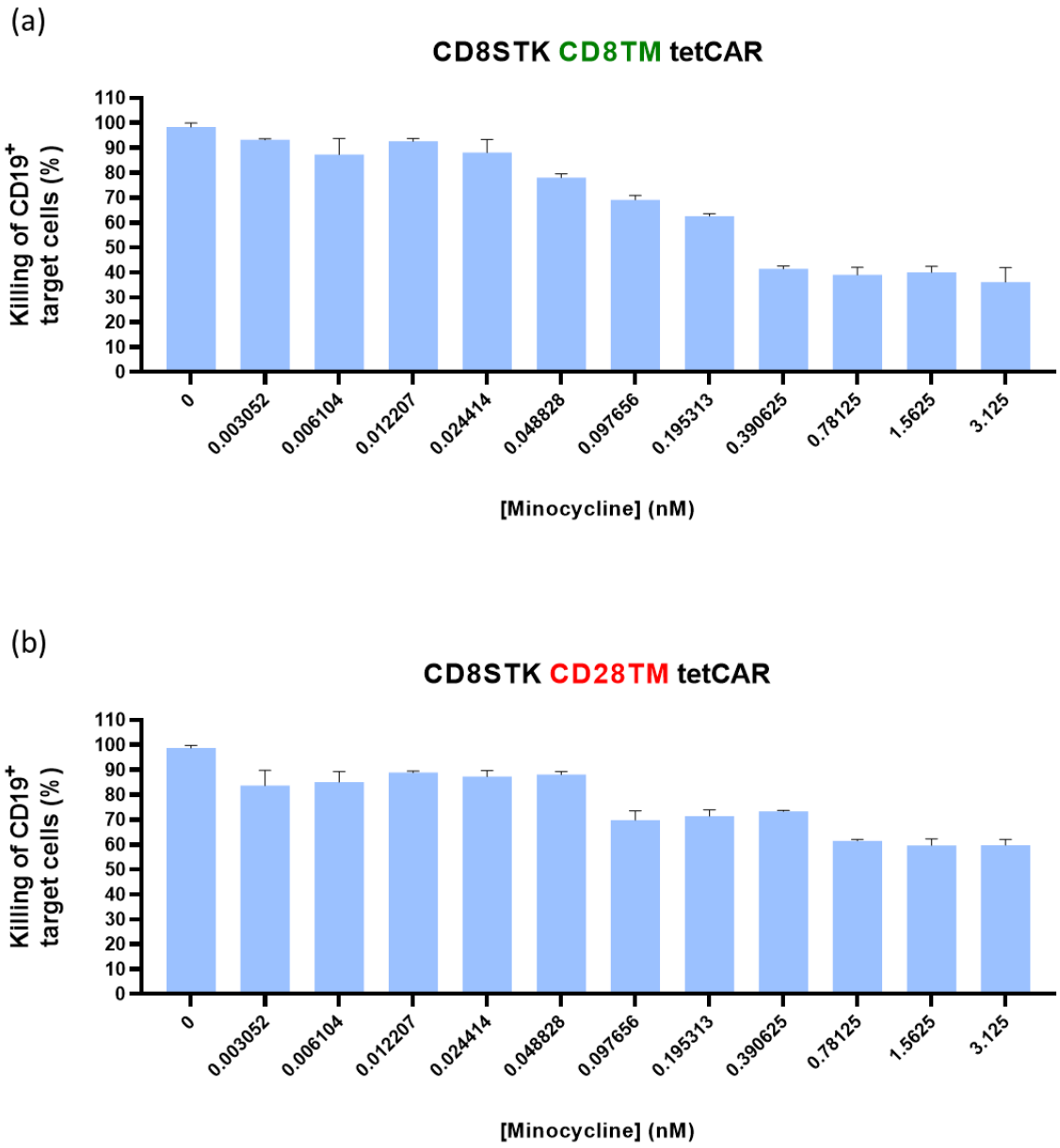

Figure 34. Control of tetCAR T-cell activity by administration of minocycline, another tetracycline analogue. Cytotoxicity activity mediated by tetCARs in a 72-hour end-point experiment. (a) Primary human T-cells expressing the 'CD8STK CD8TM' tetCAR or (b) primary human T-cells expressing the 'CD8STK CD28TM' tetCAR were challenged with SupT1 cells engineered to express CD19 at a 4:1 T-cell:target cell ratio in the absence of minocycline or in the presence of increasing concentrations of minocycline.

(c)

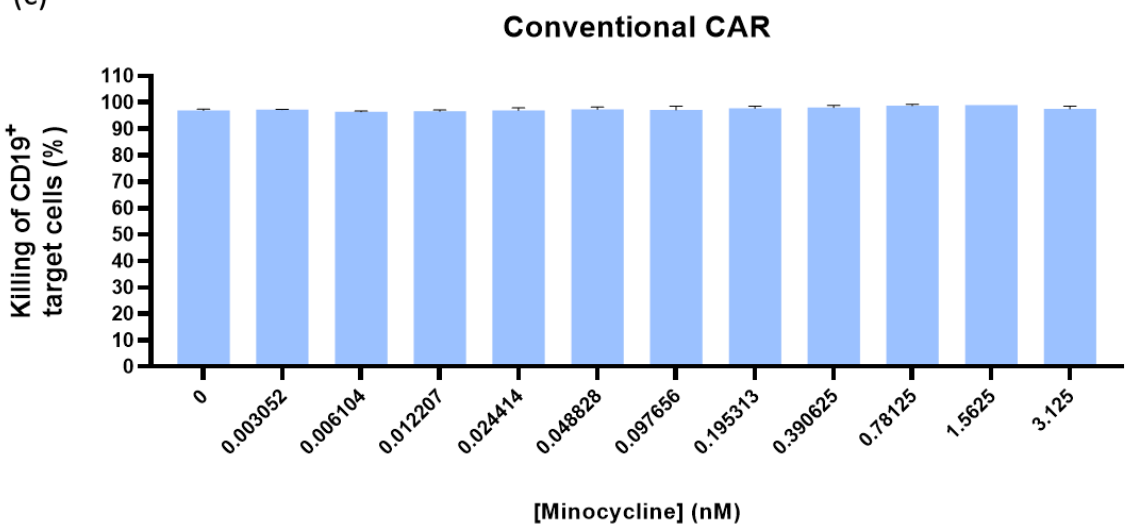

(d)

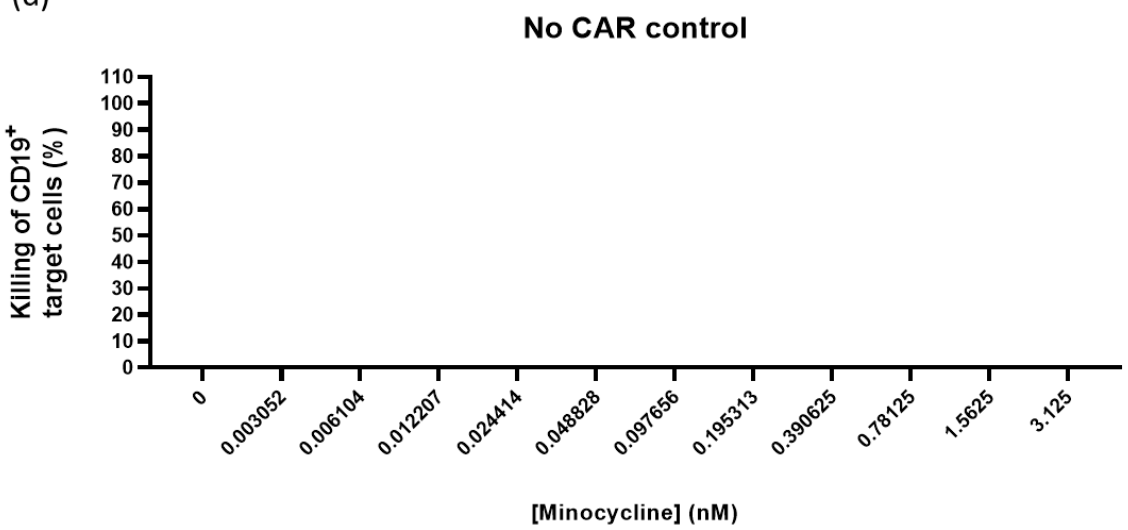

(c) Primary human T-cells expressing the conventional CAR and (d) non-transduced T-cells were set-up to serve as control. A low percentage for survival of $CD19^+$ SupT1 cells indicates a high degree of specific target cell killing by CAR T-cells; n = 2 independent experiments from separate donors, error bars denote SD.

7.2 Killing of multiple types of CD19$^+$ target cells by primary tetCAR T-cells

In our previous experiments, the cognate antigen CD19 was presented to T-cells as a cell surface protein on SupT1 target cells. The SupT1 cells provide an elegant model system, as they do not naturally express any antigen. Consequently, the introduction of CD19 into these cells was required. To confirm the relevance of our observations made with engineered SupT1 target cell lines, we investigated the killing of natural CD19$^+$ cancer cells by primary tetCAR T-cells.

Firstly, we analysed the transduction efficiency of the primary human T-cells by flow cytometry. As shown in Figure 35c, both tetCARs could be detected at the cell surface, thus indicating that these constructs were both expressed and trafficked correctly to the plasma membrane. Cell surface expression of the conventional CAR was also detected. Prior to co-culture, a further important goal was to validate the CD19 expression of all target cell lines. The presence of CD19 at the target cell surface was confirmed using flow cytometry with an anti-human CD19 antibody. The Daudi (Figure 35d), Nalm6 (Figure 35e) and Raji (Figure 35f) target cell lines naturally express CD19 in similar amounts to that seen in the CD19$^+$ SupT1 (Figure 35g) cell line. With the CD19 expression of all target cell lines validated, it was possible to test cell killing by performing a flow cytometry-based cell-killing assay. Primary human T-cells expressing the tetCARs were co-cultured with target cells at a 4:1 T-cell:target cell ratio in the absence of tetracycline or in the presence of 1600 nM tetracycline. Primary human T-cells expressing the conventional CAR were also tested. Furthermore, T-cells from the same donor that had not undergone gene transfer (designated non-transduced T-cells) were set up to serve as an additional control.

After incubation for 72 hours, surviving target cells were quantified by flow cytometry. A low percentage for survival of target cells indicates a high degree of specific target cell killing by CAR T-cells. The 72-hour end-point experiment showed that Daudi (Figure 35h), Nalm6 (Figure 35i), Raji (Figure 35j) and CD19$^+$ SupT1 (Figure 35k) cell lines were subject to killing by both ‘CD8STK CD8TM’ and ‘CD8STK CD28TM’ tetCAR T-cells in the absence of tetracycline. In the presence of 1600 nM tetracycline,

no cell killing mediated by tetCAR T-cells was observed. The conventional CAR T-cells showed a consistent killing of all $CD19^+$ target cell lines on either absence or presence of tetracycline. As expected, no cell killing mediated by non-transduced T-cells was observed on either absence or presence of tetracycline.

In summary, our results show that primary tetCAR T-cells kill multiple types of $CD19^+$ target cell populations.

Figure 35

(a) **Second-generation CD19-targeting tetCAR (with CD8STK CD8TM):**

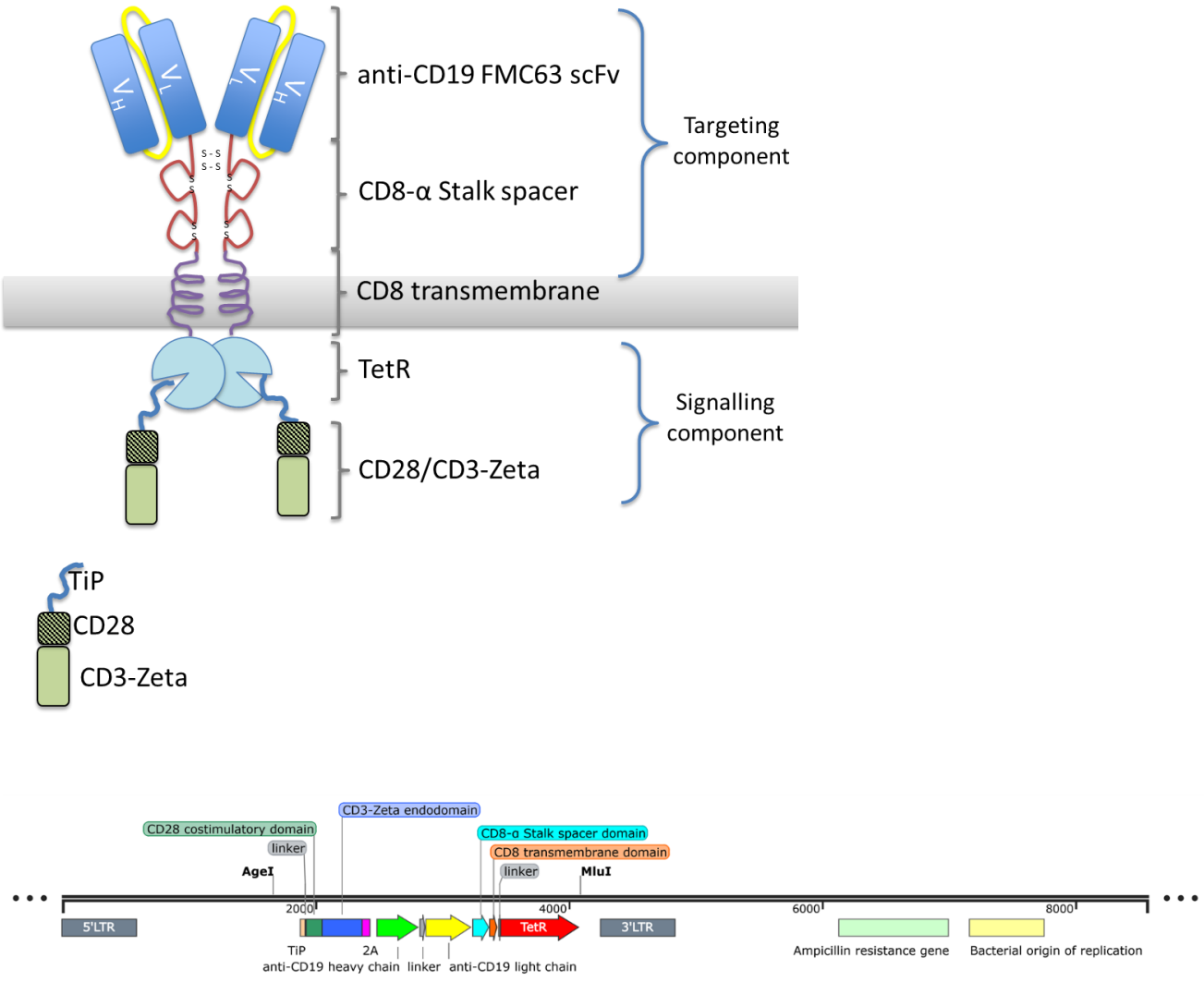

Figure 35. Killing of multiple types of CD19^{+} target cells by primary tetCAR T-cells. (a) Schematic diagram illustrating a second-generation tetCAR with CD8STK as spacer domain instead of the initial spacer derived from the Fc domain of IgG1 and with CD8TM as transmembrane domain instead of the initial CD4 derived transmembrane and intracellular domain (top). A single CAR is expressed with only one signalling component which comprises of TiP (dark blue) fused to the CD28 (diagonal stripes) and CD3-Zeta (light green) endodomain. The receptor component comprises of a CD19 recognizing scFv (blue), a CD8-α Stalk spacer domain (red), a CD8 transmembrane domain (purple), and TetR (light blue). Additionally, the plasmid map of the second-generation CD19-targeting tetCAR (with CD8STK CD8TM) is also shown (bottom).

(b) **Second-generation CD19-targeting tetCAR (with CD8STK CD28TM):**

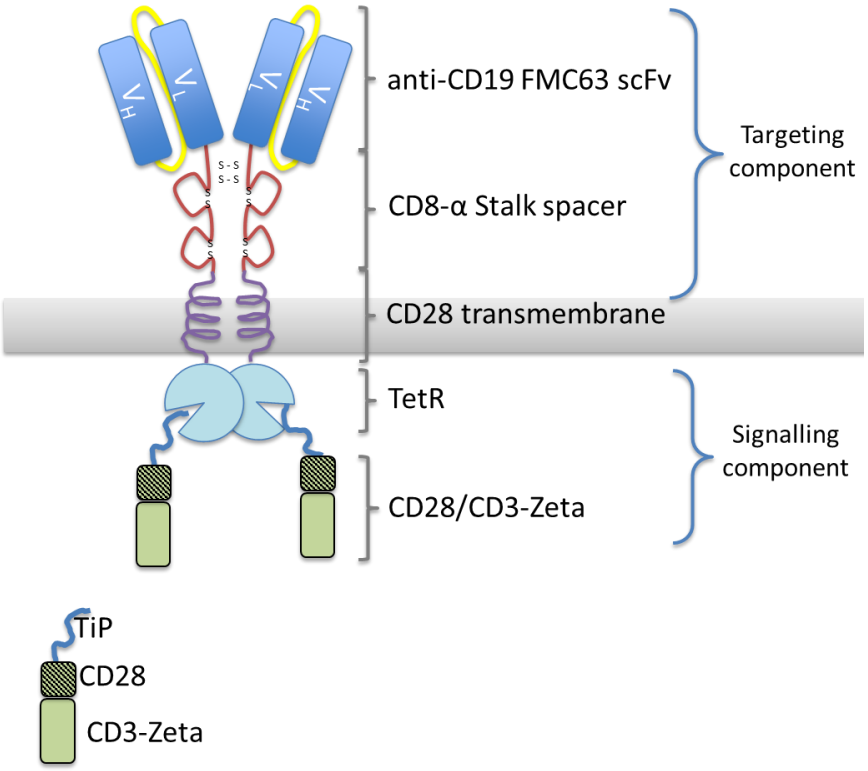

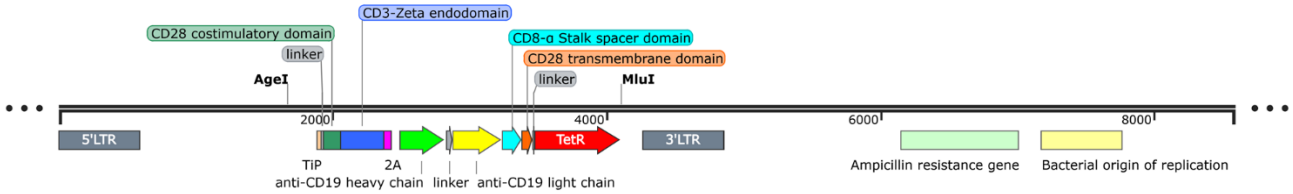

(b) Schematic diagram illustrating a second-generation tetCAR with CD8STK as spacer domain instead of the initial spacer derived from the Fc domain of IgG1 and with CD28TM as transmembrane domain instead of the initial CD4 derived transmembrane and intracellular domain (top). A single CAR is expressed with only one signalling component which comprises of TiP (dark blue) fused to the CD28 (diagonal stripes) and CD3-Zeta (light green) endodomain. The receptor component comprises of a CD19 recognizing scFv (blue), a CD8-α Stalk spacer domain (red), a CD28 transmembrane domain (purple), and TetR (light blue). Additionally, the plasmid map of the second-generation CD19-targeting tetCAR (with CD8STK CD28TM) is also shown (bottom).

(c) **Primary human T-cells:**

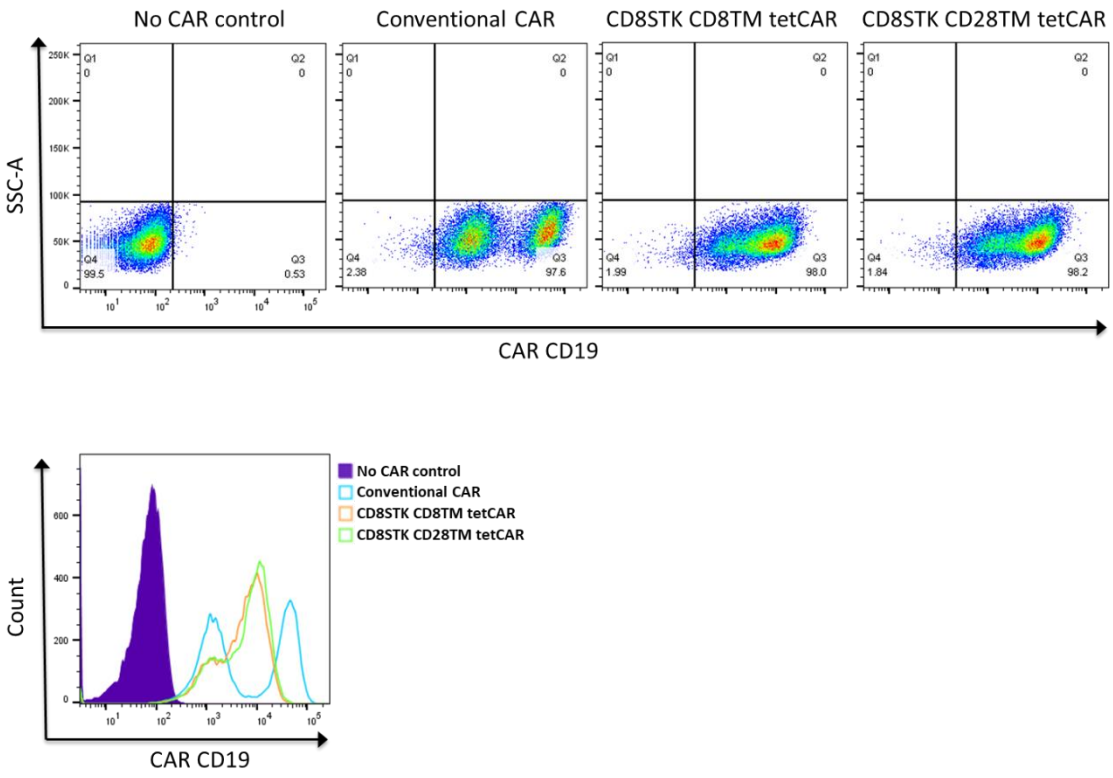

(c) Expression levels of CARs in primary human T-cells. Cells engineered with retroviral constructs encoding CAR molecules were analysed by flow cytometry. Expression of the tetCARs at the surface of primary human T-cells was compared with the expression of conventional CAR. The CARs were detected with soluble CD19 fused to rabbit IgG followed by a directly conjugated anti-Rabbit IgG antibody. Staining was compared against NT T-cells stained using the same antibodies.

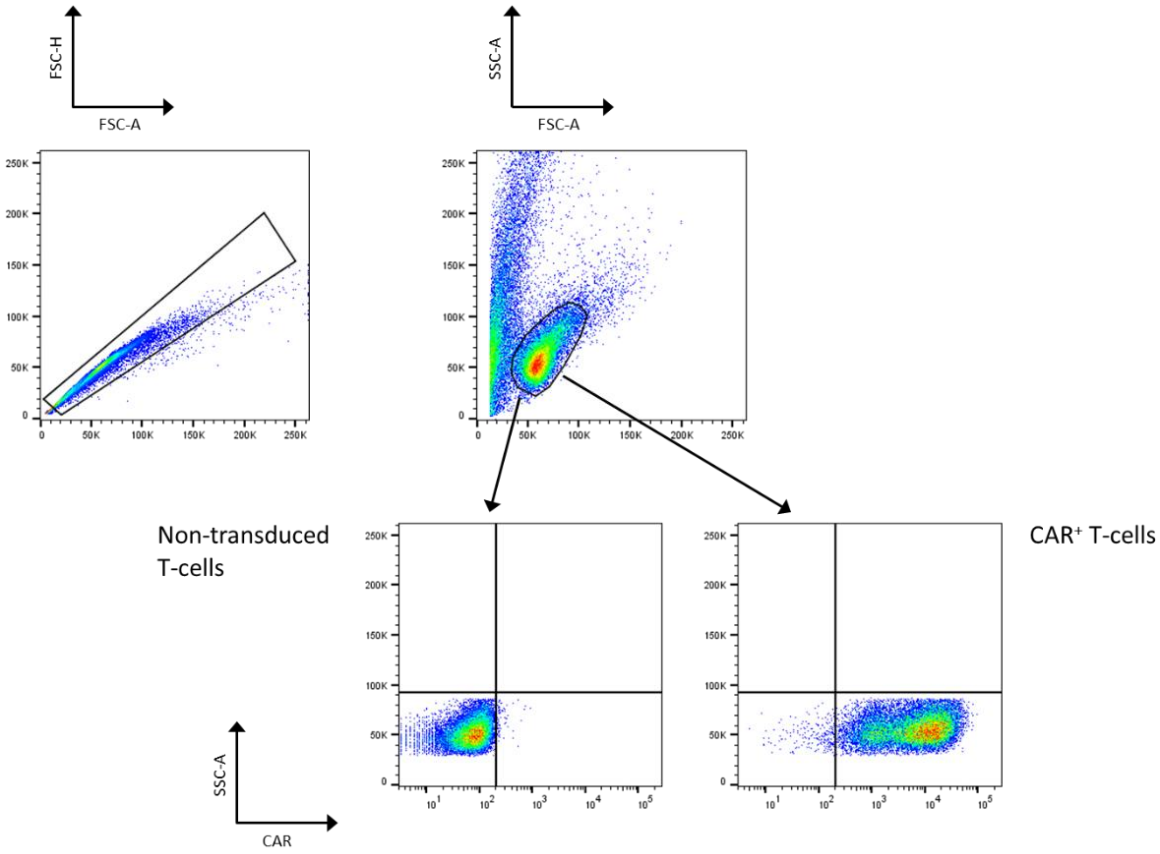

Gating strategy used to verify CAR expression on T-cells. Representative flow cytometry plots illustrating the gating strategy for assessment of CAR transduction efficiency of T-cells. Gating strategy used to identify singlet (top left), viable (top right) T-cell populations. CAR^+ T-cells were gated with reference to non-transduced control T-cells (bottom).

(d)

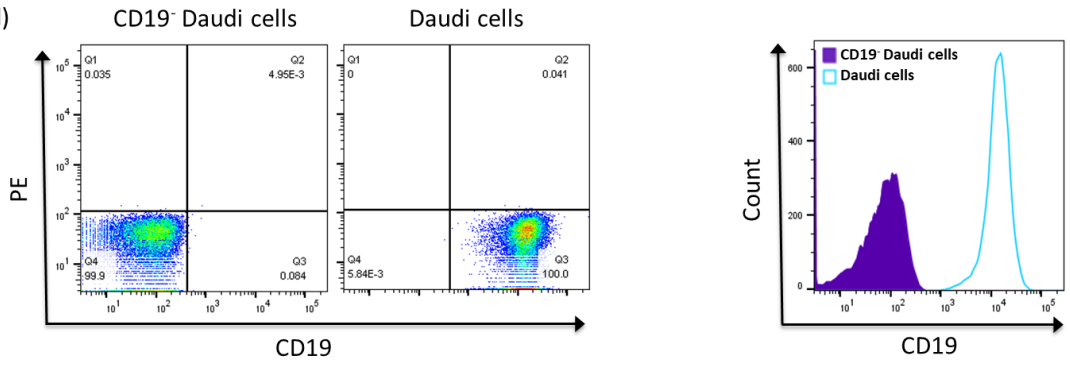
CD19- Daudi cells
Daudi cells
PE
CD19
Q1 0.035
Q2 4.95E-3
Q4 99.9
Q3 0.084
Q1 0
Q2 0.041
Q4 5.84E-3
Q3 100.0
Count
CD19- Daudi cells
Daudi cells
CD19

(e)

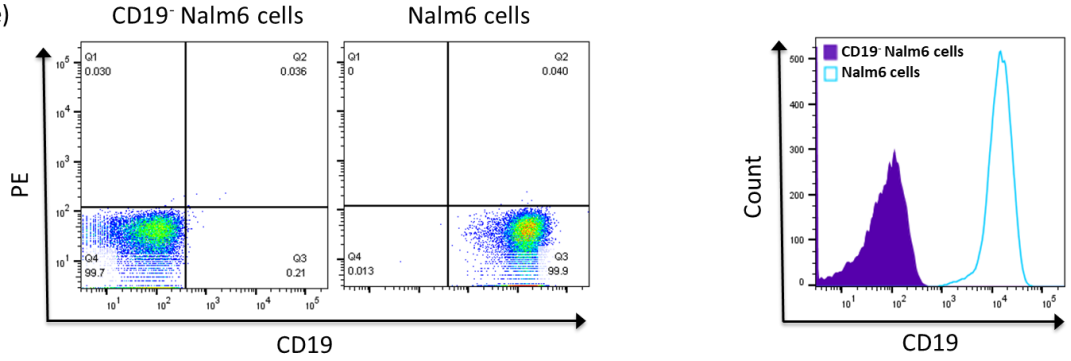
CD19- Nalm6 cells
Nalm6 cells
PE
CD19
Q1 0.030
Q2 0.036
Q4 99.7
Q3 0.21
Q1 0
Q2 0.040
Q4 0.013
Q3 99.9
Count
CD19- Nalm6 cells
Nalm6 cells
CD19

(f)

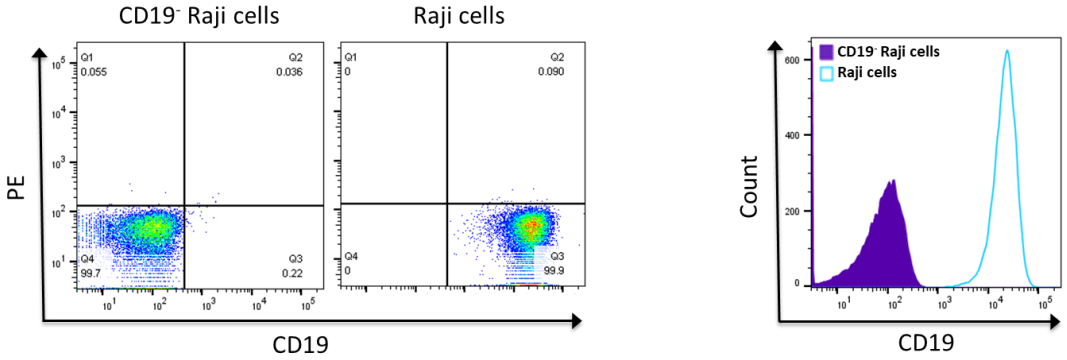
CD19- Raji cells
Raji cells
PE
CD19
Q1 0.055
Q2 0.036
Q4 99.7
Q3 0.22
Q1 0
Q2 0.090
Q4 0
Q3 99.9
Count
CD19- Raji cells
Raji cells
CD19

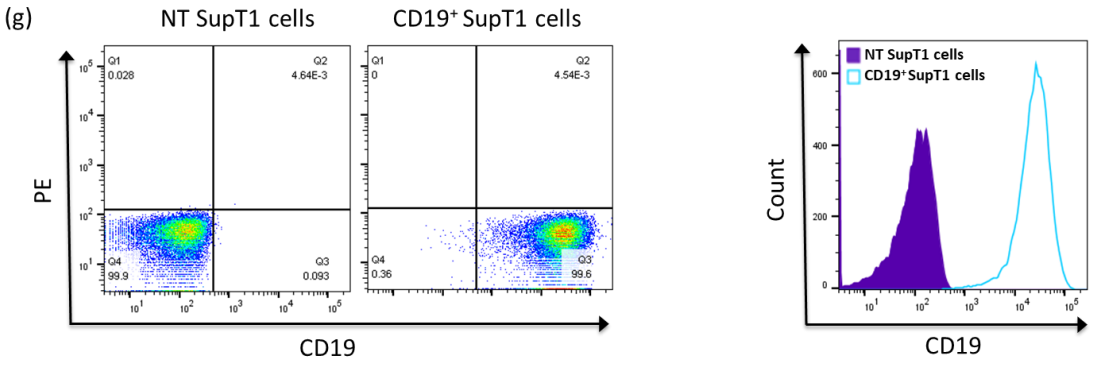

(d) Level of CD19 expression on target cell surface. (d) Daudi cells, (e) Nalm6 cells, (f) Raji cells and (g) $CD19^+$ SupT1 cells were used as target cells in co-culture assays. The cells were investigated for the presence of CD19 using flow cytometry. The expression of CD19 was detected using an anti-human CD19 antibody. The level of CD19 expression was compared with that displayed by the $CD19^-$ target cells stained with the same antibody.

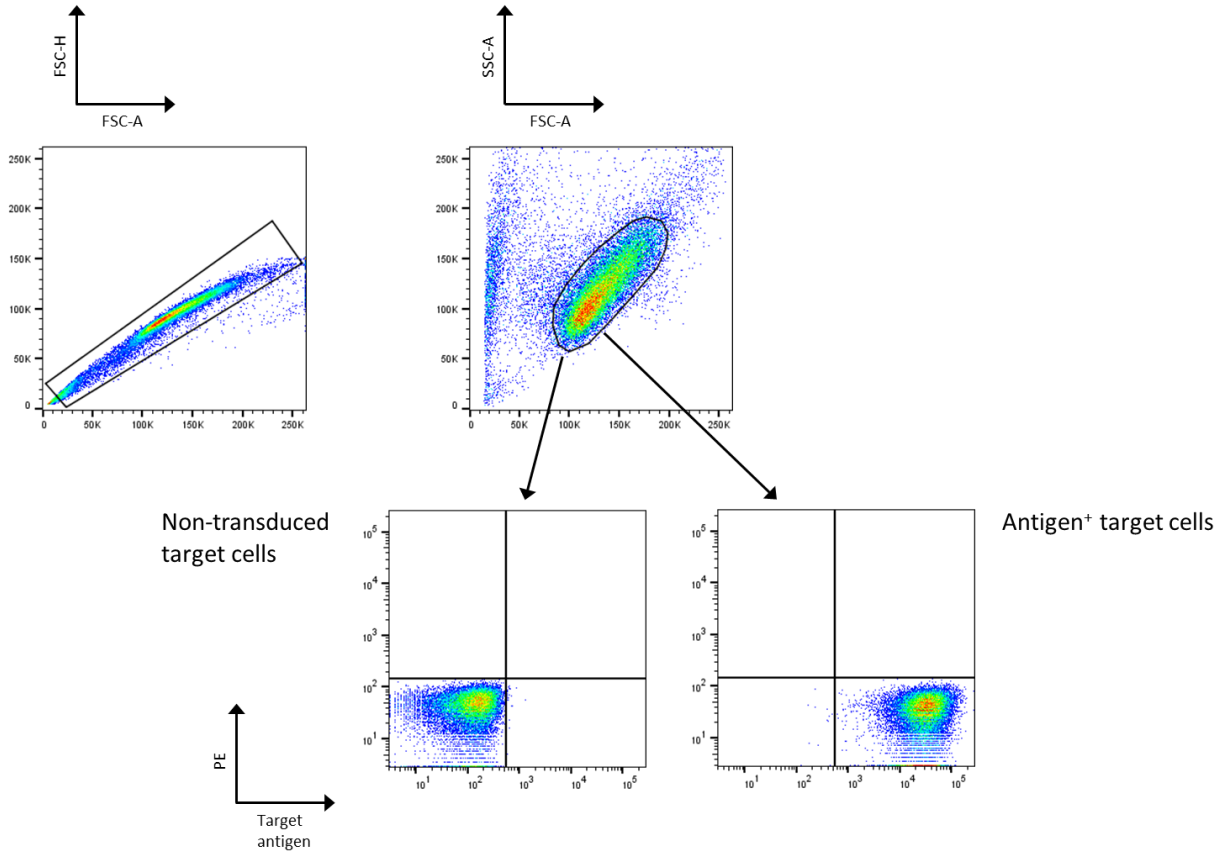

Gating strategy used to quantify antigen expression on target cells. Representative flow cytometry plots illustrating the gating strategy for assessment of the levels of antigen expression on target cell surface. Gating strategy used to identify singlet (top left), viable (top right) target cell populations. Antigen^{+} target cells were gated with reference to non-transduced control target cells (bottom).

(h)

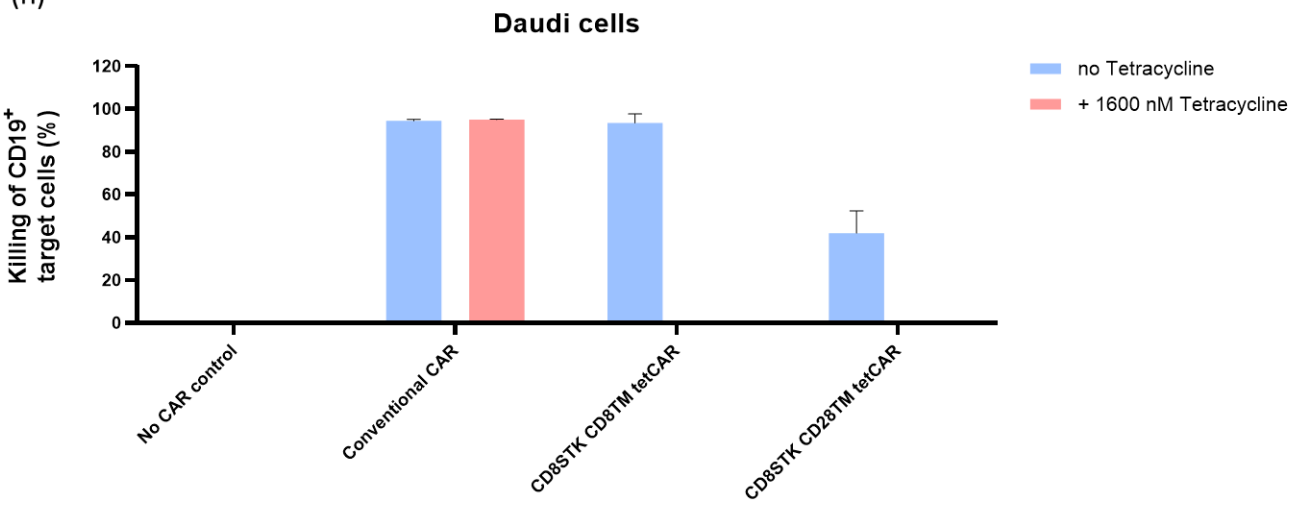
Daudi cells
Killing of CD19+ target cells (%)
120
100
80
60
40
20
0
no Tetracycline
+ 1600 nM Tetracycline
No CAR control
Conventional CAR
CD8STK CD8TM tetCAR
CD8STK CD28TM tetCAR

(i)

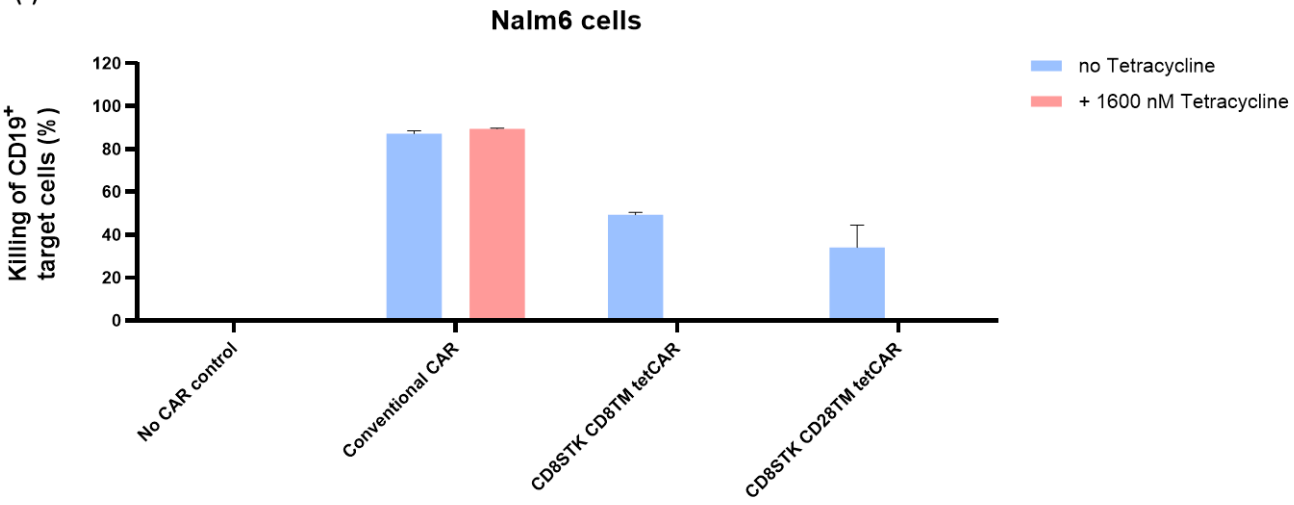
Nalm6 cells
Killing of CD19+ target cells (%)
120
100
80
60
40
20
0
no Tetracycline
+ 1600 nM Tetracycline
No CAR control
Conventional CAR
CD8STK CD8TM tetCAR
CD8STK CD28TM tetCAR

(j)

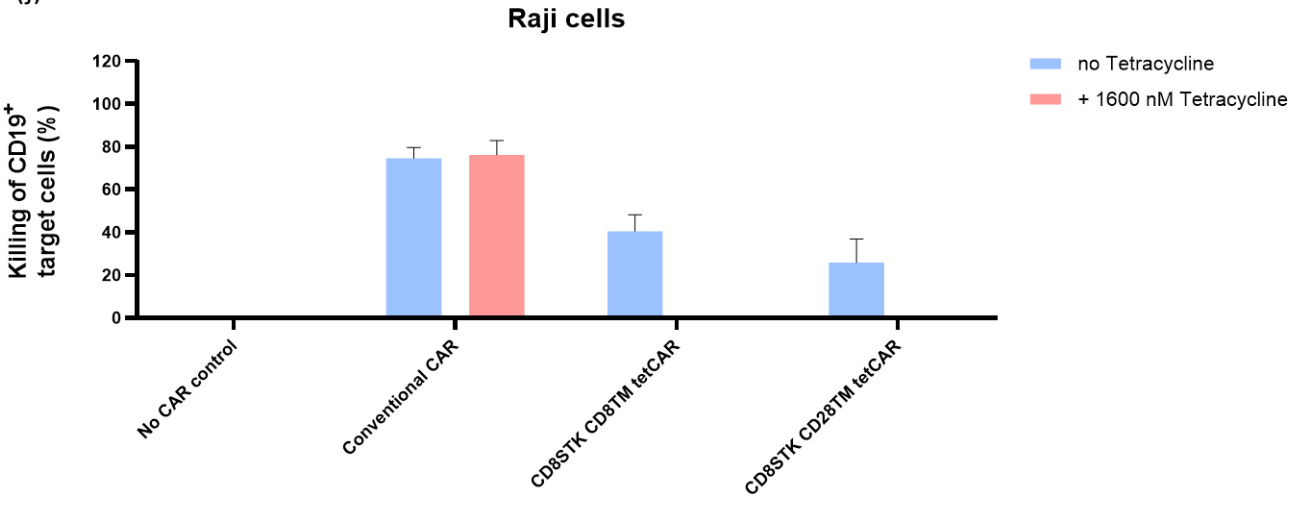
Raji cells
Killing of CD19+ target cells (%)
120
100
80
60
40
20
0
no Tetracycline
+ 1600 nM Tetracycline
No CAR control
Conventional CAR
CD8STK CD8TM tetCAR
CD8STK CD28TM tetCAR

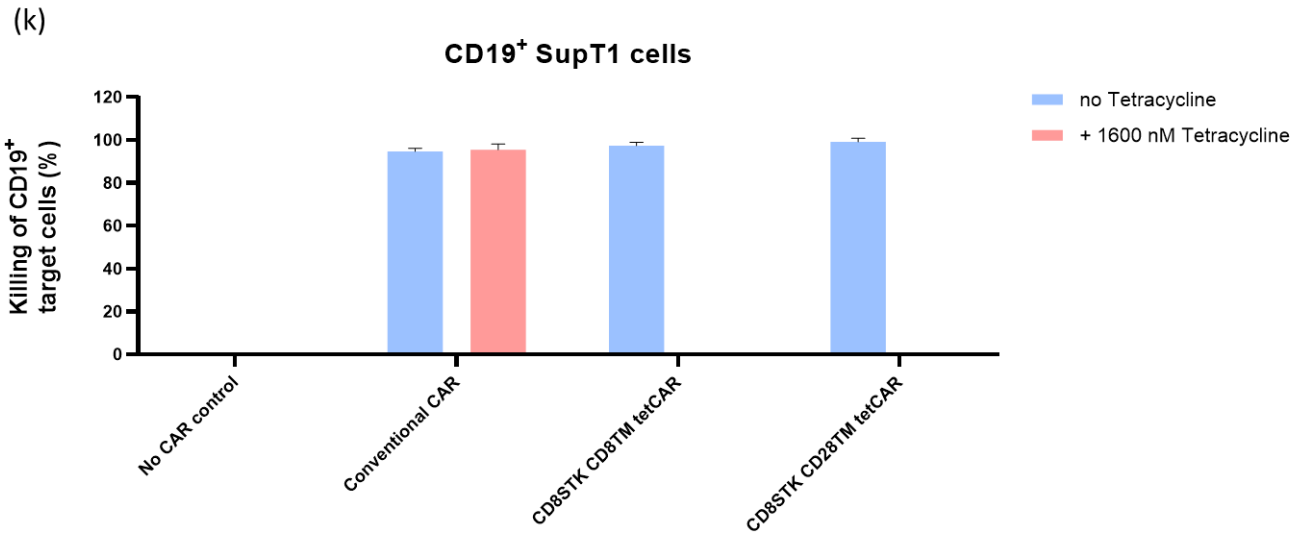

(h) Cytotoxicity activity mediated by tetCARs in a 72-hour end-point experiment. Primary human T-cells expressing the 'CD8STK CD8TM' tetCAR or the 'CD8STK CD28TM' tetCAR were challenged with (h) Daudi cells or (i) Nalm6 cells or (j) Raji cells or (k) $CD19^+$ SupT1 cells at a 4:1 T-cell:target cell ratio in the absence of tetracycline or in the presence of 1600 nM tetracycline. Primary human T-cells expressing the conventional CAR and non-transduced T-cells were set-up to serve as control. A low percentage for survival of $CD19^+$ target cells indicates a high degree of specific target cell killing by CAR T-cells; n = 3 independent experiments from separate donors, error bars denote SD.

7.3 Reversible control of tetCAR T-cell activity

7.3.1 On-Off Reversibility

Finally, it was crucial to assess the reversible control of tetCAR T-cell activity. In order to further validate the tunability of the system, we investigated the inhibition of tetracycline on a pre-activated tetCAR (also known as On-Off reversible control). From previous experiments, we had known that the tetCAR is completely switched off when 1600 nM tetracycline is added at the time of co-culture. In the On-Off reversibility experiments, we aimed to determine whether pre-activation of the tetCAR would affect the response to tetracycline.

Firstly, we analysed the transduction efficiency of the primary human T-cells by flow cytometry. As shown in Figure 36c, both tetCARs could be detected at the cell surface, thus indicating that these constructs were both expressed and trafficked correctly to the plasma membrane. Cell surface expression of the conventional CAR was also detected. Primary human T-cells expressing the tetCARs were co-cultured with SupT1 cells engineered to express CD19 at a 4:1 T-cell:target cell ratio in the absence of tetracycline. At designated time points, T-cells were washed three times with complete media and 1600 nM tetracycline was added. Primary human T-cells expressing the conventional CAR were also tested. Furthermore, T-cells from the same donor that had not undergone gene transfer (designated non-transduced T-cells) were set up to serve as an additional control.

After an overnight incubation, supernatant samples were removed and assayed for the presence of IFN-γ. Subsequent investigations into the release of IFN-γ showed that tetracycline decreases human T-cell IFN-γ secretion and hence activation of pre-activated tetCAR T-cells. The conventional CAR, which was used as a positive control, led to consistent secretion of IFN-γ by primary human T-cells in all designated time points (Figure 36f). As expected, minimal IFN-γ secretion by non-transduced T-cells was observed (Figure 36f). At the earliest time point (1-hour), both pre-activated tetCAR T-cells (Figure 36e) showed a slightly higher IFN-γ secretion when compared

to the '+ 1600 nM Tet at 0-hour' control. At the latest time point (6-hour), the amount of secreted IFN-γ was significantly lower to that seen with the 'no Tetracycline' control. These data show that pre-activation of the tetCAR T-cells does not impair the response to tetracycline.

Additionally, the On-Off reversible control was validated by a flow cytometry-based cell-killing assay.

After incubation for 72 hours, surviving target cells were quantified by flow cytometry. A low percentage for survival of $CD19^+$ SupT1 cells indicates a high degree of specific target cell killing by CAR T-cells. In the 72-hour end-point experiment, almost complete killing of the $CD19^+$ target cells was observed with the conventional CAR T-cells in all designated time points (Figure 37b). As expected, no cell killing mediated by non-transduced T-cells was detected (Figure 37b). The pre-activated 'CD8STK CD8TM' tetCAR T-cells (Figure 37a) showed a significantly lower degree of target cell killing in the 1-hour and 2-hour time points when compared to the 'no Tetracycline' control. With the pre-activated 'CD8STK CD28TM' tetCAR T-cells (Figure 37a), the percentage for killing of $CD19^+$ SupT1 cells was significantly lower in the 1-hour, 2-hour and 4-hour time points when compared to the 'no Tetracycline' control.

Taken together, these findings confirm the On-Off reversibility of the system in therapeutically relevant T-cells via the administration of tetracycline.

Figure 36

(a) **Second-generation CD19-targeting tetCAR (with CD8STK CD8TM):**

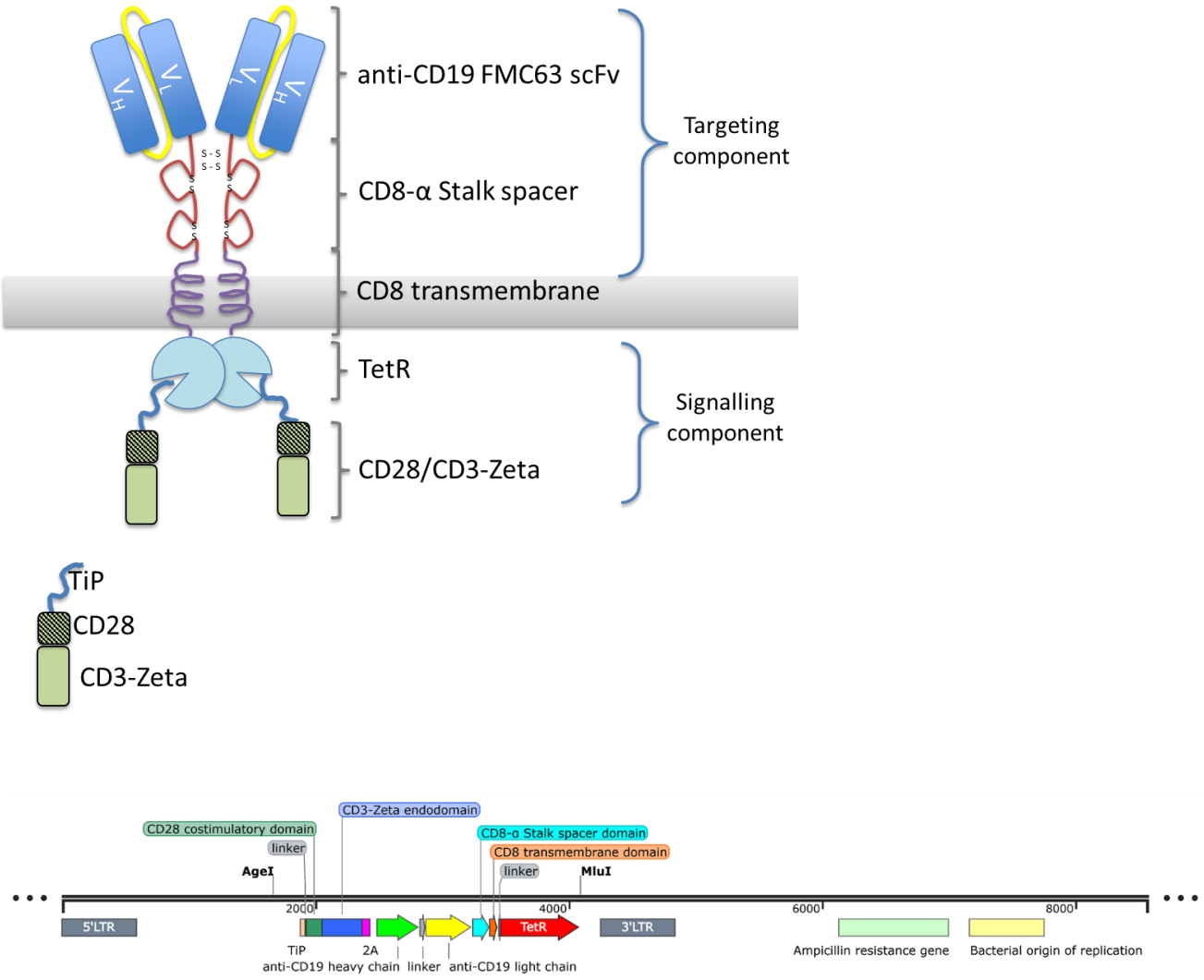

Figure 36. On-Off Reversible control of tetCAR T-cell activity. Cytokine production by primary tetCAR T-cells in the presence of $CD19^{+}$ target cells. (a) Schematic diagram illustrating a second-generation tetCAR with CD8STK as spacer domain instead of the initial spacer derived from the Fc domain of IgG1 and with CD8TM as transmembrane domain instead of the initial CD4 derived transmembrane and intracellular domain (top). A single CAR is expressed with only one signalling component which comprises of TiP (dark blue) fused to the CD28 (diagonal stripes) and CD3-Zeta (light green) endodomain. The receptor component comprises of a CD19 recognizing scFv (blue), a CD8-α Stalk spacer domain (red), a CD8 transmembrane domain (purple), and TetR (light blue). Additionally,

the plasmid map of the second-generation CD19-targeting tetCAR (with CD8STK CD8TM) is also shown (bottom).

(b) **Second-generation CD19-targeting tetCAR (with CD8STK CD28TM):**

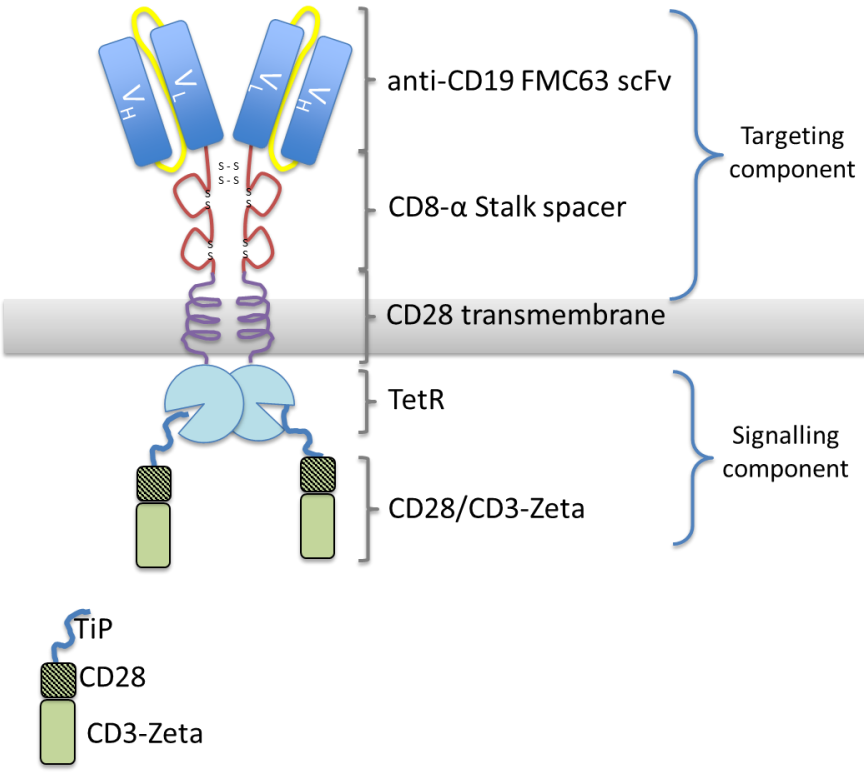

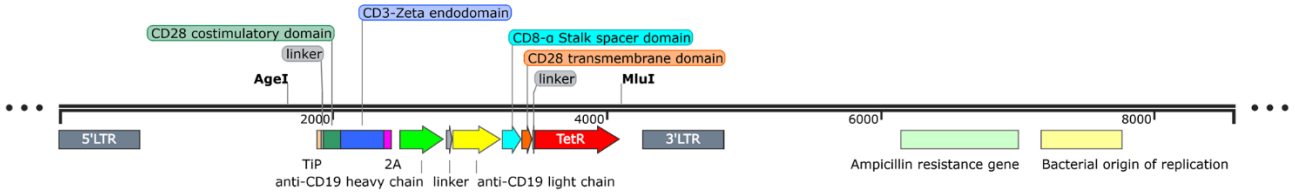

(b) Schematic diagram illustrating a second-generation tetCAR with CD8STK as spacer domain instead of the initial spacer derived from the Fc domain of IgG1 and with CD28TM as transmembrane domain instead of the initial CD4 derived transmembrane and intracellular domain (top). A single CAR is expressed with only one signalling component which comprises of TiP (dark blue) fused to the CD28 (diagonal stripes) and CD3-Zeta (light green) endodomain. The receptor component comprises of a CD19 recognizing scFv (blue), a CD8-α Stalk spacer domain (red), a CD28 transmembrane domain (purple), and TetR (light blue). Additionally, the plasmid map of the second-generation CD19-targeting tetCAR (with CD8STK CD28TM) is also shown (bottom).

(c) **Primary human T-cells:**

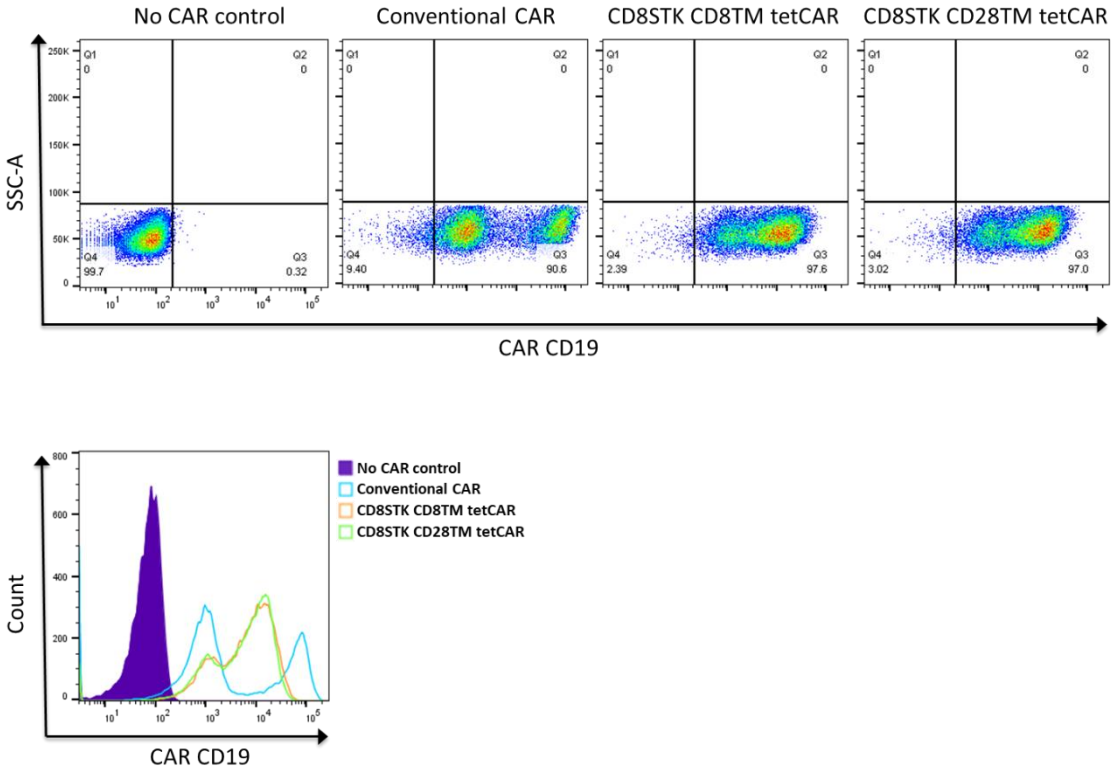

(c) Expression levels of CARs in primary human T-cells. Cells engineered with retroviral constructs encoding CAR molecules were analysed by flow cytometry. Expression of the tetCARs at the surface of primary human T-cells was compared with the expression of conventional CAR. The CARs were detected with soluble CD19 fused to rabbit IgG followed by a directly conjugated anti-Rabbit IgG antibody. Staining was compared against NT T-cells stained using the same antibodies.

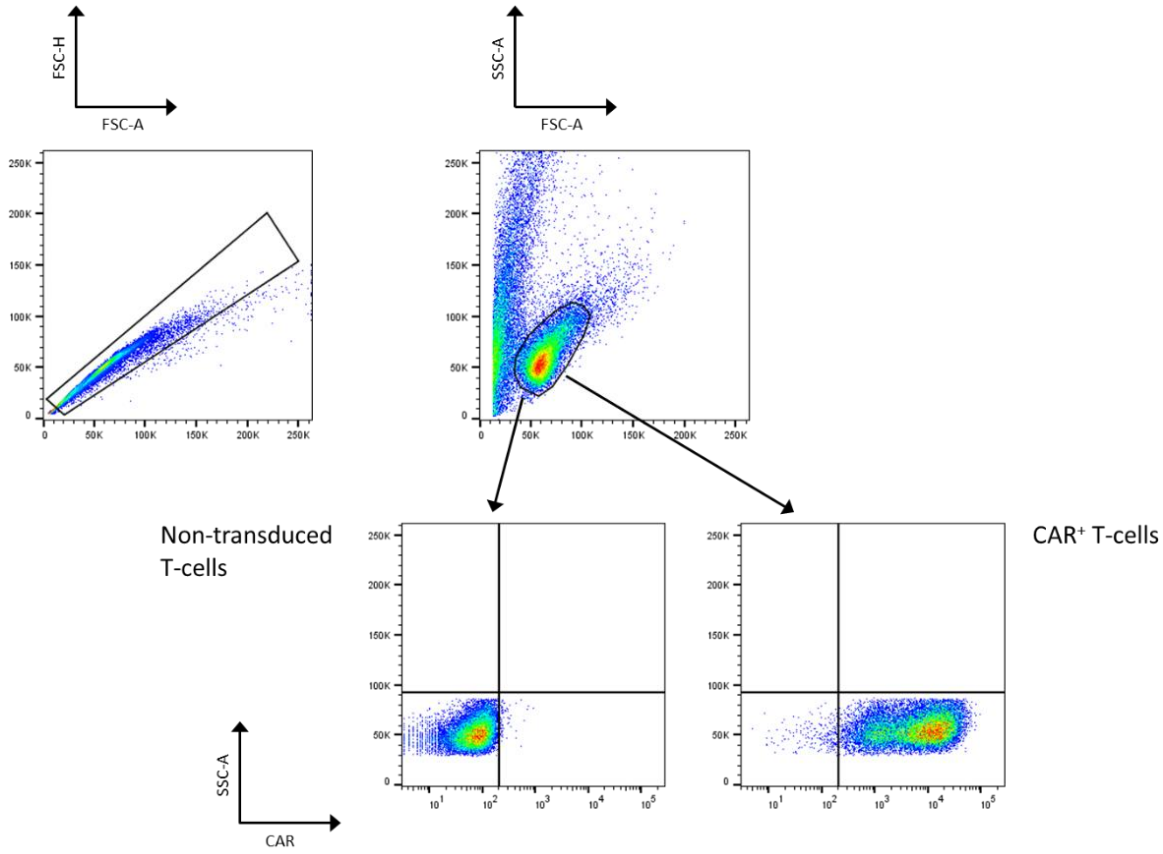

Gating strategy used to verify CAR expression on T-cells. Representative flow cytometry plots illustrating the gating strategy for assessment of CAR transduction efficiency of T-cells. Gating strategy used to identify singlet (top left), viable (top right) T-cell populations. CAR^+ T-cells were gated with reference to non-transduced control T-cells (bottom).

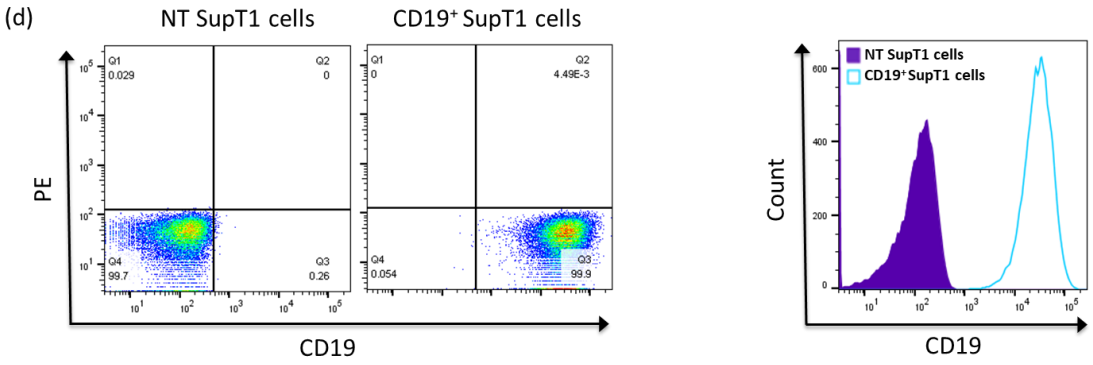

(d) Level of CD19 expression on target cell surface. SupT1 cells were used as target cells in co-culture assays. Non-transduced SupT1 were transduced to stably express CD19. The cells were investigated for the presence of CD19 using flow cytometry. The expression of CD19 was detected using an anti-human CD19 antibody. The level of CD19 expression was compared with that displayed by the NT SupT1 cells stained with the same antibody.

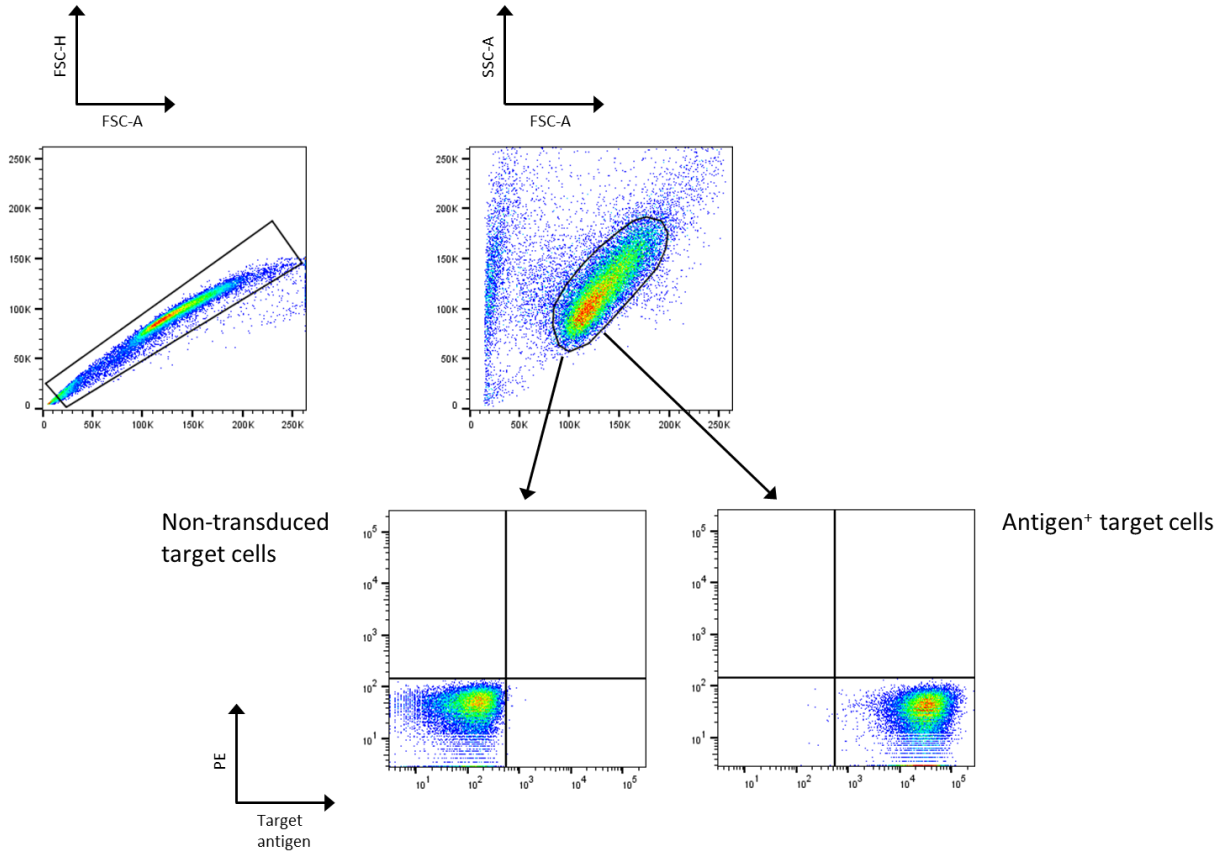

Gating strategy used to quantify antigen expression on target cells. Representative flow cytometry plots illustrating the gating strategy for assessment of the levels of antigen expression on target cell surface. Gating strategy used to identify singlet (top left), viable (top right) target cell populations. Antigen^{+} target cells were gated with reference to non-transduced control target cells (bottom).

(e)

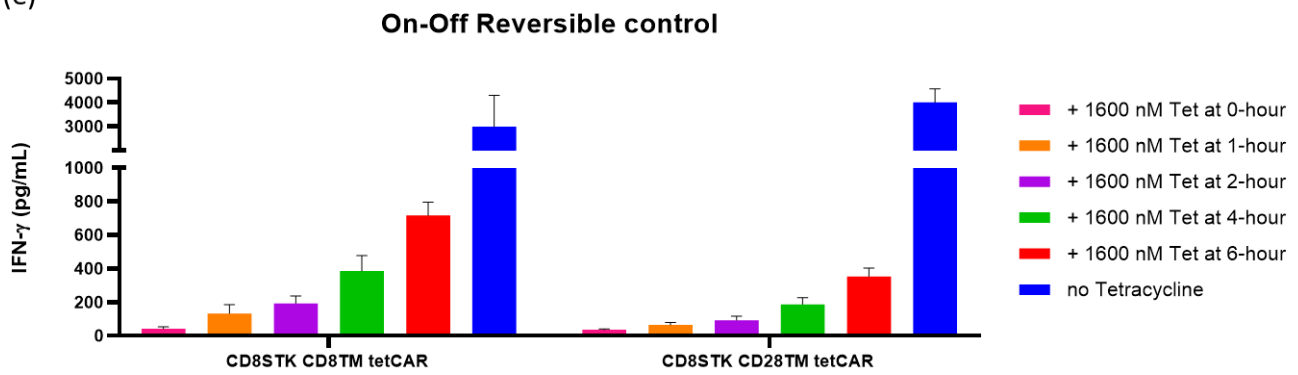

(f)

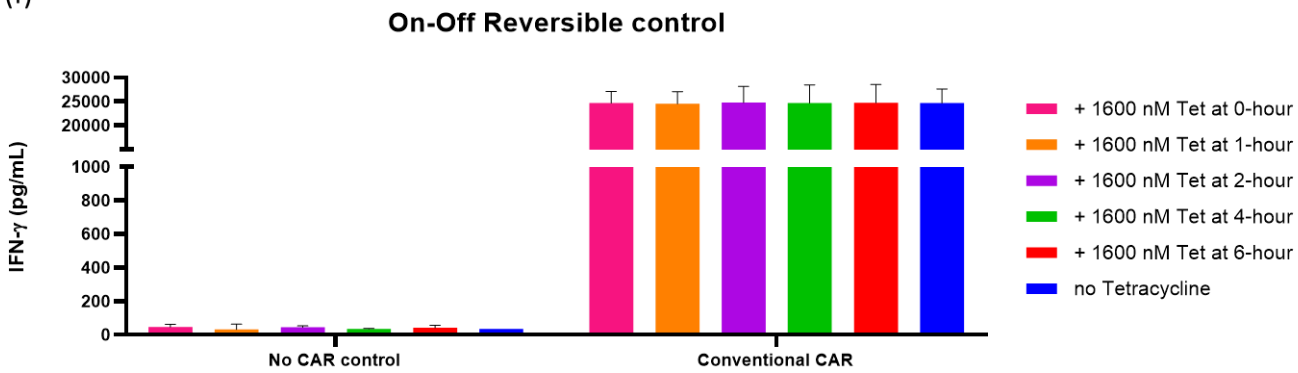

(e) Primary human T-cells expressing the 'CD8STK CD8TM' tetCAR or the 'CD8STK CD28TM' tetCAR were challenged with SupT1 cells engineered to express CD19 at a 4:1 T-cell:target cell ratio in the absence of tetracycline. At designated time points, T-cells were washed three times with complete media and 1600 nM tetracycline was added. (f) Primary human T-cells expressing the conventional CAR and non-transduced T-cells were set-up to serve as control. Production of IFN-γ after an overnight incubation was quantified by ELISA; n = 3 independent experiments from separate donors, error bars denote SD.

Figure 37

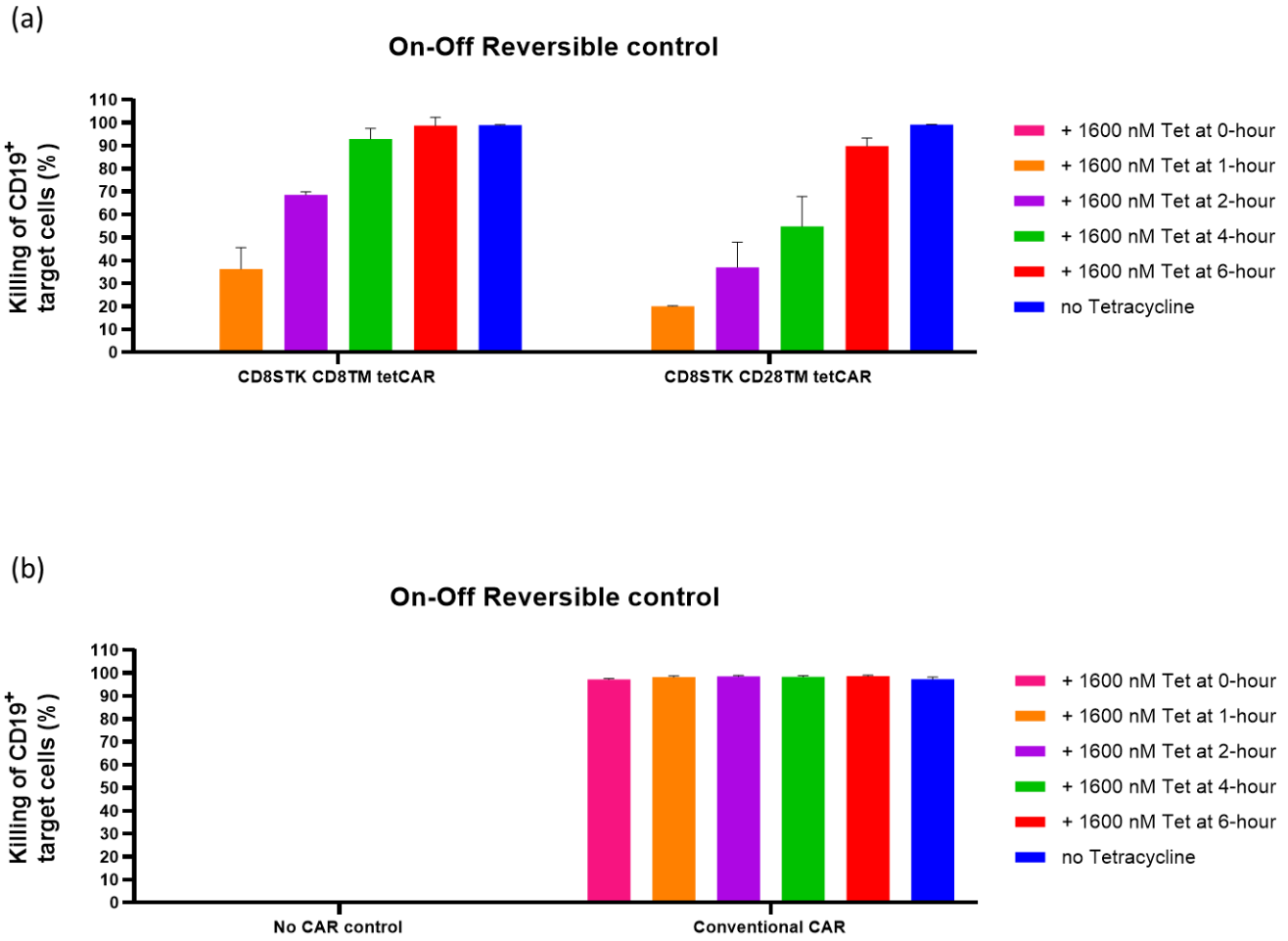

Figure 37. On-Off Reversible control of tetCAR T-cell activity. Cytotoxicity activity mediated by tetCARs in a 72-hour end-point experiment. (a) Primary human T-cells expressing the 'CD8STK CD8TM' tetCAR or the 'CD8STK CD28TM' tetCAR were challenged with SupT1 cells engineered to express CD19 at a 4:1 T-cell:target cell ratio in the absence of tetracycline. At designated time points, T-cells were washed three times with complete media and 1600 nM tetracycline was added. (b) Primary human T-cells expressing the conventional CAR and non-transduced T-cells were set-up to serve as control. A low percentage for survival of $CD19^+$ SupT1 cells indicates a high degree of specific target cell killing by CAR T-cells; n = 3 independent experiments from separate donors, error bars denote SD.

7.3.2 Off-On Reversibility

To further confirm the reversibility of the system, we also assessed the Off-On reversible control of tetCAR T-cell activity. In the Off-On reversibility experiments, we aimed to investigate whether the tetCAR T-cells would be able to regain activity upon removal of tetracycline.

In order to test the Off-On reversibility of the system, primary human T-cells expressing the tetCARs were co-cultured with SupT1 cells engineered to express CD19 at a 4:1 T-cell:target cell ratio in the presence of 1600 nM tetracycline. At designated time points, T-cells were washed three times with complete media to remove tetracycline. Primary human T-cells expressing the conventional CAR were also tested. Furthermore, T-cells from the same donor that had not undergone gene transfer (designated non-transduced T-cells) were set up to serve as an additional control.

After an overnight incubation, supernatant samples were removed and assayed for the presence of IFN-γ. Subsequent investigations into the release of IFN-γ showed that tetracycline decreases human T-cell IFN-γ secretion and hence activation. The conventional CAR, which was used as a positive control, led to consistent secretion of IFN-γ by primary human T-cells in all designated time points (Figure 38b). As expected, low IFN-γ secretion by non-transduced T-cells was observed (Figure 38b). Both ‘CD8STK CD8TM’ and ‘CD8STK CD28TM’ tetCAR T-cells (Figure 38a) showed a significantly higher IFN-γ secretion in all designated time points when compared to the ‘+ 1600 nM Tetracycline’ control.
These data show that the tetCAR T-cells are able to regain activity upon removal of tetracycline.

Additionally, the Off-On reversible control was validated by a flow cytometry-based cell-killing assay.
After incubation for 72 hours, surviving target cells were quantified by flow cytometry. A low percentage for survival of $CD19^+$ SupT1 cells indicates a high degree of specific target cell killing by CAR T-cells. In the 72-hour end-point experiment, almost complete killing of the $CD19^+$ target cells was observed with the conventional CAR T-

cells in all designated time points (Figure 39b). As expected, no cell killing mediated by non-transduced T-cells was detected (Figure 39b). Both ‘CD8STK CD8TM’ and ‘CD8STK CD28TM’ tetCAR T-cells (Figure 39a) showed an almost complete killing of the $CD19^{+}$ SupT1 cells in all designated time points while no target cell killing was observed in the ‘+ 1600 nM Tetracycline’ control.

Taken together, these findings confirm the Off-On reversibility of the system in therapeutically relevant T-cells.

Figure 38

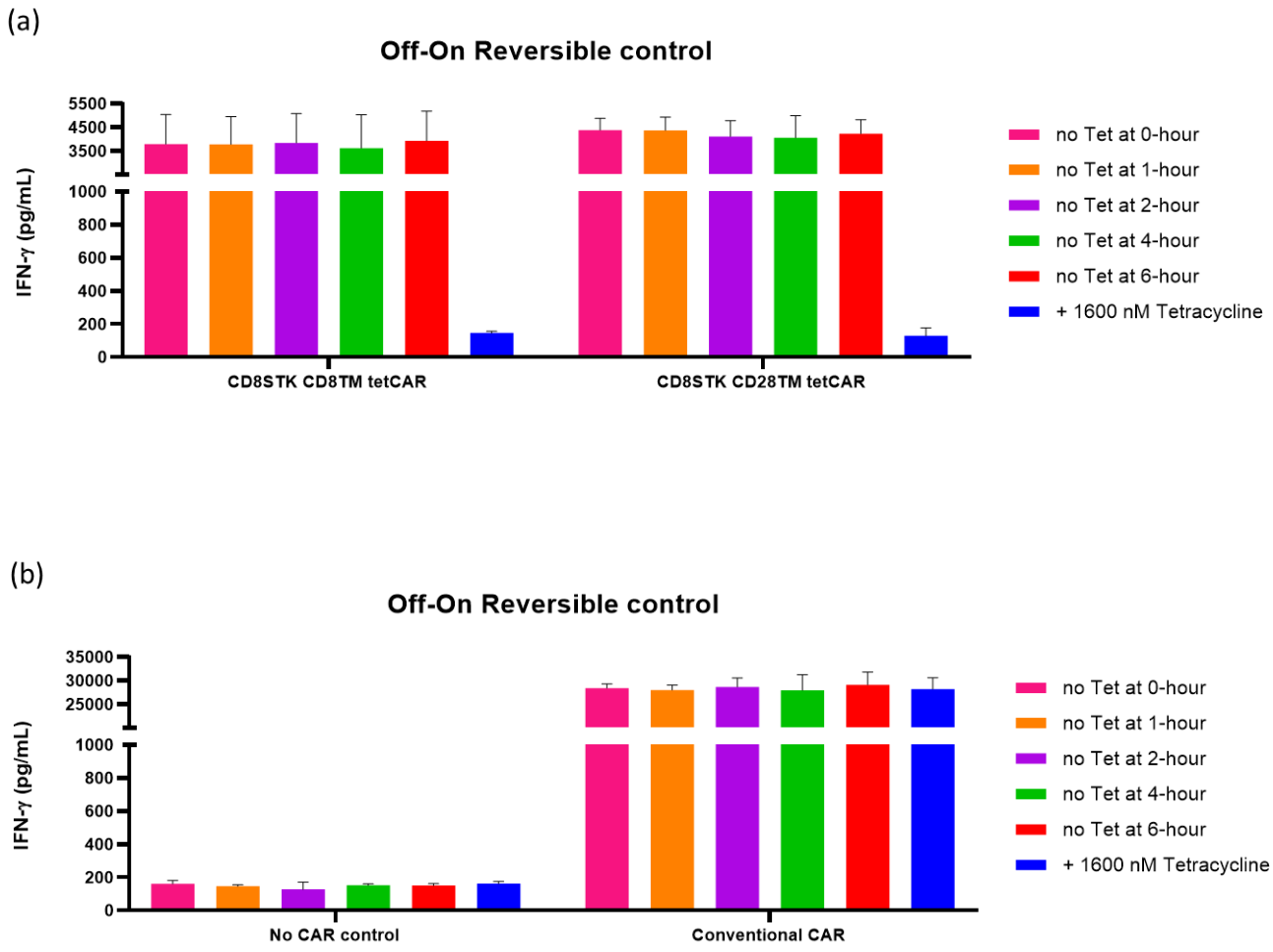

Figure 38. Off-On Reversible control of tetCAR T-cell activity. Cytokine production by primary tetCAR T-cells in the presence of $CD19^{+}$ target cells. (a) Primary human T-cells expressing the 'CD8STK CD8TM' tetCAR or the 'CD8STK CD28TM' tetCAR were challenged with SupT1 cells engineered to express CD19 at a 4:1 T-cell:target cell ratio in the presence of 1600 nM tetracycline. At designated time points, T-cells were washed three times with complete media to remove tetracycline. (b) Primary human T-cells expressing the conventional CAR and non-transduced T-cells were set-up to serve as control. Production of IFN-γ after an overnight incubation was quantified by ELISA; n = 3 independent experiments from separate donors, error bars denote SD.

Figure 39

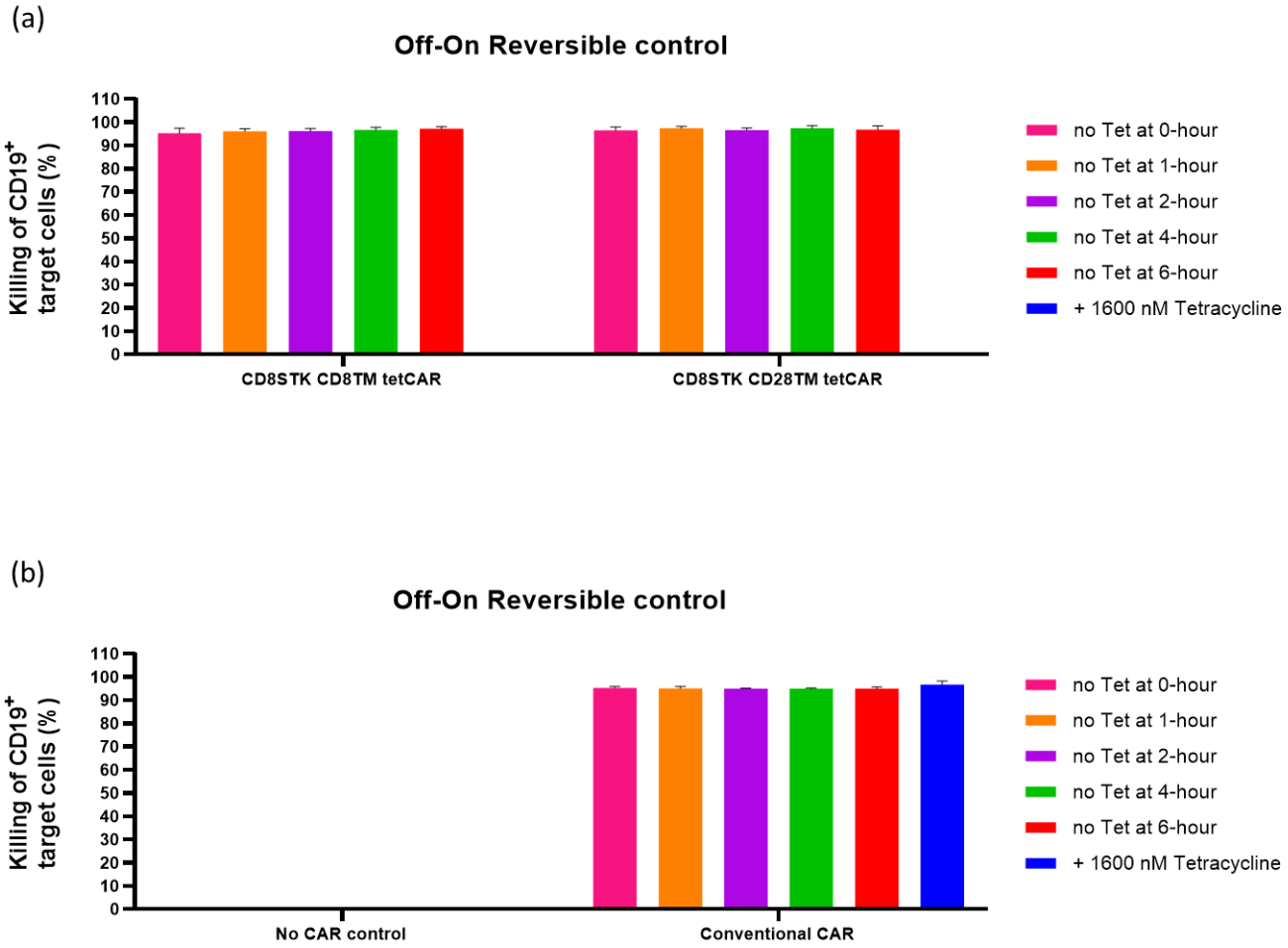

Figure 39. Off-On Reversible control of tetCAR T-cell activity. Cytotoxicity activity mediated by tetCARs in a 72-hour end-point experiment. (a) Primary human T-cells expressing the 'CD8STK CD8TM' tetCAR or the 'CD8STK CD28TM' tetCAR were challenged with SupT1 cells engineered to express CD19 at a 4:1 T-cell:target cell ratio in the presence of 1600 nM tetracycline. At designated time points, T-cells were washed three times with complete media to remove tetracycline. (b) Primary human T-cells expressing the conventional CAR and non-transduced T-cells were set-up to serve as control. A low percentage for survival of $CD19^{+}$ SupT1 cells indicates a high degree of specific target cell killing by CAR T-cells; n = 3 independent experiments from separate donors, error bars denote SD.

7.4 Discussion

In this chapter, we have demonstrated a complete *in vitro* testing of the tetCAR system. Here, we aimed to assess the titre response of the two most promising tetCAR constructs to tetracycline and analogues doxycycline and minocycline. In addition, we also aimed to assess the inhibition (On-Off) and reversibility (Off-On) of tetCAR T-cell activity.

We have offered clear evidence that the tetCAR response to tetracycline and analogues doxycycline and minocycline is complete and titratable, in therapeutically relevant T-cells. We have also demonstrated that response of the tetCAR to the different small molecules affects cytokine production and cytotoxicity. In summary, the concentration of the small molecule was inversely correlated with the production of cytokine and the cytotoxic activity of the tetCAR was increasingly impaired with higher increments of the small molecule, demonstrating an analogue response.

After using BW5 murine T-cells for our initial investigations, it was of great interest to test the three different small molecules in therapeutically relevant T-cells. Our results demonstrated that the tetCAR system works with tetracycline and also with doxycycline and minocycline. An important difference between the three small molecules, is that the tetCAR system is more sensitive to analogues doxycycline and minocycline when compared to tetracycline, as higher concentrations of tetracycline were required to inhibit the system. In addition, these results showed no significant difference between doxycycline and minocycline.

One interesting observation made in this chapter was that addition of very low concentrations of the small molecule results in undetectable levels of cytokine production, while higher concentrations of the small molecule are required to inhibit the tetCAR cytotoxic activity. A possible explanation for the difference observed is the fact that target cell killing occurs on a faster time scale (minutes) when compared to cytokine production [108, 109].

An additional interesting observation made during these studies was that different TM domains appear to affect sensitivity to the small molecule and overall function. Here, we tested the two most promising tetCAR constructs, the ‘CD8STK CD8TM’ tetCAR and the ‘CD8STK CD28TM’ tetCAR, which differed in the transmembrane domain, one bearing the CD8TM and the other bearing the CD28TM. While both tetCAR constructs had an analogue response to the different small molecules, the ‘CD8STK CD28TM’ tetCAR appeared to be more sensitive when compared to the ‘CD8STK CD8TM’ tetCAR. In addition, the ‘CD8STK CD8TM’ tetCAR showed a better overall function when compared to the ‘CD8STK CD28TM’ tetCAR, as a stronger cytotoxicity activity was observed against the natural $CD19^{+}$ cancer cells.

Finally, the reversibility of the tetCAR system was validated by inhibiting the pre-activated tetCAR T-cells with tetracycline (On-Off reversibility) and by activating the inhibited tetCAR T-cells with removal of the small molecule (Off-On reversibility). These results demonstrated that once activated, the addition of tetracycline switches off the tetCAR response. Additionally, it was also demonstrated that the shut-down of tetCAR T-cell function is reversible, as removal of tetracycline led to re-coupling of the CAR and the tetCAR T-cells regained cytotoxic activity and produced cytokines. In summary, we successfully generated a fully reversible small molecule controlled CAR-T approach that enables complete and titratable switch off over CAR T-cell activity.

CHAPTER 8

GENERAL DISCUSSION

8.1 Overview and synthesis

Our goal was to construct a CAR that can be directly inhibited by administration of a small molecule. To achieve this, we used a split-receptor design. We found that it is possible to separate the antigen-recognition and signalling components of a CAR to produce an inducible system, where the addition of small molecule inhibits the system. In the absence of small molecule, these two components dimerize to assemble a functioning receptor complex.

We investigated several ways of splitting components of the conventional CAR construct to find a configuration that would strongly impair its activity when in the presence of the small molecule but still allow for strong antigen-induced signalling, comparable to that achieved by the conventional single-component receptor, when the two components are assembled. We tested candidate receptors in the BW5 murine T-cells and primary human T-cells using two main assays. We assayed the cytotoxicity activity of T-cells transduced with a tetCAR and we also measured cytokine production (IL-2 and IFN-γ). The initial tetCAR constructs failed to signal as strongly as the conventional CAR, despite similar expression levels of both receptors in T-cells.

We thought of many different possible ways to improve the tetCAR activity. We suspected that the long endodomain of the CD4 transmembrane might be keeping the signalling domain too far from the cell membrane resulting in a weaker CAR T-cell activity. Thus, we explored replacing the entire CD4 transmembrane domain by a shorter one. We designed constructs that included the CD8TM or the CD28TM as transmembrane domain instead of the initial CD4 derived transmembrane and intracellular domain. Another modification that we expected to increase the tetCAR activity was the positioning of a 4-1BB costimulatory domain adjacent to the plasma membrane. A previous study shows that the 4-1BB costimulatory domain works best when placed adjacent to the cell membrane [110]. We also designed constructs that included the CD8STK as spacer domain instead of the initial spacer derived from the Fc domain of IgG1.

The most promising designs from this set of constructs comprised the CD8STK as spacer domain and the CD8TM (Figure 23c) or the CD28TM (Figure 23d) as transmembrane domain. When stimulated by SupT1 cells engineered to express CD19, both tetCAR constructs led to a strong cytokine production and also led to a strong cytotoxicity activity comparable to that stimulated by the conventional CAR. Furthermore, the addition of small molecule inhibited the system. These were the split-receptor designs within this subset that showed the best balance between the strong antigen-induced signalling and the impaired activity when in the presence of the small molecule. Other examples, such as the two tetCAR constructs comprising a 4-1BB costimulatory motif between the transmembrane domain and TetR (Figures 23e and 23f) showed a strong cytotoxicity activity either in the absence or presence of the small molecule, suggesting that addition of small molecule did not inhibit the system. To better understand this, we also measured IFN-γ cytokine secretion by these two tetCAR T-cells. Notably, when in the presence of the small molecule, cytokine production was undetectable. It is known that cell killing mediated by T-cells occurs on a faster time scale (minutes) when compared to cytokine production [108, 109]. Thus, we suspect that the lack of response to small molecule by these two tetCARs in the cytotoxicity assay was due to the fast target cell killing. Together these results showed that tetCAR T-cell activity can be enhanced by replacing pre-existing CAR components. Some components of the CAR molecule that we believed to have little impact on the CAR T-cell activity showed to play an important role.

While we have successfully identified two promising tetCAR constructs, an important future step will be to determine whether the tetCAR activity can be further improved. During our studies, testing of the tetCAR showed good function and responsiveness to the small molecule but lower cytokine secretion in the absence of the small molecule compared with the conventional CAR, thus suggesting a reduced activation maximum. A possible explanation for this is the potential lack of 1:1 binding between TetR and TiP. Having demonstrated the impact of replacing pre-existing CAR components, our aim is to test many other tetCAR configurations and identify the crucial domains for efficacy and small molecule responsiveness. In order to increase the possibility of interaction between TetR and TiP and improve the cytokine release capacity, we will design and test a new group of constructs bearing membrane tethered TiP, or alternative TiP peptides with increased affinity to TetR.

In addition to these, there are other optimisations regarding the tetCAR components that would be important to investigate in the future. Those optimisations will be focused on the linker between the TM domain and TetR, and the induction of dimerization through a second TetR. First, we will further investigate the effect of altering the linker fusing the transmembrane domain to TetR by designing a construct in which both CD28 and 4-1BB costimulatory domains are inserted between the TM domain and TetR, and with the TiP peptide bearing only the CD3-Zeta. The rationale behind designing these constructs is as follows: CD3-Zeta is required for activation so costimulatory signals out of the small molecule control may be stronger but will not result in activation in the presence of the small molecule. In comparison to our 'CD8TM 4-1BB' and 'CD28TM 4-1BB' tetCARs, this new design adds an additional costimulatory signal out of the small molecule control. As our results suggested that inclusion of one costimulatory domain between the TM domain and TetR is associated with an increase in cytokine production, we are hypothesising that the incorporation of two costimulatory domains in the membrane-bound moiety of the tetCAR will result in a further improvement of the tetCAR response [110]. On the other hand, it will be crucial to assess whether this expected improvement may affect the response of the tetCAR to the small molecule. To be considered a promising design, this new tetCAR construct will have to show not only the strong antigen-induced signalling, but also the strongly impaired activity when in the presence of the small molecule.

Another optimisation that we believe it can result in an improved cytokine release capacity is the introduction of a second TetR to the tetCAR protein, in order to promote the dimerization of the TetR domains. The rationale behind this new configuration is as follows: TetR needs to form a homodimer to function [111]. In our current tetCAR configurations, two TetR domains from two CARs interact. Here, we are speculating that the tetCAR activity can be improved if the TetR is expressed as a single chain with two TetRs attached together via a polypeptide linker, allowing the dimerization to form without requiring the tetCAR to be in close proximity to another CAR molecule. Our two most promising tetCAR constructs, the 'CD8STK CD8TM' tetCAR and the 'CD8STK CD28TM' tetCAR, comprise a CD8-α Stalk spacer that mediates homodimerization of the CAR proteins, bringing the TetR domains in proximity to dimerize. However, it is unknown whether the homodimerization occurs in the endoplasmic reticulum (ER) or on the membrane. The stability of the tetCAR in its monomeric form before the dimerization through CD8-α Stalk spacer is disputable. We

suspect that the stability concern might explain the lower cytokine secretion by tetCAR compared to the conventional CAR. In order to increase the stability of the tetCAR protein and improve the cytokine release capacity, we will investigate the induction of dimerization through a second TetR.

We tested whether the tetCAR would show similar response to different small molecules. We used tetracycline and analogues doxycycline and minocycline. The different small molecules were tested in BW5 murine T-cells and primary human T-cells. A direct comparison between the three different small molecules in BW5 murine T-cells showed that the system is more sensitive to doxycycline (Figure 15) and minocycline (Figure 16) as the addition of one or the other at the lowest concentration completely inhibited the system. On the other hand, to achieve a similar result with tetracycline (Figure 14) we needed a higher concentration of the small molecule. The highest tetracycline concentration used during this research was 1600 nM that is below the peak concentration of tetracycline in the bloodstream after a 500mg dose [112]. The different small molecules worked equally well in primary human T-cells. Here the system also showed to be more sensitive to doxycycline and minocycline. While the tetracycline-titratable control of engineered therapeutic T-cells through the tetCAR was confirmed by using the set of concentrations ranging from 0 to 1600 nM, to validate the tunability of the system via the administration of tetracycline analogues, we tested a new range of lower concentrations (0 to 3.125 nM). In summary, the tetCAR design works with tetracycline and also with alternative small molecules.

The tetCAR was initially designed with a single-chain antibody that recognises the antigen CD33. More recently, we reconstructed the system with a single-chain antibody that recognises the antigen CD19 instead of the antigen CD33. After testing both versions of the receptor, the results confirmed that the tetCAR design functions with alternative antigen-binding domains.

Throughout our studies, we used SupT1 target cells to show the cytotoxicity activity mediated by tetCAR constructs in primary human T-cells. To confirm the relevance of our findings made with engineered SupT1 target cells, we examined the killing of natural $CD19^{+}$ cancer cells by tetCAR T-cells (Figure 35). The Daudi, Nalm6 and Raji target cell lines naturally express CD19. Cytotoxicity experiments demonstrated that all

$CD19^+$ cell lines were subject to killing by tetCAR T-cells. Together these results showed killing of multiple types of $CD19^+$ target cell populations.

We next tested the reversibility of the tetCAR system. The aim of this study was to assess the inhibition (On-Off) and reversibility (Off-On) of tetCAR T-cell activity. In the On-Off reversibility assays (Figures 36 and 37), we investigated whether pre-activation of the tetCAR would affect the response to tetracycline. Both cytokine production and target cell killing by the pre-activated tetCAR T-cells was significantly lower than the control condition, demonstrating that pre-activation of the tetCAR T-cells does not impede the response to tetracycline. In the Off-On reversibility assays (Figures 38 and 39), we examined whether the tetCAR T-cells would be able to regain activity upon removal of tetracycline. Both cytokine production and target cell killing by the tetCAR T-cells was significantly higher than the control condition. These results confirmed that removal of tetracycline leads to re-coupling of the CAR and the tetCAR T-cells regain cytotoxic activity and produce cytokines. Altogether, our findings support the conclusion that the tetCAR design provides a flexible platform for temporal control over CAR T-cell activity.

In the course of this project, we have developed a highly innovative technology which can lead to a new generation of pharmacologically controlled cellular therapeutics. The ultimate measure of utility of tetCAR will be determined through clinical experience. After completing the required pre-clinical preparation, we aim to test our tetCAR technology in a clinical trial. T-cells engineered to express CARs have proven effective against B-cell cancers and as a result, two CAR T-cell therapies, Yescarta (axicabtagene ciloleucel) from Kite Pharma [53, 113, 114] and Kymriah (tisagenlecleucel) from Novartis [38, 115-117], have already obtained market authorization. While CAR T-cell therapies are effective, overly active CAR T-cell activity can lead to dangerous inflammatory syndromes and even be fatal [41]. With our tetCAR technology, we hope to reproduce the clinical successes seen with standard CAR T-cell therapy against haematological malignancies, but with control of immune toxicity.

The main competing technology is the suicide gene approach. However, such suicide switches result in complete deletion of the CAR T-cells with an increased risk of relapse, when actually only a transient reduction in CAR T-cell activity is required [62-68].

It is important to point out that immune toxicity related to overly active T-cells restricts CAR T-cell therapy to younger patients with little pre-existing morbidity and to only the most specialist clinical centres. If successful, our approach would increase availability of CAR T-cell therapy to more medical centres and for indications like myeloma would allow treatment of older patients where standard CAR T-cell therapy is not tolerated. This strategy might also contribute to the application of CAR T-cells for the treatment of solid cancers as a safer platform will facilitate such clinical development [118, 119]. Our tetCAR technology has the potential to be applied to any CAR T-cell product of the future. Ultimately, CAR T-cell therapy will not only be safer, but more widely applicable.

8.2 Conclusions

In summary, we successfully engineered a class of chimeric antigen receptors that allow for effective remote control of therapeutic T-cells through disruption of protein-protein interaction. The developed CAR enables complete, titratable and reversible switch off over T-cell activity. Importantly, the system uses an approved and readily available small molecule that is only needed during periods of toxicity, rather than requiring continued presence of a small molecule to sustain CAR T-cell activity as is needed with rapalog dimerizers.

8.3 Future directions

In addition to the points mentioned above, future work will be aimed at testing whether the tumour cell killing by primary tetCAR T-cells could be controlled *in vivo* in a small animal model. The model we will use is that described by Gilham et al., where mouse T-cells were transduced with a CAR which recognized murine CD19. Mice were burdened with the A20 syngeneic murine cell line. Mice developed a syndrome closely resembling human CRS/MAS as well as having B-cell depletion and efficacy against the A20 graft. We have selected this model because it realistically recapitulated the most important toxicity seen in human subjects. Also, this model is currently being established in the lab with the anti-mouse CD19 CARs being generated. Alternative human/mouse models do exist where human whole blood is engrafted in NSG mice but these models have not yet been established in UCL.

Our plan is as follows: test murine CD19 version of tetCAR in murine splenocytes *in vitro* with a simple killing / cytokine release assay in the presence and absence of tetracycline. If this is functional, we will proceed to test in the A20 syngeneic model looking for efficacy and also for the ability to modulate MAS/CRS with intraperitoneal (IP) tetracycline.

References

[1] Weinberg RA (2007) *The Biology of Cancer*. New York: Garland Science, Taylor and Francis Group, LLC, pgs. 672-91.

[2] Reiman JM, Kmieciak M, Manjili MH, Knutson KL. Tumor immunoediting and immunosculpting pathways to cancer progression. *Semin Cancer Biol* 2007; 17(4): 275-287.

[3] Farzaneh F. Tumour Immunology: interactions between the tumour and the immune system. King's College London: lecture delivered in 2012.

[4] Thomas GR, Chen Z, Oechsli MN, Hendler FJ, Van Waes C. Decreased expression of CD80 is a marker for increased tumorigenicity in a new murine model of oral squamous-cell carcinoma. *Int J Cancer* 1999; 82(3): 377-384.

[5] Wang S, Chen L. Co-signaling molecules of the B7-CD28 family in positive and negative regulation of T lymphocyte responses. *Microbes Infect* 2004; 6(8): 759-766.

[6] Ribas A, Koya RC. Adoptive cell transfer of T-cell receptor engineered lymphocytes: lessons from recent modelling. *Future Oncol* 2010; 6(11): 1671-1673.

[7] Rosenberg SA, Dudley ME. Adoptive cell therapy for the treatment of patients with metastatic melanoma. *Curr Opin Immunol* 2009; 21(2): 233-240.

[8] Ruella M, June CH. Chimeric Antigen Receptor T cells for B Cell Neoplasms: Choose the Right CAR for You. *Curr Hematol Malig Rep* 2016; 11(5): 368-384.

[9] Gross G, Waks T, Eshhar Z. Expression of immunoglobulin-T-cell receptor chimeric molecules as functional receptors with antibody-type specificity. *Proc Natl Acad Sci U S A* 1989; 86(24): 10024-10028.

[10] Kuwana Y, et al. Expression of chimeric receptor composed of immunoglobulin-derived V regions and T-cell receptor-derived C regions. *Biochem Biophys Res Commun* 1987; 149(3): 960-968.

[11] Ghorashian S, Pule M, Amrolia P. CD19 chimeric antigen receptor T cell therapy for haematological malignancies. *Br J Haematol* 2015; 169(4): 463-478.

[12] Wilkie S, et al. Selective Expansion of Chimeric Antigen Receptor-targeted T-cells with Potent Effector Function using Interleukin-4. *J Biol Chem* 2010; 285(33): 25538-25544.

[13] Eshhar Z, Waks T, Gross G, Schindler DG. Specific activation and targeting of cytotoxic lymphocytes through chimeric single chains consisting of antibody-binding

domains and the gamma or zeta subunits of the immunoglobulin and T-cell receptors. *Proc Natl Acad Sci* 1993; 90(2): 720-724.

[14] Eshhar Z, Waks T, Bendavid A, Schindler DG. Functional expression of chimeric receptor genes in human T cells. *J Immunol Methods* 2001; 248(1-2): 67-76.

[15] Guest RD, et al. The role of extracellular spacer regions in the optimal design of chimeric immune receptors: evaluation of four different scFvs and antigens. *J Immunother* 2005; 28(3): 203-211.

[16] Wilkie S, et al. Retargeting of human T cells to tumor-associated MUC1: the evolution of a chimeric antigen receptor. *J Immunol* 2008; 180(7): 4901-4909.

[17] Sadelain M. T-cell engineering for cancer immunotherapy. *Cancer J* 2009; 15(6): 451-455.

[18] Dotti G, Savoldo B, Brenner M. Fifteen years of gene therapy based on chimeric antigen receptors: "are we nearly there yet?". *Hum Gene Ther* 2009; 20(11): 1229-1239.

[19] Alarcon B, et al. T-cell antigen receptor stoichiometry: pre-clustering for sensitivity. *EMBO Rep* 2006; 7(5): 490-495.

[20] Haynes NM, et al. Redirecting mouse CTL against colon carcinoma: superior signaling efficacy of single-chain variable domain chimeras containing TCR-zeta vsFc epsilon RI-gamma. *J Immunol* 2001; 166(1): 182-187.

[21] Howard FD, et al. The CD3 zeta cytoplasmic domain mediates CD2-induced T cell activation. *J Exp Med* 1992; 176(1): 139-145.

[22] Kershaw MH, et al. A phase I study on adoptive immunotherapy using gene-modified T cells for ovarian cancer. *Clin Cancer Res* 2006; 12(20 Pt 1): 6106-6115.

[23] Park JR, et al. Adoptive transfer of chimeric antigen receptor re-directed cytolytic T lymphocyte clones in patients with neuroblastoma. *Mol Ther* 2007; 15(4): 825-833.

[24] Till BG, et al. Adoptive immunotherapy for indolent non-Hodgkin lymphoma and mantle cell lymphoma using genetically modified autologous CD20-specific T cells. *Blood* 2008; 112(6): 2261-2271.

[25] Gong MC, et al. Cancer patient T cells genetically targeted to prostate-specific membrane antigen specifically lyse prostate cancer cells and release cytokines in response to prostate-specific membrane antigen. *Neoplasia* 1999; 1(2): 123-127.

[26] Imai C, et al. Chimeric receptors with 4-1BB signaling capacity provoke potent cytotoxicity against acute lymphoblastic leukemia. *Leukemia* 2004; 18(4): 676-684.

[27] Pule MA, Straathof KC, Dotti G, Heslop HE, Rooney CM, Brenner MK. A chimeric T cell antigen receptor that augments cytokine release and supports clonal expansion of primary human T cells. *Mol Ther* 2005; 12(5): 933-941.

[28] Lim WA, June CH. The Principles of Engineering Immune Cells to Treat Cancer. *Cell* 2017; 168(4): 724-740.

[29] Davies DM, Maher J. Adoptive T-cell Immunotherapy of Cancer Using Chimeric Antigen Receptor-Grafted T-cells. *Arch Immunol Ther Exp* 2010; 58(3): 165-178.

[30] Maher J. Immunotherapy of malignant disease using chimeric antigen receptor engrafted T cells. *ISRN Oncol* 2012; 2012: 278093.

[31] Porter DL, Levine BL, Kalos M, Bagg A, June CH. Chimeric antigen receptor modified T-cells in Chronic Lymphoid Leukaemia. *N Engl J Med* 2011; 365(8): 725-733.

[32] Brentjens RJ, et al. CD19-targeted T cells rapidly induce molecular remissions in adults with chemotherapy-refractory acute lymphoblastic leukemia. *Sci Transl Med* 2013; 5(177): 177ra38.

[33] Maude SL, et al. Chimeric antigen receptor T cells for sustained remissions in leukemia. *N Engl J Med* 2014; 371(16): 1507-1517.

[34] Brudno JN, et al. Allogeneic T Cells That Express an Anti-CD19 Chimeric Antigen Receptor Induce Remissions of B-Cell Malignancies That Progress After Allogeneic Hematopoietic Stem-Cell Transplantation Without Causing Graft-Versus-Host Disease. *J Clin Oncol* 2016; 34(10): 1112-1121.

[35] Lee DW, et al. T cells expressing CD19 chimeric antigen receptors for acute lymphoblastic leukaemia in children and young adults: a phase 1 dose-escalation trial. *Lancet* 2015; 385(9967): 517-528.

[36] Turtle CJ, et al. CD19 CAR-T cells of defined CD4+:CD8+ composition in adult B cell ALL patients. *J Clin Invest* 2016; 126(6): 2123-2138.

[37] Grupp SA, et al. Chimeric antigen receptor-modified T cells for acute lymphoid leukemia. *N Engl J Med* 2013; 368(16): 1509-1518.

[38] Maude SL, et al. Tisagenlecleucel in Children and Young Adults with B-Cell Lymphoblastic Leukemia. *N Engl J Med* 2018; 378(5): 439-448.

[39] Park JH, et al. Long-Term Follow-up of CD19 CAR Therapy in Acute Lymphoblastic Leukemia. *N Engl J Med* 2018; 378(5): 449-459.

[40] Gardner RA, et al. Intent-to-treat leukemia remission by CD19 CAR T cells of defined formulation and dose in children and young adults. *Blood* 2017; 129(25): 3322-3331.

[41] Lee DW, et al. Current concepts in the diagnosis and management of cytokine release syndrome. *Blood* 2014; 124(2): 188-195.

[42] Davila ML, et al. Efficacy and toxicity management of 19-28z CAR T cell therapy in B cell acute lymphoblastic leukemia. *Sci Transl Med* 2014; 6(224): 224ra25.

[43] Maude SL, et al. Managing cytokine release syndrome associated with novel T cell-engaging therapies. *Cancer J* 2014; 20(2): 119-122.

[44] Bonifant CL, Jackson HJ, Brentjens RJ, Curran KJ. Toxicity and management in CAR T-cell therapy. *Mol Ther Oncolytics* 2016; 3: 16011.

[45] Kochenderfer JN, et al. B-cell depletion and remissions of malignancy along with cytokine-associated toxicity in a clinical trial of anti-CD19 chimeric-antigen-receptor-transduced T cells. *Blood* 2012; 119(12): 2709-2720.

[46] Kochenderfer JN, et al. Eradication of B-lineage cells and regression of lymphoma in a patient treated with autologous T cells genetically engineered to recognize CD19. *Blood* 2010; 116(20): 4099-4102.

[47] Lamers CH, et al. Treatment of metastatic renal cell carcinoma with autologous T-lymphocytes genetically retargeted against carbonic anhydrase IX: first clinical experience. *J Clin Oncol* 2006; 24(13): e20-e22.

[48] Morgan RA, et al. Case report of a serious adverse event following the administration of T-cells transduced with a chimeric antigen receptor recognizing ERBB2. *Mol Ther* 2010; 18(4): 843-851.

[49] Topp MS, et al. Safety and activity of blinatumomab for adult patients with relapsed or refractory B-precursor acute lymphoblastic leukaemia: a multicentre, single-arm, phase 2 study. *Lancet Oncol* 2015; 16(1): 57-66.

[50] Wu J, Fu J, Zhang M, Liu D. Blinatumomab: a bispecific T cell engager (BiTE) antibody against CD19/CD3 for refractory acute lymphoid leukemia. *J Hematol Oncol* 2015; 8: 104.

[51] Fan G, Wang Z, Hao M, Li J. Bispecific antibodies and their applications. *J Hematol Oncol* 2015; 8: 130.

[52] Wang Z, Guo Y, Han W. Current status and perspectives of chimeric antigen receptor modified T cells for cancer treatment. *Protein Cell* 2017; 8(12): 896-925.

[53] Neelapu SS, et al. Axicabtagene Ciloleucel CAR T-Cell Therapy in Refractory Large B-Cell Lymphoma. *N Engl J Med* 2017; 377(26): 2531-2544.

[54] Buechner J, et al. Global Registration Trial of Efficacy and Safety of CTL019 in Pediatric and Young Adult Patients with Relapsed/Refractory (R/R) Acute Lymphoblastic Leukemia (ALL): Update to the Interim Analysis. *Clin Lymphoma Myeloma Leuk* 2017; 17: S263-S264.

[55] Gust J, et al. Endothelial Activation and Blood-Brain Barrier Disruption in Neurotoxicity after Adoptive Immunotherapy with CD19 CAR-T Cells. *Cancer Discov* 2017; 7(12): 1404-1419.

[56] Schuster SJ, et al. Global Pivotal Phase 2 Trial of the CD19-Targeted Therapy CTL019 in Adult Patients with Relapsed or Refractory (R/R) Diffuse Large B-Cell Lymphoma (DLBCL)-An Interim Analysis. *Hematol Oncol* 2017; 35: 27.

[57] Abramson JS, et al. High Durable CR Rates in Relapsed/Refractory (R/R) Aggressive B-NHL Treated with the CD19-Directed CAR T Cell Product JCAR017 (TRANSCEND NHL 001): Defined Composition Allows for Dose-Finding and Definition of Pivotal Cohort. *Blood* 2017; 130: 581.

[58] Mei H, et al. Neurological toxicities and coagulation disorders in the cytokine release syndrome during CAR-T therapy. *Br J Haematol* 2018; 181(5): 689-692.

[59] Prudent V, Breitbart WS. Chimeric antigen receptor T-cell neuropsychiatric toxicity in acute lymphoblastic leukemia. *Palliat Support Care* 2017; 15(4): 499-503.

[60] Fry TJ, et al. CD22-targeted CAR T cells induce remission in B-ALL that is naive or resistant to CD19-targeted CAR immunotherapy. *Nat Med* 2018; 24(1): 20-28.

[61] Wang Z, Han W. Biomarkers of cytokine release syndrome and neurotoxicity related to CAR-T cell therapy. *Biomark Res* 2018; 6: 4.

[62] Ciceri F, et al. Infusion of suicide-gene-engineered donor lymphocytes after family haploidentical haemopoietic stem-cell transplantation for leukaemia (the TK007 trial): a non-randomised phase I-II study. *Lancet Oncol* 2009; 10(5): 489-500.

[63] Greco R, et al. Improving the safety of cell therapy with the TK-suicide gene. *Front Pharmacol* 2015; 6: 95.

[64] Di Stasi A, et al. Inducible apoptosis as a safety switch for adoptive cell therapy. *N Engl J Med* 2011; 365(18): 1673-1683.

[65] Straathof KC, et al. An inducible caspase 9 safety switch for T-cell therapy. *Blood* 2005; 105(11): 4247-4254.

[66] Vogler I, et al. An improved bicistronic CD20/tCD34 vector for efficient purification and in vivo depletion of gene-modified T cells for adoptive immunotherapy. *Mol Ther* 2010; 18(7): 1330-1338.

[67] Serafini M, et al. Characterization of CD20-transduced T lymphocytes as an alternative suicide gene therapy approach for the treatment of graft-versus-host disease. *Hum Gene Ther* 2004; 15(1): 63-76.

[68] Philip B, et al. A highly compact epitope-based marker/suicide gene for easier and safer T-cell therapy. *Blood* 2014; 124(8): 1277-1287.

[69] Jones BS, Lamb LS, Goldman F, Di Stasi A. Improving the safety of cell therapy products by suicide gene transfer. *Front Pharmacol* 2014; 5: 254.

[70] Urbanska K, et al. A universal strategy for adoptive immunotherapy of cancer through use of a novel T-cell antigen receptor. *Cancer Res* 2012; 72(7): 1844-1852.

[71] Ma JS, et al. Versatile strategy for controlling the specificity and activity of engineered T cells. *Proc Natl Acad Sci U S A* 2016; 113(4): E450-E458.

[72] Cao Y, et al. Design of Switchable Chimeric Antigen Receptor T Cells Targeting Breast Cancer. *Angew Chem Int Ed Engl* 2016; 55(26): 7520-7524.

[73] Rodgers DT, et al. Switch-mediated activation and retargeting of CAR-T cells for B-cell malignancies. *Proc Natl Acad Sci U S A* 2016; 113(4): E459-E468.

[74] Viaud S, et al. Switchable control over in vivo CAR T expansion, B cell depletion, and induction of memory. *Proc Natl Acad Sci U S A* 2018; 115(46): E10898-E10906.

[75] Tamada K, et al. Redirecting gene-modified T cells toward various cancer types using tagged antibodies. *Clin Cancer Res* 2012; 18(23): 6436-6445.

[76] Cartellieri M, et al. Switching CAR T cells on and off: a novel modular platform for retargeting of T cells to AML blasts. *Blood Cancer J* 2016; 6(8): e458.

[77] Cartellieri M, et al. A novel ex vivo isolation and expansion procedure for chimeric antigen receptor engrafted human T cells. *PLoS One* 2014; 9(4): e93745.

[78] Loureiro LR, et al. Development of a novel target module redirecting UniCAR T cells to Sialyl Tn-expressing tumor cells. *Blood Cancer J* 2018; 8(9): 81.

[79] Duong CP, et al. Enhancing the specificity of T-cell cultures for adoptive immunotherapy of cancer. *Immunotherapy* 2011; 3(1): 33-48.

[80] Fedorov VD, Themeli M, Sadelain M. PD-1- and CTLA-4-based inhibitory chimeric antigen receptors (iCARs) divert off-target immunotherapy responses. *Sci Transl Med* 2013; 5(215): 215ra172.

[81] Grada Z, et al. TanCAR: A Novel Bispecific Chimeric Antigen Receptor for Cancer Immunotherapy. *Mol Ther Nucleic Acids* 2013; 2: e105.

[82] Juillerat A, et al. An oxygen sensitive self-decision making engineered CAR T-cell. *Sci Rep* 2017; 7: 39833.

[83] Juillerat A, et al. Design of chimeric antigen receptors with integrated controllable transient functions. *Sci Rep* 2016; 6: 18950.

[84] Krause A, et al. Antigen-dependent CD28 signaling selectively enhances survival and proliferation in genetically modified activated human primary T lymphocytes. *J Exp Med* 1998; 188(4): 619-626.

[85] Morsut L, et al. Engineering Customized Cell Sensing and Response Behaviors Using Synthetic Notch Receptors. *Cell* 2016; 164(4): 780-791.

[86] Roybal KT, et al. Precision Tumor Recognition by T Cells With Combinatorial Antigen-Sensing Circuits. *Cell* 2016; 164(4): 770-779.

[87] Wilkie S, et al. Dual targeting of ErbB2 and MUC1 in breast cancer using chimeric antigen receptors engineered to provide complementary signaling. *J Clin Immunol* 2012; 32(5): 1059-1070.

[88] Sakemura R, et al. A Tet-On Inducible System for Controlling CD19-Chimeric Antigen Receptor Expression upon Drug Administration. *Cancer Immunol Res* 2016; 4(8): 658-668.

[89] Wu CY, et al. Remote control of therapeutic T cells through a small molecule-gated chimeric receptor. *Science* 2015; 350(6258): aab4077.

[90] Mata M, et al. Inducible Activation of MyD88 and CD40 in CAR T Cells Results in Controllable and Potent Antitumor Activity in Preclinical Solid Tumor Models. *Cancer Discov* 2017; 7(11): 1306-1319.

[91] Bayle JH, et al. Rapamycin analogs with differential binding specificity permit orthogonal control of protein activity. *Chem Biol* 2006; 13(1): 99-107.

[92] Liberles SD, et al. Inducible gene expression and protein translocation using nontoxic ligands identified by a mammalian three-hybrid screen. *Proc Natl Acad Sci U S A* 1997; 94(15): 7825-7830.

[93] Choi J, et al. Structure of the FKBP12-rapamycin complex interacting with the binding domain of human FRAP. *Science* 1996; 273(5272): 239-242.

[94] Cunha BA, Comer JB, Jonas M. The tetracyclines. *Med Clin North Am* 1982; 66(1): 293-302.

[95] Klein NC, Cunha BA. Tetracyclines. *Med Clin North Am* 1995; 79(4): 789-801.

[96] Cunha BA, Sibley CM, Ristuccia AM. Doxycycline. *Ther Drug Monit* 1982; 4(2): 115-135.

[97] Cunha BA. Doxycycline re-revisited. *Arch Intern Med* 1999; 159(9): 1006-1007.

[98] Jonas M, Cunha BA. Minocycline. *Ther Drug Monit* 1982; 4(2): 137-145.

[99] Cunha BA. New uses for older antibiotics: nitrofurantoin, amikacin, colistin, polymyxin B, doxycycline, and minocycline revisited. *Med Clin North Am* 2006; 90(6): 1089-1107.

[100] Cunha BA, Baron J, Cunha CB. Similarities and differences between doxycycline and minocycline: clinical and antimicrobial stewardship considerations. *Eur J Clin Microbiol Infect Dis* 2018; 37(1): 15-20.

[101] Klotzsche M, Berens C, Hillen W. A peptide triggers allostery in tet repressor by binding to a unique site. *J Biol Chem* 2005; 280(26): 24591-24599.

[102] Luckner SR, Klotzsche M, Berens C, Hillen W, Muller YA. How an agonist peptide mimics the antibiotic tetracycline to induce Tet-repressor. *J Mol Biol* 2007; 368(3): 780-790.

[103] Birnboim HC, Doly J. A rapid alkaline extraction procedure for screening recombinant plasmid DNA. *Nucleic Acids Res* 1979; 7(6): 1513-1523.

[104] Hanenberg H, et al. Colocalization of retrovirus and target cells on specific fibronectin fragments increases genetic transduction of mammalian cells. *Nat Med* 1996; 2(8): 876-882.

[105] Pollok KE, et al. High-efficiency gene transfer into normal and adenosine deaminase-deficient T lymphocytes is mediated by transduction on recombinant fibronectin fragments. *J Virol* 1998; 72(6): 4882-4892.

[106] Almasbak H, et al. Inclusion of an IgG1-Fc spacer abrogates efficacy of CD19 CAR T cells in a xenograft mouse model. *Gene Ther* 2015; 22(5): 391-403.

[107] Zhang T, Wu MR, Sentman CL. An NKp30-based chimeric antigen receptor promotes T-cell effector functions and anti-tumor efficacy in vivo. *J Immunol* 2012; 189(5): 2290-2299.

[108] Huppa JB, Gleimer M, Sumen C, Davis MM. Continuous T cell receptor signaling required for synapse maintenance and full effector potential. *Nat Immunol* 2003; 4(8): 749-755.

[109] Purbhoo MA, Irvine DJ, Huppa JB, Davis MM. T cell killing does not require the formation of a stable mature immunological synapse. *Nat Immunol* 2004; 5(5): 524-530.

[110] Milone MC, et al. Chimeric receptors containing CD137 signal transduction domains mediate enhanced survival of T cells and increased antileukemic efficacy in vivo. *Mol Ther* 2009; 17(8): 1453-1464.

[111] Schnappinger D, Schubert P, Pfleiderer K, Hillen W. Determinants of protein–protein recognition by four helix bundles: changing the dimerization specificity of Tet repressor. *EMBO J* 1998; 17(2): 535-543.

[112] Agwuh KN, MacGowan A. Pharmacokinetics and pharmacodynamics of the tetracyclines including glycylcyclines. *J Antimicrob Chemother* 2006; 58(2): 256-265.

[113] Jacobson CA, Farooq U, Ghobadi A. Axicabtagene ciloleucel, an anti-cd19 chimeric antigen receptor t-cell therapy for relapsed or refractory large b-cell lymphoma: Practical implications for the community oncologist. *Oncologist* 2020; 25(1): e138-e146.

[114] Locke FL, et al. Long-term safety and activity of axicabtagene ciloleucel in refractory large b-cell lymphoma (zuma-1): A single-arm, multicentre, phase 1-2 trial. *Lancet Oncol* 2019; 20(1): 31-42.

[115] Vairy S, Garcia JL, Teira P, Bittencourt H. Ctl019 (tisagenlecleucel): Car-t therapy for relapsed and refractory b-cell acute lymphoblastic leukemia. *Drug Des Devel Ther* 2018; 12: 3885-3898.

[116] Laetsch TW, et al. Patient-reported quality of life after tisagenlecleucel infusion in children and young adults with relapsed or refractory b-cell acute lymphoblastic leukaemia: A global, single-arm, phase 2 trial. *Lancet Oncol* 2019; 20(12): 1710-1718.

[117] Schuster SJ, et al. Tisagenlecleucel in adult relapsed or refractory diffuse large b-cell lymphoma. *N Engl J Med* 2019; 380(1): 45-56.

[118] Ma S, et al. Current progress in car-t cell therapy for solid tumors. *Int J Biol Sci* 2019; 15(12): 2548-2560.

[119] Martinez M, Moon EK. Car t cells for solid tumors: New strategies for finding, infiltrating, and surviving in the tumor microenvironment. *Front Immunol* 2019; 10: 128.

[120] Pule M, Finney H, Lawson A. Artificial T-cell receptors. *Cytotherapy* 2003; 5(3): 211-226.

[121] Finney HM, Lawson AD, Bebbington CR, Weir AN. Chimeric receptors providing both primary and costimulatory signaling in T cells from a single gene product. *J Immunol* 1998; 161(6): 2791-2797.

[122] Maher J, Brentjens RJ, Gunset G, Riviere I, Sadelain M. Human T-lymphocyte cytotoxicity and proliferation directed by a single chimeric TCRzeta /CD28 receptor. *Nat Biotechnol* 2002; 20(1): 70-75.

[123] James JR, Vale RD. Biophysical mechanism of T-cell receptor triggering in a reconstituted system. *Nature* 2012; 487(7405): 64-69.

[124] Ylitalo P, Hinkka H, Neuvonen PJ. Effect of exercise on the serum level and urinary excretion of tetracycline, doxycycline and sulphamethizole. *Eur J Clin Pharmacol* 1977; 12(5): 367-373.

[125] Kalos M, et al. T Cells with Chimeric Antigen Receptors Have Potent Antitumor Effects and Can Establish Memory in Patients with Advanced Leukemia. *Sci Transl Med* 2011; 3(95): 95ra73.

[126] Traversari C, et al. The potential immunogenicity of the TK suicide gene does not prevent full clinical benefit associated with the use of TK-transduced donor lymphocytes in HSCT for hematologic malignancies. *Blood* 2007; 109(11): 4708-4715.

[127] Bridgeman JS, et al. The optimal antigen response of chimeric antigen receptors harboring the CD3zeta transmembrane domain is dependent upon incorporation of the receptor into the endogenous TCR/CD3 complex. *J Immunol* 2010; 184(12): 6938-6949.

[128] Savoldo B, et al. CD28 costimulation improves expansion and persistence of chimeric antigen receptor-modified T cells in lymphoma patients. *J Clin Invest* 2011; 121(5): 1822-1826.

[129] Hinrichs W, et al. Structure of the Tet repressor-tetracycline complex and regulation of antibiotic resistance. *Science* 1994; 264(5157): 418-420.

[130] Kisker C, Hinrichs W, Tovar K, Hillen W, Saenger W. The complex formed between Tet repressor and tetracycline-Mg2+ reveals mechanism of antibiotic resistance. *J Mol Biol* 1995; 247(2): 260-280.

[131] Klotzsche M, Goeke D, Berens C, Hillen W. Efficient and exclusive induction of Tet repressor by the oligopeptide Tip results from co-variation of their interaction site. *Nucleic Acids Res* 2007; 35(12): 3945-3952.

[132] Loskog A, et al. Addition of the CD28 signaling domain to chimeric T-cell receptors enhances chimeric T-cell resistance to T regulatory cells. *Leukemia* 2006; 20(10): 1819-1828.

[133] Pule MA, et al. Virus-specific T cells engineered to coexpress tumor-specific receptors: persistence and antitumor activity in individuals with neuroblastoma. *Nat Med* 2008; 14(11): 1264-1270.

[134] Quintarelli C, et al. Co-expression of cytokine and suicide genes to enhance the activity and safety of tumor-specific cytotoxic T lymphocytes. *Blood* 2007; 110(8): 2793-2802.

[135] Suntharalingam G, et al. Cytokine storm in a phase 1 trial of the anti-CD28 monoclonal antibody TGN1412. *N Engl J Med* 2006; 355(10): 1018-1028.

[136] Szymczak AL, et al. Correction of multi-gene deficiency in vivo using a single 'self-cleaving' 2A peptide-based retroviral vector. *Nat Biotechnol* 2004; 22(5): 589-594.

[137] Zhao Y, et al. A herceptin-based chimeric antigen receptor with modified signaling domains leads to enhanced survival of transduced T lymphocytes and antitumor activity. *J Immunol* 2009; 183(9): 5563-5574.

[138] Bluestone JA, Bour-Jordan H. Current and future immunomodulation strategies to restore tolerance in autoimmune diseases. *Cold Spring Harb Perspect Biol* 2012; 4(11): a007542.

[139] Sadelain M, Brentjens R, Rivière I. The basic principles of chimeric antigen receptor design. *Cancer Discov* 2013; 3(4): 388-398.

[140] Kalos M, June CH. Adoptive T cell transfer for cancer immunotherapy in the era of synthetic biology. *Immunity* 2013; 39(1): 49-60.

[141] Kochenderfer JN, Rosenberg SA. Treating B-cell cancer with T cells expressing anti-CD19 chimeric antigen receptors. *Nat Rev Clin Oncol* 2013; 10(5): 267-276.

[142] Fischbach MA, Bluestone JA, Lim WA. Cell-based therapeutics: the next pillar of medicine. *Sci Transl Med* 2013; 5(179): 179ps7.

[143] Roberts MR, et al. Targeting of human immunodeficiency virus-infected cells by CD8+ T lymphocytes armed with universal T-cell receptors. *Blood* 1994; 84(9): 2878-2889.

[144] Maus MV, Grupp SA, Porter DL, June CH. Antibody-modified T cells: CARs take the front seat for hematologic malignancies. *Blood* 2014; 123(17): 2625-2635.

[145] Sato T, et al. Engineered human tmpk/AZT as a novel enzyme/prodrug axis for suicide gene therapy. *Mol Ther* 2007; 15(5): 962-970.

[146] Weiss A, Littman DR. Signal transduction by lymphocyte antigen receptors. *Cell* 1994; 76(2): 263-274.

[147] Miyamoto T, et al. Rapid and orthogonal logic gating with a gibberellin-induced dimerization system. *Nat Chem Biol* 2012; 8(5): 465-470.

[148] Murase K, Hirano Y, Sun TP, Hakoshima T. Gibberellin-induced DELLA recognition by the gibberellin receptor GID1. *Nature* 2008; 456(7221): 459-463.

[149] Boyman O, Sprent J. The role of interleukin-2 during homeostasis and activation of the immune system. *Nat Rev Immunol* 2012; 12(3): 180-190.

[150] Ikeda H, Old LJ, Schreiber RD. The roles of IFN gamma in protection against tumor development and cancer immunoediting. *Cytokine Growth Factor Rev* 2002; 13(2): 95-109.

[151] Banaszynski LA, Wandless TJ. Conditional control of protein function. *Chem Biol* 2006; 13(1): 11-21.

[152] Bacchus W, Fussenegger M. The use of light for engineered control and reprogramming of cellular functions. *Curr Opin Biotechnol* 2012; 23(5): 695-702.

[153] Toettcher JE, Gong D, Lim WA, Weiner OD. Light-based feedback for controlling intracellular signaling dynamics. *Nat Methods* 2011; 8(10): 837-839.

[154] Levskaya A, Weiner OD, Lim WA, Voigt CA. Spatiotemporal control of cell signalling using a light-switchable protein interaction. *Nature* 2009; 461(7266): 997-1001.

[155] Kennedy MJ, et al. Rapid blue-light-mediated induction of protein interactions in living cells. *Nat Methods* 2010; 7(12): 973-975.

[156] Wu YI, et al. A genetically encoded photoactivatable Rac controls the motility of living cells. *Nature* 2009; 461(7260): 104-108.

[157] Prehoda KE, Scott JA, Mullins RD, Lim WA. Integration of multiple signals through cooperative regulation of the N-WASP-Arp2/3 complex. *Science* 2000; 290(5492): 801-806.

[158] Dueber JE, Yeh BJ, Bhattacharyya RP, Lim WA. Rewiring cell signaling: the logic and plasticity of eukaryotic protein circuitry. *Curr Opin Struct Biol* 2004; 14(6): 690-699.

[159] Liu E, et al. Use of CAR-Transduced Natural Killer Cells in CD19-Positive Lymphoid Tumors. *N Engl J Med* 2020; 382(6): 545-553.

[160] Blank CU, et al. Defining 'T cell exhaustion'. *Nat Rev Immunol* 2019; 19(11): 665-674.

[161] Boroughs AC, et al. Chimeric antigen receptor costimulation domains modulate human regulatory T cell function. *JCI Insight* 2019; 5(8): e126194.

[162] Chen J, et al. NR4A transcription factors limit CAR T cell function in solid tumours. *Nature* 2019; 567(7749): 530-534.
[163] Majzner RG, et al. Tuning the Antigen Density Requirement for CAR T-cell Activity. *Cancer Discov* 2020; 10(5): 702-723.
[164] Choi BD, et al. CAR-T cells secreting BiTEs circumvent antigen escape without detectable toxicity. *Nat Biotechnol* 2019; 37(9): 1049-1058.
[165] Cohen AD, et al. B cell maturation antigen-specific CAR T cells are clinically active in multiple myeloma. *J Clin Invest* 2019; 129(6): 2210-2221.
[166] Finney OC, et al. CD19 CAR T cell product and disease attributes predict leukemia remission durability. *J Clin Invest* 2019; 129(5): 2123-2132.
[167] Leung WH, et al. Sensitive and adaptable pharmacological control of CAR T cells through extracellular receptor dimerization. *JCI Insight* 2019; 5(11): e124430.
[168] Lynn RC, et al. c-Jun overexpression in CAR T cells induces exhaustion resistance. *Nature* 2019; 576(7786): 293-300.
[169] Majzner RG, Mackall CL. Clinical lessons learned from the first leg of the CAR T cell journey. *Nat Med* 2019; 25(9): 1341-1355.
[170] Stadtmauer EA, et al. CRISPR-engineered T cells in patients with refractory cancer. *Science* 2020; 367(6481): eaba7365.
[171] Majzner RG, et al. CAR T Cells Targeting B7-H3, a Pan-Cancer Antigen, Demonstrate Potent Preclinical Activity Against Pediatric Solid Tumors and Brain Tumors. *Clin Cancer Res* 2019; 25(8): 2560-2574.
[172] Mestermann K, et al. The tyrosine kinase inhibitor dasatinib acts as a pharmacologic on/off switch for CAR T cells. *Sci Transl Med* 2019; 11(499): eaau5907.
[173] Ormhoj M, et al. Chimeric Antigen Receptor T Cells Targeting CD79b Show Efficacy in Lymphoma with or without Cotargeting CD19. *Clin Cancer Res* 2019; 25(23): 7046-7057.
[174] Raje N, et al. Anti-BCMA CAR T-Cell Therapy bb2121 in Relapsed or Refractory Multiple Myeloma. *N Engl J Med* 2019; 380(18): 1726-1737.
[175] Ramakrishna S, et al. Modulation of Target Antigen Density Improves CAR T-cell Functionality and Persistence. *Clin Cancer Res* 2019; 25(17): 5329-5341.